Characterisation of Primary Porcine Hepatocyte Culture Systems for use in Bioartificial Liver Devices

Leonard Joseph Nelson

A thesis submitted for the degree of Doctor of Philosophy (PhD) at the University of Edinburgh

May 2002

Declaration of originality

I hereby declare that the work presented in this thesis is my own, unless otherwise stated. It has not been submitted previously for a higher degree. This work was undertaken at the University of Edinburgh Liver Cell Biology Laboratory, Department of Medicine (Clinical and Surgical Sciences) and the Department of Clinical Biochemistry, Royal Infirmary of Edinburgh, and in collaboration with the Roslin Institute (Edinburgh) and Department of Preclinical Veterinary Sciences (Dick Vet School), University of Edinburgh.

Leonard Joseph Nelson

Certificate

We certify that Leonard Joseph Nelson has completed 48 months (part-time) of experimental research and that he fulfilled conditions of ordinance 39 of the University of Edinburgh, so that he is qualified to submit the following thesis in application for the Degree of Doctor of Philosophy (PhD).

Professor Peter C Hayes

Dr Simon Walker

Dedication

I would like to dedicate this thesis to my son, David, my mother, Jean, and my family: Pat, Maureen, Mike, Teresa, Peter and in memory of my father, Len and brother, David, for their love, support and encouragement always.

Contents outline

Page

Table of Contents **Page**

Contents **Page**

Contents **Page**

Contents **Page**

Contents **Page**

Contents ..... **Page**

Figures and Tables **Chapter - Page**

Abbreviations

% GE	Percentage galactose elimination
λ	Wavelength
$\alpha_5\beta_1$	Integrin $\alpha_5\beta_1$ heterodimer
2D	2-dimensional
3D	3-dimensional
AB	Albumin blue 580 dye [2-chloro-3-(2,2-dicyanoethenyl)-2-cyclohexen-1-xylidene]methylpropanedinitrile potassium salt
Acetyl Co-A	Acetyl Coenzyme-A
A-Gal epitope	alpha galactose alpha-1,3-galactose epitope
ALF	Acute liver failure
ANOVA	Analysis of variance
AO	Acridine orange
ASR	Albumin synthesis rate
ATP	Adenosine triphosphate
BAL	Bioartificial Liver
C3A	Human hepatoblastome cell line
CSK	Cytoskeleton
CV	Coefficient of variance
Cy3	conjugated donkey anti-goat IgG
CYP2A	Cytochrome P450 isoenzyme 2A
CYP3A4	Cytochrome P450 isoenzyme 3A4
DMEM	Dulbecco's modified Eagle's medium
DNA	Deoxyribonucleic acid
E	Extinction coefficient
ECM	Extracellualr matrix
EDTA	ethylene di-amino tetra acetic acid
EGF	Epidermal growth factor
EGTA	ethylene glycol-bis[β-aminoethyl ether]-N,N,N`N`-tetraacetic acid

EHS	Engelbreth Holm Sarcoma Natrix (gel biomatrix)
ELAD	Extracorporeal liver assist device
ER	Endoplasmic reticulum
F1	Fraction 1 (supernatant)
F2	Fraction 2 (cytosolic)
FBS	Foetal bovine serum
FCS	Foetal calf serum
FDA	Fluorescein diacetate
FHF	Fulminant hepatic failure
GE	Galactose elimination
GSH	Glutathione (reduced form)
H&E	Haematoxylin and eosin (nuclear / cytoplasmic stain)
HARV	High aspect ratio vessel
HBAI	Hepatocyte biological activity index
HBSS	Hanks' Balanced Salt Solution
HDM	Hormonally defined medium
HE	Hepatic encephalopathy
HEPES	N-2-Hydroxyethylpiperazine-N`-2-ethanesulfonic acid
HepG2	Human hepatoblastoma cell line
HGF	Hepatocyte growth factor
HM	Hepatocyte Medium
IgG	Immunoglobulin G
IgM	Immunoglobulin M
ITU	Intesive therapy unit
IVC	Inferior vena cava
KAB	Krebs Albumin Buffer
KHB	Krebs HEPES Buffer
KHBS	Krebs-Henseleit Buffer Stock Solution
LDH	Lactate dehydrogenase
L-EGF	Long- Epidermal growth factor
LSD	Least significant difference

M1640	Roswell Park Memorial Institute (RPMI) Medium 1640
M199	Medium 199
MEM	minimum essential medium
MOPS	3-N-morpholinopropanesulphonic acid (free acid)
mRNA	messenger ribonucleic acid
n	Number (n) of separate experiments
NAD^+	Nicotinamide adenine dinuleotide (reduced form)
NADH	Nicotinamide adenine dinuleotide (oxidized form)
NAPQI	N-acetyl parabenzoquinoneimine
NDS	normal donkey serum
NPC	Non-parenchymal cells
OLT	Orthotopic liver transplantation
p-value	observed significance level
P450	Cytochrome P450 system
P4501A1	Cytochrome P450 isoenzyme 1A1
P4501A1/2	Cytochrome P450 isoenzyme 1A1 and 1A2
PAS	periodic acid schiff
PB	Perfusion buffer
PBS	phosphate-buffered saline
PC	Parenchymal cells
Pen-Strep	Penicillin-Streptomycin
PERV	Porcine endogenous retrovirus
PGA	Polyglycolic acid
PHLC	Primary human liver cells
pO_2	partial pressure of oxygen
PPH(s)	Primary porcine hepatocyte(s)
QC	Quality control
r^2	Correlation coefficent
RCCS	Rotary cell culture system
RER	Rough endoplasmic reticulum
SCB	sodium cacodylate buffer

SDS	Sodium dodecyl sulphate
SECs	Sinusiodal endothelial cells
SEM	Scanning electron microscopy
SEM	Standard error mean
SER	Smooth endoplasmic reticulum
SLTU	Scottish Liver Transplant Unit
ST	Sub-total
SUBU	Strathclyde University Bioengineering Unit
TCA	Tricarboxylic acid cycle
TCP	Tissue culture plastic
TEM	Transmission electron microscopy
TP	Total cellular protein content
tP450	total cellular cytochrome P450 content
UDP-galactose	Uridine diphosphate-galactose
UDP-galactose-s-epimerase	Uridine diphosphate- galactose-s-epimerase
UDP-glucose	Uridine diphosphate-glucose
USR	Urea synthesis rate
v/v	Volume per volume
w/v	Weight per volume
WB	Wash buffer
WE	Williams Medium E
WE+	Supplemented Williams Medium E

Acknowledgements

I would like to express my sincere thanks and appreciation to my supervisors, Professor Peter Hayes, Dr Simon Walker and Dr John Plevris for their enthusiasm, help, guidance, encouragement, support and friendship throughout the project.

I would also like to warmly thank Drs Forbes Howie and Moira Nicol (Clinical Biochemistry) for many practical hints and advice on cell biochemistry protocols, 'lending' of reagents and equipment and for their friendship since the early days of the project. Also thanks to Professor Ian Mason for allowing me to work in this department and for advice on cytochrome P450 measurement and biochemistry. Thanks to Dr Ken Humphreys for help with the albumin assay development, dot blots and assessment of gross morphology, to Steve Keatch for help with P450 assays, and to Irene Beldon for help with urea and galactose measurements.

I greatly appreciate the support of Roy Dawkes and the other technical staff, particularly, Derek Christie, Bill Wight and Dr Harry Brash for designing and constructing the 4-station rotary cell culture system (microgravity simulator) as well as help with computing and equipment 'emergencies'. Thanks to staff of the Dept of Pathology, particularly Dr Chris Bellamy and Helen Caldwell, for technical help and advice on hepatic histology and image analysis.

For helpful advice and many discussions on all aspects of the project I would like to express my gratitude to the 'old school'; Drs Paddy Hadoke and Christine Buckley (for hands-on help with the cell isolation), Zahur Islam and Carol-Ann McIntyre, and the 'new school' - Phil (the stem cell) Newsome. Thanks also to Dr Ahmed Helmy for guidance on statistical analysis. Special thanks to Dr Celine Filippi for critical reading of the thesis and help with biochemical analysis. For expertise in scanning and electron microscopy and helpful advice on sample preparation, production and interpretation of electron micrographs - thanks to Steve Mitchell; and for histology staining, Gordon Goodall, in the Dept of Veterinary Medicine, Dick Vet School.

Abstract

Introduction

Paracetamol-induced acute liver failure causes disruption of normal hepatic architecture and function, and where there is massive cellular necrosis, resulting in poor prognosis heralded by hepatic coma, liver transplantation is the only effective treatment. This procedure is however limited by a shortage of donor organs. Alternative treatment strategies under development include hepatocyte-based bioartficial liver systems (BALS) which may allow time for temporary support of the failing liver until a donor organ becomes available. This approach, may even allow regeneration of the native liver and full recovery. Primary porcine hepatocytes (PPHs) are the preferred biological component for BALS as they have similar morphology and biochemical functionality to human hepatocytes. Conventional *in vivo* isolation of PPHs can give high yield and viability required of BALS, although such methods are time-consuming, expensive and require specialist surgical facilities. The consensus view is that PPH-based BALS should retain synthetic, detoxifying, metabolic and excretory functions. Despite this, systematic studies on the optimisation and characterisation of different *in vitro* culture conditions following high yield extraction of PPHs, is lacking.

Principal Aims of Thesis

The principal aims of this thesis were to develop a high viability, high yield, reproducible *ex vivo* method for obtaining PPHs and to characterise, using functional and morphological criteria, PPHs under different fully-defined culture conditions, for use in BAL devices.

Methods

PPH isolation was optimised using a novel 5-step *ex vivo* retrograde collagenase perfusion method. Purified cells were subsequently cultured in four separate serum-free chemically-defined medium (SFCD) formulations (Medium 199 (M199), Williams Medium E (WE), RPMI 1640 (M1640), and Hepatocyte Medium (HM)) for 6 days on biomatrix-free, unmodified tissue culture plastic, or in a rotary cell culture simulated microgravity system (RCCS) in WE for 12 days. Differentiated characteristics of morphology and function were then assessed. Functional assays of urea synthesis rates (USR) and galactose elimination (GE) of medium-*conditioned* cultures, and assays of total cellular protein content (TP), total P450 content (tP450) and lactatc dehydrogenase activity (cell viability) were measured using spectrophotometry. Albumin synthesis rates (ASR) in test media, were determined by a novel fluorimetric albumin 580 dye-binding assay.

Statistics:

For each biochemical measurement, and for image analysis, multiple comparisons were made of: 1) between-media evaluations on each day of culture and 2) between-day evaluations for each medium formulation using one-way single factor ANOVA (assuming equal variances) and *Post Hoc* tests of least significant differences. Results are expressed as mean±SEM (n=x, experiments).

In order to define an index of global functional capacity, a scoring system (hepatocyte biological acitivity index; HBAI) was devised as an integrated measure of overall functional capability of cell cultures, on each day or cumulatively. Gross morphology and ultrastructure were assessed using phase contrast and both scanning and transmission electron microscopy, and by image analysis techniques. Integrin expression, bile functionality, and viability of RCCS spheroids were detected by immunofluorescent (IF) staining using confocal and IF microscopy.

Results

Cell Isolation A **yield** of 2.4±0.5 x 10^{10} cells from 12±1 kg piglets (n=20), with a **viability** of 85±6% was obtained in <2 hours. Isolate **purity** was 97±3 % hepatocytes (n=4). Image analysis data proved more discriminatory, in assessment of plating efficiencies (PE), than assessment of total protein, or LDH activity. *Between-media comparisons*: **PE** (n=3) on d1 for WE, HM, M199, and, M1640 maintained cells were 71±14, 38±3, 78±5, and 55±10 %, respectively; PE was significantly greater in both WE ($p<0.05$) and M199 ($p<0.01$) cells *vs* HM cells, up to d4. HM was significantly lower than all test media on d2 ($p<0.05$) and d4 ($p<0.01$). **USR** of cultures *conditioned* in test media (n=3): d2 was significantly greater at 147±21nmol/hour/mg TP for M1640 *vs* WE (104±11), but not M199 (115±17) or HM (126±20) cells. By d4, USR of HM (221±25) and M1640 (176±31) cells was significantly higher ($p<0.01$), than WE (93±14) or M199 (79±4) cultures. **USR** was attenuated in all media by d6. **GE** of cultures *conditioned* in test media (n=3): GE for WE, HM, M199 and RPMI 1640 on culture day 2 (420±66, 436±54, 416±33, 516±44 nmol/h/mg TP, respectively) was significantly greater ($p<0.05$) *vs* day 4 (266±56, 298±78, 231±41, 277±101) cultures. GE remained stable up to day 6. **tP450** decreased significantly ($p<0.001$), from 120 pmol/mg TP for fresh cells, to ≈40 pmol/mg TP in all media tested on d2. Specifically, tP450 was maintained at 36±3 in HM (n=3), significantly greater ($p<0.05$) than WE (24±3) or M1640 (25±5) at d2, and declining most significantly in WE (17±1, $p<0.05$) by d6. *Between-day comparisons*: **PE** was significantly greater ($p<0.05$) in all media by d4 (≈95%) *vs* d1 (≈70%) cultures, except HM (≈40%) cells. **USR** increased significantly ($p<0.05$) only in day 4 HM-*conditioned* cells (221±25) compared with day2. **Morphology** Hepatocytes maintained in M199 and WE, but not HM and M1640 media formulations, preserve ultrastructural, and gross morphological features of healthy cells up to culture day 4. The HBAI utility for multiple comparisons, reinforced by morphological observations, ranked the media on day 2 as: M199>WE>M1640>HM, M199 retaining primacy up to day 6. The RCCS modality retains stable, liver-

specific metabolic functions of PPHs, morphological features characteristic of 3D hepatocyte cultures, and integrin α5 expression over a 12 day culture period.

Conclusions

High yield PPHs isolations, with high viability and purity, cultured under separate SFCD formulations, allow maintenance of viable hepatocyte cultures following high plating efficiencies, compatible with retention of functional activity, for up to 6 days. Moreover, the type of medium formulation appears to modulate, to varying degrees, both cell culture morphology and functional activity *in vitro*. USR, ASR, tP450, and GE functions for day 2 test media cultures, were up to 300%, 90%, 20%, and 50%, respectively, of *in vivo* values for human liver. Medium 199 is the most suitable synthetic media for culturing PPHs in BALS, which require rapid attachment of cells with an *in* vivo-like morphology, whilst maintaining a diverse repertoire of hepatic support functions. Furthermore, compared with 2D static cultures, the RCCS modality promotes culture longevity, and cellular functionality (on a per viable cell basis), while the presence of bile canalicular-like structures, and integrin α5expression, suggest the viable cell population maintained a differentiated, 3D-hepatospheroid cytoarchitecture with evidence of polarity. Further study is required to enhance the viable cell population, phenotype, polarity and thus functional activity of such liver constructs, for future therapeutic use.

Structure of thesis

Background

This thesis deals with the characterisation and optimization of primary porcine hepatocyte (PPH) culture systems for use in bioartificial liver devices (BAL) to treat acute liver failure (ALF). PPHs are considered the most suitable cell source for BAL devices. Although it is unclear which specific hepatic support functions are required in a BAL device, the consensus view is that these cells should have a repertoire of synthetic, detoxification and metabolic functions.

Despite this assertion, there are no systematic studies which seek to characterize optimal, defined culture conditions for PPHs, in terms of biochemical functionality and morphology. To achieve this a novel high yield, high viabilty *ex vivo* retrograde collagenase perfusion and isolation technique was first developed. Subsequently, the modulatory effects of different medium formulations on hepatocyte biochemical functionality and morphology was assessed in a fully-defined culture system. In order to define an index of global functional capacity, a scoring system (hepatocyte biological acitivity index; HBAI) was devised as an integrated measure of overall functional capability. Finally, the formation of 3-dimensional hepatosheroids in a simulated microgravity culture system is investigated as a novel environment for enhancing hepatocyte function, morphology and lifespan, applicable for BAL devices.

Structure

The first part of the thesis (Introduction, Chapter 1) outlines the normal anatomy, microstructure and selected functional aspects of liver metabolism, which enable normal physiological homeostasis to be maintained. The therapeutic potential of primary porcine hepatocytes (PPHs) is introduced in the context of their application to the treatment of acute liver failure, as the biological component of bioartificial liver systems. Finally, potential strategies used to retain *in* vivo-like

morphological and functional characteristics of isolated hepatic cells *in vitro* are presented.

In the second part of the thesis (experimental work, Chapters 2-5), each chapter is divided into: Introduction, Aim, Materials and Methods, Results, and Discussion. The 'Introductory' sections extend the discourse of chapter 1 by giving a more detailed account of each experimental chapter topic. For example, Chapter 5 defines the physical conditions which promote 3D cell configurations in the simulated microgravity environment. The 'Discussion' sections at the end of each experimental chapter give an overall critical discussion of results, offer new insights introduced by the experimental work regarding PPH culture for BAL systems, as well as future studies emerging from this work.

Chapter 2 deals with the development of a novel high yield, high viabilty *ex vivo* retrograde collagenase perfusion and isolation technique. Chapter 3 is a study of the viability, attachment efficiency, as well as gross and ultrastructural morphology of PPHs cultured under different, serum-free chemically defined culture conditions. In Chapter 4, the work of Chapter 3 is extended, by measuring biochemical functionality of PPHs under these defined conditions. In chapter 4 also, the concept of the 'hepatocyte biological activity index' is defined and explained. Finally, Chapter 5 deals with the morphology and function of PPHs grown in a simulated microgravity environment.

Chapter 6 (Concluding remarks) reviews the findings of this thesis and suggests future work, which may help improve both the biological component and design criteria, of BAL systems.

The bibliography, appendices and published papers arising from this thesis comprise Chapter 7.

Chapter 1

1.0 Introduction

1.1 General introduction

The liver is strategically situated between the splanchnic and systemic circulations to perform its primary global function – the regulation of the supply of substances to the systemic circulation and from the intestine. Liver cells are the most versatile cells in the body. Hepatocyte heterogeneity within the liver acinus, morphological variability and an abundance and variety of subcellular organelles, reflect the functional diversity of this remarkable organ. Modulation of the supply of substrates to distant organs is accomplished by several processes or functional capabilities of liver cells. These cells, operating within a highly structured organization, perform both endocrine and exocrine functions, uptake and removal of substances from sinusoidal blood, as well as synthetic, detoxification and metabolic duties including storage of metabolites.

Derangement of hepatic function, such as in paracetamol-induced acute liver failure, cause disruption of normal hepatic architecture and function due to massive cellular necrosis. Patients with this dramatic clinical syndrome have high morbidity and mortality with liver transplantation being the only effective treatment, albeit severely limited by a shortage of donor organs, and cost. Alternative treatment strategies include hepatocyte-based bioartficial liver systems which may allow time for temporary support of the failing liver until a donor organ becomes available or even to regeneration of the native liver and full recovery. The consensus view is that the biological component used in these devices should maintain synthetic, detoxifying, metabolic and excretory functions. However, systematic studies concerning optimisation of *in vitro* culture conditions following high yield extraction of hepatocytes is lacking.

This chapter outlines the normal anatomy, microstructure and selected functional aspects of liver metabolism, which enable normal physiological homeostasis to be maintained. The therapeutic potential of primary porcine hepatocytes (PPHs) is introduced in the context of their application to the treatment of acute liver failure, as the biological component of bioartificial liver systems. Finally, potential strategies used to retain *in* vivo-like phenotypic and functional characteristics of isolated hepatic cells *in vitro* are presented.

1.2 Gross anatomical features of human and pig liver

The human liver, weighing approximately 1500g (≈2 % of body weight) in adults, is the largest solid organ in the body and is surrounded by Glisson's capsule; it is situated in the right upper quadrant of the abdomen largely protected by the rib cage (Ham, 1953). In pigs, the liver comprises up to 5 % of body weight, perhaps reflecting the high intrinsic metabolic capacity of this species. Although many aspects of microanatomy are similar, there are major differences in gross anatomy between human and pig liver. For example, in humans the liver is traditionally divided into two uneven lobes by the falciform ligament, the right lobe being about six times larger than the left. In contrast, the pig's liver has deep fissures which clearly divide into distinct left lateral and left medial and right lateral and right medial lobes (Sack, 1982); centrally are the short quadrate and a caudate process with the gall bladder lying between the quadrate and right medial lobes (Figure 1.1). Like human liver, the concave visceral surface of pig liver contains the porta hepatis into which the hepatic artery and portal vein enter with hepatic veins running in the opposite direction, collecting blood from the sinusoids to the main hepatic veins, which drain into the inferior vena cava. Through the portal vein, the liver receives 75 % of its blood supply from the splanchnic circulation and 25 % through the hepatic artery. Blood flows into the sinusoids from these vessels (Moseley, 2000).

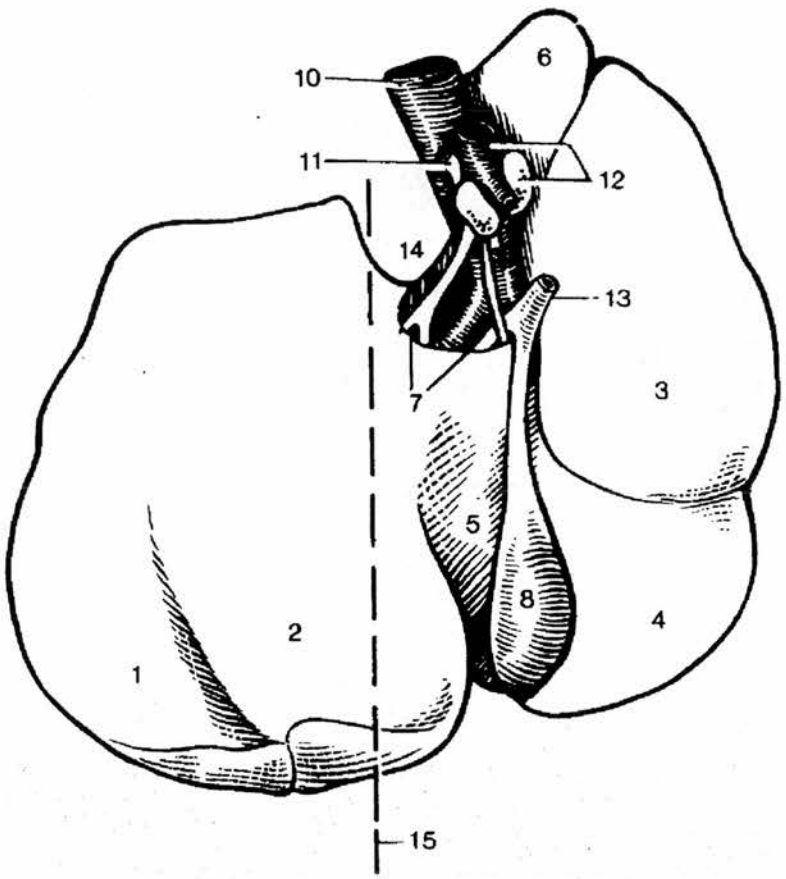

Figure 1.1 Schematic drawing of visceral surface of pig liver Modified from Sack, (1982) 1. Left lateral lobe; 2. Left medial lobe; 3. Right lateral lobe; 4. Right medial lobe; 5. Quadrate lobe; 6. Caudate process; 7. Porta; 8. Gall bladder; 10. Caudal vena cava; 11. Hepatic artery; 12. Portal vein and lymphatic nodes; 13. Bile duct; 14. Oesophageal notch; 15. Median plane.

1.3 Microstructural organization of the liver

Hepatocytes occupy 78 % of the total liver volume in humans and pigs (Sack, 1982). The cells are arranged in irregularly shaped plates, 1-2 cells thick along the hepatic sinusoids (Figure 1.2), which appear as 'cords' in two-dimensions under the microscope. The plates are branching and anastomosing laminae, arranged radially around small venules to form anatomical units called hepatic lobules (Rhodin, 1974). In pigs, the Kiernan's or classic lobule is about 0.7 x 2 mm in size, number about one million per liver and, unlike human lobules, have sharply deliminated boundaries of thin interlobular septa of connective tissue, which is hexagonal in outline (Junqueira, 1977). Each peripheral angle of the hexagonal lobule is occupied by portal spaces containing branches of the hepatic arteries, portal veins and bile ducts. The centrilobular hepatic veins are found at the centre of the liver lobule (Figure 1.3).

The functional unit of the liver is the simple liver acinus, defined as a unit of liver parenchyma irrigated by a single blood supply from hepatic arterial and portal venous branches in a small terminal portal space (Rappaport, 1976). In other words, the hepatic acinus comprises the region irrigated by one distributing vein (diamond shape in Figure 1.3). In addition to the terminal branches of the portal vein, an arterial branch and bile ductile are in the centre of this mass of hepatic parenchyma, which is situated in adjacent areas of two different classical hepatic lobules (Figure 1.3). Blood perfuses hepatic cells unidirectionally, becoming progressively poorer in oxygen and nutrients from acinar zone 1 to zone 3. Interestingly, this zonal arrangment may explain why potentially hepatotoxic drugs such as paracetamol, induce centrilobular or zone 3 necrosis, since it is predominantly zone 3 hepatocytes that participate in drug metabolism and disposition (Moseley, 2000).

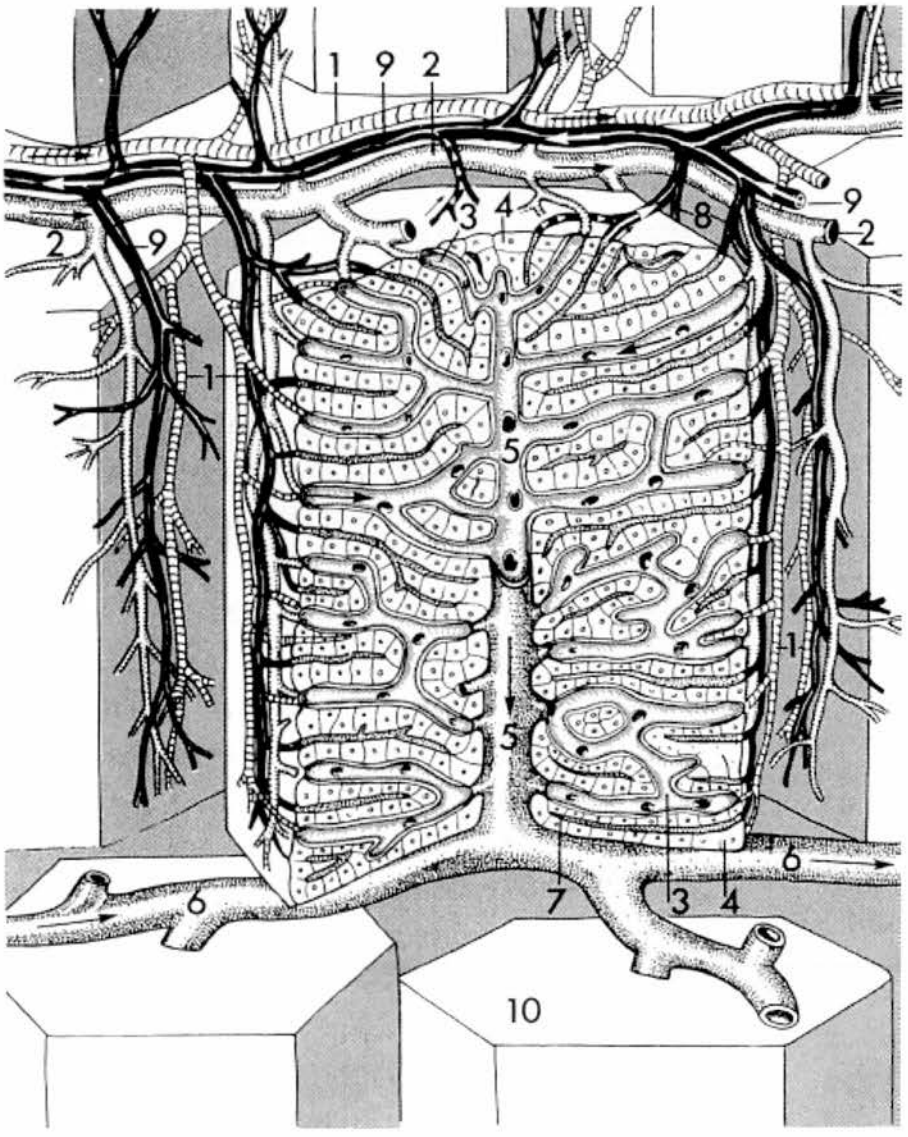

Figure 1.2 Three-dimensional diagram of the classic hepatic lobule [Rhodin *et al* 1974]. 1. Interlobular portal veins; 2. Interlobular hepatic arteries; 3. Hepatic sinusoids; 4. Plates of hepatic cells; 5. Central venule; 6. Sublobular hepatic vein; 7. Bile canalicui; 8. Bile ductules; 9. Bile ducts; 10. Perilobular surfaces of adjoining hepatic lobules. Hepatic arteries, veins and bile ducts occupy the portal spaces. Direction of blood flow is indicated by black arrows, bile fluid by white arrows.

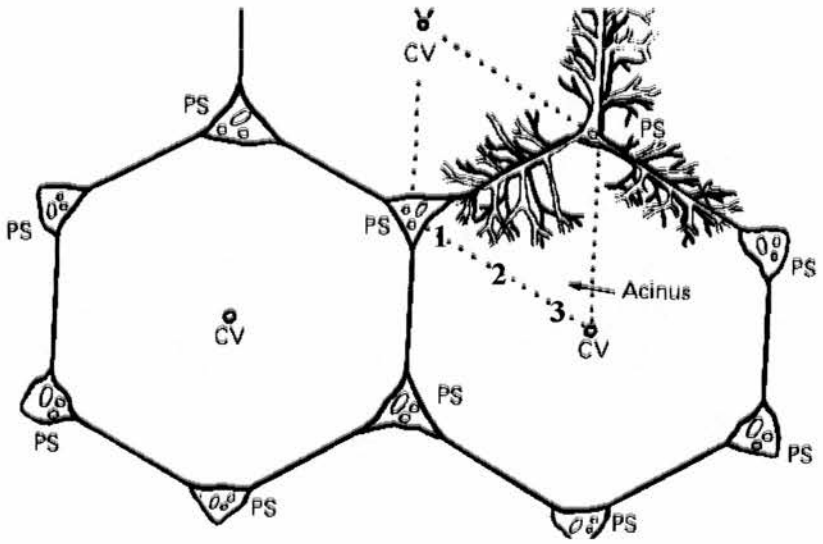

Figure 1.3 Schematic illustration of the territories of the liver lobules and hepatic acini [Modified from Junqueira, (1977)]

The classical lobule has a central vein (CV) and is outlined by the (solid) lines that bind the portal spaces (PS). The hepatic acinus comprises the region irrigated by one distributing vein (dotted triangles forming a diamond shape). Blood becomes progressively poorer in oxygen and nutrients from zone 1 (periportal) to zone 3 (perivenous).

In addition to hepatocytes and bile duct epithelial cells, four types of nonparenchymal cells populate the liver which are organized into liver acini (Figure 1.4): Sinusoidal endothelial cells (SECs), Kupffer cells (hepatic macrophages), hepatic stellate cells (Vitamin A-storing cells) and Pit cells (natural killer cells). In adult liver, hepatocyte constitute 78 % of the tissue volume, nonparenchymal cells account for 6 % and the extracellular space about 16 % (Fan, 2000). Fenestrated SECs line the hepatic sinusoids, which separate adjacent plates of hepatocytes. Unlike other endothelia, SECs lack an underlying basement membrane allowing the direct, selective exchange of substances, such as secretion of proteins or uptake of protein-bound bile acids or drugs, between the plasma and hepatocytes via the perisinusoidal Space of Disse (Moseley, 2000). Hepatocytes typically form one-cell thick plates, which are joined by junctional complexes demarcating the canalicular space from the sinusoidal domain. Kupffer cells and pit cells lie within the sinusoidal lumen whereas endothelial cells separate this lumen from the Space of Disse, wherein lie stellate cells (lipocytes) (Figure 1.4).

Within the thickness of the hepatic plates the bile canaliculi form an anastomosing polygonal network, constantly separated by a half-cell thick layer of cytoplasm from the hepatic sinusoids. The canaliculi secrete bile into periportal cholangioles or canals of Hering, which connect canaliculi to the smallest interlobular bile ducts (Figure 1.2), composed of cuboidal epithelial cells. These ducts convey bile to the extrahepatic bile duct, the gallbladder and the duodenum where bile facilitates fat digestion and absorption. These differences in the structure and function of the sinusoidal and canalicular membrane define the hepatocyte as a highly polarized epithelial cell (Rhodin, 1974; Moseley, 2000).

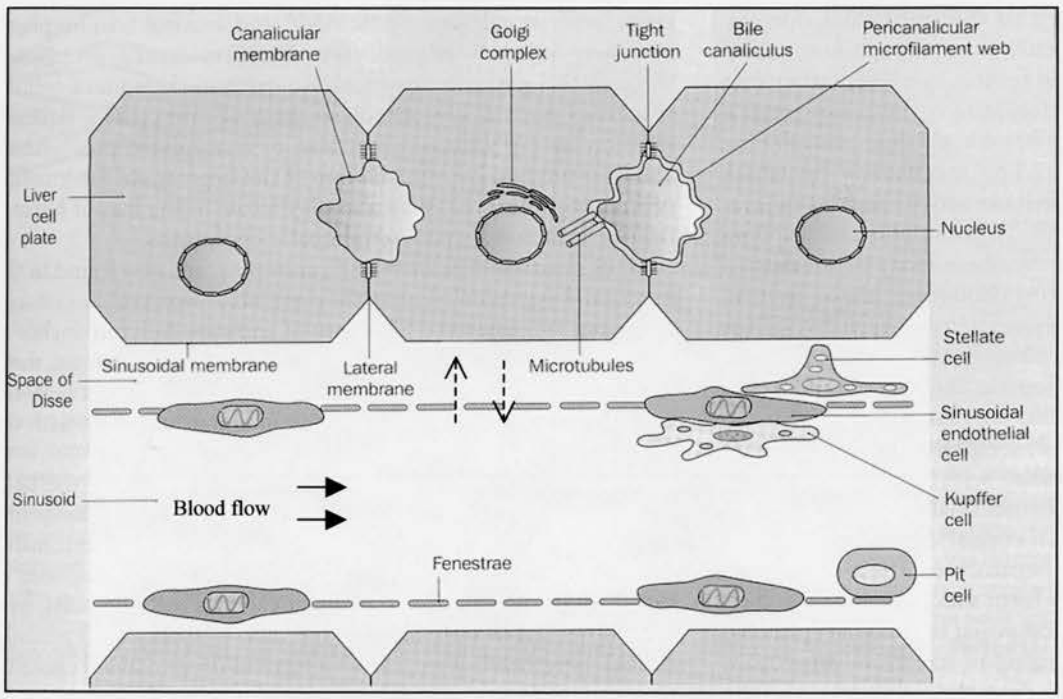

Figure 1.4 Schematic illustration of the microanatomy of the liver cell plate [Modified from Moseley, (2000)].

The relationship between hepatocytes, the four types of nonparenchymal cells and sinusoids in a part of the liver acinus is shown (not to scale). Hepatocytes typically form one-cell thick plates, which are joined by junctional complexes demarcating the canalicular space from the sinusoidal domain. Blood (solid arrows) passes through the sinusoidal lumen allowing exchange of solutes (broken arrows) with hepatocytes via fenestrae and the Space of Disse. Kupffer cells and pit cells lie within the sinusoidal lumen whereas endothelial cells separate this lumen from the Space of Disse, wherein lie stellate cells (lipocytes).

1.4 Microanatomy and ultrastructure of hepatocytes

Hepatocytes are polyhedral cells with a diameter of 20-30 μm. The nucleus is large, often binucleate with one or two prominent nucleoli. Nuclei vary in size due to polyploidy, increases in DNA content being associated with both age and pathology. In histological sections stained with haematoxylin and eosin, the cytoplasm of hepatocytes is eosinophilic due in part to the presence of smooth endoplasmic reticulum but mainly because of the presence of large numbers (1000-2000) of mitochondria (Junqueira, 1977), giving the cytoplasm a granular appearance under light microscopy (Burkitt *et al.*, 1993).

The large surface area of basolateral microvilli projecting into the perisinusoidal Space of Disse allows direct contact with sinusoidal blood so enabling the high absorbtive and secretory activity of hepatocytes. As well as exhibiting a distinct polarity, hepatocytes have uptake mechanisms for the bidirectional exchange of solutes including amino acids, hexose sugars, and organic anions such as bile acids fatty acids and bilirubin; receptor mediated endocytotic processes; Na^+,K^+-ATPase; and export processes for albumin, lipoproteins and clotting factors (Finlayson, 1997; Moseley, 2000)

Electron microscopy, subcellular fractionation and biochemical techniques have revealed great ultrastructural and functional diversity of hepatocytes. Mitochondria are respiratory organelles which are particularly numerous in hepatocytes and assume a spherical or ovoid shape. The primary function of mitochondria is the conservation of energy, from the oxidation of substrates by oxygen, in the form of ATP. Their inner membranes and cristae are involved with oxidative phosphorylation and fatty acid oxidation whereas the matrix is a concentrated protein solution of enzymes of the tricarboxylic acid and urea cycles (Berry *et al.*, 1991; Desmet, 1994).

The endoplasmic reticulum (ER) and Golgi complexes are involved in the synthesis, processing, packaging and sorting of cellular proteins prior to exocytosis. The ER is a collection of continuous membranous tubules, vesicles and flattened sacs that extends throughout the cytoplasm. Only granular ER, which is more developed in acinar zone 1 (periportal hepatocytes), has cisternae with attached polyribosomes, which are sites of protein synthesis. Smooth ER, on the other hand, has no ribosomes and functions in lipid biosynthesis, calcium regulation and detoxification through biotransformation. The Golgi complex is usually closely associated with the granular ER from which it receives newly synthesized proteins for subsequent processing and export to different destinations within the cell and to the cell surface. Peroxisomes are spherical structures smaller than mitochondria which provide important metabolic links between both anabolic and catabolic biochemical reactions of carbohydrates, lipids, fats, proteins and nucleic acids. Lysosomes are membrane-bound vesicles containing more than fifty hydrolytic enzymes involved in the digestion and catabolism of various endogenous and exogenous substances (Berry *et al.*, 1991; Burkitt *et al.*, 1993; Hargreaves, 1968; Junqueira, 1977).

1.5 Extracellular matrix, cell-matrix and cell-cell interactions

Normal liver lacks a true basement membrane and the stromal compartment is greatly reduced. As a result, the density, distribution and organization of hepatic extracellular matrix (ECM) is unique. Immunohistochemistry and electron microscopy analysis, reveal that some ECM proteins in the acini reside in the Space of Disse, including: collagen types I, III, IV, V and VI; fibronectin and laminin; and various proteoglycans and glycosaminoglycans. The main producers of ECM are hepatic stellate cells and hepatocytes and to a lesser extent SECs. (Fan, 2000; Maher, 1998; Portmann, 2000).

ECM in normal liver is considered important in the structural organization of liver parenchyma and in the regulation and modulation of hepatocyte function in the acinus. The ECM provides intercellular cohesiveness and communication, gene expression and function as well as induction of cell polarity and maintenance of

differentiated cell phenotype. These events appear to be regulated by specific cell-matrix and cell-cell interactions that are modulated by ECM geometry and binding to cell surface adhesion molecules called integrins (Berthiaume *et al.*, 1996; Fan, 2000). The first identified ligands of integrins were matrix proteins and the first identified matrix-specific receptor of the integrin family was fibronectin integrin $\alpha_5\beta_1$, which is particularly abundant in liver. Integrin receptors bind to ECM proteins and mediate attachment of ECM to intracellular cytoskeletal elements eliciting a signal transduction cascade influencing the physiological activity of the cell including, in addition to the above, cell motility and proliferation (Berman and Kozlova, 2000).

The microstructural organization and anatomy of liver described above, suggests a significant role for heterotypic cell-cell interactions, in concert with various growth factors including epidermal growth factor (EGF) and cytokines, in coordinated liver function. In both developing and adult liver, such cell-cell interactions between parenchymal and nonparenchymal neighbours appear to modulate cell growth, migration and differentiation (Bhatia *et al.*, 1999; Maher, 1998).

1.6 Hepatic biochemical function

As outlined above, the multiplicity of function of hepatic cells is related to their great morphological and ultrastructural diversity. The liver is well recognized as being central to the metabolism of lipids, proteins and carbohydrates as well as xenobiotic substances (Gumucio, 1992). The interplay between some of these metabolic pathways is outlined in Figure 1.5. In this section we concentrate on selected functional aspects of liver. In particular, albumin, ammonia, galactose, and cytochrome P450 metabolism are examples of important specific metabolic functions of liver.

Figure 1.5 Central metabolic pathways of proteins, carbohydrates and lipids in the liver (Modified from Moseley, 2000).

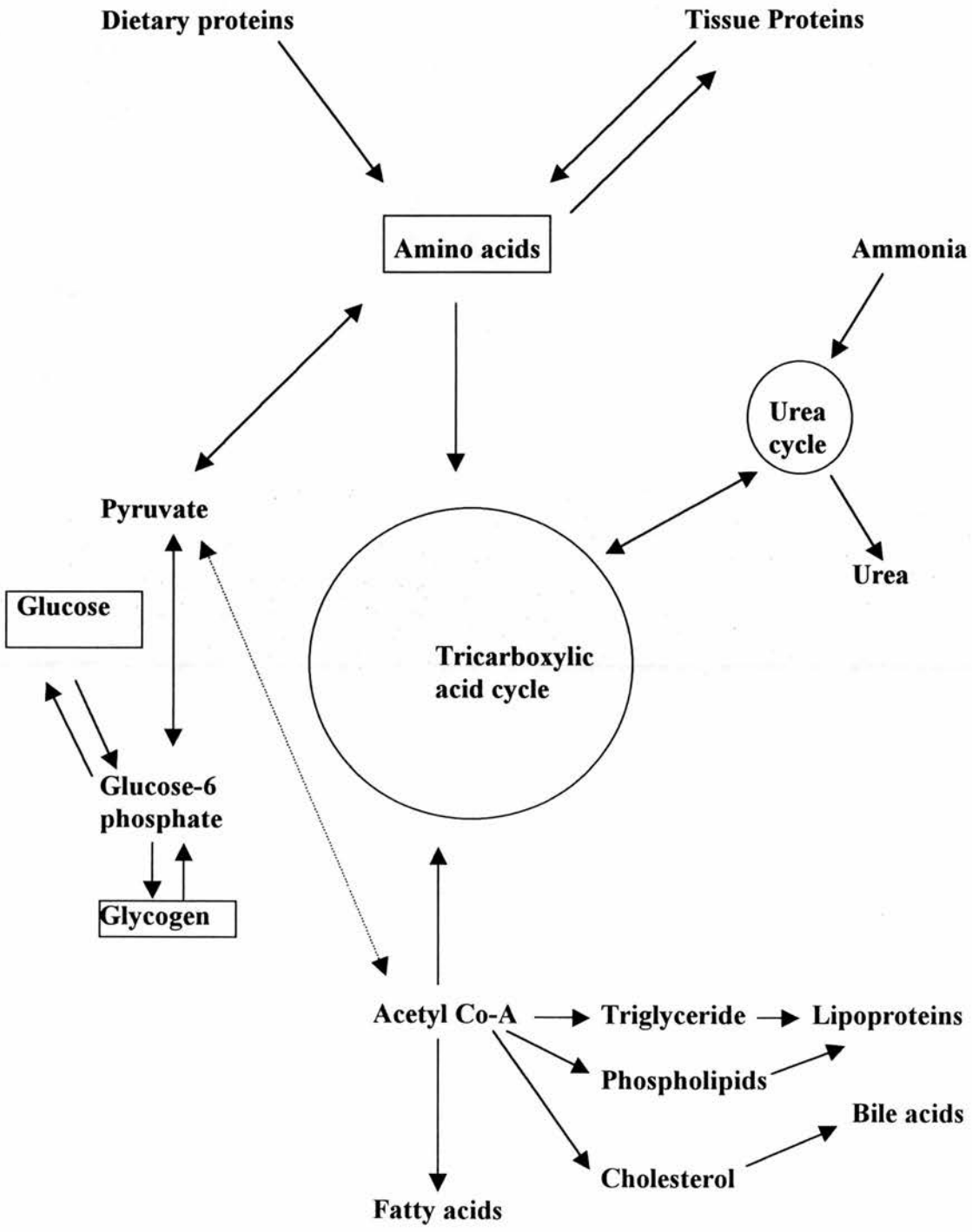

1.6.1 Albumin metabolism

Albumin production is unique to the adult liver and is the predominant product of hepatic protein synthesis with an average synthesis of 8-14 grams daily. The normal serum albumin levels are 35-50 g/L accounting for about 50 % of the serum proteins. Its main functions are to maintain the colloid oncotic pressure of blood, as a blood buffer and as a carrier vehicle for the transport of many substances including xenobiotics, bile acids, bilirubin, fatty acids and hormones (Percy-Robb and Finlayson, 1997; Finlayson, 1997; Doweiko and Nompleggi, 1991a; Doweiko and Nompleggi, 1991b).

Polyribosomes bound to the (granular) endoplasmic reticulum synthesise and secrete albumin into the sinusoidal blood via the Golgi complex (Rothschild *et al.*, 1973). Release of albumin from the hepatocyte appears to be sensitive to the concentration of both potassium and tryptophan. Albumin synthesis is regulated by changes in nutritional status, osmotic pressure and systemic inflammation. In addition, the hormonal milieu of the hepatocyte is important; corticosteroids, growth hormones and insulin alter albumin production and their effects may be additive (Doweiko and Nompleggi, 1991a; Doweiko and Nompleggi, 1991b).

Albumin is also important as a diagnostic and prognostic determinant as well as a useful therapeutic agent. In culture, hepatocytes readily produce albumin under a variety of conditions and is considered a marker of protein synthetic function and differentiation *in vitro*. Of course, the liver produces other important proteins such as vitamin K-dependent coagulation-factor pro-enzymes (factors II, VII, IX and X) involved in normal blood coagulation; α_1-antitrypsin; α_2-macroglobulin; ceruloplasmin; and iron transport proteins, to name but a few (Percy-Robb and Finlayson, 1997; Desmet, 1994; Finlayson, 1997; Moseley, 2000).

1.6.2 Ammonia metabolism

Excess nitrogen resulting from proteolysis and amino acid degradation is converted to non-toxic urea in hepatocytes by the Krebs-Henseleit ornithine cycle. The entry of ammonia into the systemic circulation must be prevented because at plasma levels >50 μM, it is highly toxic to the central nervous system (Meijer *et al.*, 1990). Carbamoyl phosphate synthetase catalyses the products of amino acid catabolism, NH_4^+ and HCO_3^-, to form carbamoyl phosphate (Figure 1.6). A further four enzymatic steps result in the formation of urea. The urea cycle occurs partially in the mitochondrion and partially in the cytosol with ornithine and citrulline being transported across the mitochondrial membrane by specific transport systems (Voet, 1995). Carbamoyl phosphate synthetase controls flux through the cycle and is the key regulatory enzyme in urea synthesis from ammonia. The concept of metabolic zonation of the liver acinus accepts that hepatic nitrogen metabolism including ureogenesis and all five enzymes of this cycle, confirmed by histochemical observations, occur in the periportal zone of the acinus. Urea thus formed is secreted into the blood and sequestered by the kidneys for excretion in the urine (Moseley, 2000). Glutamine synthetase, on the other hand, is located in the last few perivenous hepatocytes surrounding the terminal hepatic venule and converts ammonia to glutamine – essentially serving as a 'scavenger' for stray ammonium ions (Meijer *et al.*, 1990). Glutamine is subsequently released into the terminal hepatic venule and the systemic circulation. Ammonium chloride (1-10 mM) added to hepatocyte cultures is readily converted to urea and is a convenient biochemical method of determining the detoxifying capability of cells *in vitro* (Flendrig *et al.*, 1997a; Koebe and Schildberg, 1996; Naik *et al.*, 1996; te Velde *et al.*, 1995).

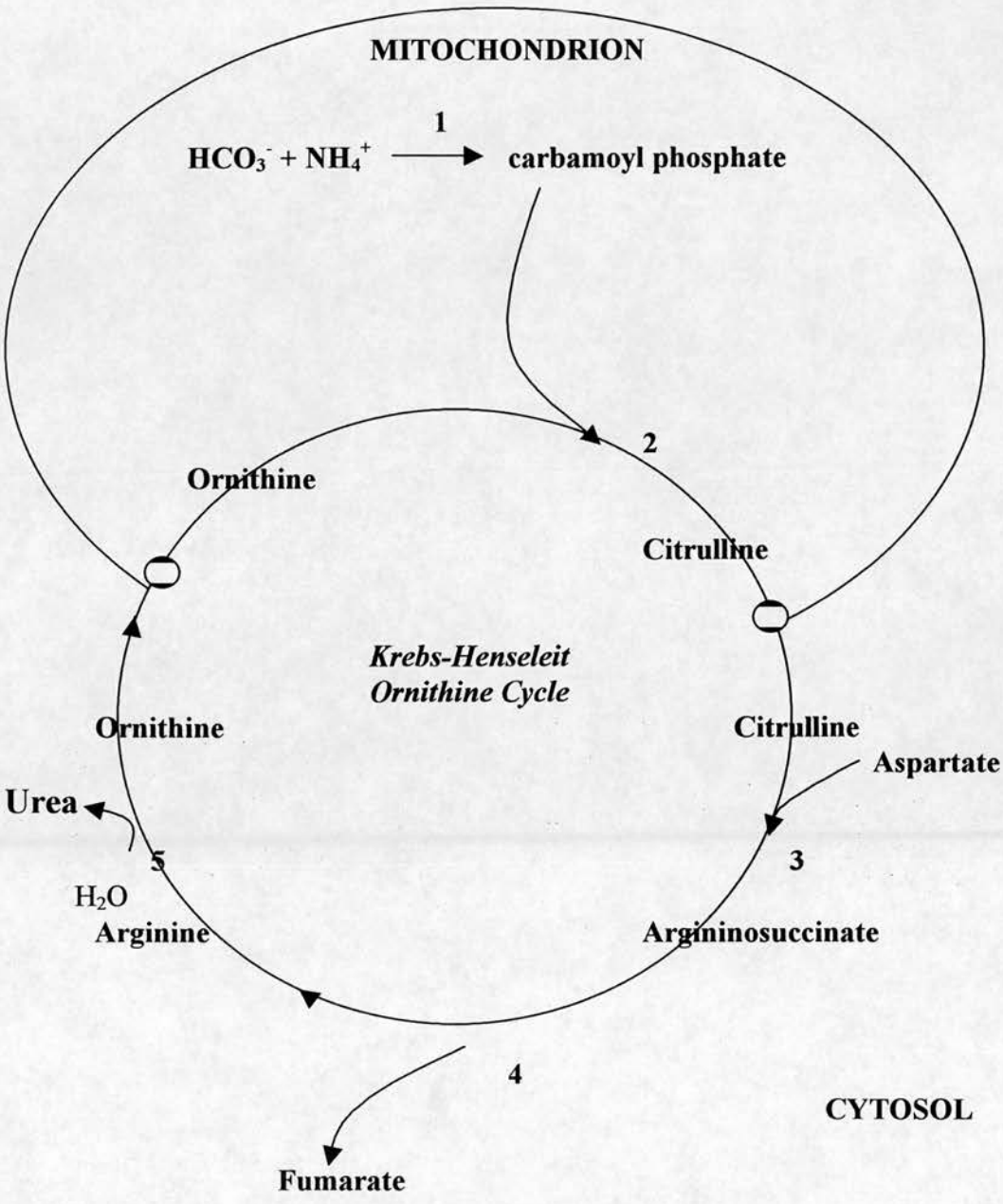

Figure 1.6 Highly simplified drawing of ammonia metabolism in periportal hepatocytes (Modified from Voet, 1995). Ammonia is removed from the circulation by periportal hepatocytes and converted to urea by the Krebs-Henseleit Ornithine Cycle (Urea Cycle), which occurs partially in the mitochondrion and partially in the cytosol with ornithine and citrulline being transported across the mitochondrial membrane by specific transport systems (shaded circles). The five enzymes of the urea cycle are 1) carbamoyl phosphate synthetase, 2) ornithine transcarbamoylase, 3) argininosuccinate synthetase, 4) argininosuccinase, and 5) arginase.

1.6.3 Galactose metabolism

Following a meal rich in carbohydrate, glucose is preferentially taken up by perivenous hepatocytes from the portal blood, where it undergoes glycolysis and / or may be converted to and stored as glycogen. In the postabsorptive or fasting state, periportal hepatocytes facilitate the supply of glucose that can be oxidized in peripheral tissues, to provide energy by glycogenolysis of stored glycogen and by gluconeogenesis from substrates such as lactate, pyruvate or alanine. However, glucose is not the only ingested carbohydrate that can be metabolised by the liver. Galactose occurs in milk in the form of lactose. Since galactose and glucose are epimers that differ in their configuration about Carbon-4, an epimerization reaction must occur before galactose can enter the glycolytic pathway. This metabolic conversion in human liver follows the Leloir pathway (Leloir, 1951) outlined in Figure 1.7.

Depending on the metabolic state of the liver, glucose-1-phosphate formed in the transferase reaction can be converted to glucose-6-phosphate and enter the glycolytic pathway for oxidation and provision of energy. Also, UDP-glucose arising in the epimerase reaction may be directed toward glycogenesis (Seifter and Englard, 1994).

Galactose loading is useful clinically as an index of functional liver cell mass (Winkler *et al.*, 1993), in fact, galactose elimination may be a useful prognostic indicator in patients with fulminant hepatic failure (Baker, 1992). Galactose elimination is also a convenient measure of hepatocyte carbohydrate metabolism in culture (Flendrig *et al.*, 1997a; Sajiki *et al.*, 2000).

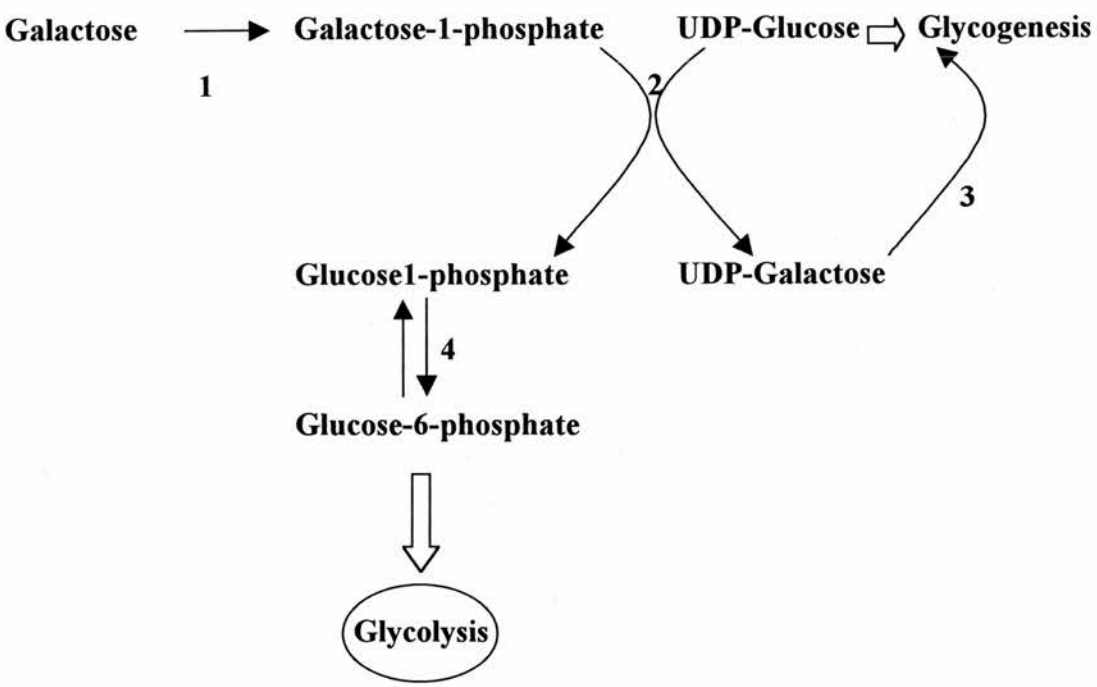

Figure 1.7 The metabolism of galactose – the Leloir pathway. Four enzymes participate in the conversion of galactose to the glycolytic intermediate glucose-6-phosphate: 1) galactokinase, 2) galactose-1-phosphate uridylyl transferase, 3) UDP-galactose-5-epimerase, and 4) phosphoglucomutase (Modified from Voet, 1995).

1.6.4 Cytochrome P450 metabolism

Cytochrome P450, present within smooth ER membranes, is the major component of the liver mixed function oxidase system and plays a central role in the detoxification and metabolism of many exogenous and endogenous compounds (Monshouwer *et al.*, 1998). Hepatic biotransformation is performed by these mixed function oxidases which involve phase I oxidation or reduction reactions of the parent compound. Conjugation by sulfation or glucuronidation by phase II reactions, render the compound highly water soluble for urinary elimination (Neuberger and Finlayson, 1997). Not all xenobiotics however undergo sequential phase I and II reactions (Moseley, 2000). Certain drugs such as paracetamol may produce toxic intermediates under certain conditions.

In cell culture systems, the functional activity of the many P450 isoenzymes is typically measured by their ability to detoxifiy compounds such as lidocaine, diazepam, 7-ethoxycoumarin or paracetamol; the metabolites are usually detected by high performance liquid chromatography (Flendrig *et al.*, 1997a; Jauregui *et al.*, 1997; Gregory *et al.*, 2000; Liu *et al.*, 1999). Alternatively, total cytochrome P450 content (tP450) of cultured hepatocytes can be measured in whole cell or microsomal samples as a indicator of retained liver function, interpreted as the biotransformation potential of the culture system (Mitaka, 1998; Nelson *et al.*, 2000; Watts *et al.*, 1995). Rather than measure the functional activity of a particular component of the cytochrome P450 system, whilst it remains unclear which isoenzyme is centrally involved in ALF or may be down-regulated in hepatocytes, we consider tP450 to be useful 'global' marker of the liver cytochrome P450 monooxygenase system.

1.7 Pathophysiology of paracetamol-induced acute liver failure

Paracetamol, in therapeutic doses, is detoxified by a combination of phase I and phase II reactions involving glucuronidation, sulfation and renal excretion. Following an overdose, these pathways become saturated and a greater proportion of paracetamol is metabolised through the cytochrome P450 system, leading to production of the toxic metabolite, N-acetyl parabenzoquinoneimine (NAPQI). Glutathione (GSH) detoxifies NAPQI and thus protects hepatic cellular constituents from its direct toxic effect. However, once GSH levels are depleted by large amounts of NAPQI, as occurs in significant overdose, centrilobular hepatic necrosis results which may lead to the dramatic clinical condition of acute liver failure (ALF) (Newsome *et al.*, 2000; Neuberger and Finlayson, 1997).

1.7.1 The need for bioartificial liver systems

Paracetamol-induced severe hepatocellular dysfunction and necrosis is the commonest cause of ALF in Britain and the United States. This syndrome is defined by the appearance of hepatic encephalopathy (HE) in patients with acute liver injury (Blei, 2000; Plevris *et al.*, 1998). The annual incidence in Scotland is 0.4 per 100 000 of the population with paracetamol overdose accounting for 73 % of all ALF cases [Dr A Bathgate, personal communication]. Mortality is high (70-90%) due to multi-organ failure and cerebral oedema, which often leads to brain stem herniation and death. In the 8 years since the opening of the Scottish Liver Transplant Unit (SLTU), over 300 cases of FHF have been referred for management. Approximately 50% required ITU support, of whom, 20% were transplanted. Currently, orthotopic liver transplantation (OLT) is the most effective therapeutic option, but is limited by a shortage of donor organs. A significant proportion of patients die on the emergency list as they rapidly deteriorate before a donor liver becomes available. For these patients temporary bioartificial liver (BAL) support may be beneficial by prolonging survival until a liver graft becomes available or, since ALF is potentially reversible, by promoting the regenerative capacity of the diseased, native liver and full recovery. Development of a

large animal model of paracetamol-induced ALF, ongoing in our laboratory, will allow characterisation of underlying pathophysiological mechanisms and evaluation of bioartificial liver support systems (Newsome *et al.*, 2000).

1.7.2 Pathogenesis of hepatic encephalopathy in ALF

HE and renal failure are major complications of ALF. Although the pathogenesis of the HE component is unknown it is generally accepted that accumulation of a variety of toxic substances from the portal system as well as from the necrotic liver itself play a significant role. Endotoxins, ammonia, aromatic amino acids, fatty acids, mercaptans, bile acids, cytokines, transforming growth factor-1 and gamma-amino butyric acid (GABA) have all been implicated in such deleterious systemic and local effects. (Maddrey, 2000; Plevris *et al.*, 1998; Jauregui and Gann, 1991a; Cao *et al.*, 1998) Even though none of these substances have been identified as being pathognomonic for ALF, both hyperammonemia and increased GABA levels, are considered to be intimately connected with the development of HE. In ALF plasma ammonia concentrations are frequently elevated (with depletion of brain glutamate) and can rapidly reach toxic levels (Record, 1991; Clemmesen *et al.*, 1999). Ammonia is neurotoxic to brain astrocytes, the site of brain ammonium detoxification, and contributes to brain oedema whereas GABA, a major inhibitory neurotransitter, may induce neural inhibition through endogenous benzodiazepine accumulation and $GABA_A$ receptor activation (Ampola, 1994; Jauregui and Gann, 1991b; Jones and Schafer, 1986; Albrecht and Jones, 1999) In this context, failure of the detoxification capacity of the liver is accepted as playing an important role in this disorder. This has directed study of PPH function to ammonia detoxification and phase I drug metabolising enzymes and phase II conjugating enzymes.

1.8 Liver support systems

Poor prognosis heralded by hepatic coma has led investigators to develop liver support systems that might control the accumulation of potentially toxic substances ordinarily metabolised or excreted by the liver. Strategies for liver support have utilized both non-biological and biological systems.

1.8.1 Historical perspectives

Many of the aforementioned toxins are small (<5 kDa) and middle (5-15 kDa) molecular weight compounds which, it was hypothesized, could essentially be physically removed from the circulation by detoxification, usually involving sorption therapy (Cao *et al.*, 1998). Techniques employed since the 1950's have included: blood exchange, plasma exchange (plasmapheresis), haemodialysis, haemofiltration, total body blood washout, charcoal or resin haemoperfusion, and haemadsorption using non-biological adsorbents (Demetriou, 1998). Despite anecdotal reports of beneficial clinical effects, none of these systems has been consistently proven in controlled trials to treat ALF. Problematic in the use of sorption therapy is that, since many toxins are bound to plasma proteins such as albumin, it is difficult to remove these substances from a patient's circulation without causing other problems. For instance, haemadsporption uses sorbents which can efficiently remove protein-bound toxins directly from the circulation; unfortunately, sorbents are equally efficient at removing important components such as platelets, leukocytes, clotting factors, and other humoral regulatory factors. Some of these techniques may however be useful as adjuncts of more complex detoxification devices, such as hepatocyte-based systems.

In the late 1960's and early 1970's, whole blood, *ex vivo* liver perfusions were used to treat patients with liver failure using a variety of species including baboon , porcine, dog, calf and human cadaveric livers (Abouna *et al.*, 1970; Eiseman *et al.*, 1965). In most cases transient improvements in HE were noted although many problems related to the use of xenografts were encountered including rapid rejection, bleeding, haemolysis and cessation of function (Demetriou, 1998). For these reasons,

notwithstanding the cumbersome and costly nature of the procedure, this technique has been largely precluded as a treatment therapy for ALF. Recently, however (Horslen *et al.*, 2000) successfully 'bridged' 9 of 14 patients with severe ALF by extracorporeal liver perfusion using human and pig livers. Intracranial pressure and cerebral perfusion pressure were stabilized whereas both ammonia and bilirubin levels were reduced.

1.8.2 Bioartificial extracorporeal liver support systems

Primarily because of the limited success of non-biological liver support systems and *ex vivo* liver perfusions, the continuing disparity between the supply and demand of cadaveric human livers for transplantation, and the high levels of morbidity and mortality associated with ALF – despite advances in modern clinical management - has led to development of hepatocyte-based bioartificial liver (BAL) support devices.

The development of a BAL device represents a formidable challenge. Unlike the heart, lung or kidney, which essentially perform one primary task, the liver performs thousands of functions. As stated above, the highly complex structure-function relationships of the liver allow it to perform its synthetic and degradative functions which impact upon almost every aspect of body metabolism and physiological regulatory processes. Moreover, the aetiology of ALF is still not well defined and therefore it is not clear what is essential to keep ALF patients alive in the BAL setting. Despite these obvious shortcomings, the consensus view is that a clinically successful BAL device should maintain a range of metabolic, excretory and synthetic functions to support a patient with ALF. Using exogenous hepatocytes in this context, may provide the opportunity to achieve more than just removal of toxins, specifically, by optimising metabolic and excretory hepatic support functions (Cao *et al.*, 1998; Demetriou, 1998; Hoofnagle *et al.*, 1995; Maddrey, 2000).

The key features of a BAL system are: a) the biological component; b) a bioreactor which can accommodate these cells and c) an efficient circuit between the patient and the BAL in order to provide optimal exchange of nutrients, oxygen and permit detoxification of the patient's plasma.

1.8.2.1 Biological component

Mammalian hepatocytes, in particular porcine-derived, are the most popular cellular component of BAL devices. In theory, human hepatocytes are the cells of choice, however the problem of relative scarcity is compounded by competing demands of whole organ liver transplantation and hepatocyte transplantation. As with whole organ transplantation, immune rejection is also a problem although hyper-acute rejection, which often applies in xeno-transplantation, is generally not relevant. Finally, sourcing of human hepatocytes from resected liver tissue from partial hepatectomy/hepatocellular carcinoma operations has raised concern about transmission of malignancy or infection into the patient. As a consequence of these problems human hepatocytes have not been widely used in BAL devices and attention has turned to immortalised human hepatocyte lines or xenogeneic hepatocytes (Tsiaoussis *et al.*, 2001).

Immortalised human hepatocyte cell lines can provide an unlimited resource for BAL systems (Ellis *et al.*, 1996; Sussman *et al.*, 1992), but concerns exist about their relatively poor metabolic function (Stange *et al.*, 1995). Enosawa *et al.*, (1996) demonstrated that primary rat hepatocytes outperformed 31 types of hepatocyte cell lines, including HepG2 and HuH 6 human hepatoblastoma derived lines, in terms of ammonia removal and 7-ethoxycoumarin deethylation activities. Nyberg *et al.*, (1994) showed that ureagenesis and biotransformation performance of primary rat hepatocytes, seeded into their gel-entrapment BAL device, were superior to HepG2 cells in this environment. Transmission of immortalised cells or tumourigenic substances into the patients' circulation is also a potential risk factor (Zeidl-Engelhart and Rabes, 1992). This concern is particularly relevant in that patients with liver

failure are immuno-compromised for long periods of their lifetime, either acutely or post-transplantation thus decreasing their ability to remove such malignant cells from the circulation. This does however still remain a theoretical concern, as there is no evidence of transmission so far (Paradis *et al.*, 1999). However, transmigration of HepG2 cells into the extracapillary compartment (analogous to the patient's compartment during clinical application) was observed in a prototype BAL device (Nyberg *et al.*, 1994; Nyberg *et al.*, 1994). The extracorporeal liver assist device (ELAD) developed by Sussman and coworkers (Ellis *et al.*, 1996; Sussman *et al.*, 1992), utilises the C3A cell line, a clonal derivative of the human hepatoblastoma HepG2 cell line which exhibit strong contact inhibition of growth. C3A cells are reported to have a more differentiated hepatic phenotype than HepG2 and other cell lines (Sussman *et al.*, 1992). Metabolic studies of the C3A line have shown levels of synthetic function such as albumin and alpha-fetoprotein production and also nitrogen-metabolizing activity, similar to that of perfused rat livers (Ellis *et al.*, 1997). However, when compared with primary porcine hepatocytes, the C3A cell line has lower levels of cytochrome P450IA1 activity, ammonia removal and amino acid metabolism (Wang *et al.*, 1998).

The ready availability, high viability and yield of primary porcine hepatocytes (PPHs) -which support the requirements of a BAL device - coupled with anatomical, physiological, and a range of metabolic function similar to that of human hepatocytes, confer PPHs with significant advantages over other xenogeneic mammalian cell sources. Large cell numbers are required for BAL systems since it is estimated from recent animal studies that at least 20 % of host liver mass is required for effective support, corresponding to approximately 2x 10^{10} hepatocytes. High yield isolation of PPHs usually involves anterograde collagenase perfusion of the portal and / or hepatic artery (Sheil *et al.*, 1998; Sharda *et al.*, 1996; Rozga *et al.*, 1993b; Naruse *et al.*, 1996b; Naik *et al.*, 1996; Morsiani *et al.*, 1998; Gerlach *et al.*, 1996a; Flendrig *et al.*, 1997a), such techniques are cumbersome, time-consuming, expensive, and require expert licensed personnel with appropriate surgical expertise and facilities. To circumvent this, we developed a retrograde *ex vivo* whole liver collagenase perfusion

technique that gives the required yield and viability for large-scale BAL devices and can be performed in any standard cell biology research facility (Nelson *et al.*, 2000). PPHs exhibit a wide range of differentiated functions under a variety of *in vitro* culture conditions including performance testing in protoype and scaled-up BAL devices. Functional activity has been evaluated in terms of urea and albumin synthesis; numerous biotransformatory functions; carbohydrate and bile metabolism; as well as proliferative activity (De Bartolo *et al.*, 2000; Demetriou, 1998; Desille *et al.*, 1999; Flendrig *et al.*, 1997a; Gregory *et al.*, 2000; Jauregui *et al.*, 1997; Nelson *et al.*, 2000; Rozga *et al.*, 1993b; Waring *et al.*, 1995; Bader *et al.*, 2000) These attributes of PPHs support their candidacy as the premier cell source for BAL systems.

1.8.2.2 The bioreactor

The majority of current bioreactor designs utilize hollow-fibre technology based upon original proposals by Wolf and Munkelt, (1975). Synthetic semi-permeable (hollow-fibre capillary) membranes act both as a cell support and as a channel for the transport of perfusates in the bioreactor. The design is based on the counter-current blood flow principle used in conventional renal haemodialysis systems where the patient's blood is perfused through the hollow-fibre lumen with functional hepatocytes on the extra-luminal side and enclosed in a plastic shell housing. Bi-directional solute transport and oxygen delivery is achieved by fluid convection (Starling flow) driven across the membrane by a trans-fibre pressure drop, which is proportional to the axial flow rate (Demetriou, 1998; Cao *et al.*, 1998).

The complexity and diversity of liver function are reflected in the range of innovative bioreactor designs under development. Novel bioreactor models include configurations based upon: various hollow-fibre systems; microcarrier systems; flat membrane bioreactors (see Figure 1.8); spirally-wound ('Swiss-roll') nonwoven polyester sheets; spouted-bed and packed-bed bioreactors; and intra-luminal gel-entrapment devices (Nyberg *et al.*, 1993; Gerlach *et al.*, 1994a; Flendrig *et al.*, 1997a; Demetriou, 1998; De Bartolo *et al.*, 2000). The two major BAL systems under

evaluation in clinical trials are briefly described as well as some of the prototype BAL configurations currently under assessment – all of which incorporate PPHs as the biological component.

Demetriou & Rozga (Chen *et al.*, 1996; Chen *et al.*, 1997; Kong *et al.*, 1996) developed a novel, hybrid extracorporeal liver support device using plasma separation and high-performance sequential plasma perfusion through a column loaded with activated cellulose-coated charcoal particles and through a hollow-fibre bioreactor with viable, collagen matrix/microcarrier-anchored, cryopreserved PPHs. This device has been used to treat some 38 patients with ALF of varying aetiologies; all but one survived and were successfully transplanted; with one patient recovering fully without transplantation. Significant decreases in intracranial pressure, plasma ammonia levels and bilirubin were described with an increased cerebral perfusion pressure, neurological improvement and reduction in cerebral oedema. No adverse reactions to PPHs after intermittent (6 hours) multiple treatments were observed. However there was no significant reduction in prothrombin time.

The ELAD used by Sussman's group (Ellis *et al.*, 1996) utilized high density C3A cell cultures (described above), attached directly to the extraluminal domain of uncoated hollow-fibre membranes. No charcoal sorbent column was used. Continuous (≈72 hours) perfusion of heparinized whole blood did not result in significant improvement in survival of 24 patients with ALF compared with controls. However, galactose elimination was improved and there was a 4-fold increase in human growth hormone after 6 hours of haemoperfusion. Whether the ELAD can effectively remove inhibitors of regeneration remains unclear.

Gerlach and coworkers (Gerlach *et al.*, 1995; Gerlach *et al.*, 1994a) developed a bioreactor system whereby separate bundles of hollow-fibres, were arranged in a 3-dimensional network enclosed in a plastic casing. Four capillary systems were apposed in different directions in the bioreator space for: plasma inflow; oxygenation as well as CO_2 removal; and coculture with SECs. This system recreated *in vivo*-like

liver microarchitecture to some extent, by attachment of PPH aggregates to the extra-luminal compartment capillaries coated with Matrigel™. Albumin synthesis, galactose elimination and P450 function was maintained for up to seven weeks. This system has not been tested in clinical trials.

Another innovative system developed by (Flendrig *et al.*, 1997a), comprises spirally-wound nonwoven polyester sheets in a 'Swiss-roll' formation which allows a high density 3-dimensional framework for PPH immobilization and aggregation. Functional activity (galactose elimination; urea and albumin synthesis; lidocaine and amino acid metabolism) was well maintained over the four-day test period. Significantly, no ECM material was required and the bioreactor was autoclavable; resulting in a safer, cheaper and more convenient device. Moreover, this device prolonged survival and plasma ammonia and total bilirubin levels, in pigs with complete liver ischaemia, using 14 x 10^9 PPHs, with no adverse effects (Flendrig *et al.*, 1999).

Finally, Bader's group in Germany (De Bartolo *et al.*, 2000; Bader *et al.*, 1995a; Bader *et al.*, 1995b) attempted to reconstruct hepatic-specific tissue microarchitecture in their modular flat membrane bioreactor (Figure 1.8). Liver cells are organized as 'acinar-like' plates within a collagen gel sandwich, on either side of the sandwich are gas permeable hollow fibre membranes, supplying culture medium (or plasma, in clinical test mode) or CO_2 / O_2. After 18 days in culture cells retained polarity and differentiated function including albumin and urea synthesis as well as biotransformation activity. Clinical trials of this device are eagerly awaited.

Unlike Demetriou's BAL device described above which uses an external oxygenator, this device and that of both Gerlach and Flendrig, provide integral oxygenation – considered an essential parameter for modern BAL systems encompassing 3D cellular configurations (De Bartolo *et al.*, 2000; Balis *et al.*, 1999).

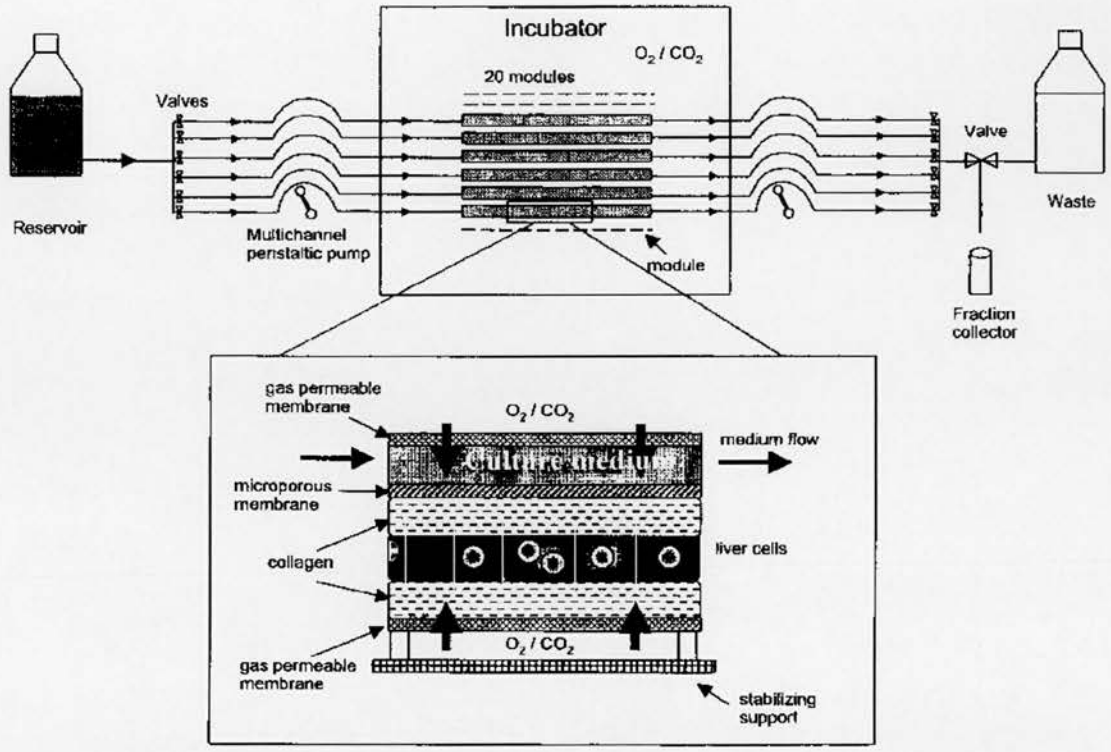

Figure 1.8 Schematic illustration of a flat membrane bioreactor (Modified from De Bartolo *et al.*, 2000)

The bioreactor is a modular stackable plate arrangement that can accommodate 10^{10} cells (50 plates in parallel). Cells and serum-free medium are oxygenated by diffusion of humidified air (CO_2 / O_2) across a 35μm non-porous gas permeable membrane and perfused via a multi-channel persistaltic pump, at a flow rate of 9 ml/hour. Following seeding and attachment of cells onto a single layer of Type I collagen, a second layer of matrix is placed on top, creating a 'collagen gel sandwich' configuration.

A novel prototype bioreactor has been developed the University of Strathclyde (US) Bioengineering Unit (SUBU) and Dept of Chemical and Process Engineering, our collaborators in the development of a PPH-based BAL device (Smith *et al.*, 1996; Smith *et al.*, 1997a; Smith *et al.*, 1997b). The SUBU bioreactor (Figure 1.9) has a modular, stacked-plate configuration incorporating hollow-fibres for integral oxygenation which allows improved control of cell surface pO_2 and optimal mass transfer capability. Hepatocytes are arranged as both small aggregates and monolayers attached to the extracapillary space allowing optimal exchange of nutrients, oxygen and removal of toxins. The scaled-up bioreactor will utilise at least 10^{10} freshly isolated hepatocytes representing >10% of total functional liver mass, which is the required theoretical mass to treat a 30kg pig model of paracetamol-induced ALF, being developed in our laboratory (Newsome *et al.*, 2000).

This represents a configuration of twenty (30cm x 60cm) stacked-plates with a cell density of 0.18×10^6 cm^{-2}. Further scale-up to accommodate $>10^{10}$ cells is underway. Functional assessment of the bioreactor, in terms of urea synthesis, galactose elimination and albumin production show promising results.

Figure 1.9 Prototype bioreactor developed at the University of Strathclyde Bioengineering Unit (Dr J Gaylor, personal communication)

Panel A shows a schematic illustration of the general bioreactor geometry. **Panel B** In pre-clinical mode, each module is comprised of 2 plates (P1, P2), which are sealed together by a gaskit (g). Cells attach directly to the plastic surface (P1) as monolayers and small aggregates. Medium (or plasma in clinical mode) is perfused through the inlet port (in) and flows over the attached cells via a channel reservoir (ch) and exits at the outlet port (out). Hollow-fibres for integral oxygenation are incorporated into plate P2, which allow improved control of cell surface pO_2 and optimal mass transfer capability. A configuration of sixty (30cm x 60cm) stacked-plates (0.5 cm thick) with a cell density of 0.18×10^6 cm^{-2} would allow attachment of approximately 10^{10} cells. **Panel C** The plate stacks are clamped and held in place by the bioreactor housing.

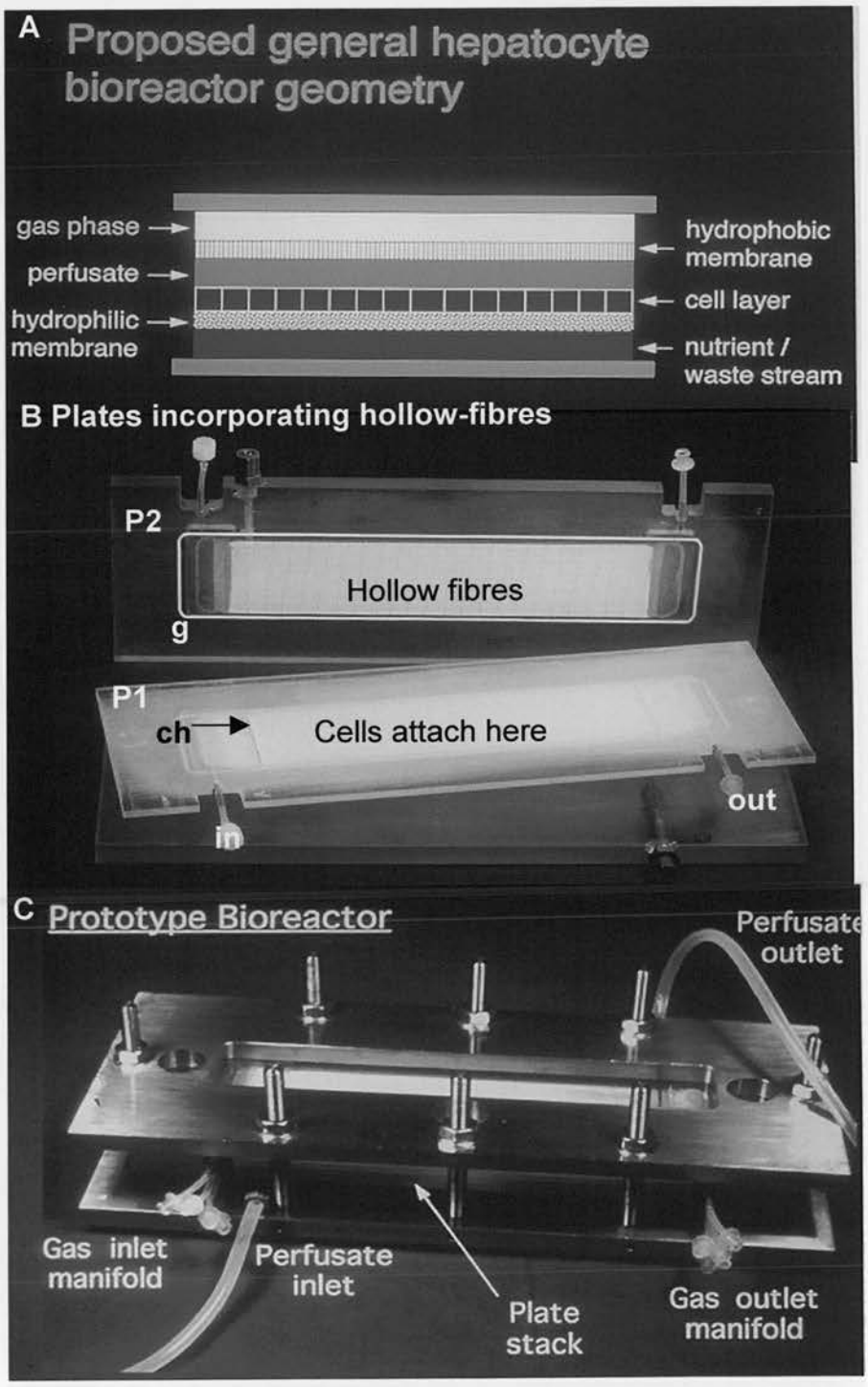
A Proposed general hepatocyte bioreactor geometry
gas phase
perfusate
hydrophilic membrane
hydrophobic membrane
cell layer
nutrient / waste stream
B Plates incorporating hollow-fibres
P2
Hollow fibres
g
P1
ch
Cells attach here
out
in
C Prototype Bioreactor
Perfusate outlet
Gas inlet manifold
Perfusate inlet
Plate stack
Gas outlet manifold

1.9 Background and Aims of Research Project

Modulation of function and morphology of primary hepatocyte cultures

The need for species-specific characterization of cellular function for optimal BAL device implementations is crucial. Numerous hormonal, medium and substrate conditions have been described in the literature for restoring and maintaining well differentiated functional and morphological properties of cultured hepatocytes using the rat as model (LeCluyse *et al.*, 1996). In the field of BAL development, such data gleaned from studies using rat hepatocytes has inevitably been translated or extrapolated to porcine hepatocytes. However, not only do distinct species differences exist in terms of attachment efficiency, functional, morphological and proliferative properties, but very few comprehensive comparisons of culture conditions have been reported with physiologically relevant endpoints pertaining to the use of PPHs for BAL support therapy.

As described above, many types of bioreactors with variable cell culture configurations, medium composition / supplements, and ECM are used. Similarly, the endpoints used, to analyse function, for example, are equally variable due in part to the lack of understanding of the precise requirements for an effective BAL device. As proposed by Skett and Bayliss, (1996), standardization of both isolation and culture conditions will allow for more reproducible and relevant evaluation of *in vitro* data. This will allow direct comparisons between laboratories of the performance efficacy of different BAL systems.

The major interdependent factors which enhance the liver-specific function and phenotype in primary hepatocyte cultures are recognized as: a) the medium composition (soluble components), b) the ECM, and c) cell-cell contacts (Gerlach *et al.*, 1995; Bhatia *et al.*, 1999; Berthiaume *et al.*, 1996; Ben-Ze'ev *et al.*, 1988; LeCluyse *et al.*, 1996). This implies that both cell shape and the microenvironment may have an important influence on liver cell function both in culture and *in vivo*.

Evidence that cell shape, cell-cell and cell-matrix interactions were important in preservation of liver-specific phenotype and maintenance of function came from studies of densely packed confluent monolayers of hepatocytes cultured on collagen gels or Matrigel™ and hepatocytes cultured as spheroids (Berthiaume *et al.*, 1996; Bhatia *et al.*, 1999; Koide *et al.*, 1989; Koide *et al.*, 1990; Landry *et al.*, 1985; Sakai *et al.*, 1996; Yuasa *et al.*, 1993). Furthermore, gross morphological observations of *in vitro* hepatocyte cultures and ultrastructural analysis, give important clues as to cell 'fitness' and differentiative state, respectively.

In BAL devices, the significance of cell aggregation in improving *in vitro* performance of PPHs has been emphasized (Bader *et al.*, 1995b; De Bartolo *et al.*, 2000; Demetriou, 1998; Flendrig *et al.*, 1997a; Gerlach *et al.*, 1994a; Jauregui *et al.*, 1997). To achieve this, all of the aforementioned BAL devices, except for Flendrig *et al* (1997a), utilize some form of ECM substrata; while all of the above systems use medium formulations such as William's medium E, Medium 199 or RPMI 1640 medium, supplemented with foetal bovine serum. The latter has been routinely employed with medium formulations culturing rat hepatocytes as prerequisite for improving attachment, survival and morphology. However, detrimental effects of serum on hepatocyte differentiation have been observed including cytostatic and cytotoxic effects, leading to cellular dedifferentitation, which may preclude its use in pre-operational, clinical BAL systems (Berry *et al.*, 1997; LeCluyse *et al.*, 1996).

Moreover, studies from our laboratory, and others, have shown that PPHs do not require serum supplementation or ECM substrates for high viability culture and function (Gregory *et al.*, 2000; Nelson *et al.*, 2000; te Velde *et al.*, 1995). The reasons for this are unknown. Perhaps the small clusters (5-20 cells) of PPHs, typical of isolates following collagenase digestion, retain sufficient endogenous ECM components 'trapped' within the aggregates. Alternatively, this three dimensional organization may retain expression of cell adhesion molecules, including integrins, for more efficient attachment and establishment in culture, compared with other mammalian hepatocytes.

The commercially available (basic) media formulations mentioned above contain a complex mixture of amino acids, vitamins, trace elements and cofactors. Despite the large number of media used for rat hepatocyte culture (LeCluyse *et al.*, 1996), very few studies have compared the effects of medium formulation on the maintenance (or potential modulatory influence) on liver-specific function and morphology for *in vitro* rat models (Jauregui *et al.*, 1986; LeCluyse *et al.*, 1999; Michalopoulos *et al.*, 1999; Turner and Pitot, 1989; Williams *et al.*, 1977). The influence of medium formulation may be significant. For instance, LeCluyse *et al.* (1999) showed that medium formulation and culture dish material had significantly greater effects on the induction of cytochrome P4502B by phenobarbital than either collagen or Matrigel™ sandwich cultures of rat hepatocytes. As mentioned, distinct species differences are known to exist. For example, cell proliferation studies have shown porcine hepatocytes to have a much greater proliferative potential than rat hepatocytes cultured on collagen in hormonally-defined medium (Joly *et al.*, 1997; Wegner *et al.*, 1992). In addition, pig hepatocytes reproduced cytochrome P450-dependent oxidative metabolism of human hepatocytes to a greater extent than either rat, rabbit or dog primary cells, or the HepG2 hepatoma cell line (Donato *et al.*, 1999). Finally, oxygen uptake rates, an important parameter in BAL design, were significantly higher for PPHs than rat hepatocyte monolayer cultures (Balis *et al.*, 1999). These studies highlight the need for species-specific characterisation of hepatic cellular function to optimise performance for BAL systems.

However, there is no information available on the influence of medium composition on liver-specific function and morphology using porcine hepatocytes. It seems reasonable to assume that serum-free medium, containing soluble supplemental factors - including the use of hormones such as insulin and dexamethasone, growth hormones as well as growth factors (eg EGF or HGF) - may improve cell survival, morphology and function of PPHs *in vitro*. However, very little is known about whether PPHs can be maintained under such chemically-defined culture conditions on simple uncoated surfaces, such as tissue culture plastic or hollow-fibre membranes, without either serum or ECM substrata. Importantly, BAL configurations which

utilize Engelbreth Holm Sarcoma Natrix (EHS) or Matrigel as substrata, may risk leaking potentially tumourigenic or murine proteins, respectively, into the patients circulation, raising questions of potential immunogenicity and bioreactor safety. Unlike PPHs, rat and human hepatocytes, have an absolute requirement for exogenous matrix proteins for cell attachment (Christiansen *et al.*, 1988; Odenthal *et al.*, 1992). We propose that identifying *in vitro* culture conditions, which could maximize differentiated hepatic function of PPHs, under serum-free fully defined conditions on simple, unmodified surfaces, such as tissue culture plastic, may improve efficacy, safety, and reduce costs of BAL devices. Furthermore, improving the hepatic culture environment would contribute to being able to provide the required cell mass for more ergonomic BAL designs.

This thesis will address some of these issues by attempting to delineate the optimal test medium for retention of liver-specific function and phenotype, and assess whether different medium formulations modulate these parameters *in vitro*. Furthermore, we introduce the concept of a 'hepatocyte biological activity index' (HBAI), to simplify analysis of the multiple (functional) comparisons requisite of such a study. The HBAI normalises each hepatic functional parameter with respect to an equally weighted scoring system. Additionally, the impact of media formulation on culture morphology and phenotype is taken into account.

Finally, the feasibility of using a novel simulated microgravity (rotary cell culture system) modality is investigated, in order to improve the hepatic culture environment by growing PPHs as 3-dimensional 'hepatospheroids' which may more closely resemble *in vivo*-like tissue architecture and enhance cell-cell cell matrix interactions. Recently, human liver cells grown in microgravity were shown to exhibit liver tissue-specific morphological and functional characteristics over a 60-day culture period (Khaoustov *et al.*, 1999; Yoffe *et al.*, 1999). Characterisation of the optimal culture conditions for PPHs will help further clarify their therapeutic potential for use as the biological component of BAL systems.

Inasmuch as media supplementation, biomatrices and cell-cell contacts have been shown to maintain, enhance or prolong hepatocyte differentiated performance *in vitro*, alternative strategies are available which may elicit these effects, including: a) Preferential cell isolation b) Coculture, c) Chemical modulators, and d) The use of spheroid cultures. Future developments that may be implemented to enhance the hepatic culture environment are discussed within the framework of relevant experimental chapters.

Aims of research project

- To develop a rapid, low-cost, high viability, high yield and reproducible *ex vivo* method for obtaining functional primary hepatocytes from whole livers of weanling piglets for use in BAL systems.

- To assess the modulatory effects on hepatocyte morphology of different serum-free chemically-defined media formulations on cultured porcine hepatocytes in terms of:
    1) Gross cellular morphology under phase contrast light microscopy
    2) Cell ultrastructure under transmission electron microscopy
    3) Biochemical parameters related to cellular attachment and viability

- To assess differential effects of separate, serum-free chemically-defined medium formulations on differentiated hepatic support functions of cultured porcine hepatocytes for future BAL devices.

- Using biochemical, histological, ultrastructural and immunocytochemistry studies, we sought to identify whether spheroid aggregate formation in the unique environment of simulated microgravity, maintained stable, liver-specific metabolic capacity and characteristic hepatic morphology for an extended period. The expression of integrin $\alpha 5$, as a marker of hepatic differentiation and structural integrity, was investigated and the findings compared with conventional static cultures.

Chapter 2

An Improved *Ex Vivo* Method Of Primary Porcine Hepatocyte Isolation For Use In Bioartificial Liver Systems

2.1 Introduction

Primary porcine hepatocytes (PPHs) are used for *in vitro* studies of hepatocyte function including studies on hepatotoxicology, transfection / gene transfer, hepatocyte transplantation and bioartificial liver (BAL) systems for treatment of acute liver failure (ALF) (Demetriou, 1998; Guillouzo *et al.*, 1997).

Immortilized human hepatocyte cell lines' such as Hep G2, can theoretically provide an unlimited resource for use in BAL systems (Sussman *et al.*, 1992). However, problems associated with possible transfer of tumourigenic proteins to the patient via the BAL, and the rather limited functional range of these dedifferentiated cells, have severely limited usage of cell lines in BAL devices (Jauregui *et al.*, 1997; Jauregui and Gann, 1991; Nyberg *et al.*, 1994; Plevris *et al.*, 1998). Hepatocyte viability from standard rat liver perfusions is similar to that obtained from pigs (Nyberg *et al.*, 1993b), but yields of 10^8 hepatocytes are not sufficient to be incorporated into a scaled-up clinical device for use in humans. Since primary human hepatocytes are not readily available (Plevris *et al.*, 1998) and large yields of functional hepatocytes are required for a clinically effective BAL, PPHs are the cells of choice for BAL devices. They are differentiated hepatocytes with similar biochemical and metabolic functions to human hepatocytes and can be obtained with good viability and yield (Clement *et al.*, 1998; Gerlach *et al.*, 1994c; Gerlach *et al.*, 1996a; Jauregui *et al.*, 1997; Jauregui and Gann, 1991). A concern in the use of PPHs for clinical BAL application, however, remains the possible transfer of pig endogenous retroviruses to humans (Martin *et al.*, 1998).

Conventional *in vivo* isolation of PPHs involves anterograde perfusion of the portal vein, sometimes in combination with perfusion of the hepatic artery. However, although producing excellent cell viability and yield, this technique requires large perfusion volumes with the associated high collagenase costs with increased perfusion times (Flendrig *et al.*, 1997a; Fremond *et al.*, 1996; Gerlach *et al.*, 1994c; Hu *et al.*, 1997; Sheil *et al.*, 1998; Sielaff *et al.*, 1995b). Moreover, *in vivo* techniques involve anaesthetic maintenance regimes and extensive surgical facilities requiring expert licensed personnel. These requirements may preclude many laboratories from obtaining and utilizing the considerable research potential of porcine hepatocytes.

Ex vivo isolation of PPHs from livers of abattoir origin can attain acceptable viabilities (Donini *et al.*, 1997; Koebe and Schildberg, 1996) but with several disadvantages including insufficient yield for BAL devices, availability and locality constraints of the abattoir source, relatively high collagenase costs and potential infection problems with abattoir-derived organisms.

Since an effective high yield and high viability method of obtaining functionally active PPHs is prerequisite for efficient BAL devices, different perfusion methods and conditions were tested to establish a reproducible isolation technique suitable for subsequent morphological and functional evaluation under different culture conditions.

2.2 Aim

The aim of this study was to develop a rapid, low-cost, high viability, high yield and reproducible *ex vivo* method for obtaining functional primary hepatocytes from whole livers of weanling piglets for use in BAL systems.

2.3 Materials and methods

2.3.1 Animals

2.3.1.1 Method I: Liver wedge isolations

Livers (1.5 kg) were retrieved from 60 kg pigs obtained from Forth Meat Supplies Abattoir (Galashiels, Scotland, UK). Prior to liver retrieval, animals were killed instantly with a captive bolt gun to the cranium before immersion in a 65°C water bath. The whole liver was then removed from the carcass before the liver wedge was dissected out for subsequent perfusion.

2.3.1.2 Methods II and III: Whole liver isolations

The animals were treated in accordance with UK Home Office Guidelines (Scientific Procedures Act, 1986). Following euthanasia, all procedures were performed *post mortem*. Piglets (*Large white*; <15 kg) were obtained from the Roslin Institute (Roslin, Scotland) on the day of isolation and maintained on standard feed and water *ad libitum* up to the time of sacrifice. Animals were anaesthetized with 30 mg/kg body weight (bwt) of pentobarbitone sodium via the auricular vein and then killed with an i.v. bolus dose of 150 mg/kg bwt. The abdominal cavity and lower chest were opened with a midline incision exposing the viscera and the suprahepatic inferior vena cava (IVC) clamped just below the heart, cannulated with a Foley catheter and secured with a ligature. The infrahepatic IVC was also clamped (Figure 2.1).

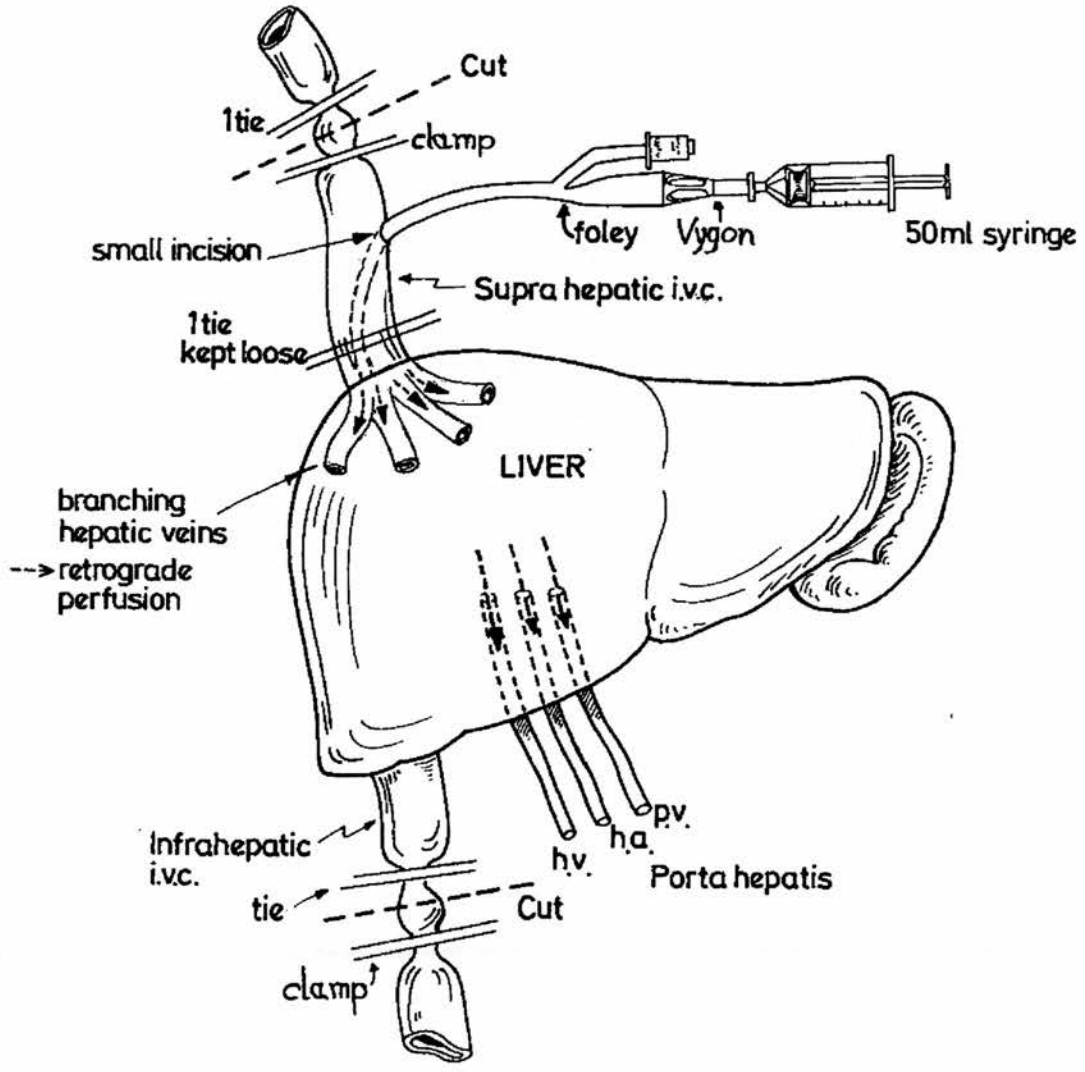

Figure 2.1 Diagram showing the Foley catheter / perfusion assembly

Diagram shows the Foley catheter assembly in the supra-hepatic inferior vena cava (IVC) and positioning of tie clamps for retrograde perfusion of whole piglet liver (not to scale). Perfusate enters the liver through the supra-hepatic IVC, while clamping the infra-hepatic IVC shunts the perfusate to exit via the porta hepatis; (ha) hepatic artery, (hv) hepatic vein, (pv) portal vein. Broken lines with arrow heads depict the direction of retrograde perfusion.

2.3.2 Reagents

Type IV collagenase (from *Clostridium histolyticum*), ethylene glycol-bis[β-aminoethyl ether]-N,N,N`N`-tetraacetic acid (EGTA), N-2-Hydroxyethylpiperazine-N`-2-ethanesulfonic acid (HEPES), albumin (Fraction V), long epidermal growth factor (L-EGF), Triton X-100, and Williams E (WE) medium were obtained from Sigma Chemical Co. (St Louis, Mo, USA). Penicillin-Streptomycin, Gentamycin, Fungizone (Amphotericin B), L-Glutamine, phosphate-buffered saline (PBS, pH 7.4) and Hanks' Balanced Salt Solution (HBSS; Ca and Mg free, pH 7.4) were cell culture grade supplied by Gibco (Paisley, UK). Analar grade chemicals for the perfusion solutions and P450 buffer were obtained from Life Technologies (BDH Merck). University of Wisconsin (UWS) preservation solution (Viaspan™) was obtained from DuPont Chemical Co (USA). Other reagents were: Dexamethasone (David Bull Labs, England), Aprotinin (Trasylol™, Bayer) and porcine insulin (Pork Velosulin™, Novo Nordisk, Denmark).

2.3.3 Perfusion and washing buffers

2.3.3.1 Methods I and II [Drs J Gerlach, M Smith; personal communication];

Perfusion Stock Solutions: 1) For 1L [10x] Hanks Buffer Stock Solution: 80g NaCl, 4g KCl, 2g $MgSO_4.7H_2O$, 0.6g $Na_2HPO_4.2H_2O$, and 0.6g KH_2PO_4 were dissolved in distilled water (dH_2O), made up to 1L and stored at 4°C (for <3 months). 2) For 2L [2x] Krebs-Henseleit Buffer Stock Solution (KHBS): *Solution A*: in the following order, 785ml dH_2O 200ml 16.09% NaCl (32.18g NaCl / 200ml), 150ml 1.1% KCl (1.605g / 150ml), 25ml 0.22M KH_2PO_4 (0.748g / 25ml), 50ml 2.74% $MgSO_4.7H_2O$ (1.37g / 50ml) and 100ml 0.12M $CaCl_2.6H_2O$ (2.628g / 100ml) were added to a 2L brown bottle and equilibrate with 95%O_2/5%CO_2 gas for 10 minutes; *Solution B*: 9.71g $NaHCO_3$ was dissolved in 1L dH_2O and gassed as above. Add *solution A* (1310ml) to 690ml *solution B* for 2L KHBS. Store at 4°C. NB Solution must be clear upon mixing (if a precipitate was evident the solution was discard). Liver Perfusion Solutions: Hanks I: Add 2.1g $NaHCO_3$, 3.0g HEPES, 6.66g Bovine Serum Albumin (BSA), 228mg EGTA, and 100ml [x10] Hanks Stock Solution to 600ml dH_2O, mix well, make up to 1L and pH to 7.4 with 5N NaOH then sterile-filter. Store at 4°C. Hanks II: Add 2.1g $NaHCO_3$ 3.0g HEPES, 294mg $CaCl_2.2H_2O$ and 100ml [x10] Hanks Stock solution to 600ml dH_2O, mix well, make up to 1L and pH to 7.4 with 5N NaOH and sterile-filter. Store at 4°C. Krebs Albumin Buffer (KAB): For 1L KAB; add 3.0g HEPES, 10g BSA and 500ml [x2] Krebs Stock Solution to 300ml dH_2O (adding BSA last), mix well, make up to 1L and pH to 7.4 with 5N NaCl then sterile-filter solution. Store at 4°C. Cell Washing Solutions: (Krebs HEPES Buffer (KHB)): For 1L KHB; add 3.0g Hepes and 500ml [x2] Krebs Stock Solution to 300ml dH_2O, mix well, make up to 1L and pH to 7.4 with 5N NaOH then sterile-filter. Store at 4°C.

2.3.3.2 Method III

Stock solution: 2 litres of a stock Perfusion Buffer (PB) containing 154 mmol/L NaCl, 5.6 mmol/L KCl, 5 mmol/L glucose, 25 mmol/L $NaHCO_3$ and 20 mmol/L HEPES was made up with distilled H_2O, adjusted to pH 7.4 and sterile filtered. PB1 consisted of 500ml stock PB supplemented with EGTA (at 1mmol/L), 20 mg dexamethasone and 1.4 mg aprotinin; PB2 contained 500ml stock PB with EGTA (at 1mmol/L) alone; PB3 consisted of 100ml PB stock only; PB4 was 500ml stock PB containing 5mmol/L $CaCl_2$, and either 0.03, 0.04, or 0.05 % (w/v) Type IV collagenase; PB5 was 200ml Williams E medium only.

2 litres of washing buffer (WB) containing 120 mmol/L NaCl, 6.2 mmol/L KCl, 0.9 mmol/L $CaCl_2$, 10 mmol/L HEPES and 0.2% (w/v) albumin, was made up with distilled H_2O, adjusted to pH 7.4 and sterile filtered. All equipment was sterilized by autoclaving (Koebe and Schildberg, 1996).

2.3.4 Perfusion methods

2.3.4.0 General description

Four perfusion methods were tested to permit isolation of primary porcine hepatocytes (PPHs) with high viability and yield for use in BAL systems. Method I: Liver wedge isolation from 60kg abattoir-sourced pigs; Method IIa: Whole liver isolation from piglets (<15kg). Both these preliminary methods utilized perfusion solutions previously used for *in vivo* isolation techniques (Drs J Gerlach, M Smith; personal communication). Method IIb: This procedure was identical with Method IIa except that heparin was added to the initial saline flush solution. The above mentioned methods utilized 0.05% (w/v) Type IV collagenase. Method III: Modified whole liver retrograde isolation technique (Adapted from Koebe & Schildberg, 1996): Different concentrations (0.03-0.05% (w/v)) of collagenase were tested and the optimal

(0.03%) was adopted as the final (most favorable) method for isolating PPHs (Nelson *et al.*, 2000) and used for all subsequent experiments presented in this thesis. The advantages and disadvantages of each method will be discussed in Section 2.6.

2.3.4.1 Method I: Liver wedge isolation from abattoir-sourced pigs

On site (in the abattoir), a 400-500g central wedge portion of liver was removed so that medium-sized hepatic veins were clearly visible (thin-walled vessels with a brown appearance). These veins were flushed with 1 litre of UWS using a sterile 50 ml syringe. The liver was stored on ice in UWS in a sterile sealed container for transport back to the lab.

Perfusion solutions Hanks I, Hanks II, Krebs Albumin Buffer (KAB), and Krebs Hepes wash Buffer (KHB) were prewarmed to 37°C in a water bath and equilibrated with 95% O_2 / 5% CO_2. Inside a Class II hood, the liver wedge was kept in UWS on ice and 4 to 8 hepatic veins cannulated using Venflon™ catheters sutured into place. The liver was then placed into a sterile bowl kept at 37°C and connected to a 4-cannulae perfusion rig. Perfusion was performed either open loop or closed loop using a Watson-Marlow peristaltic pump to transport perfusate to (or from) the liver via sterilized 5mm bore silicon tubing connected (via luer caps) to the Foley catheter and the adapted perfusion bottle lid. The pump was run briefly with perfusate to expunge any air bubbles. The liver was then perfused with: (1) 1 litre Hanks I buffer at 50 ml/min (open loop); (2) Closed loop (recirculating flow) of 500 ml Hanks II buffer with 0.05% (w/v) type IV collagenase at 100 $mlmin^{-1}$, until there was clear evidence of regional tissue disruption (liver wedge shows pallor and becomes flaccid). The collagenase-digested portions of the liver wedge were, using sterile gloves, gently sloughed off into 500ml KAB solution. The crude cell suspension was sterile-filtered sequentially through 1000, 360, 190, and 70 μm mesh filters. Parenchymal cells were allowed to sediment in KAB and the non-parenchymal cell fraction (supernatant) aspirated. The hepatocytes were then washed with KHB, using 3 centrifuge-wash

cycles at 50g (room temperature) for 5 minutes. Finally, cells were resuspended in 100ml KHB.

2.3.4.2 Method II: Whole liver isolation

Method IIa: The liver was perfused retrogradely *in situ* with 500ml ice-cold 0.9% sterile iv saline solution (Baxter) via the Foley catheter which was coupled to a Vygon™ connector and 50ml syringe both with luer locks (Figure 2.1). The whole liver was excised and exsanguinated with a further 500ml 0.9% saline confirmed by a clear perfusate emerging from the portahepatis (leaving the Foley assembly and infrahepatic IVC clamp in place), the whole organ was then rinsed with 250ml University of Wisconsin Solution (UWS), placed in a polythene bag with 750ml UWS on ice, and transported to the laboratory.

For this isolation method of *ex vivo* retrograde perfusion, Hanks I, Hanks II and KAB were pre-warmed in a water bath at 37°C and directly oxygenated with 95%O_2 / 5%CO_2 gas. The liver was transferred from UWS storage to a warmed container. Perfusion was open loop or closed loop at a flow rate of 75 ml min^{-1}. Organ Perfusion: An initial open loop perfusion with 1.5 L of Hanks I solution was performed followed by a closed loop recirculating perfusion of 1.5 L Hanks II perfusate containing 0.05% w/v collagenase Type IV for 45-60 minutes. Following the completion of each perfusion step the perfusate was discarded. A final closed loop perfusion with 750ml KAB was effected. Following this step, the perfusate was discarded and 750ml (37°C) KAB added (at this stage, the liver appears flaccid, shows pallor and easily ruptures upon testing with a blunt instrument). Whole Liver Dissociation: The liver was then gently disrupted manually into KAB using sterile gloves, removing non-perfused tissue and the intact gall bladder. The hepatocyte suspension was cooled on ice and the cell suspension filtered using 300, 200 and 100 μm stainless steel filters into a 2 litre sterile Duran bottle. Next, 300ml oxygenated (4°C) KHB was added and the parenchymal cells allowed to sediment for 15-30 minutes, and supernatant aspirated. This step was repeated with KHB, followed by 2

centrifuge wash cycles in KHB at 4°C. Finally, the washed cell suspension was resuspended in then oxygenated Williams E media, and cell viability and yield assessed on a haemocytometer under phase contrast microscopy, incorporating the trypan blue exclusion test.

Method IIb: In one series (n=3; animals 11.2±0.9 kg bwt), following euthanasia, 25000 U heparin was added to the 0.9% saline flush solution. Otherwise, the protocol was identical with Method IIa.

2.3.4.3 Method III: Modified whole liver retrograde isolation technique

The liver was retrogradely perfused *in situ* with 250ml PBS at 4°C, via the Foley catheter which was coupled to a Vygon™ connector and 50ml syringe both with luer locks (Figure 2.1). The whole liver was excised and exsanguinated with a further 250 ml of PBS, confirmed by a clear perfusate emerging from the portahepatis (leaving the Foley assembly and infrahepatic IVC clamp in place), the whole organ was then rinsed with PBS, placed in a polythene bag with 200 ml PBS on ice, and transported to the laboratory.

Prewarmed perfusion buffers (PB1-4) were saturated with 95% O_2 / 5% CO_2 and the liver transferred to a stainless-steel bowl and placed in a 37°C water bath with the buffers (Figure 2.2). Perfusion was either open loop (non-recirculated; PB 1-3, PB5) or closed loop (recirculated; PB4). The liver was sequentially perfused via the Foley catheter connected to a peristaltic pump (Watson-Marlow, USA) set at 50 ml/min via silastic tubing thus: PB1 (≈8 mins), PB2 (≈8 mins), PB3 (≈2 mins), PB4 (≈16mins) and PB5 (at 4°C for ≈3mins). Perfusate was removed following steps PB1, PB2 and PB3.

Figure 2.2 Photographs showing the general perfusion set-up for *ex* vivo retrograde perfusion and the effects of collagenase digestion on whole piglet liver

These photographs show the general set-up of a successful Method III isolation procedure. Panel A Perfusion buffers (PB1-4) were connected to a coupling lid which allowed either open- or closed-loop retrograde perfusion of the liver via silastic tubing and a peristaltic pump. Panel B This ventral view of the liver shows closed-loop perfusion whereby the collagenase solution is pumped retrogradely (green arrow) into the superior IVC (not visible) via the Foley catheter / Vygon connector assembly. Clamping of the infrahepatic inferior vena cava (Inf. IVC) shunts perfusate through the porta hepatis (ph). After 10 minutes collagenase perfusion, the liver is very pale in colour and there are signs of tissue blanching (black asterisks). Panel C This dorsal view of the liver shows that, after 16 minutes collagenase perfusion, the liver capsule has ruptured (white asterisks) and cells released into the perfusate. See Section 2.3.4.

A


Silastic tubing
Coupling
PB2-4
2 3 4
PB1
Water bath
(37^{0}C)

B

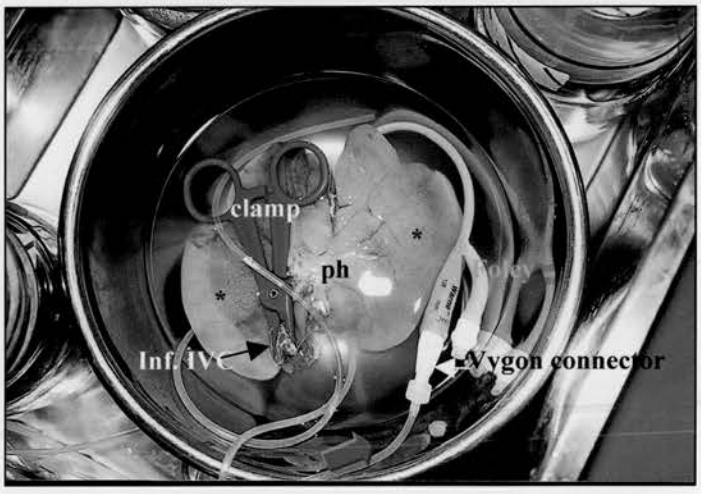
clamp
ph
Inf. IVC
Vygon connector

C

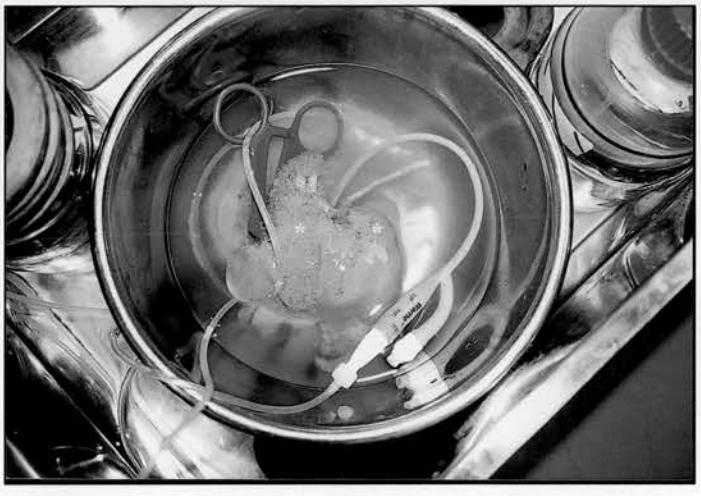

2.3.5 Method III: Hepatocyte Isolation

Following perfusion the whole liver was dissected aseptically with sharp scissors into $\approx 1 cm^3$ pieces and the disrupted tissue placed in an orbital shaker at moderate speed for 5 minutes at 37°C in the presence of PB4 and PB5. The resulting cell suspension was transferred to a laminar flow hood and sequentially filtered through a stainless-steel collander and meshes of grid size 200, 150 and 100 μm respectively into collection bottles placed on ice. Collagenase activity was neutralised by adding 500 ml WB at 4°C (containing 0.2% albumin) to the filtered suspension to achieve a final volume of 1200ml. The predominantly parenchymal cell fraction was allowed to sediment on ice and the non-parenchymal fraction aspirated. The hepatocytes were then washed with WB, using 3 centrifuge-wash cycles at 25 g (4°C) for 5 minutes. Finally the hepatocyte pellets were resuspended in Williams E medium at 4°C. Cell number and viability were initially determined by the trypan blue exclusion test using a Neubauer brightfield haemocytometer (BDH, Merck). Aliquots of fresh cell suspension were analysed for total protein content, total cytochrome P450 content, LDH activity and for urea synthesis rate following ammonium chloride challenge.

2.3.6 Method III: Hepatocyte cultures

Cells were seeded at a density of $8x10^6$ viable cells per 90mm culture dish (Dow Corning, USA) in 8ml WE medium at 37°C. The culture medium consisted of serum-free, hormonally-defined Williams E media (WE+) supplemented with 50 ng/ml L-EGF; 10μg/ml porcine insulin; 1 μmol/L dexamethasone; 2 mmol/L L-Glutamine; 50 mg/ml Gentamycin; 50 mg/ml Penicillin-Streptomycin and 2.5 μg/ml Fungizone. The culture dishes were shaken gently to aid dispersal of cells for attachment and placed in a humidified incubator under a 95% air: 5% CO_2 atmosphere. For the initial cell attachment phase, the incubator was gassed with 30% O_2 / 5% CO_2 for 2 hours (Sharda *et al.*, 1996). Next day (day 1), the culture dishes were aspirated and fresh WE+ medium added.

2.3.7 Method III: Biochemical assays

On the day of isolation (day 0) and on day 2, total protein (TP) and total cytochrome P450 content, lactate dehydrogenase (LDH) activity and urea synthesis rate (USR) of the cells were measured. This was performed in 5 separate isolations, unless stated otherwise.

2.3.7.1 Treatment of fresh cell suspension for total protein and LDH measurements

On day 0, 10ml ($5x10^7$) fresh cell suspension in WE medium was centrifuged at 25g (4^0C) for 5 minutes and 1ml samples of the supernatant taken (F1 fraction) and stored at -70^0C until analysis of extracellular LDH activity (Marsh *et al.*, 1991; Poullain *et al.*, 1992). The cell pellet was resuspended in 10ml 0.25% Triton X-100 in HBSS and frozen to -70^0C, thawed, centrifuged at 200g (4^0C) for 5 minutes and 1ml samples of supernatant (F2 fraction) taken as above for analysis of cytosolic LDH and total protein (TP). TP was analysed using the Bradford assay (Bradford, 1976) modified for a COBAS FARA centrifugal analyser (Roche Diagnostics); results are expressed as mg protein / 10^6 cells. LDH activity was determined in the F1 and F2 fractions by following the rate at which NADH is converted to NAD^+ at λ_{340} nm in the presence of pyruvate as enzyme substrate (Sigma Diagnostics LDH kit DG1340-K) adapted for use on the COBAS FARA. The percentage of total extracellular LDH released into the medium is calculated as follows: %LDH = F1 / (F1 + F2) x 100 whereas the percentage of total cellular (cytosolic) LDH = 100 - F1 / (F1 + F2) x 100.

2.3.7.2 Treatment of day 2 monolayer cell cultures for total protein and LDH measurements

On day 2, 1 ml samples of medium (F1 fraction) were taken from duplicate dishes and stored at -70^0C until analysis for extracellular LDH. The medium was then aspirated completely, the cell monolayer washed twice with HBSS (4^0C) and 5ml 0.25%

Triton-X 100 in HBSS added. Dishes were freeze-thawed and cells scraped from the dish using a pastette. Residual cells were rinsed from the dish with 5ml HBSS, added to the lysed cell homogenate and centrifuged at 200g (4^0C) for 5 mins, and 2x1ml samples of supernatant (F2 fraction) stored at -70^0C until analysis for TP and LDH activity (as above).

2.3.7.3 Treatment of fresh cell suspension and day 2 monolayer cultures for total cellular cytochrome P450 levels

On day 0, $2x10^7$ freshly isolated cells in WE medium were centrifuged at 25g (4^0C) for 5 mins and the supernatant aspirated. 2ml of ice-cold P450 buffer (Watts *et al.*, 1995) (0.1M sodium phosphate buffer pH 7.6, 0.02% Nonidet P-40, 20% glycerol, 1mM EGTA and 1mM Dithiothreitol) was added to the cell pellet and the crude suspension homogenised using 7 strokes of a teflon-glass Dounce homogeniser and stored at -70^0C until analysis. Day 2 monolayer cultures were washed twice with HBSS (4^0C), 2ml P450 buffer added and the cells scraped from the culture dish; the crude homogenate was collected and treated as above. Following assay of the TP content as above, both fresh and cultured cells were diluted with P450 buffer to 4mg protein / ml and 1ml of sample placed into each of two 1cm quartz glass sample and reference cuvettes with blackened sides. 1 mg sodium hydrosulphite was added to both cuvettes; 2 minutes later the sample cuvette was bubbled at 2 bubbles / second for 20 seconds with 99% pure CO gas. The P450 content was assessed by carbon monoxide-difference spectroscopy of the sodium hydrosulphite-reduced samples (Omura and Sato, 1964) using a Kontron dual beam spectrophotometer scanning between λ_{400}-λ_{500} nm. The difference in absorbance between λ_{450} and λ_{490} nm was recorded, using an extinction coefficent, ε = 91 mM cm^{-1}, and path length of 1cm, to calculate the P450 concentration (c) according to Beer's law, thus:

$$\textbf{Absorbance} = \varepsilon l c$$

$$\textbf{[P450]} = \textbf{Absorbance} / \varepsilon l \qquad \textbf{(pmol)}$$

Results are expressed as pmol/mg protein (corrected for total cellular protein content). A representative P450 spectrum is shown in Figure 2.3.

Figure 2.3 Representative Carbon Monoxide-difference Spectra of Freshly Isolated Primary Porcine Hepatocyte Lysates

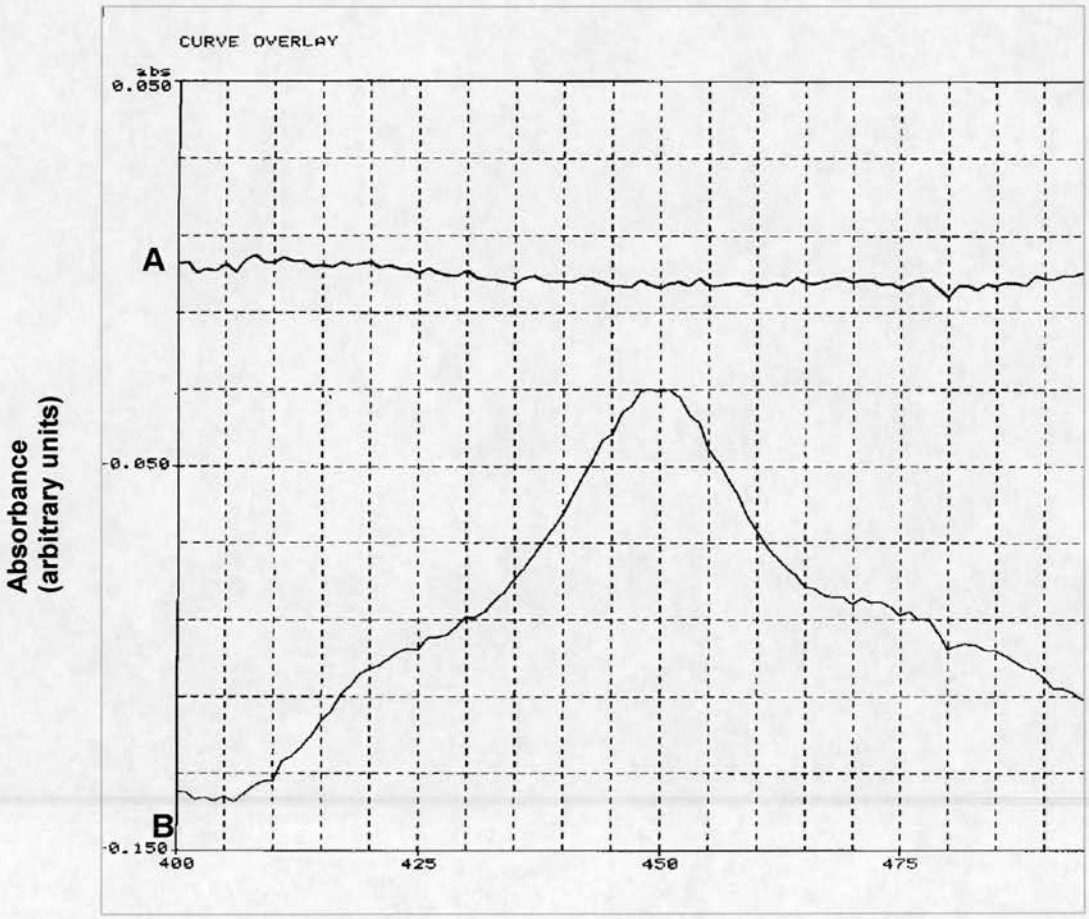

Freshly isolated cells were solubilized in 'P450 buffer', homogenized and the protein content determined. Following addition of 1 mg sodium hydrosulphite to both sample and reference cuvettes, a baseline (curve A) was recorded using a Kontron dual beam spectrophotometer scanning between λ_{400}-λ_{500} nm. Two minutes later the sample cuvette were bubbled at 2 bubbles / second for 20 seconds with 99% pure CO gas, the P450 spectrum recorded (curve B) and the P450 content assessed by carbon monoxide-difference spectroscopy of the sodium hydrosulphite-reduced samples (Omura and Sato, 1964) as detailed in Section 2.3.7.3. Cultured hepatocytes in each test media were scraped from the culture dishes and treated as above.

2.3.8 Urea synthesis

2.3.8.1 Calculation of urea concentration

The absorbances for the chromogenic reaction were measured for each time point at λ_{525} nm in a Pye Unicam spectrophotometer and the **[urea]**, $\mathbf{C_1}$ (at t_0) **and** $\mathbf{C_2}$ (at t_2) calculated in **mmol/L**, using the equation derived from the slope of the urea standard curve (Figure 2.4), **x**, of the form:

$$\mathbf{y = ax + b} \qquad \textit{Equation 1}$$

Rearranging, $\mathbf{x = y-b / a}$ *Equation 2*

Where, **x** is defined as **[urea]**, $\mathbf{C_1}$ or $\mathbf{C_2}$ in **mmol/L**

2.3.8.2 Calculation of urea synthesis rate (USR) in primary porcine hepatocytes cultures

$$\mathbf{USR = [C_2V_2] - [C_1V_1] / NT}$$

where, $\mathbf{V_2 = V_1 - V_s}$

2.3.8.3 Definition of parameters:

- $\mathbf{V_1}$ volume of medium in the dish prior to sampling at t_o
- $\mathbf{t_o}$ that time at which the assay is just beginning
- $\mathbf{V_2}$ that volume of medium in the dish prior to sampling at t_2
- $\mathbf{t_2}$ that time at which the assay is just finishing (in hours)
- $\mathbf{V_s}$ that sample volume removed from the dish between t_0 and t_2

$\mathbf{C_1}$ that concentration of solute quantified on the t_0 sample (from *equation 2* above)

$\mathbf{C_2}$ that concentration of solute quantified on the t_2 sample (from *equation 2* above)

T that time which has elapsed between t_0 and t_2

N the value of total protein in the culture dish (mg/dish)

Units: nmol urea synthesized / hour / mg total protein

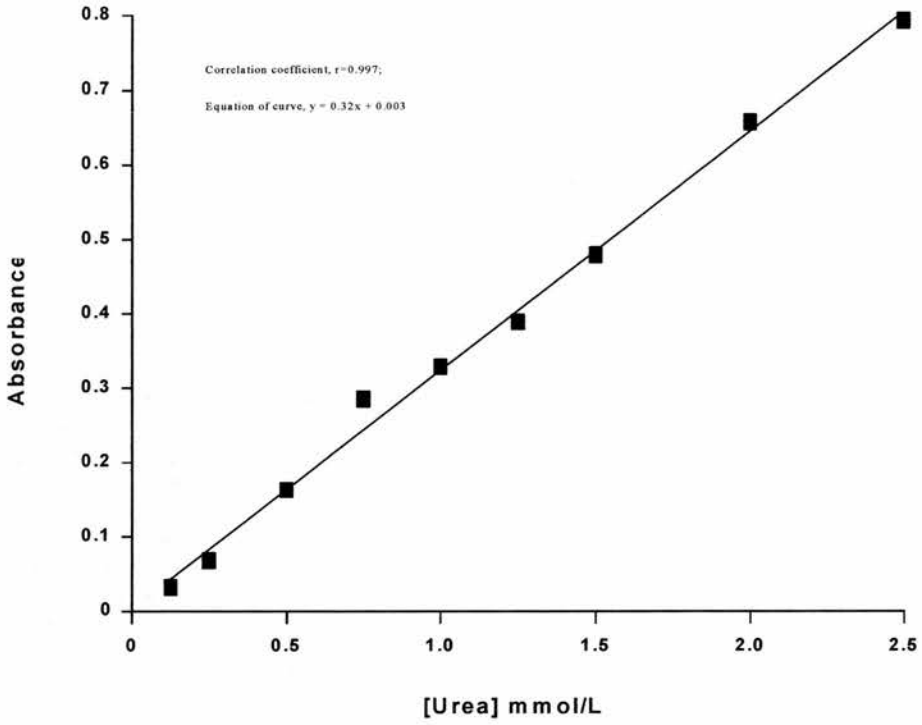

Figure 2.4 Representative Urea Standard Curve

Representative standard curve for the determination of urea concentration in the test media. Standard solutions of urea standard (0 - 2.5 mM) were assayed in duplicate according to the manufacturer's instructions, and the absorbances for the chromogenic reaction measured for each concentration. The data was fitted to a linear regression curve (y = 0.32x + 0.003) using FigP (version 2.5) software programme. The concentrations in 'unknown' samples were derived from the slope of the standard curve (see Sections 2.3.8.1-3).

2.3.8.4 Preliminary work

Previous studies of urea synthesis rates following NH_4Cl challenge of primary hepatocytes have used NH_4Cl concentrations of between 2 (Dr P Gregory, pers. comm.) and 10 mmol/L (Watt *et al.*, 1995). In our study, urea production was assessed in day 2 cultured porcine hepatocytes in HBSS reference medium:

(a) Using different concentrations of NH_4Cl (1-10 mmol/L) to find the saturating [NH_4Cl], and
(b) As a function of time to test for constant urea synthesis.

(a) Cells cultures were incubated in duplicate with 1, 2, 4, 8 or 10 mmol/L of NH_4Cl in HBSS for 2 hours. Urea production rate (UPR) is expressed as mM/hour/mg TP (Figure 2.5A).

(b) Cells were incubated as in a), except with 2mmol/L NH_4Cl only for 2 hours; samples were taken at 0, 30, 60, 90, and 120 minutes and the urea concentration measured as described above. Urea production is expressed as mM/mg TP (Figure 2.5B).

The data was fitted to a linear regression curve of the form y=0.003x-0.0274, where UPR=0.003t–0.0274, corresponding to a USR = 153 nmol/h/mg TP with a correlation coefficient, R^2=0.955. Although the saturating concentration of NH_4Cl was ≈10mM we chose to perform the experiments at 2mM because (i) it ensured a stable urea synthesis over the 2 hours and (ii) it is more likely to reflect the supraphysiological concentration encountered in a BAL device. The linearity of urea synthesis was confirmed in later experiments under different culture conditions (see Chapter 4, page 4-17, Figure 4.2).

2.3.8.5 Protocol

Fresh Cells (Day 0): Freshly isolated hepatocytes were inoculated at a density of $8x10^7$ in 55ml WE+ medium containing 2 mmol/L NH_4Cl (Flendrig *et al.*, 1997a), into a rotary cell culture vessel (high aspect ratio vessel; Cellon-Sarl, Luxembourg) and rotated at 10 revolutions per minute for 2 hours in a humidified incubator at 37°C under an atmosphere of 95% air / 5% CO_2.

Day 2: Duplicate cell culture dishes were washed 2x with HBSS (37°C) and incubated in 8ml WE+ with 2 mmol/L NH_4Cl for 2 hours at 37°C as above. Cells were subsequently collected and analysed for total protein content using the Bradford assay.

The urea synthesis rate (USR) was determined for each day in 0.5 ml samples taken at t=0 and t=2 hours using a modified colourimetric urea nitrogen kit (Sigma kit 535-B) and corrected for total protein content for each culture modality.

Figure 2.5 (opposite page) Urea production of cultured porcine hepatocytes was measured as a function of (a) [NH_4Cl], and (b) time.

(a) Cells cultures were incubated in duplicate with 1, 2, 4, 8 or 10 mmol/L of NH_4Cl in HBSS for 2 hours. Urea production rate (UPR) is expressed as mM/hour/mg TP; (b) Cells were incubated as in (a), except with 2mmol/L NH_4Cl only for 2 hours; samples were taken at 0, 30, 60, 90, and 120 minutes and the urea concentration measured as described above. Urea production is expressed as mM/mg TP. The data was fitted to a linear regression curve of the form y=0.003x-0.0274, where UPR=0.003t–0.0274, corresponding to a USR = 153 nmol/h/mg TP with a correlation coefficient, R^2=0.955.

Figure 2.5 Urea production response to ammonium chloride challenge of primary porcine hepatocytes cultured in HBSS reference medium

A) Urea production rate as a function of [NH_4Cl]

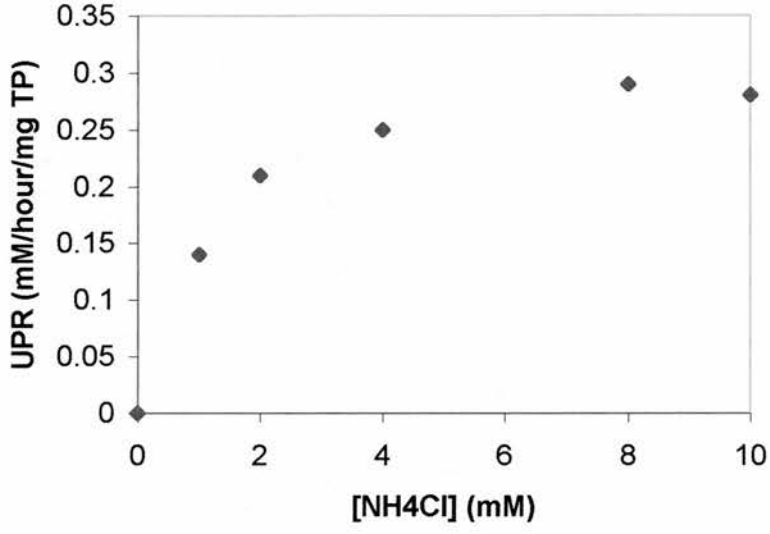

B) Urea production as a function of time

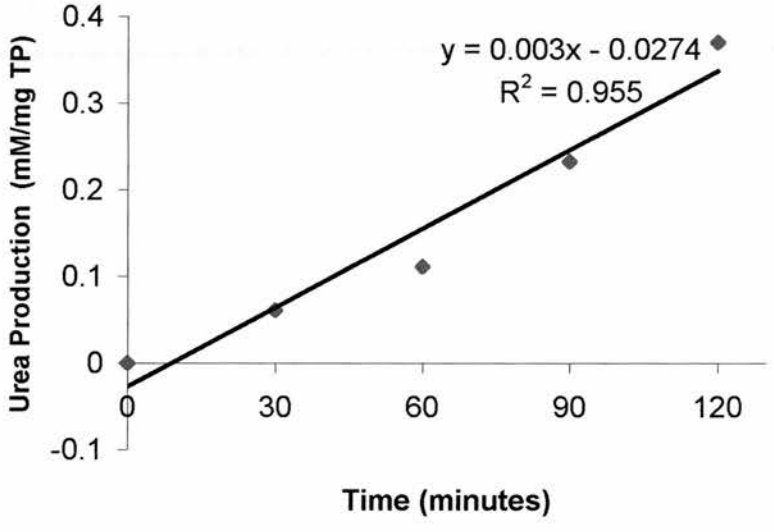

2.3.9 Morphology and isolate purity

Morphology was assessed using a Zeiss inverted microscope (Zeiss, Germany) under phase-contrast on both day 0 and day 2 of culture. Photomicrographs recorded hepatocytes in suspension and monolayer culture. The purity of the freshly isolated cell suspension was assessed by histological staining and manual cell counting, and confirmed by an independent expert observer (Dr C Bellamy, Dept. of Pathology, University of Edinburgh). Following cytospin (200 g; $2x10^5$ cells), cells were stained with hematoxylin and eosin (H&E) and counted using the above microscope (using x20 objective lens) fitted with an eye piece graticule. Three random fields per slide were scored (n=4 separate isolations) for the presence of parenchymal cells (hepatocytes: large distinct round nuclei, eosinophilic-positive cytoplasm; high cytoplasmic to nuclear ratio; visible nucleoli; diameter 20-30 μm) and non-parenchymal cells (irregular nuclei; diameter <10 μm). Periodic Acid Schiff (PAS) stain was used to verify glycogen replete hepatocytes.

2.3.10 Statistics

Results are expressed as mean ± standard error. Student's t-test was used to compare means of different groups. A p value of <0.05 was taken as significant (two tailed test of significance).

2.4 Results

Table 2.1 summarizes the results of the 4 methods tested for large-scale isolation of primary porcine hepatocytes using a collagenase concentration of 0.05 % (w/v).

Cell Isolation Method	Isolation Time (h)	Body Weight (kg) (Range)	[Collagenase] % (w/v)	% Viability (Trypan blue) (Range)	Yield ($x10^{9}$) (Range)
I (n=8) Wedge	4	62±5 (57-67 kg)	0.05	70±14 (53-90)	0.14±0.12 (0.05-0.5)
IIa (n=13) Whole liver retrograde	3	13.4±2 (10-18 kg)	0.05	66±14 (34-90)	36±33 (4-89)
IIb (n=3) Whole liver Retrograde/ heparin	3	11.2±0.9 (10-12 kg)	0.05	45±13 (31-62)	4.6±2.6 (5-12)
III (n=5) Modified whole liver retrograde	<2	12.8±1.3 (9-14 kg)	0.05	82±9 (76-94)	4.3±2.2 (2.1-6.7)

Table 2.1 Comparison of the different isolation methods used in this study to isolate primary porcine hepatocytes from livers of weanling piglets. Table compares isolation time, cell viability, yield and body weight. In this series, the collagenase concentration was maintained at 0.05% (w/v). Liver wedges' or whole livers were processed as described in Materials and Methods (Sections 2.3.1 to 2.3.5). Results are expressed as mean ± standard error. The number n, of hepatocyte isolations performed is shown in parentheses.

2.4.1 Method I: Liver wedge isolation from abattoir-sourced pigs

Warm ischaemic time was 10-20 minutes before the liver was removed from the carcass, cold ischaemic time was 2 hours. Perfusion time was ≈90 minutes. Total isolation time (from animal sacrifice to final cell wash) was ≈4 hours (n=8). Cell viability was 70±14% (trypan blue exclusion test) with a yield of 140±120 x 10^6 cells from 62±5 kg pigs using 0.05% (w/v) collagenase (n=8; Table 2.1). Hepatocytes from 4/8 isolations were successfully plated and grown in monolayer culture, only if viability >70%. Microbiological tests of cell cultures showed sensitivity to gentamicin. The latter was subsequently added to test cultures derived from this method.

2.4.2 Method II: Whole liver isolation

2.4.2.1 Total isolation time (from animal sacrifice to final cell wash) was reduced to <3 hours (n=13), compared with Method I.

2.4.2.2 Method IIa Cell viability was 66±16% (trypan blue exclusion test) with a yield of 36±33 x 10^9 cells from 13±2 kg pigs using 0.05% (w/v) collagenase (n=13; Table 2.1). Hepatocytes from 6/11 isolations were successfully plated and grown in monolayer culture only if viability >70%. Less infection was evident with these cultures (supplemented with pen-strep / gentamicin) compared with Method I cultures.

2.4.2.3 Method IIb

Cell viability was 45±13% (trypan blue exclusion test) with a yield of 4.6±2.6 x10^9 cells from 13.4±2 kg pigs using 0.05% (w/v) collagenase (n=3; Table 2.1). No cells plated from isolations containing heparin in the saline flush solution.

2.4.3 Method III: Modified whole liver retrograde isolation technique

Table 2.2 summarizes the results obtained using Method III and shows the influence of collagenase concentration on cell viability and yield.

Table 2.2 Influence of collagenase concentration on hepatocyte viability and yield using Method III

Cell Isolation Group	Body Weight (kg)	[Collagenase] % (w/v)	% Viability (Trypan blue)	Yield ($x10^{9}$)
1 (n=5)	12.8±1.3	0.05	82±9	4.3±0.22
2 (n=5)	14.1±0.6	0.04	76±6	7.0±0.20
3 (n=20)	12±1	0.03	85±6	24±0.5

Table 2.2 Hepatocyte isolation from whole livers of weanling piglets using Method III (Section 2.3) showing the influence of collagenase concentration on cell viability and yield. Results are expressed as mean ± standard error. The number n, of hepatocyte isolations performed is shown in parentheses.

Times from animal sacrifice to initial PBS flush and PBS flush to cold storage using 0.03% (w/v) collagenase, were 12±4 (n=20) and 16±6 (n=20) minutes, respectively. Transport time to the lab was 12±3 minutes, while hepatocyte isolation time (PB1 to final cell wash) was 65±6 minutes (n=20). Total isolation time (from animal sacrifice to final cell wash) was 105±5 minutes (n=20). Similar times were noted for isolations using the higher collagenase concentrations.

The common *Large White* strain of pig (<15kg; costing 15 pounds sterling each) was used in the hepatocyte isolation experiments. Reducing the collagenase concentration from 0.05 to 0.03% (w/v) produced a 5-fold increase in cell yield, $p<0.05$ (Table 2.2) whilst maintaining high viabilities, and significantly reduced the cost of the isolation (130 pounds sterling per g).

Cell viability was 85±6% (trypan blue exclusion test) with a yield of 2.4±0.5 x 10^{10} cells from 12±1 kg piglets using 0.03% (w/v) collagenase (n=20; Table 2.2). Hepatocytes from all isolations were successfully plated and grown in monolayer culture. Microbiological sensitivity tests of cell cultures showed no evidence of infection.

2.4.2 Method III: Biochemical and morphological analysis

Biochemical measurements of both the isolate and cultured PPHs are summarized in Table 2.3. In freshly isolated hepatocytes (day 0), total protein content (TP) was 1.2±0.1 mg/10^6 cells (n=5) and 1.2±0.3 mg/10^6 cells (n=5) for day 2 monolayer cultures, corresponding to approximately 9x10^6 hepatocytes/dish; percentage of total LDH released into the medium was 13±4% for day 0 and 8±4% at day 2; conversely, intracellular LDH activities were 87±4% and 92±4% of total, respectively; the urea synthesis rate was 196±36 nmol/hour/mg protein at day 0 (n=4) and 292±62 nmol/hour/mg protein (n=9) at day 2. Total P450 content was 99±11 pmol/mg TP for fresh cells (n=5) and maintained at 89±35 pmol/mg TP (n=3) in day 2 cultures.

Table 2.3 Biochemical parameters of freshly isolated porcine hepatocytes (Method III) and subsequent day 2 monolayer cultures

Biochemical Parameter	Fresh Cells (day 0)	Cultured Cells (day 2)
% LDH in medium (F1)	13±4	8±4
% LDH retained in cells (F2)	87±4	92±4
Total Protein (mg / 10^6 cells)	1.2±0.10	1.17±0.27
Urea Synthesis Rate (nmol hr^{-1}/ mg protein)	196±36	292±62 (n=9)
Total P450 (pmol / mg protein)	99±11	89±35

Table 2.3 Biochemical parameters of freshly isolated hepatocytes (day 0) and for day 2 hepatocyte monolayer cultures: Cells were isolated using Method III (0.03% collagenase). Cell viability was assessed as a function of percentage total lactate dehydrogenase (LDH) released into the medium (F1) and retained as cytosolic LDH (F2); total protein (TP) approximates to cell number and urea synthesis rate (USR) to detoxification capacity. Total P450 content indicates cellular biotransformation potential. Results are means (± standard error) from at least five separate hepatocyte isolations measured in duplicate for each parameter.

2.4.2 Method III: Biochemical and morphological analysis (continued)

Phase contrast microscopy (Figure 2.6A) showed that the cell suspension was composed of single cells and small aggregates of between 5-20 cells showing bright cytoplasm, sharply defined borders, commonly with round or polygonal shape and little physical damage (blebbing). In monolayer culture, hepatocytes showed a flattened morphology with typical trabecular arrangement, sharp refractile borders and dark cytoplasm with a pronounced nucleus often with 2 or more nucleoli (Figure 2.6B). Hepatocyte purity for freshly isolated cells was 97±3 % (n=4) (Figure 2.6, C-E). PAS staining revealed a high hepatocyte glycogen content (Figure 2.6F).

Figure 2.6 Morphology of primary porcine hepatocytes

Panel A Freshly isolated porcine hepatocyte suspension following the final washing step: under phase contrast microscopy, hepatocytes show bright cytoplasm, sharply defined borders with round or polygonal shape and little physical damage (blebbing). **Panel B** Hepatocytes in confluent monolayer culture show flattened morphology with typical trabecular arrangement, sharp refractile borders and dark cytoplasm with pronounced nucleus and often with 2 or more nucleoli. **Panels C-F** Histological staining of fresh cell isolate to estimate purity of preparation: Following cytospin and standard staining with H&E, at least 200 cells were counted in each of 3 random fields per slide (n=4 separate isolations) for the presence of parenchymal and non-parenchymal cells (NPCs). The purity of the isolate was >95%, which was confirmed by an independent expert observer (Dr C Bellamy, Dept of Pathology, University of Edinburgh). Hepatocytes (diameter 20-30 μm) typically displayed large distinct round nuclei, eosinophilic-positive cytoplasm; high cytoplasmic:nuclear ratio and visible nucleoli. **Panel C** Under low power (x100, scale bar 100μm) several hundred hepatocytes are shown (open arrows) with very few 'contaminating' NPCs evident (irregular nuclei, diameter <10 μm: Closed arrows in **C**, and **D** (x200, bar 50μm)). Large distinct round nuclei (closed arrows) and eosinophilic-positive cytoplasm (open arrows) are clearly shown in **E** (x400, bar 25μm). Periodic Acid Schiff (PAS) stain was used to verify glycogen replete hepatocytes in **F** (x400, bar 25μm); PAS positive hepatocytes (magenta colour, open arrows) with nuclei counterstained with haemotoxylin (closed arrows). Cell samples were processed as described in Materials and Methods (Sections 2.3.5-6 and 2.3.9).

Panel A: Freshly isolated hepatic cells

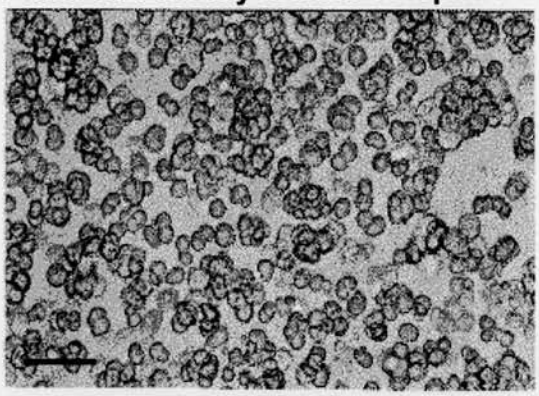

Panel B: Day 2 cultured porcine hepatocytes

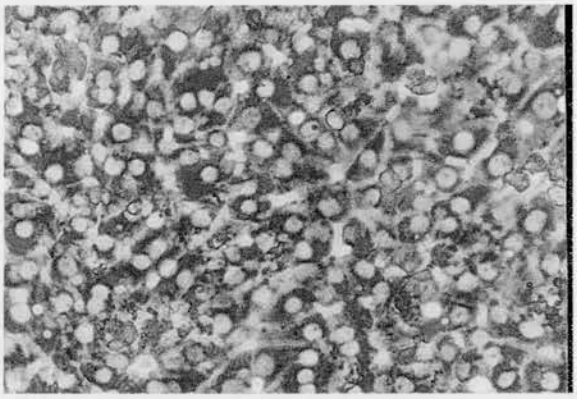

Panels C-F: Histological staining of isolate following cytospin

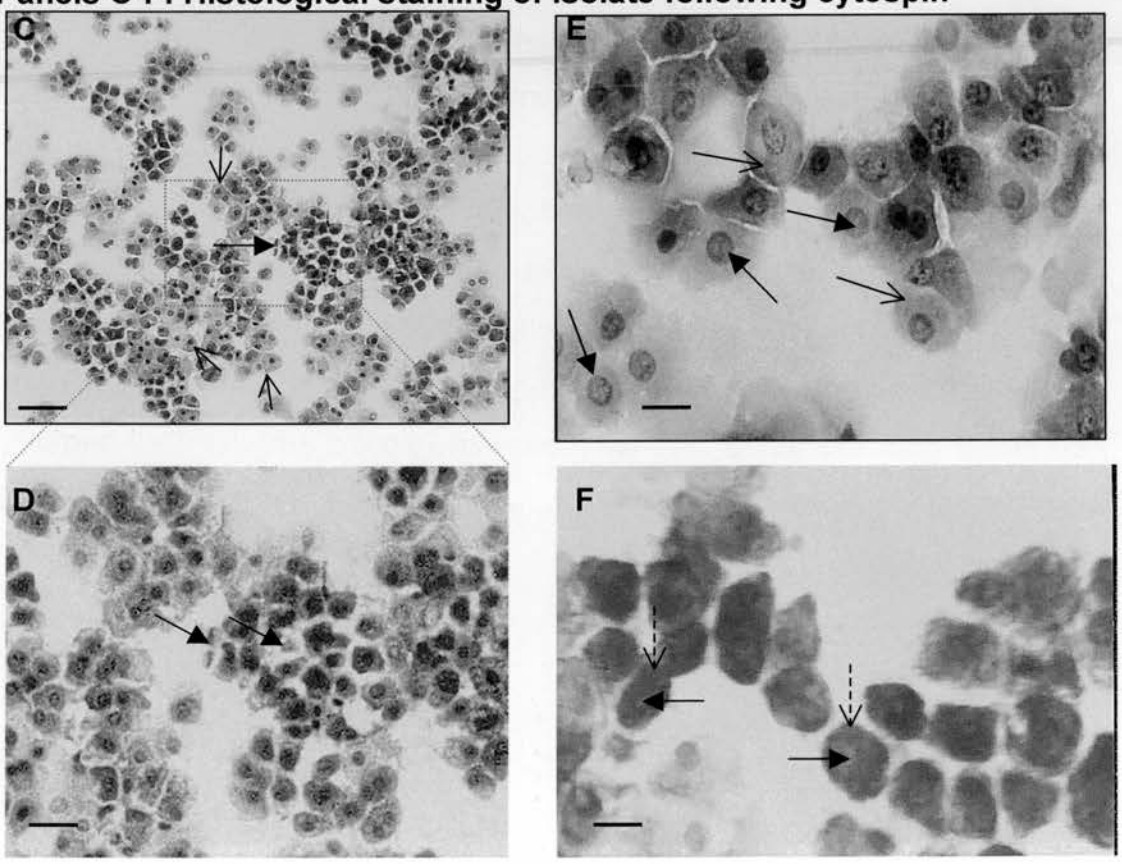

2.6 Discussion

Hepatocyte based BAL systems for treatment of FHF require large numbers of hepatocytes capable of synthetic, metabolic and detoxifying functions. Inadequate yield from rat livers and other small mammals prohibits direct scale-up to clinical BAL application, whereas human-derived liver cell lines have a dedifferentiated metabolic profile and may introduce tumourigenic proteins into the patient. Moreover, because primary human hepatocytes are scarce, PPHs are currently used in scaled-up BAL systems. These cells are considered to be biocompatible with normal human hepatocytes and can be obtained in sufficiently high yield and viability (Demetriou, 1998; Donato *et al.*, 1999; Jauregui *et al.*, 1995; Jauregui and Gann, 1991; Naruse *et al.*, 1996a).

The most common perfusion method for isolating porcine hepatocytes is *in vivo* anterograde collagenase perfusion via the portal vein which can provide sufficient yield for BAL systems, with viabilities over 85% reported (Clement *et al.*, 1998; Demetriou, 1998; Flendrig *et al.*, 1997a; Fremond *et al.*, 1996; Gerlach *et al.*, 1994c; Sheil *et al.*, 1998). However, shortcomings of the *in vivo* technique are its relative complexity, expense, time-consuming nature and above all animal welfare considerations. To conduct an *in vivo* anterograde perfusion under general anaesthesia in the UK would require a licence from the Home Office under the Animals (Scientific Procedures) Act 1986. The Act states: "The Secretary of State shall not grant a project license unless he is satisfied:

(a) That the purpose of the programme to be specified in the licence cannot be achieved satisfactorily by any other reasonably practicable method not entailing the use of protected animals; and

(b) That the regulated procedures to be used are those which use the minimum number of animals, involve animals with the lowest degree of neurophysiological sensitivity, cause the least pain, suffering, distress or lasting harm, and are most likely to produce satisfactory results".

(Animal (Scientific Procedures) Act, Chapter 14, section 5(5); http://www.homeoffice.gov.uk/animact/aspag6.htm#Personal)

The *in-vivo* technique could not satisfy the above requirements if the *ex-vivo* technique could produce comparable results using a protocol which is judged to cause less pain, suffering or lasting harm. In fact the pigs used in this study did not require licensing under the Act because they were killed humanely, using an approved method under the Act (Animal (Scientific Procedures) Act 1986, Schedule 1; http://www.homeoffice.gov.uk/animact/aspag9.htm) prior to any procedures being conducted. Because animal welfare is the overriding consideration a comparison of *in* vivo versus *ex* vivo techniques regarding their relative complexity and cost is less relevant. However the *in vivo* technique would require the assistance of several personnel skilled and appropriately licensed in veterinary anaesthesia and surgery. The method is technically more challenging due to the requirement of obtaining intravenous access to the portal vein while maintaining stable anaesthesia and circulation. The cost of conducting this procedure is estimated to be ten times that of the *ex-vivo.* In this regard, the major advantages of developing *ex vivo* methods are: improved animal welfare, increased reproducibility of the procedure, easier accessibility for perfusion (via the suprahepatic IVC), no animal licensing requirements, and a major reduction in costs.

Previous *ex vivo* methods attempting large-scale isolation of PPHs have attained comparable viabilities but with low yields, probably due to the use of liver wedges as the tissue source (Donini *et al.*, 1997; Koebe and Schildberg, 1996; te Velde *et al.*, 1995).

To circumvent these problems we aimed to develop a simple, reproducible and cost-effective *ex* vivo method of isolating high quality PPHs from whole piglet livers suitable for BAL usage. A comparison of the different methodologies used in this study to achieve this objective is shown in Table 2.1.

In preliminary experiments using liver wedge portions (Method I) from 60kg abattoir-sourced pigs both yield and viability were compromised compared with similar techniques. For example, Koebe & Schildberg (1996) achieved significantly higher viabilities (84±5%) and yield (2.2±0.5 x10^9) than our method. Whole liver retrograde perfusion (Method II) improved yield by up to two orders of magnitude, with similar viabilities as reported with Method I (Table 2.1), with the exception of Method IIb (Section 2.3.4.2). Here, when heparin was used in the initial saline flush solution, viability decreased markedly compared with all the other methods tested. Interestingly, in the absence of heparin under the same conditions (Method IIa) yield was greater by up to an order of magnitude (along with improved viability), in comparison with Method IIb. Reports of a direct, dose-related hepatotoxic effect of heparin in rat hepatocyte cultures (resulting in cell damage and death) may explain this phenomenon (Sanders *et al.*, 1984), although other investigators have demonstrated an hepatotrophic function *in vivo* (Matsumoto & Nakamura, BBRC 1996). Several studies administered iv heparin as a prelude to *in vivo* isolation (Seilaf *et al.*, 1995; Wang *et al.*, 2000) with excellent yields and viabilities reported (see also Table 2.5 below). Perhaps the apparently negative effect of heparin on whole pig liver (Method IIb) occurs predominantly under *ex vivo* conditions, or that too high a dosage was used in our study.

Adaptation of Method IIa allowed more consistent reproducibility in both viability and yield (Table 2.1) resulting in Method III. The methodological modifications undertaken to achieve the stated aims of this study are outlined in Table 2.2, where the collagenase concentration was set at 0.05 % (w/v). Further refinement of Method III was made by titrating the [collagenase] to its optimum of 0.03% for this technique (see Table 2.2), which gave more consistent high viabilities as well as sufficient yield for most BAL devices.

Whilst acknowledging that it is virtually impossible to identify exactly which were the primary factors in the much improved isolation technique, it is possible to consider some of the major changes and the criteria by which modifications were made.

Table 2.4 outlines methodological modifications undertaken in this study to improve the *ex vivo* isolation of primary porcine hepatocytes.

Table 2.4 Comparison of methodological modifications undertaken in this study to improve the *ex vivo* isolation of primary porcine hepatocytes

Parameter	Method I	Method IIa	Method IIb	Method III	Comment
Mean Body Wt (kg)	62 (Adult*)	13 (Weanling)	11 (Weanling)	13 (Weanling)	*Abattoir-sourced
Perfusion Route	Hepatic veins	Supra hepatic IVC	Supra hepatic IVC	Supra hepatic IVC	All Retrograde
Flush / Storage Solutions	UWS only	Saline / UWS	Saline/hep/ UWS	PBS only	All 4°C
Perfusion Buffers 0.05% (w/v) [collagenase]	Hanks/Krebs Wash steps at RT	Hanks/Krebs KHB wash at 4°C	Hanks/Krebs KHB wash at 4°C	PB1-5 PB5 at 4°C	Hanks / PB1-4 at 37°C; PB1 contains aprotinin, dex/glucose;
Perfusion Volumes (L)	Up to 1L	Up to 1.5L	Up to 1.5L	All 0.5L	
Flow Rates (ml/min)	50 (Hanks) 100 (Krebs)	50 (Hanks) 100 (Krebs)	50 (Hanks) 100 (Krebs)	50 constant	
Total Isolation Time (hrs)	4	3	3	<2	
Blood Clots	Some	Some	Some	Rare	
% Viability (range)	53-90	34-90	31-62	76-94	
Mean Cell Yield (x10^9)	0.14	36	4.6	4.3 (24)	(at 0.03% collagenase)

In general Methods I and II gave inconsistent yields and viabilities from pig livers. Since liver wedges were obtained from 60kg adult pigs, weanling piglets were subsequently used since Gerlach *et al.* (1996a) had established that viability and yield

declined with increasing pig weight (6-40 kg). This may reflect an increase in fibrous tissue content in the more mature pig liver compared with the livers of weanling piglets. However, *ex vivo* perfusion of liver wedges from 35-115 kg abattoir-sourced pigs gave high viability but inadequate yield for BAL use (Donini *et al.*, 1997; Koebe & Schildberg, 1996). Initial experiments using saline and UWS as flush and storage solutions surprisingly did not improve the quality of the isolate whereas heparin appeared hepatotoxic using Method II. The cost of UWS (200 pounds / L) was also prohibitive for multiple isolations required for subsequent experimental work.

Method II used large volumes of complex perfusion buffers designed for, and perhaps more suited to, use with *in vivo* procedures (Dr J Gerlach, personal communication) which could more efficiently handle increased perfusion times and flow rates (up to 300ml/min) since the liver could be more extensively perfused *in situ* (with the animals heart beating) down to the microcirculatory or sinusoidal level - not achievable with the *ex vivo* scenario. Another problem encountered for preliminary *ex vivo* isolations was incomplete perfusion due to blood clots. On the other hand, attempts to cannulate the portal vein and/or hepatic artery for anterograde perfusion of whole liver, following Method II, proved unsuccessful (data not shown) and resulted in many more blood clots, and increased pre-perfusion time (ie prior to initiation of PB1).

Koebe & Schildberg (1996) as mentioned, attained high viabilities using an *ex vivo* technique of isolation from abattoir-sourced liver wedges. Although yield was insufficient for scaled-up BAL devices, it was surmised that using *whole* piglet liver (with an intact Glisson's capsule) may well increase the yield whilst maintaining high viability. Empirically, we observed that any damage or lesions to the whole piglet liver during the isolation / perfusion steps, decreased yield, viability and quality of the isolate. *Ex vivo* isolations using liver wedges have one or two open cut surfaces where perfusate can extrude and which results in decreased efficiency of the perfusion and subsequent yield. It was reasoned that lower perfusion volumes and an accessible perfusion route (retrograde, via the suprahepatic IVC) would decrease the overall

isolation time and improve outcome. Moreover, the use of aprotinin (as a fibrinolytic to prevent blood clots) in the initial perfusion step (PB1) may improve efficacy of the technique by increasing perfusate flow down to the microcirculatory level, whereas the addition of dexamethasone and glucose at this stage would stabilize cell integrity by stimulating protein synthesis and the redox potential, respectively, of isolated cells. Finally, a constant reduced flow rate of 50ml/min, coupled with the initial flush with ice-cold PBS, and the aforementioned modifications, ensured that the liver showed early signs of uniform perfusion (very pale colour and flaccidity) even after the first perfusion step (PB1). Perfusion with cooled Williams E (after the collagenase recirculation step) prior to disruption and mechanical handling of the digested liver acts as a cytoprotectant (Gerlach *et al.*, 1994c), whilst the relatively high amino acid content contributes to preservation of nitrogen balance (Berry *et al.*, 1991c) Finally, all purification and washing steps were stringently undertaken at 4°C, and at low centrifugation (x25g) which improved overall isolate quality, reproducibility and consistency. Indeed, Kreamer *et al.*, (1986) suggests that NPC contamination is less with methods employing both cooled washing steps with low speed centrifugation (< x50g) as well as shorter exposures to collagenase, as for Method III (≈16 minutes).

Under these conditions, further refinement of Method III involved determination of the optimal [collagenase]. This factor appeared important since demonstrable improvements in cell yield (5-fold) whilst maintaining high viability (Table 2.2) were evident. Determination of the optimal [collagenase] may be critical in the isolation process for the reasons of batch-to-batch variation, unknown composition and variable enzymatic activity of Type IV collagenase (which also contains other proteolytic enzymes such as pronase and dispase). Collagenase is also known to alter plasma membrane components, decrease transcription of liver-specific genes and protein synthesis, as well as causing many other phenotypic changes even under optimal conditions (LeCluyse *et al.*, 1996). Consequently, excess collagenase may further damage cells, so reducing viable cell yield and isolate quality (Alpini *et al.*, 1994).

Comparative yields and viabilities of differing methods of PPH isolation reported in the literature are outlined in Table 2.5. With a mean cell viability of 85% and a viable cell yield of 2.4 $x10^{10}$, our data compare favourably with *in vivo* techniques (Clement *et al.*, 1998; Demetriou, 1998; Fremond *et al.*, 1996; Gerlach *et al.*, 1994c; Jauregui *et al.*, 1997; Sheil *et al.*, 1998; Sielaff *et al.*, 1995b), while outperforming yields obtained using comparable *ex vivo* isolation methods by an order of magnitude (Donini *et al.*, 1997; Koebe and Schildberg, 1996). Considering that a 12 kg piglet's liver weighs ≈500g and the wet weight of undigested liver was ≈150g, then the yield approximates to $60x10^6$ viable cells/g wet weight of liver, or, 60% of all hepatic parenchymal cells were harvested as viable hepatocytes, assuming the liver contains $\approx 10^8$ cells/g. This is 3 times more efficient than the *in vivo* method of Morsiani *et* al., (1998) although viability was slightly higher at 93±3 %. Moreover, the isolated hepatocytes successfully form high viability confluent monolayer cultures, as demonstrated by high intracellular LDH activity (Marsh *et al.*, 1991; Poullain *et al.*, 1992) and total protein content (Baserga, 1995; Sharda *et al.*, 1996). The cultured cells maintain cytosolic total protein levels comparable to fresh hepatocytes and are capable of detoxification of ammonia through conversion to urea.

The functional liver mass required for a clinically effective BAL is at least 10^{10} hepatocytes (Allen *et* al., 2001, Demetriou, 1998; Fremond *et al.*, 1996; Jauregui *et al.*, 1997; Sielaff *et al.*, 1995b, Strain & Neuberger, 2002), which could be accommodated using our *ex vivo* method or conventional *in vivo* techniques (Demetriou, 1998; Flendrig *et al.*, 1997a; Fremond *et al.*, 1996; Gerlach *et al.*, 1994c; Jauregui *et al.*, 1997; Jauregui and Gann, 1991; Joly *et al.*, 1997; Sharda *et al.*, 1996; Sheil *et al.*, 1998; Sielaff *et al.*, 1995b).

Most of these *in vivo* isolation procedures have adapted the two-step collagenase perfusion techniques originally described in rat isolations by Seglen (1976). Following anaesthesia, intubation and mechanical ventilation, the pig liver is perfused (via the portal vein) *in situ* with perfusion buffer containing EGTA. The liver is then excised and perfused *ex vivo* with a recirculating collagenase buffer and disrupted.

Table 2.5 Comparative data of various techniques employed to isolate primary porcine hepatocytes (See text for details)

Perfusion Route	Body Weight (kg)	[Collagenase] (% w/v) or [specific activity]	% Viability (Trypan blue)	Mean Cell Yield ($x10^9$)	Reference
Retro/*ex vivo*	12±1	0.03	85±6	24	Nelson 2000
Retro/*in vivo*/hep	12	0.08	79±6	24	Naik 1996
ex vivo/LW	35-115	0.05	84±5	0.22	Koebe 1996
pv/hep	8±3	[1mg/ml]	90	8	Gregory 2000
fv/LW*	22±3	[60U/ml]	88±4	<1	teVelde 1995
pv	8±2	0.1	90	20	Lazar 1995
pv/hep	8±3	0.1	92±2	26	Wang 2000
pv	12±2	0.05	85	30	Naruse 1996a
pv	9±1	0.05	95	<20	Kawazoe 1999
pv/hep	8±2	0.1	95	21	Seilaff 1995
pv	8.5±1	0.1	71±7	12	Waring 1995
pv	20	0.05	90	25	Morsiani 2001
pv	12	0.1	90±4	24	Iwata 1999
pv/hep	9±1	0.05	92±2	15	Kong 1996
Pv	22±2	0.06	>95	75	Joly 1997

Table 2.5 Table compares mean values of body weight, collagenase concentration, cell viability and yield (±SEM, if data reported in literature) of different hepatocyte isolation methodologies from pig livers. All methods cited are whole liver *in vivo* (anterograde perfusion) procedures, except where indicated: **Retro**., refers to retrograde perfusion via the inferior vena cava. **Pv**, portal vein; **hep**, iv heparin administration (prior to perfusion); **fv**, femoral vein; **LW**, (*subsequent) liver wedge isolation.

Table 2.5 shows that most of these *in vivo* procedures result in both viabilities and yields comparable with our *ex vivo* technique (Method III; see Table 2.2). Improvements in outcome however have been achieved. Using this methodology, Joly *et al* (1997) obtained yields of $5\text{-}10\text{x}10^{10}$ and viabilities >95% from 20kg pigs. Gerlach *et al.*, (1994c) reported very similar results with 5kg piglets by means of a sophisticated 5-step *in* vivo method (with 0.08% collagenase) combined arterial and portal vein perfusion. Nonetheless, this technique gave lower viability (70%) and yield in 12 kg piglets compared with our *ex* vivo method, using only 0.03% enzyme (Table 2.2). Thus although producing improved outcome under certain conditions, the final method reported here (Nelson *et al.*, 2000) enabled large scale isolation of high viability PPHs appropriate for most BAL devices under development, and this method was commensurate with both the majority of *in vivo* methods reported in the literature (Table 2.5) and the requirements of the Animals (Scientific Procedures) Act 1986.

In practical terms, development of an improved *ex vivo* isolation method has achieved savings in both the cost and time of large-scale isolation of PPHs. This has been realized by: a) substituting UWS for PBS as the initial flush / storage solution; b) obviating the need for expensive anaesthetic procedures and licensed personnel; c) reducing collagenase concentrations and perfusate volumes, and d) using an inexpensive strain of pig. In terms of logistics, we have found it is more satisfactory to utilize pigs killed on the day of isolation as demand dictates, with comparable viabilities and inherently higher viable cell yield than other *ex vivo* methods. This permits more flexibility in cell usage without the greater risks of introducing infection, as is the case for abattoir methods, while eliminating the logistical constraints of the latter. In addition, we have successfully applied our technique to isolation of human hepatocytes from unused donor livers (data not shown).

Cell purity assessment requires morphological, biochemical, histochemical, or immunohistochemical techniques (Alpini *et al.*, 1994). Hepatocytes are readily identified on the basis of morphological characteristics (ie size and appearance) whereas cell-specific assays are preferable in the identification of NPCs. Using

Method III, histological staining and morphological analysis indicated that at least 95% of the isolated cells were hepatocytes (Figure 2.6). Hepatocytes, 20-30 μm in diameter, typically displayed large distinct round nuclei, eosinophilic-positive cytoplasm, high cytoplasmic:nuclear ratio, and visible nucleoli, whereas non-parenchymal cells with diameter of <10 μm appeared irregular in shape. Periodic Acid Schiff (PAS) stain was also used to verify glycogen replete hepatocytes. Biochemical measurements of LDH activity (and trypan blue exclusion) showed the high viability of the isolate, suggesting preservation of hepatocyte membrane integrity. Further, indirect evidence of the high parenchymal cell content of the fresh cell isolate is observed under SEM (see Chapter 5, Figure 5.9), where large hepatocytes with intact membranes and characteristic abundant microvilli (Arterburn *et* al., 1995) are evident. Whilst freshly isolated cells showed ultrastructural characteristics typical of hepatocytes (Figure 3.3, page 3-17). In our experience, and others (Donini *et al.*, 1997; Koebe and Schildberg, 1996;), Percoll™ density gradient purification enhances viability by ≈10% (up to 98%; Kreamer *et al.*, 1986) but reduces yield by 40-50%. In preliminary experiments, day 2 (WE+) cell cultures seeded from Percoll-purified cells (obtained using Method III; Nelson *et al.*, 2000) were morphologically and functionally (urea and albumin synthesis) very similar (data not shown) to non-Percoll treated cells (see Table 2.3) from the same isolate, which is considered to be consistent with high initial purity (Gregory *et al.*, 2000). However, Percoll may render cells unsuitable for BAL use due to membrane damage and reduction of the inherent nonparenchymal cell population present, which may have implications if heterotypic cell interactions are important for optimal BAL function.

Fresh cell suspensions showed a tendency of the hepatocytes to aggregate into small clusters of 5-20 cells (Figure 2.6A). This might be advantageous for cells expediently seeded into a bioartificial liver device. Indeed, there is evidence that isolated hepatocytes arranged into multicellular formations, establish cell-cell and cell-matrix contacts which result in improved differentiation and liver-specific function, when compared with single cell culture monolayers (Bhatia *et al.*, 1999; Koide *et al.*, 1989; Kong *et al.*, 1996; Naruse *et al.*, 1996b; Watts *et al.*, 1995). It is thought that

formation of cell aggregates may provide an *in vivo*-like liver microarchitecture promoting maintenance of viability and differentiated functions (Ben-Ze'ev *et al.*, 1988; Flendrig *et al.*, 1997a; Jauregui *et al.*, 1997; Lazar *et al.*, 1995a; Yuasa *et al.*, 1993).

Total protein (TP) content of freshly isolated cells was 1.2 mg per 10^6 cells, consistent with recent reports (Gregory *et* al., 2000; Sharda *et al.*, 1996). While TP content is only a rough guide to cell number, the day 2 TP content of monolayer cultures could be approximately equated to $9x10^6$ cells per dish. This level of cell count accorded with morphological observations (Figure 2.6B), which confirmed cell confluence. LDH is a reliable indicator of hepatocyte viabilty, attachment and membrane integrity (Jauregui *et al.*, 1981; Marsh *et al.*, 1991; Poullain *et al.*, 1992). Thus high cytosolic LDH activity, increasing from 87% (of total LDH) for freshly isolated cells to 92% in day 2 monolayer hepatocyte cultures, confirms both the high viability of the cell isolation (initially assessed by trypan blue exclusion) and establishes that the cells have recovered from the trauma of isolation and consolidated their structural integrity. Hepatocyte-specific synthesis of urea from ammonium chloride in both freshly isolated cells and day 2 cell cultures, was obtained at levels comparable to those reported in previously (Flendrig *et al.*, 1997a). Ammonia (NH_3) is a putative neurotoxin in the development of hepatic encephalopathy and brain oedema in FHF, so that NH_3 detoxification is considered an essential prerequisite for an effective BAL device in clinical treatment (Gerlach *et al.*, 1994a; Gerlach *et al.*, 1996b; Jauregui *et al.*, 1997; Sharda *et al.*, 1996; Strain, 1994). In addition, we have shown that these cells retain P450 function and thus have metabolic biotransformation potential (Table 2.3). Although cellular P450 content is known to decline with culture age in most species, it can be enhanced by modulating culture conditions (Watts *et al.*, 1995) or by administration of phenobarbital prior to cell isolation. Recently, pig hepatocytes have been shown to outperform both rodent and dog hepatocytes in maintenance of phase 1 and phase 2 activities, whilst high metabolic similarities were found between pig and human hepatocytes (Donato *et al.*, 1999). These attributes of

pig hepatocytes support their usage as the most appropriate species forming the biological component of BAL devices.

For hepatocyte cultures, we use serum-free, hormonally-defined medium containing long-EGF and insulin. Porcine hepatocytes cultured this way show much greater growth potential than rat hepatocytes cultured under the same conditions (Wegner *et al.*, 1992). Indeed density-dependent inhibition of cell growth was less pronounced with the porcine hepatocytes even after reaching confluency (Hughes and Williams, 1996; Yuasa *et al.*, 1993). Morphologically, we have observed overgrowth of pig hepatocytes even after reaching confluence on day 1/day 2 and up to day 6 (not shown). This may be important in terms of maintaining differentiated, multicellular formations in BAL devices as discussed above.

The possible transfer of pig endogenous retroviruses (PERV) to humans via PPHs used in BAL systems at the clinical level may be problematic (Dixit V., 1994; Omura and Sato, 1964). However, recent studies have shown no evidence of pig DNA or PERV infection in patients with short-term extracorporeal connection to pig kidneys or from porcine islet-cell xenografts (Donato *et al.*, 1999; Watts *et al.*, 1995).

In conclusion, our method provides a high viability, high yield and rapid isolation technique, which is easy to perform in a standard research laboratory. Outcome is similar to most *in vivo* protocols reported, although improvements in yield and viabilities are attainable with the latter. Nevertheless, the method obviates the need for relatively complex, *in vivo* surgical techniques and facilities, which are time-consuming and require highly trained, licensed personnel. Cells can be deployed in a variety of *in vitro* liver model systems in under two hours, whilst maintaining viability and hepatocyte functionality. In this study, yield, viability and function of isolated hepatocytes compare favourably with results obtained using *in vivo* techniques.

Chapter 3

Light and Transmission Electron Microscopy Reveal Modulatory Effects of Serum-Free Chemically-Defined Media Formulations on Gross Morphology and Ultrastructure of Primary Porcine Hepatocytes

3.1 Introduction

Hepatocyte shape and structure are considered to be intimately related to functional activity (Gerlach *et al.*, 1995; Ben-Ze'ev *et al.*, 1988; Mitaka, 1998; Folkman and Moscona, 1978; Goulet *et al.*, 1988). The idealized cellular component of bioartificial liver (BAL) systems should maintain a well-differentiated *in vivo*-like phenotype and undergo controlled rounds of proliferation *in vitro* (Jauregui and Gann, 1991; Riordan *et al.*, 1998). That this has not yet been achieved is primarily due to the well documented deterioration of both liver-specific metabolic activities and hepatocyte morphology which occurs within days of culture (Clayton and Darnell, 1983; Gerlach *et al.*, 1995; LeCluyse *et al.*, 1996; Moshage and Yap, 1992; Reid and Jefferson, 1984).

Various strategies have been adopted to address this problem, such as the use of complex biomatrices, microcarriers or synthetic membranes to improve attachment and function of cells (Demetriou, 1998; Gerlach *et al.*, 1994a). Recently however, primary porcine hepatocytes cultured on tissue culture plastic were shown to perform equally well compared with cells grown on a variety of exogenous attachment substrates (te Velde *et al.*, 1995; Gregory *et al.*, 2000). In Chapter 2, it was shown that under defined, serum-free conditions, primary porcine hepatocytes (PPHs) retain characteristic gross morphological and functional features of hepatic monolayer cultures *in vitro* (Nelson *et al.*, 2000). Furthermore, culture morphology was

indistinguishable from that reported in previous studies in which PPHs were similarly grown in William's E medium in the presence of serum on tissue culture plastic alone or with various biomatrices including: Type I and IV collagen, laminin, fibronectin, Engelbreth-Holm-Swarm Natrix (EHS) and Matrigel™ (Gregory *et al.*, 2000; te Velde *et al.*, 1995). The latter have been shown to be a suitable substrata with which to maintain differentiated function and improve cellular polarity, in rat hepatocytes (Berry *et al.*, 1991a; Michalopoulos *et al.*, 1999). In contrast, porcine hepatocytes appear unique in their ability to maintain these desired attributes without the aid of exogenous substrates or serum (te Velde *et* al., 1995; Gregory *et al.*, 2000; Nelson *et al.*, 2000; te Velde *et al.*, 1995). Formation of 3-dimensional tissue-like cultures of PPHs, cultured on a Matrigel-coated, polypropylene hollow fibre bioreactor design, was reported to retain ultrastructural features of liver parenchyma *in vivo* (Gerlach *et al.*, 1994a; Gerlach *et al.*, 1995).

A major concern of this type of BAL configuration is the leakage of potentially tumourigenic or murine proteins from EHS or Matrigel, respectively, into the patients circulation, raising questions of potential immunogenicity and bioreactor safety. Non-autologous serum, on the other hand, introduces unknown factors and contains selective inhibitors, bacterial endotoxins and lipids which may contribute to the observed cytostatic and cytotoxic effects, which are inhibitory to the expression of differentiated, liver-specific functions and selective for the growth of non-parenchymal cells (Enat *et al.*, 1984; Berry *et al.*, 1991a). Moreover batch variation of sera, particularly in comparative studies, present difficulties of adequate characterization of the culture system.

For these reasons, we have used serum-free chemically-defined media formulations to study their influence on the gross cellular and ultrastructural morphology of primary porcine hepatocytes cultured on unmodified tissue culture plastic. William's E Medium (Flendrig *et al.*, 1997a; Bader *et al.*, 1996; De Bartolo *et al.*, 2000; Flendrig *et al.*, 1998a), Medium 199 (Gerlach *et al.*, 1989; Gerlach *et al.*, 1990) and Medium 1640 (Kong *et al.*, 1996) are commonly used in current BAL systems; whereas

Hepatocyte Medium is a new formulation which apparently maintains *in vitro* differentiated function in other mammalian species (Sigma-Aldrich Technical Services, personal communication).

The marked functional diversity of the hepatocyte, including protein synthesis, bile secretion, storage of metabolites and detoxification, is reflected in the great variety of cytoplasmic organelles visible under transmission electron microscopy. The presence of an intact cytoplasmic membrane, plentiful mitochondria, endoplasmic reticulum, glycogen storage granules and bile canaliculi structures are considered to be the 'gold standard' when assessing morphological markers of differentiation (Peshwa *et al.*, 1996; Portmann, 2000; Fan and Steer, 2000; Shatford *et al.*, 1992; Mitaka, 1998; Junqueira, 1977; Gerlach *et al.*, 1995; Berry *et al.*, 1991b; Hargreaves, 1968). The morphological characteristics of hepatocyte cultures were studied in parallel with biochemical parameters of plating efficiency, viability and total cellular protein content.

3.2 Aims

The aims of this study were to assess the modulatory effects on hepatocyte morphology of different serum-free chemically-defined media formulations on cultured hepatocytes in terms of:

1. Gross cellular morphology under phase contrast light microscopy
2. Cell ultrastructure under transmission electron microscopy
3. Biochemical parameters related to cellular attachment and viability

3.3 Materials and methods

3.3.1 Reagents

All reagents used were as detailed in Chapter 2 with the following additions: Culture media (Williams E (WE), Hepatocyte medium (HM), Medium 199 (M199), RPMI 1640 (M1640)), and Hanks' Balanced Salt Solution (HBSS, pH 7.4) were obtained from Sigma Chemical Co. (Sigma, Poole, UK). LDH and urea kits were obtained from Sigma Diagnostics. Reagents for TEM were obtained from BDH Merck (UK).

3.3.2 Hepatocyte isolation

Hepatocytes were isolated from weanling piglets (<15kg) using our *ex vivo* collagenase perfusion method described in Chapter 2 (Nelson *et al.*, 2000).

3.3.3 Hepatocyte cultures

Cells were seeded at a density of 10^7 viable cells per 100mm tissue culture plastic (TCP) dish (Dow Corning, USA) in 8ml of each of the four test media (WE, HM, M199, M1640) at 37^0C. Each culture medium consisted of serum-free, chemically-defined medium (either WE, HM, M199, M1640) supplemented with 50 ng/ml Long-Epidermal Growth Factor (L-EGF); 10μg/ml porcine insulin; 1 μmol/L dexamethasone; 2 mmol/L L-Glutamine; 50 mg/ml Gentomycin; 50 mg/ml Penicillin-Streptomycin and 2.5 μg/ml Fungizone. The culture dishes were shaken gently to aid dispersal of cells for attachment and placed in a humidified incubator under a 95% air: 5% CO_2 atmosphere. For the initial cell attachment phase, the incubator was gassed with 30% O_2 / 5% CO_2 for 2 hours. Next day (day 1), the culture media were aspirated and fresh medium added which was subsequently changed on days 2 and 4.

3.3.4 Biochemical and metabolic assessment

3.3.4.1 General description

For each test medium hepatocytes were cultured on duplicate TCP dishes and evaluated at the time points indicated. On the day of isolation (day 0) and on culture days 2, 4 and 6 the total cellular protein content (TP) and lactate dehydrogenase (LDH) activity of the cell lysates was measured. In addition, samples of culture media and cellular lysate were analysed for LDH activity. Samples were stored at -70°C until analysis. This was performed on 10 separate isolations. Plating efficiency was assessed by measuring TP of day 1 cultures (defined below), whereas the degree of confluency (% confluency) was measured quantitatively, using computer aided image analysis, for each time point.

3.3.4.2 LDH and total protein measurements

Intra- and extracellular LDH activity and total protein (TP) content were determined in fresh cell suspensions and for hepatocytes cultured in each medium on days 2, 4 and 6 in duplicate culture dishes, as described in detail previously (Nelson *et al.*, 2000); see Chapter 2, Sections 2.3.7.1 and 2.3.7.2). Plating efficiency, measured on day 1 cultures for each test media, was defined as the TP content as the percentage of the TP content measured, compared to the number of fresh cells seeded into each dish (Watts *et al.*, 1995).

3.3.5 Morphology

3.3.5.1 Light microscopy: phase contrast microscopy

An objective assessment was made of the gross morphology of the cells cultured on TCP dishes in the different media by: (a) Two independent, blinded observers, and (b) computer-aided image analysis of percentage confluency (see below). Healthy cells

were defined as having (under phase contrast light microscopy): A confluent monolayer of densely packed cells; compact polygonal shape delimited by sharply-defined refractile borders; large bright nuclei; evidence of bile canaliculi (lucent, refractile rim surrounding each hepatocyte), according to Arterburn *et* al., 1995; Berry *et al.*, 1991a; and Moghe *et al.*, 1995. A inverted microscope (Zeiss, Germany) was used to assess culture morphology under phase contrast light microscopy. Photographs recorded hepatocytes in culture using Kodak™ 400 film and a Canon EOS camera. To examine gross morphology, TCP cultured cells were examined under phase-contrast on days 1, 2, 4 and 6 of culture for each test medium and were photographed.

3.3.5.2 Computer-aided image analysis of cultured porcine hepatocytes

Semi-automated computer-aided image analysis was used to quantitatively measure the percentage confluency of each test culture. This was achieved by measurement of the surface area covered by hepatocytes. Images were acquired, processed, and analysed using Image-Pro Plus™ software.

To obtain a representative estimate of culture dish surface area covered by attached cells the following analysis was undertaken. Primary porcine hepatocytes were cultured as described above (Section 3.3.3) for up to 6 days. On days 1, 2, 4, and 6 culture dishes were washed 2x in HBSS, fixed in formal saline, and stained with H&E using standard histological techniques. Images were acquired using a Coolsnap™ CCD camera (RS Photometrics) attached to a BH2 BHS microscope (Olympus™) via a 0.63x C-mount adapter. Acquisition and analysis were performed using Image-Pro Plus™ (version 4.5, MediaCybernetics™). Five randomly selected fields were acquired per culture dish, one for each test medium, and the percentage area containing no cells assessed using Image-Pro Plus. This was performed in duplicate for 3 separate isolations. Images were acquired at 1392 x 1040 pixels and saved as TIFF files. Microsoft Excel was then used to collate data and statistical analysis was performed

with the SPSS 9.0 statistical software package using ANOVA and Post Hoc tests as described below (Section 3.3.7).

3.3.6 Transmission electron microscopy

On days 2 and 6, cells cultured in each test medium, obtained from the same isolation as used for the phase-contrast study, were washed in HBSS buffer to remove dead or loosely attached cells and trypsinized with [0.5x] normal trypsin-EDTA (Sigma, St Louis, Mo, USA). Following low-speed centrifugation (20 g; 5 minutes) and washing steps in HBSS / 5 % FBS to neutralize trypsin activity, the cell pellet was resuspended and fixed with 3% glutaraldhyde in O.l M sodium cacodylate buffer solution (Sabatini *et al.*, 1963) at pH 7.3 for two and a half hours at room temperature. Fresh liver tissue and freshly isolated cells were similarly treated as controls. After several washings with cacodylate buffer solution the samples were post-fixed with 1% osmium tetroxide in O.l M cacodylate buffer solution (Palade, 1952) at pH 7.3 for one hour at room temperature. Following dehydration in a graded series of acetone solutions (50, 70, 90, and 100 % (3 times)), the tissue was infiltrated and embedded in araldite mixture. In order to orientate and select an area for the ultrastructural observations, 1 μm semi-thin sections were cut with glass knives, stained with 1% toluidine blue and examined under the light microscope. Ultra-thin sections with silver gold interference colour (approximately 70-80 nm in thickness) were cut on an OMU4-Reichert Ultracut ultramicrotome and collected on 200 mesh uncoated copper grids. The sections were double stained in saturated uranyl acetate in 50% methanol for 30 minutes followed by lead citrate in water (Hayat, 1970) for 5 minutes. Ten areas from each of 4 copper grids were selected for investigation and representative grids examined and photographed in a Philips CM12 electron microscope at 80kV.

3.3.7 Statistical analysis

For each parameter, multiple comparisons were made using ANOVA of: 1) between media evaluations on each day of culture and 2) between day evaluations for each medium formulation. One-way single factor ANOVA (assuming equal variances) was subsequently performed followed by *Post Hoc* multiple comparisons tests of *least significant differences* using the SPSS 9.0 statistical software package. The mean difference was considered significant at the 0.05 level. Statistical tables (Tables 3.1-3.6) show relevant p-values for multiple comparisons of either or both 1) and 2) above.

3.4 Results

3.4.1 Morphology, plating efficiency and viability of porcine hepatocytes

3.4.2 Cell isolation viability and yield

The hepatocytes were isolated using our *ex vivo* method described in detail in Chapter 2. For these experiments, cell viability was 87±5% (Mean±SEM) with a yield of 2.2±0.8 x 10^{10} (Mean±SEM) cells from 12±1 kg piglets (n=10). Trypan blue viability of fresh cell suspensions was verified by assessing *in vitro* cell attachment efficiencies (see below) after 16 hours (day 1) culture in each medium formulation (Gerlach *et al.*, 1994c).

3.4.3 Total cellular protein content

Between media evaluations of total cellular protein content were made on each day of culture (Figure 3.1 and Table 3.1). Plating efficiencies on day 1 for WE, HM, M199 and M1640 were 86±9, 75±9, 99±12 and 87±12 %, respectively. Although medium formulation did not appear to significantly influence establishment of cell culture on

day 1, the plating efficiencies confirmed the high quality isolate, initially determined with the trypan blue exclusion test. Total protein content for freshly isolated hepatocytes was 0.84 mg/10^6 cells determined from the slope of a linear regression curve constructed over a range of counted cell samples (0.6-20 x 10^6 cells) shown in Figure 3.1.1. Total protein content for the cells cultured for 2 days in WE, HM, M199 and RPMI 1640 media were 9.8±0.6, 7.3±1.0, 10.5±1.0 and 7.0±0.9 mg/ culture dish; corresponding to 11.7±0.7, 8.7±1.2, 12.5±1.2 and 8.3±1.1 x10^6 cells/ dish, respectively. Total protein content was significantly higher in M199 than HM ($p=0.013$) and RPMI 1640 ($p=0.006$), whereas WE medium attained significantly greater cellular protein levels than HM ($p=0.043$) and RPMI 1640 ($p=0.028$). This suggests that the type of medium influenced cell proliferation by culture day 2 with M199 in particular stimulating growth. Total protein content up to day 6 of culture averaged ≈9mg/ culture dish, with the exception of RPMI 1640 grown hepatocytes at 6.1±1.1 mg; although the difference was not found to be statistically significant. All other media comparisons (Table 3.1) and between day comparisons for each medium formulation were not significantly different at the 5% level.

Figure 3.1 Total Protein Content Of Porcine Hepatocytes Cultured In Four Separate Chemically-Defined Media Formulations

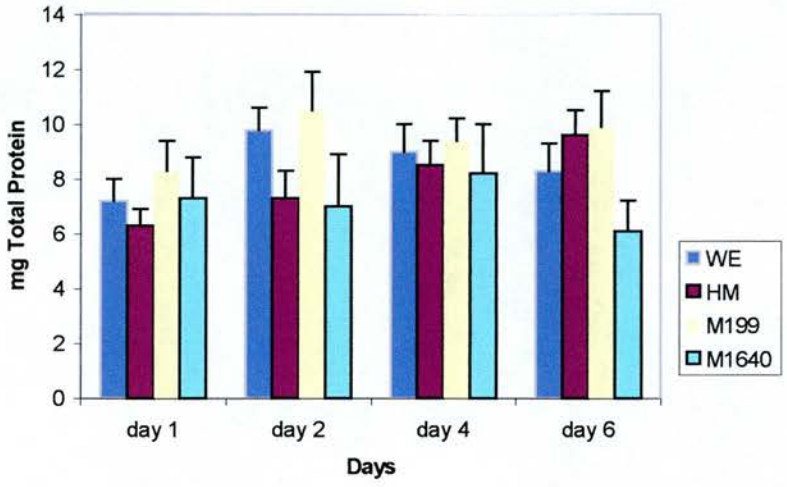

Figure 3.1 Porcine hepatocytes were seeded at 10^7 viable cells per 100mm dish in William's E, HM, M199 and M1640 chemically-defined media for up to 6 days. Cells were scraped from dishes on days 1, 2, 4 and 6 and total protein content determined using the Bradford assay. Results are expressed as mg total protein per dish as a measure of biomass (cell number). All values represent the mean±SEM of seven (day 1) and ten (days 2, 4, 6) experiments performed in duplicate culture dishes.

Table 3.1 Showing p-values for Post Hoc (least significant difference; LSD) Pairwise Multiple Comparisons of Total Protein Following Oneway ANOVA Single Factor Analysis

Media	p-value Day 1	Day 2	Day 4	Day 6
WE *vs* HM	0.511	0.043*	0.786	0.557
WE *vs* M199	0.411	0.544	0.820	0.476
WE *vs* M1640	0.922	0.028*	0.669	0.348
HM *vs* M199	0.131	0.013*	0.618	0.899
HM *vs* M1640	0.433	0.776	0.876	0.131
M199 *vs* M1640	0.451	0.006**	0.513	0.103

* Significant at the level $p<0.05$; **Significant at the level $p<0.01$**

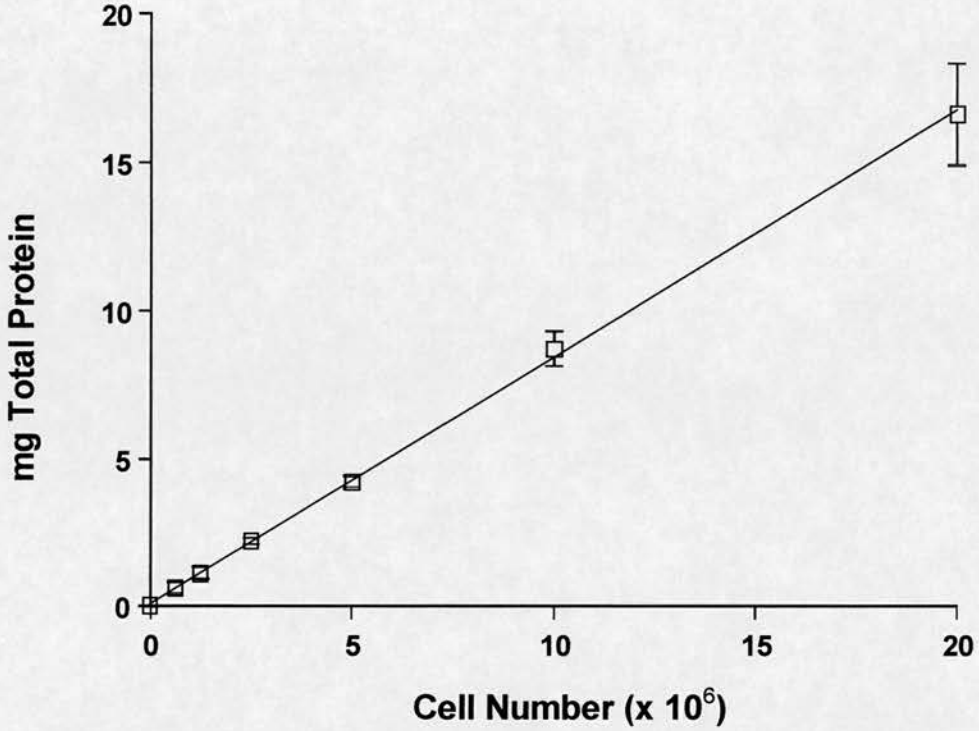

Figure 3.1.1 Graph Showing Total Protein Content of Freshly Isolated Primary Porcine Hepatocytes as a Function of Cell Number Counted

Following the cell purification procedure (Chapter 2), isolated hepatocytes were stained with trypan blue and viable cells counted using a Neubauer haemocytometer. Aliquots of 0.6, 1.2, 2.5, 5.0, 10, and 20 x 10^6 cells were taken in duplicate from 4 separate isolations and total protein content analysed using the Bradford assay modified for a COBAS FARA centrifugal analyser (Chapter 2, Section 2.3.7.1). The data was fitted to a linear regression curve ($y = 0.84x + 0.1$) using FigP (version 2.5) software programme. Total protein content was 0.84 mg/10^6 cells determined from the slope (x) of the curve. The correlation coefficient, r^2 was 0.999 while the intra-assay coefficient of variance (CV) was 5% and the inter-assay CV was 8%.

3.4.4 Hepatocyte culture viability as a function of percentage retained LDH activity

Primary porcine hepatocytes were shown to retain high viability throughout the culture period. The choice of medium had significant influence on retained LDH activity in HM medium on day 2. Between-media comparisons of cell viability were made on each day of culture (Figure 3.2 and Table 3.2). Both WE and M199 media displayed significantly higher viability ($p<0.05$) compared to HM medium on culture day 2 (96±1, 96±1, 85±6 %, respectively). Viability in RPMI 1640 was higher (87±11) than HM medium, although the difference was not significant. By day 4 of culture, the greatest difference in viability was observed between M199 and RPMI 1640 (96±2 *vs* 82±8 %, respectively; $p=0.063$). Viability remained very stable at 93±2% in all test media except RPMI 1640, which appeared markedly lower at 77±11%, while tending towards statistical significance (M1640 *versus*: WE, $p=0.061$; HM, $p=0.052$; M199, $p=0.057$, respectively). All other media comparisons (Table 3.2) and between day comparisons for each medium formulation were not significantly different at the 5% level.

Figure 3.2 Cell Viability of Porcine Hepatocytes in Four Separate Chemically-Defined Media Formulations Expressed as Percentage Retained Intracellular LDH Activities

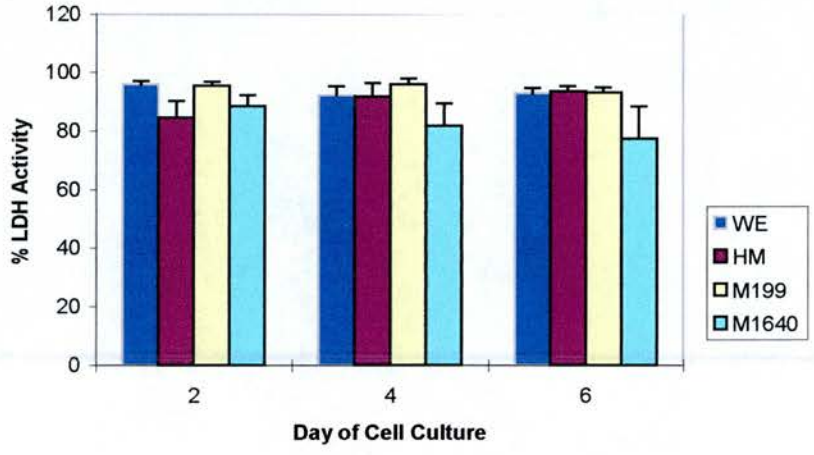

Figure 3.2 Porcine hepatocytes were cultured at 10^7 viable cells per 100mm dish in William's E, HM, M199 and M1640 chemically-defined media for up to 6 days. Samples were taken on days 1, 2, 4 and 6. and LDH activity determined for each medium using a modified LDH assay as described in *Materials and Methods*. Results are expressed as a % of total cytosolic LDH, as an indicator of cell viability. All values represent the means±SEM of eight experiments in duplicate.

Table 3.2 Showing p-values for Post Hoc (least significant difference) Pairwise Multiple Comparisons of LDH Activity Following Oneway ANOVA Single Factor Analysis

Media	p-value Day 2	Day 4	Day 6
WE *vs* HM	0.027*	0.948	0.938
WE *vs* M199	0.919	0.632	0.975
WE *vs* M1640	0.147	0.159	0.061
HM *vs* M199	0.034*	0.587	0.963
HM *vs* M1640	0.404	0.179	0.052
M199 *vs* M1640	0.176	0.063	0.057

* Significant at the level $p<0.05$.

3.5 Hepatocyte morphology

3.5.1 Morphology of fresh hepatic tissue and cultured hepatocytes

3.5.1.1 Transmission electron microscopy of fresh liver tissue and isolated hepatocytes

Figure 3.3 shows that fresh liver tissue (panels, A-D) and isolated hepatocytes (panel E) share many common fine structural features. These included one or two nuclei with nucleoli; well-defined plasma- and nuclear membranes; abundant mitochondria and rough endoplasmic reticulum (RER) interspersed between the mitochondria; smooth endoplasmic reticulum (SER); numerous dense glycogen β-particles and rosettes (α-particles) between SER and in close proximity to mitochondria; peroxisomes and lysosomes. Bile canalicula-like structures are evident in both fresh liver tissue (B and D; x28000) and in isolated hepatocytes (E; x3800).

3.5.2 Morphology and image analysis of cultured porcine hepatocytes

3.5.2.1 Morphology of Day 1 cultures under phase contrast light microscopy and computer-aided image analysis (see Section 3.5.6)

The effects of medium formulation on gross cellular morphology and overall culture integrity of day 1 cultures are shown in Figure 3.4. Plating efficiencies (Section 3.4.3), assessed by TP content (Figure 3.1) were not statistically significant between test media. However, quantitative image analysis (Figure 3.13A; Section 3.5.6, page 3-42) supported the morphological observations (Figure 3.4) in terms of confirming differences in the degree of confluency observed between test medium. In particular, M199 appeared superior to both HM and M1640 in promoting initial cell attachment (see also Figure 3.13B). Figure 3.4 shows hepatocytes maintained in HM medium (panels B, F) and to a lesser extent, in M1640 (panels D, H) display the formation of discrete colonies of piled up cells (denoted by asterisks in Figure 3.4) as evidenced by the difficulty in obtaining an even plane of focus throughout the field. Monolayer formation is more evident in M1640. In contrast, cells grown in both M199 (A, E)

and WE (panels C, G) media, establish more classical features of monolayer cultures although with some loosely attached cells still present.

Figure 3.3 (opposite page) Transmission electron microscopy of fresh liver tissue and isolated hepatocytes

Fresh liver tissue and isolated hepatocytes exhibited common fine structural features: Round nuclei (N) with nucleoli (Nu) and well-defined plasma- (Pm, arrows) and nuclear- (Nm) membranes and lysosomes (L, arrow head) (panel A; x3800); abundant mitochondria (Mt) and granular endoplasmic reticulum (ger) interspersed between the mitochondria (panels A, B; x10000 and C; x17000); smooth endoplasmic reticulum and Golgi apparatus (Ga, panel D, x28000); peroxisomes (P) are evident, as well as numerous dense glycogen (G) β-particles and rosettes (α-particles) between smooth endoplasmic reticulum and in close proximity to mitochondria (panels B and C). Bile canalicula-like structures (Bc) are formed between adjacent hepatocytes in both fresh liver tissue (panels B and D;) and in isolated hepatocytes (panel E; x3800).

A

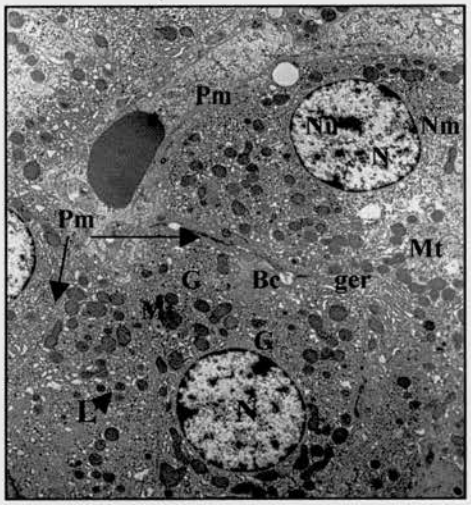
Pm
ND
Nm
N
Pm
Mt
G
Bc
ger
M
G
L
N

B

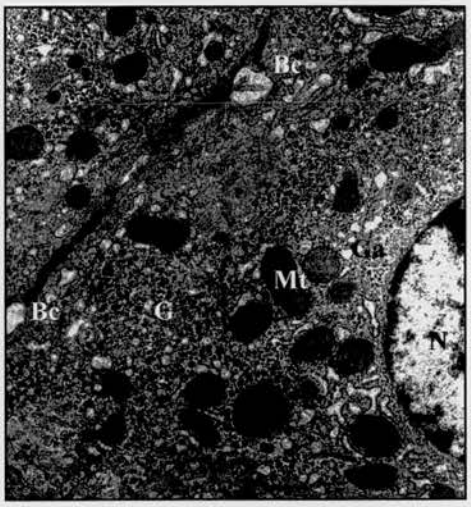
Bc
Ga
Mt
Bc
G
N

C

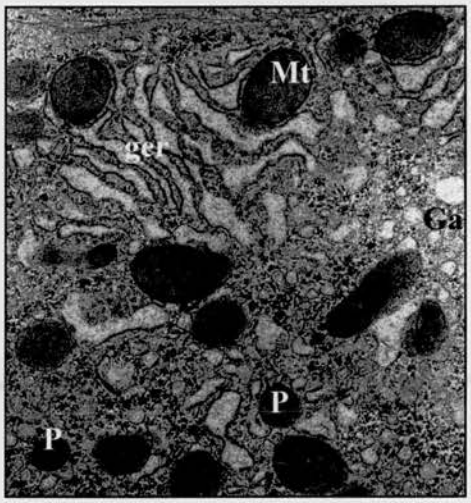
Mt
ger
Ga
P
P

D

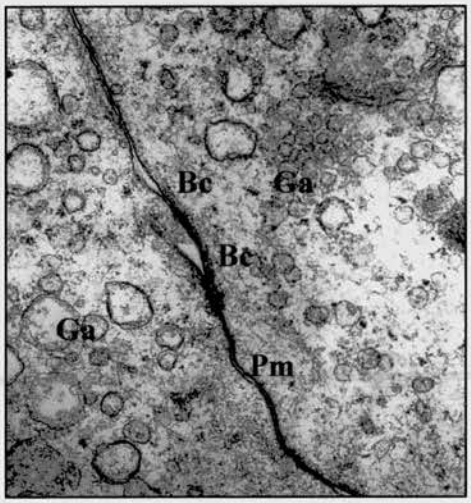
Bc
Ga
Bc
Ga
Pm

E

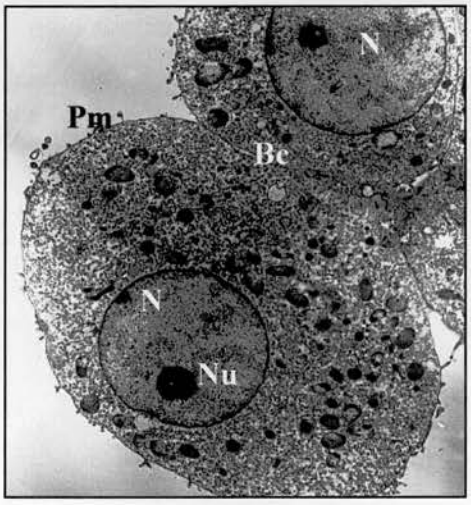
N
Pm
Bc
N
Nu

Figure 3.4 Gross Morphology of Primary Porcine Hepatocytes on Day 1 of Culture

Phase contrast photomicrographs showing gross morphology of primary porcine hepatocyte cultures, 16 hours post-seeding in serum-free chemically-defined WE, HM, M199 and M1640 media (A-D respectively; x100; scale bar 100μm) and corresponding higher magnification photographs (E-F; x200; scale bar 50μm). Cells were seeded at a density of 10^7 viable cells per 100mm tissue culture plastic (TCP) dish in 8ml of each of the four test media (WE, HM, M199, M1640) at 37^0C as described in Section 3.3.3. The appearance of cultured cells was assessed for day 1 (and subsequent cultures) using an inverted phase contrast microscope, by 2 independent blinded observers using the criteria outlined in Section 3.3.5.1. These images show the influence of test media on the attachment efficiency or degree of confluency on culture day 1. The corresponding total protein content and image analysis data is shown in Sections 3.4.3 and 3.5.6, respectively. Cells grown in both WE (panels A, E) and M199 (panels C, G) media appear as almost confluent monolayers whereas HM (panels B, F) and M1640 (panels D, H) maintained cells form partial monolayers with discrete colonies of piled up cells (asterisks).

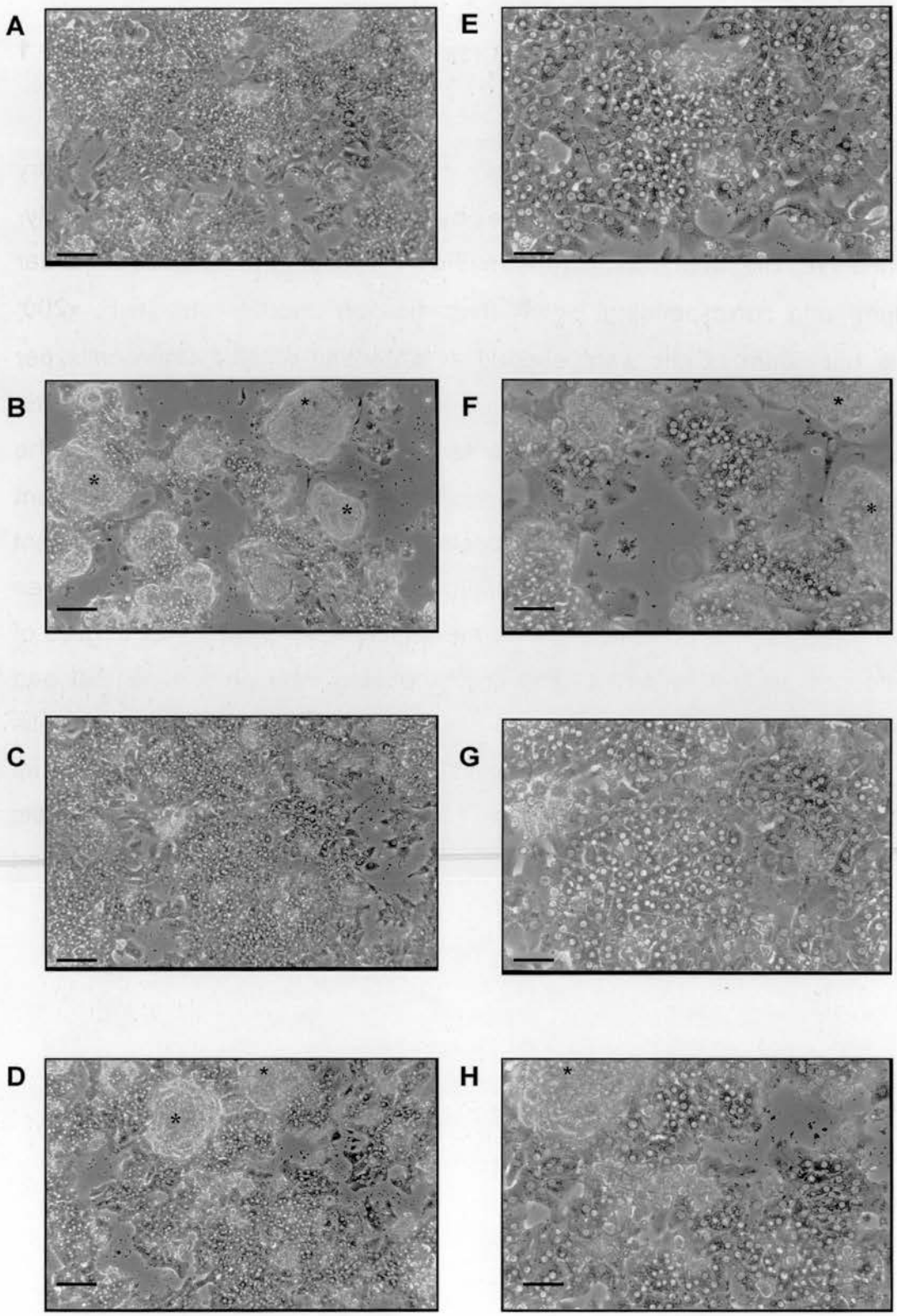
A
E
B
F
C
G
D
H

3.5.3 Morphology and image analysis of day 2 cultures

3.5.3.1 Phase contrast light microscopy and image analysis

Hepatocytes maintained for 2 days in both WE (Figure 3.5, A-B) and M199 (Figure 3.7, A-B) show characteristic morphology of healthy cell culture monolayers. This was confirmed by 2 independent observers. These cultures, under phase contrast reached an almost confluent monolayer of densely packed cells, which exhibited a compact polygonal cell shape delimited by sharply-defined refractile borders, containing bright nuclei. The lucent rim surrounding each hepatocyte represents the presence of bile canaliculi-like structures. Percentage confluency was also enhanced in WE and M199 cells as confirmed by image analysis (Section 3.5.6; Figure 3.13) and supported by TP data (Figure 3.1). Contrastingly, discrete cell colonies (denoted by asterisks in Figures 3.6 and 3.8) were conspicuous in HM- (Figure 3.6, A-B) and M1640-grown (Figure 3.8, A-B) day 2 cultures, which persisted up to day 4 in HM maintained cultures (not shown). In both media, monolayers of hepatocytes were more evident than on day 1, although with areas devoid of cells. In addition, hepatocyte monolayers cultured in HM and, to a lesser extent in M1640, were generally more spread out (see Figure 3.6, A-B) on the TCP surface compared to WE and M199 cultures often showing cellular processes including pseudopodia (Figure 3.6, B). These morphological characteristics were evident up to day 4 of culture (not shown).

3.5.3.2 Transmission electron microscopy (TEM)

All day 2 cells had a non-polyhedral, rounded appearance probably as a result of the trypsinization process. However, only WE (Figure 3.5, C-F) and M199 (Figure 3.7, C-F) cultured hepatocytes showed many of the classical ultrastructural features of fresh liver tissue. Some WE grown hepatocytes, uniquely, showed bile canaliculi-like structures (Figure 3.5, panels C, E) (confirmed using fluorescein diacetate fluorescence microscopy; not shown) and Golgi saccules (with very low density lipoprotein granules). On the other hand, M199 grown hepatocytyes contained a much greater RER network (which correlated with high total protein content and albumin synthesis rate on day 2) and glycogen content (which correlated with high PAS staining; not shown) than all other test media. In contrast, both HM (Figure 3.6, C-D) and M1640 (Figure 3.8, C-D) cultures exhibited less mitochondria, lipid droplets, discrete fluid filled vacuoles and showed asymmetric swelling of the outer mitochondrial compartment.

Figure 3.5 Gross and Ultrastructural Morphology of Hepatocytes Cultured In William's E Medium for 2 Days

Panels A and B: Representative phase contrast photographs showing gross morphology of primary porcine hepatocyte cultures, 2 days post-seeding in serum-free chemically-defined WE medium (A, x100; scale bar 100μm) and corresponding higher magnification photographs (B; x200; scale bar 50μm). These images show the influence of WE medium on the attachment efficiency or degree of confluency on culture day 2. The corresponding total protein content and image analysis data is shown in Sections 3.4.3 and 3.5.6, respectively. Note the classical confluent monolayer of densely packed cells, exhibiting a compact polygonal cell shape delimited by sharply-defined refractile borders containing bright nuclei. Cells were cultured and analysed as outlined in Figure 3.4.

Panels C-F: Transmission electron micrographs of the cultured hepatocytes shown in panels A and B. The micrographs in panels C (x 5000), D (x8000) and E (x8000) demonstrate a uniform distribution of the classical ultrastructural features of fresh liver tissue including: intact plasma membrane (Pm) with microvilli (Mv), large round nucleus (N) with nucleoli (Nu), abundant mitochondria (Mt), lysosomes (L, arrow heads) and granular endoplasmic reticulum (ger) surrounding mitochondria; panel E shows clearly electron-dense glycogen granules (G) and the presence of a bile canalicula (Bc) whereas panel F (x75000) shows hepatocyte fine structure including mitochondrial cristae (Mtc), granular endoplasmic reticulum with attached ribosomes and part of the nucleus (N). Cells were cultured and processed as described in *Materials and Methods* (Section 3.3.6).

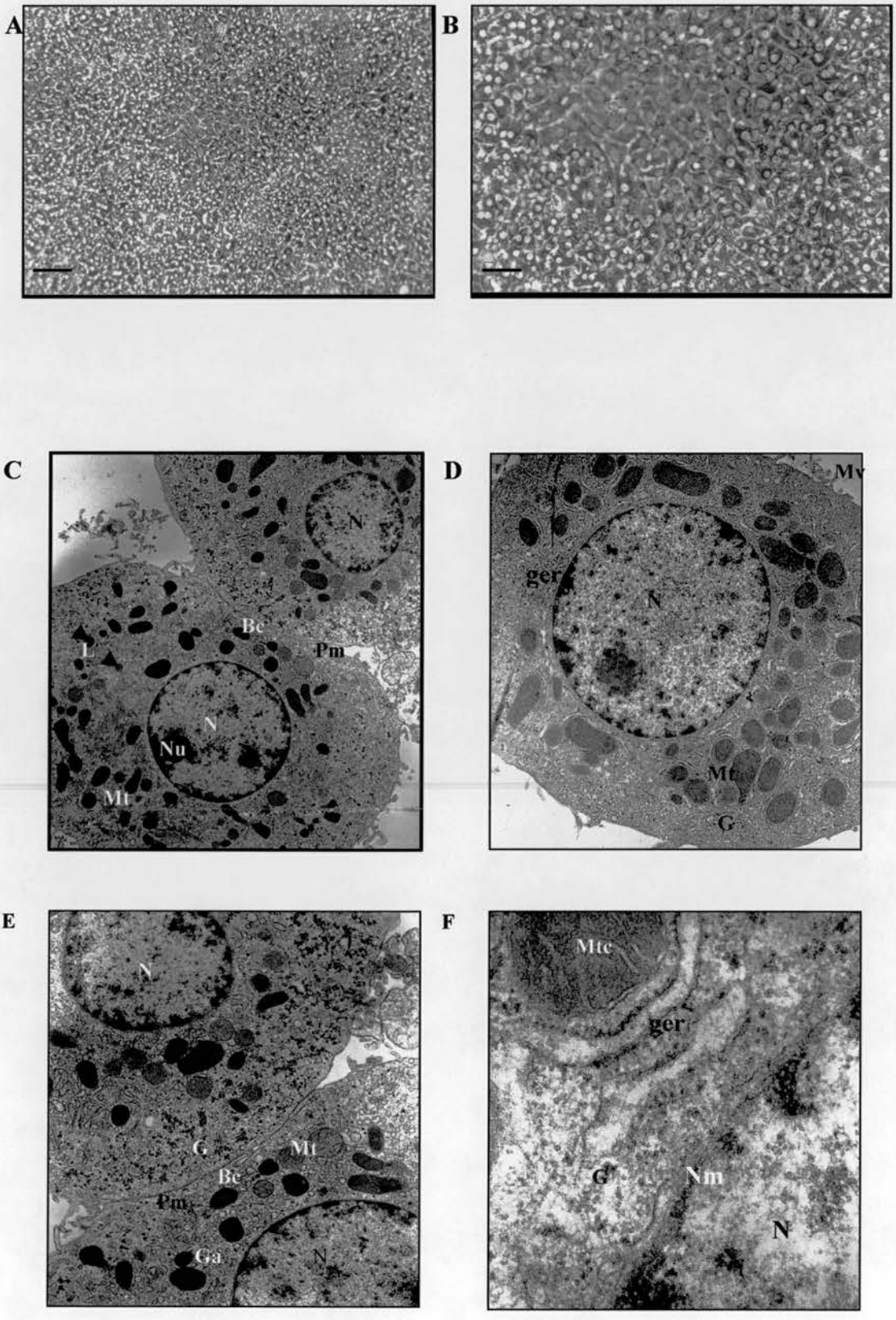
A
B
C
N
Bc
L
Pm
N
Nu
Mt
D
Mv
ger
N
Mt
G
E
N
G
Mt
Bc
Pm
Ga
N
F
Mtc
ger
G
Nm
N

Figure 3.6 Gross and Ultrastructural Morphology of Hepatocytes Cultured In Hepatocyte Medium for 2 Days

Panels A and B: Representative phase contrast photographs showing gross morphology of primary porcine hepatocyte cultures, 2 days post-seeding in serum-free chemically-defined HM medium (A, x100; scale bar 100μm) and corresponding higher magnification photographs (B; x200; scale bar 50μm). These images show the influence of HM medium on the attachment efficiency or degree of confluency on culture day 2. The corresponding total protein content and image analysis data is shown in Sections 3.4.3 and 3.5.6, respectively. Discrete cell colonies (black asterisk) are a conspicuous feature, which persisted up to day 4 (not shown) Monolayers of hepatocytes were more evident than on day 1, although with areas devoid of cells (white asterisks). In addition, hepatocyte monolayers cultured in HM were generally more spread out on the TCP surface (compared to WE and M199 cultures) often showing cellular processes including pseudopodia (arrow heads, panel A). Cells were cultured and analysed as outlined in Figure 3.4.

Panels C-D: Transmission electron micrographs of the cultured hepatocytes shown in panels A and B. Panel C (x 6500) displays a binucleate hepatocyte although with evidence of degenerative cell abnormalities such as vacuolation (V), few mitochondria and other organelles, and asymmetric mitochondrial swelling (aMt). Panel D (x75000) shows that some normal fine structure is maintained with mitochondrial cristae (Mtc), granular endoplasmic reticulum (ger) and glycogen storage granules (G) in evidence. Cells were cultured and processed as described in *Materials and Methods*.

A

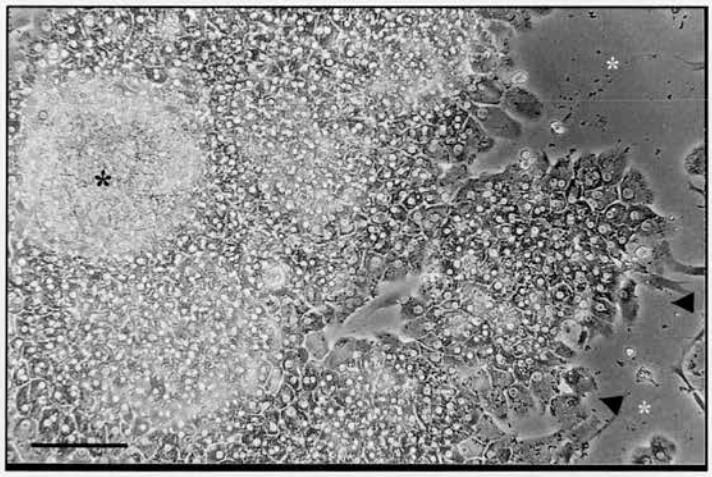

B

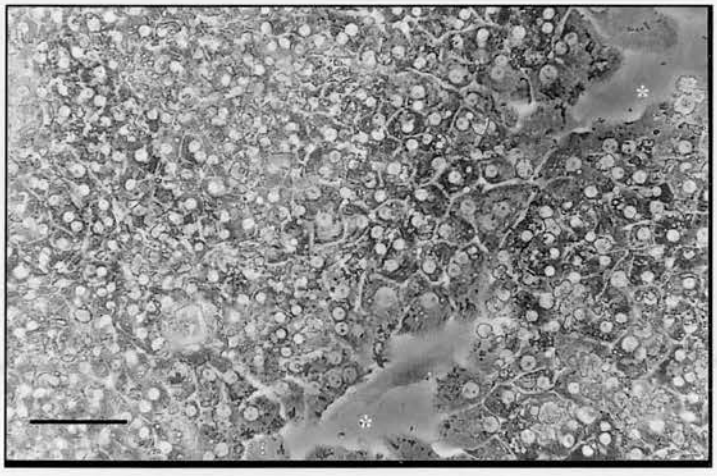

C

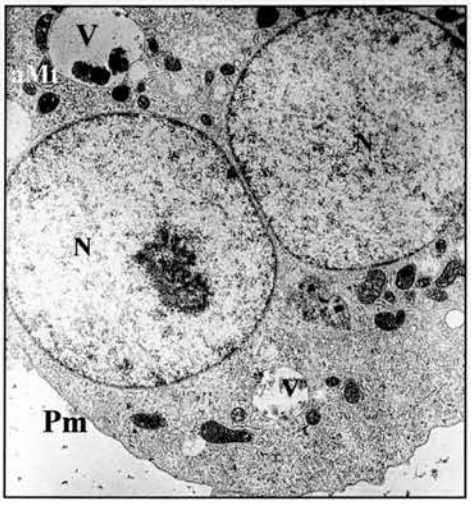

D

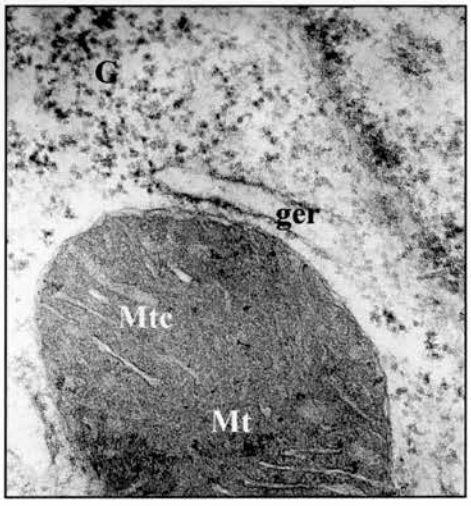

Figure 3.7 Gross and Ultrastructural Morphology of Hepatocytes Cultured In Medium 199 for 2 Days

Panels A and B: Representative phase contrast photographs showing gross morphology of primary porcine hepatocyte cultures, 2 days post-seeding in serum-free chemically-defined M199 medium (A, x100; scale bar 100μm) and corresponding higher magnification photographs (B; x200; scale bar 50μm). These images show the influence of M199 medium on the attachment efficiency or degree of confluency on culture day 2. The corresponding total protein content and image analysis data is shown in Sections 3.4.3 and 3.5.6, respectively. In common with WE-grown hepatocytes, these cells exhibit a classical confluent monolayer of densely packed cells and a compact polygonal cell shape delimited by sharply-defined refractile borders containing bright nuclei. Cells were cultured and analysed as outlined in Figure 3.4.

Panels C-F: Transmission electron micrographs of the cultured hepatocytes shown in panels A and B. Panel C (x 6500) shows a binucleate hepatocyte with prominent nucleoli (Nu), and classical ultrastructural features of fresh liver tissue including: many mitochondria, granular endoplasmic reticulum (ger), glycogen particles (G) and other sub-cellular organelles. Panels D (x22000), E (x28000) and F (x75000) shows clearly electron-dense glycogen granules (G) and free ribosomes (R), and many mitochondria surrounded by granular endoplasmic reticulum. Part nucleus (N) is indicated in D and E. Cells were cultured and processed as described in *Materials and Methods*.

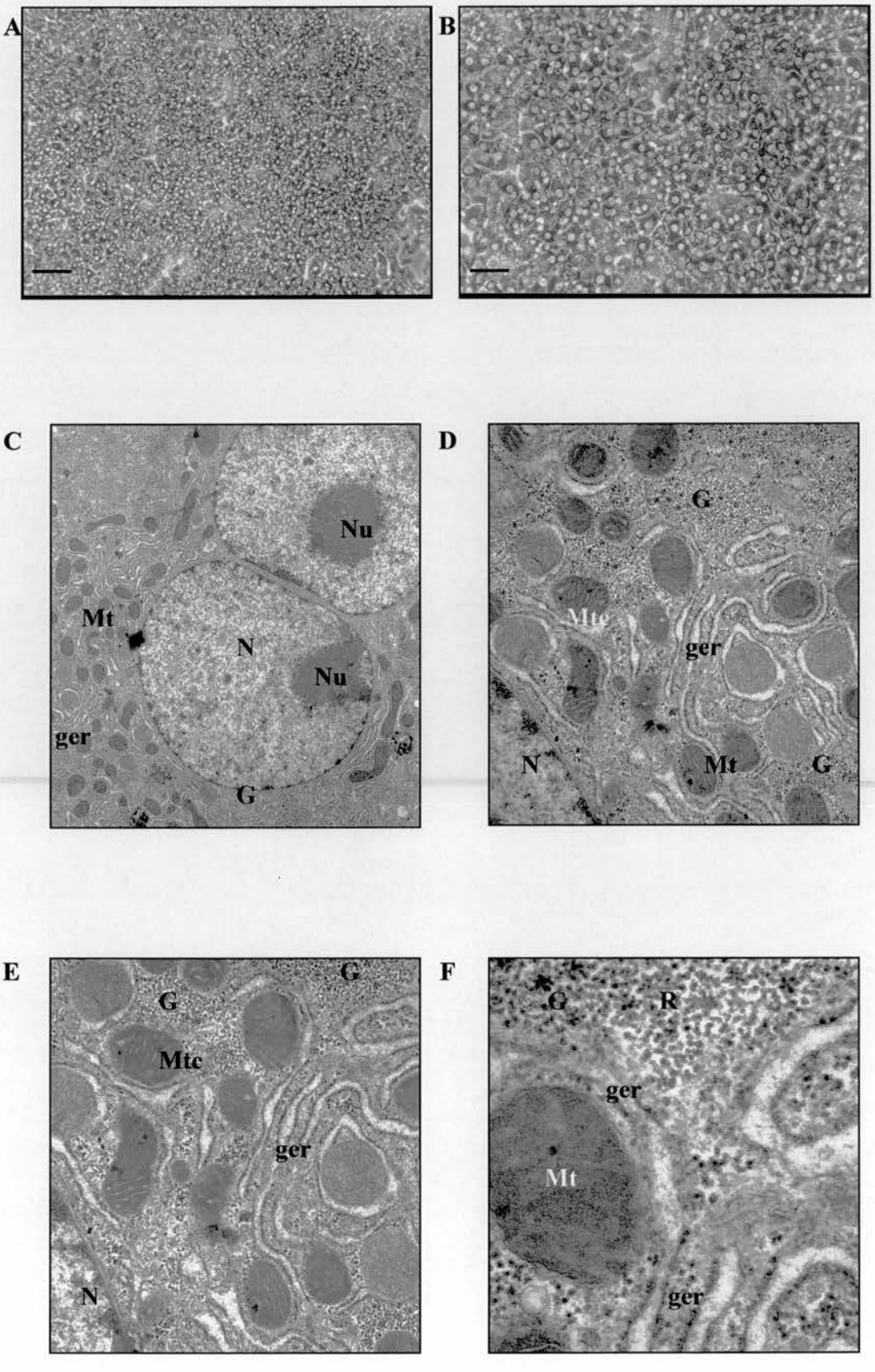
A
B
C
Nu
Mt
N
Nu
ger
G
D
G
Mtc
ger
N
Mt
G
E
G
G
Mtc
ger
N
F
G
R
ger
Mt
ger

Figure 3.8 Gross and Ultrastructural Morphology of Hepatocytes Cultured In RPMI 1640 Medium for 2 Days

Panels A and B: Representative phase contrast photographs showing gross morphology of primary porcine hepatocyte cultures, 2 days post-seeding in serum-free chemically-defined M1640 medium (A, x100; scale bar 100μm) and corresponding higher magnification photographs (B; x200; scale bar 50μm). These images show the influence of M1640 medium on the attachment efficiency or degree of confluency on culture day 2. The corresponding total protein content and image analysis data is shown in Sections 3.4.3 and 3.5.6, respectively. Discrete cell colonies are a prominent feature (black asterisks), which persisted up to day 4 (not shown). In addition, hepatocyte monolayers cultured in M1640 displayed areas of compact and 'spread out' monolayers and some regions devoid of cells (white asterisk in panel A). Cells were cultured and analysed as outlined in Figure 3.4.

Panels C-E: Transmission electron micrographs of the cultured hepatocytes shown in panels A and B. Panels C (x 5000) and D (x6300) display hepatocytes with normal nuclei (N) and nucleoli (Nu, panel C), although with clear evidence of degenerative cell abnormalities including extensive vacuolation (V), lipid droplets (Ld) and asymmetric mitochondrial swelling (aMt). Panel E (x28000) shows that some normal fine structure is maintained with normal mitochondria (Mt), granular endoplasmic reticulum (ger) and glycogen storage granules (G) in evidence. Cells were cultured and processed as described in *Materials and Methods*.

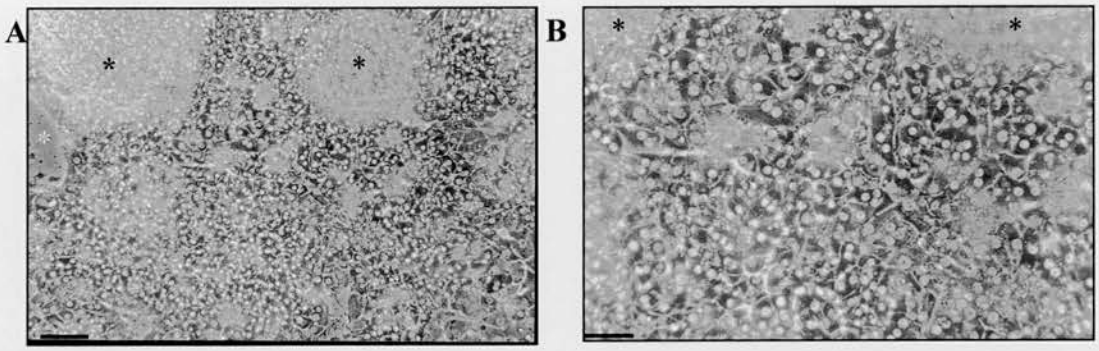
A
B

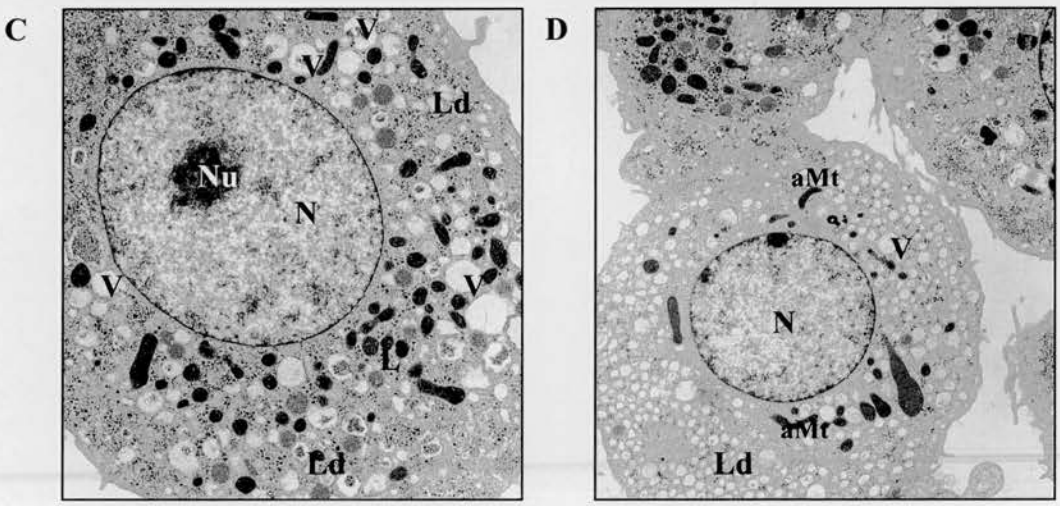
C
V
V
Ld
Nu
N
V
V
L
Ld
D
aMt
V
N
aMt
Ld

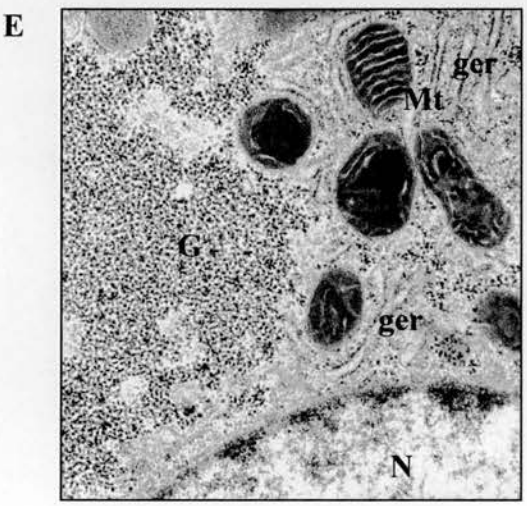
E
ger
Mt
G
ger
N

3.5.4 Morphology and image analysis of day 6 cultures

3.5.4.1 Phase contrast light microscopy and image analysis

All cultures maintained in each test medium showed distinct but varying signs of degeneration by day 6 (Figures 3.9-3.12) including cell detachment, general loss or 'blurring' of delineating cell borders, nuclear fragmentation and the appearance of necrotic and apoptotic cells. A striking feature of WE medium was the appearance in culture of discrete foci of small cell aggregates (denoted by F^* in Figure 3.9, A-B) with a radiating cord-like arrangement of hepatocytes reminiscent of the *in vivo* cell microenvironment. However, although cell detachment was clearly evident, hepatocyte morphology was well preserved and similar to day 4 cultures. A distinct feature of HM cultures was the presence of small rounded structures, possibly lipid droplets or small vacuoles (Figure 3.10C). No quantitative differences in % confluency were observed between media on day 6 (Figure 3.13A)

3.5.4.2 Transmission electron microscopy

By day 6, vacuolation, organellar swelling, ER vesiculation and irregular hepatocyte shape were more exaggerated and widespread in HM (Figure 3.10, C-D) and M1640 (Figure 3.12, C) cultures compared with WE (Figure 3.9, C) and M199 (Figure 3.11, C) maintained cells.

Figure 3.9 Gross and Ultrastructural Morphology of Hepatocytes Cultured In William's E Medium for 6 days

Panels A and B: Representative phase contrast photographs showing gross morphology of primary porcine hepatocyte cultures, 6 days post-seeding in serum-free chemically-defined WE medium (A, x100; scale bar 100μm) and corresponding higher magnification photographs (B; x200; scale bar 50μm). These images show the influence of WE medium on the attachment efficiency or degree of confluency on culture day 6. The corresponding total protein content and image analysis data is shown in Sections 3.4.3 and 3.5.6, respectively. Note the appearance in culture of discrete foci (denoted by F^*) of small cell aggregates (Figure 4.3 A and B) with a radiating cord-like arrangement of hepatocytes, reminiscent of the *in vivo* cell microenvironment. However, both cell detachment and poor overall morphology compared with day 2 cultures was evident. Cells were cultured and analysed as outlined in Figure 3.4.

Panels C: Transmission electron micrograph of the cultured hepatocytes shown in panels A and B. The micrograph in panel C (x 5000) shows some features of degenerating and damaged hepatocytes; including irregular shape, vacuolation (V) more prevalent in the lower cell (devoid of mitochondria), and both normal (Mt) abnormally shaped (aMt) mitochondria. Cells were cultured and processed as described in *Materials and Methods*.

A

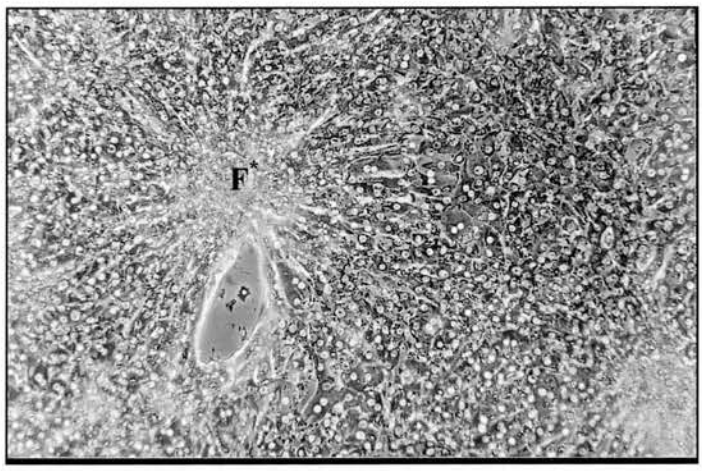

B

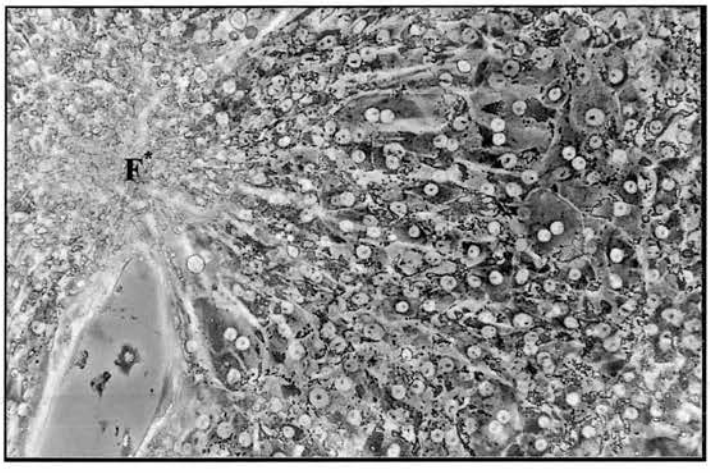

C

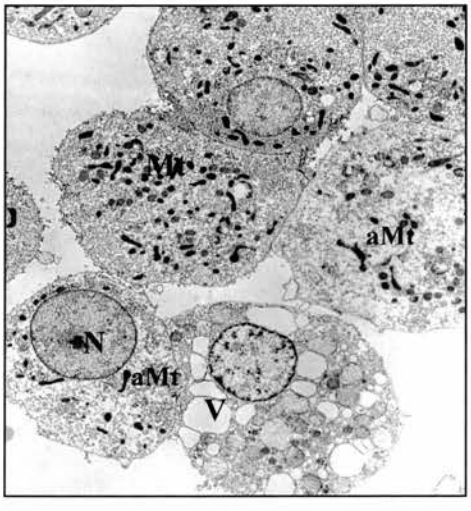

Figure 3.10 Gross and Ultrastructural Morphology of Hepatocytes Cultured In Hepatocyte Medium for 6 Days

Panels A and B: Representative phase contrast photographs showing gross morphology of primary porcine hepatocyte cultures, 6 days post-seeding in serum-free chemically-defined HM medium (A, x100; scale bar 100μ) and corresponding higher magnification photographs (B; x200; scale bar 50μ). These images show the influence of HM medium on the attachment efficiency or degree of confluency on culture day 6. The corresponding total protein content and image analysis data is shown in Sections 3.4.3 and 3.5.6, respectively. Discrete cell colonies are less common (panels A and B, black asterisks) and signs of cell degeneration, including cell detachment (panel A, white asterisks), general loss of delineating cell borders (panels A and B, black arrows) and the appearance of lipid droplets and / or vacuoles (panel B, white arrow). Cells were cultured and analysed as outlined in Figure 3.4.

Panel C: Transmission electron micrograph of the cultured hepatocytes shown in panels A and B. The micrograph in panel C (x 3800) shows features of degenerating and damaged hepatocytes including: extensive vacuolation (V), abnormally shaped mitochondria (aMt) and areas devoid of organelles. Panel D (x17000) shows loss of integrity of the endoplasmic reticulum and adjacent to the large vacuole is a mitochondria with asymmetric swelling (aMt) of the outer compartment. Glycogen particles (G) are however, in evidence. Cells were cultured and processed as described in *Materials and Methods*.

A

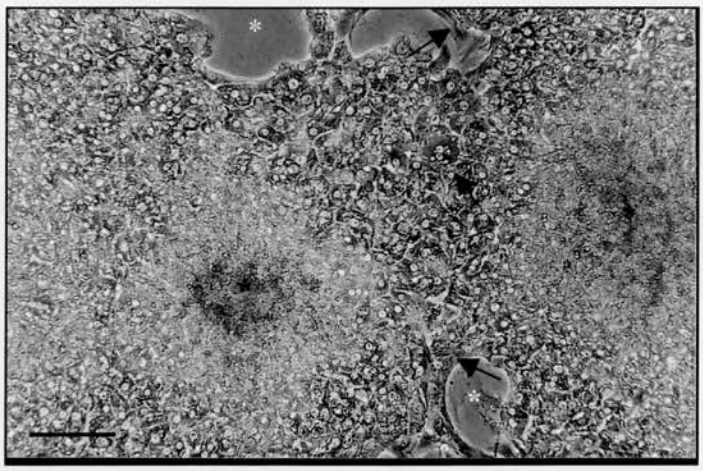

B

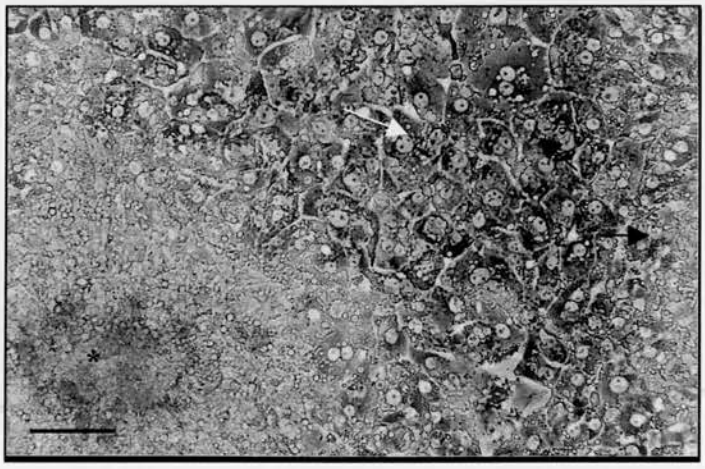

C

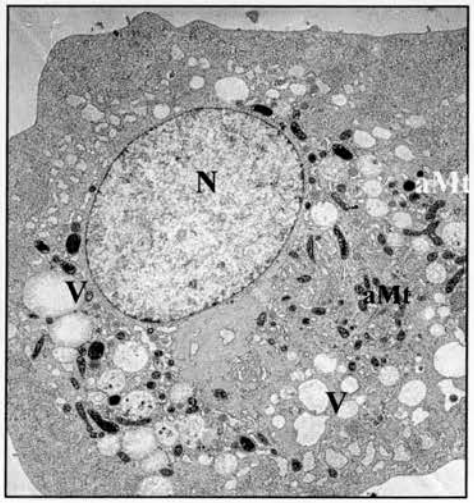

D

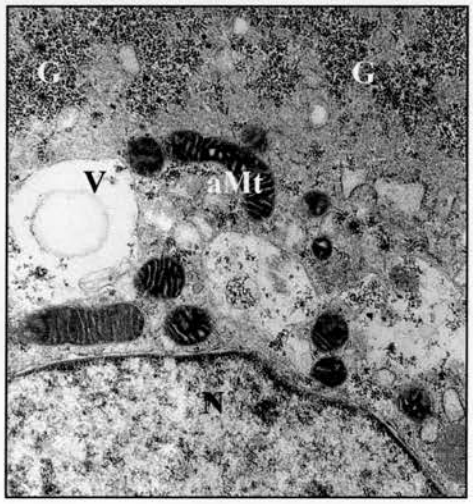

Figure 3.11 Gross and Ultrastructural Morphology of Hepatocytes Cultured In Medium 199 for 6 days

Panels A and B: Representative phase contrast photographs showing gross morphology of primary porcine hepatocyte cultures, 6 days post-seeding in serum-free chemically-defined M199 medium (A, x100; scale bar 100μm) and corresponding higher magnification photographs (B, x200; scale bar 50μm). These images show the influence of M199 medium on the attachment efficiency or degree of confluency on culture day 6. The corresponding total protein content and image analysis data is shown in Sections 3.4.3 and 3.5.6, respectively. Cell detachment is evident (asterisks) and general signs of cell degeneration such as loss of delineating cell borders and the appearance of apoptotic cells, with cell blebbing (arrows), are clearly seen. Cells were cultured and analysed as outlined in Figure 3.4.

Panels C: Transmission electron micrograph of the cultured hepatocytes shown in panels A and B. The micrograph in panel C (x 3800) shows some features of damaged hepatocytes, including vacuolation (V), fewer cyoplasmic organelles and abnormal nuclear shape (N). Cells were cultured and processed as described in *Materials and Methods*.

A

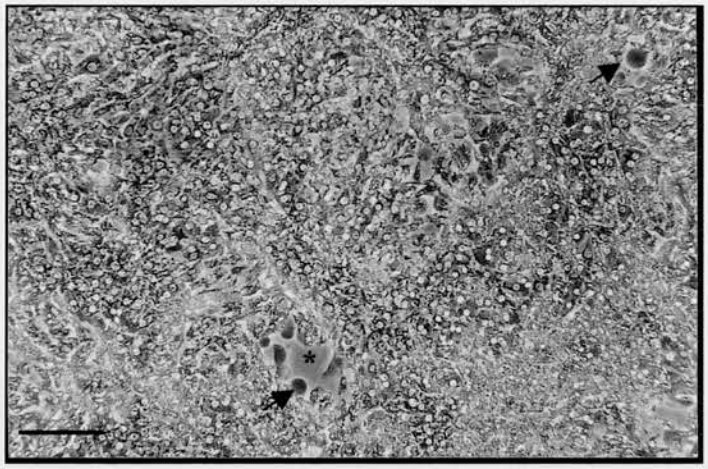

B

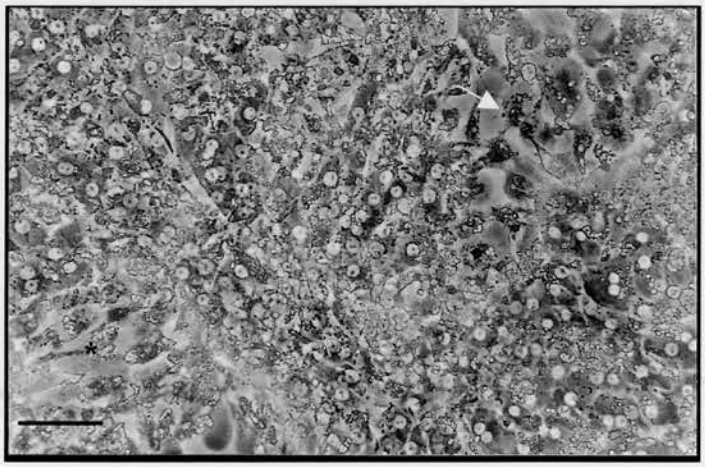

C

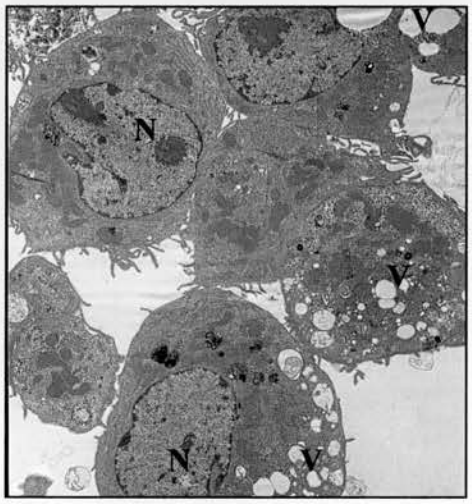

Figure 3.12 Gross and Ultrastructural Morphology of Hepatocytes Cultured In RPMI 1640 Medium for 6 Days

Panels A and B: Representative phase contrast photographs showing gross morphology of primary porcine hepatocyte cultures, 6 days post-seeding in serum-free chemically-defined M1640 medium (A, x100; scale bar 100μm) and corresponding higher magnification photographs (B; x200; scale bar 50μm). These images show the influence of M1640 medium on the attachment efficiency or degree of confluency on culture day 6. The corresponding total protein content and image analysis data is shown in Sections 3.4.3 and 3.5.6, respectively. The cell colonies evident in earlier cultures are no longer present. Cell detachment (asterisks) and degeneration are well under way including general loss of delineating cell borders and the appearance of apoptotic cells (arrows). Cells were cultured and analysed as outlined in Figure 3.4.

Panels C: Transmission electron micrographs of the cultured hepatocytes shown in panels A and B. The micrograph in panel C (x 10000) shows an irreversibly damaged hepatocyte with extensive vacuolation (V), abnormally shaped mitochondria (aMt), areas devoid of organelles and an absent nucleus. Panel D (x3800) shows that some hepatocytes remained intact although there is an abnormal distribution of organelles and little evidence of endoplasmic reticular components and glycogen particles. Cells were cultured and processed as described in *Materials and Methods*.

A

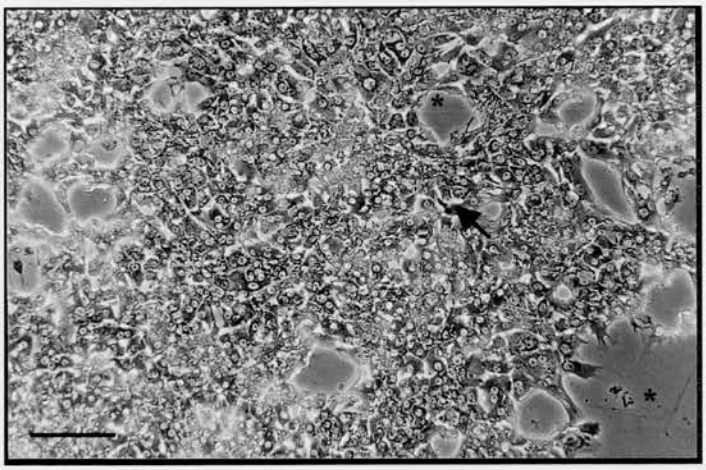

B

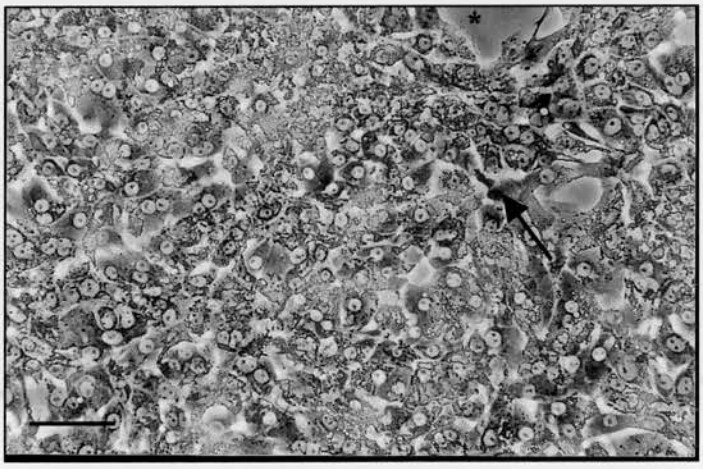

C

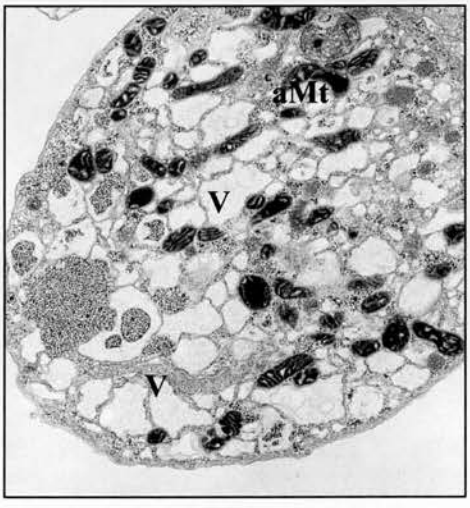

D

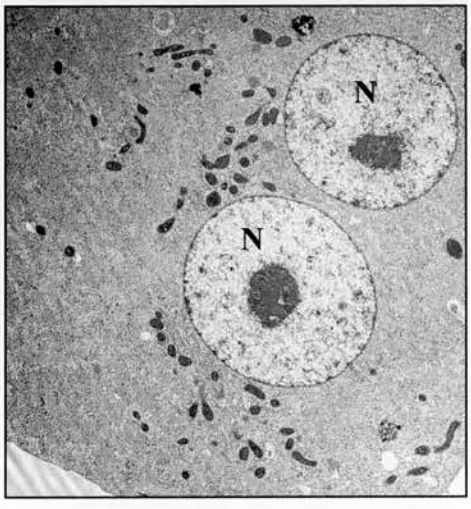

3.5.5 Relative frequencies of cytoplasmic organelles and bile canaliculi examined under TEM

Table 3.3 shows a comparison of relative frequencies of cytoplasmic organelles and bile canaliculus structures on days 2 and 6 of culture for each test medium. Ten areas from each of 4 copper grids per sample for 3 separate isolations were investigated and the number of organelles (nuclei, mitochondria, GER, glycogen granules, and Golgi complex) counted. In addition the presence of bile canaliculi in TEM sections was assessed. Day 2 cultures in WE and M199 appeared to have a full complement of organelles, as observed for fresh liver sections (Figure 3.3) whereas in both HM- and M1640-grown hepatocytes the number of organelles was depleted. Although the relative number of organelles had declined in all media by day 6, the effects were more exaggerated in HM and M1640.

Table 3.3 Relative Frequencies of Cytoplasmic Organelles and Bile Canaliculi Examined Under TEM in Primary Porcine Hepatocytes on Days 2 and 6 of Culture In Chemically-Defined Serum-free Medium Formulations

Organelles	Nuclei	Mitochondria	Ger	Glycogen Granules	Golgi Apparatus	Bile Canaliculi
DAY 2						
WE	+++	+++	+++	+++	+++	+++
HM	+++	++	+	++	+	
M199	+++	+++	+++	+++	+++	
M1640	+++	++	+	++	+	
DAY 6						
WE	++	++	+	++	+	+
HM	+	+	-	++	-	-
M199	++	++	+	++	+	-
M1640	+	+	-	-	-	-

Table 3.3 shows the relative frequencies of cytoplasmic organelles and bile canaliculus structures on days 2 and 6 of culture for each test medium. Ten areas from each of 4 copper grids per sample for 3 separate isolations were investigated and the number of organelles (nuclei, mitochondria, granular endoplasmic reticulum (Ger), glycogen granules, and Golgi complex) counted. In addition the presence of bile canaliculi in TEM sections was assessed.

3.5.6 Computer-aided image analysis of cultured porcine hepatocytes

Semi-automated computer-aided image analysis was performed (in duplicate dishes for each test medium in 3 separate experiments) to make a more objective assessment of morphological differences, such as attachment and adhesion efficiency, between the test media cultures. Between media evaluations on each day of culture were made (Figure 3.13A). In contrast with the total protein data (Section 3.4.3), statistical significance was shown for culture days 1, 2, and 4. In particular, plating efficiencies (PE) on day 1 for WE, HM, M199, and, M1640 maintained cells were 71±14, 38±3, 78±5, and 55±10 respectively; PE being greater in WE ($p<0.05$) and the difference highly significant ($p<0.01$) in M199 cells, compared with HM cells. Percentage confluency was significantly lower ($p<0.01$), notably in HM cultures in relation to all other test media on days 2 and 4; although no statistical significance was observed on day 6. Between day evaluations of each medium revealed (with the exception of HM) significant increases ($p<0.05$) in % confluency in all test media cultures by day 4 compared with initial day 1 cultures suggesting either cell proliferation and/or increased cell spreading had occurred. Mean % confluency values for all test media declined by day 6, although an unexpected significant increase ($p<0.05$) was observed in HM on day 6 compared with day 4. This could be due to the aforementioned, or a delay in cell spreading with culture age.

Opposite page: Figure 3.13B shows examples of image capture photomicrographs (x25) of day 2 WE, HM, M199, and M1640 cultures prior to analysis with the Image-Pro Plus image analysis system. Test culture dishes were washed 2x in HBSS, fixed in formal saline, and stained with H&E using standard histological techniques as described in Materials and Methods (see Section 3.3.5.2). Images were acquired, processed, and analysed using Image-Pro Plus™ software.

Figure 3.13 Percentage confluency of porcine hepatocytes cultured in four separate chemically-defined media formulations assessed by computer-aided image analysis

A) Degree of confluency of hepatocyte cultures on days 1, 2, 4, and 6

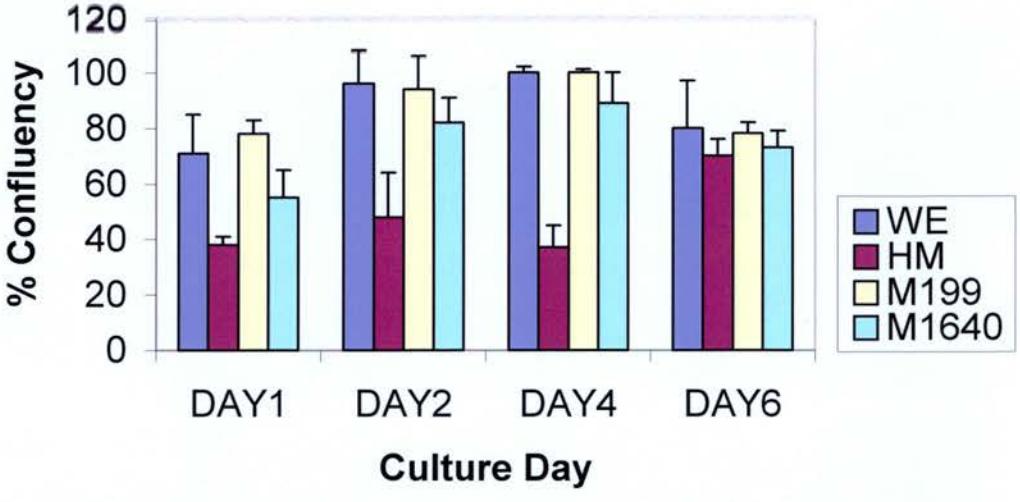

B) Image capture photomicrographs showing degree of confluency of cultured porcine hepatocytes on day 2 following staining with H&E

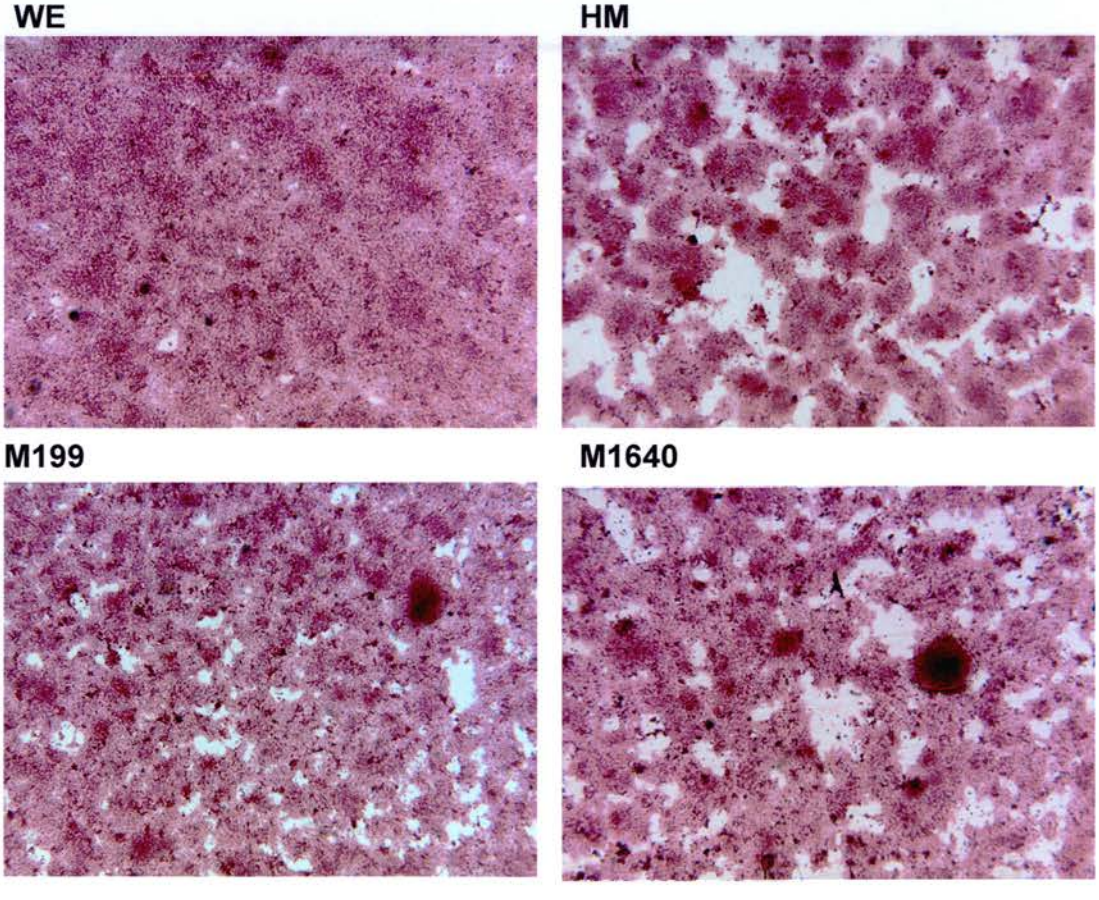

3.6 Discussion

This study was undertaken to evaluate the effect of culture conditions on hepatocyte morphology. Despite the acceptance of PPHs as being the best candidates for current BAL devices, the relative scarcity of morphological (or functional) studies using cultured porcine hepatocytes is increasingly being highlighted (Allen *et al.*, 2001; Joly *et* al., 1997; Gregory *et al.*, 2000; Seilaff *et al.*, 1995b). In contrast, there exists an extensive literature describing the characteristics of rat cultures *in vitro* (LeCluyse *et al.*, 1999). Typical approaches include promotion of homotypic or heterotypic cell-cell interactions, and manipulation of biomatrices or media composition (Allen *et al.*, 2001). Given the importance of these factors in promoting optimal *ex* vivo maintenance of hepatocytes for BAL systems (Selden *et* al., 1999; Strain & Neuberger, 2002), identifying the most favourable medium which preserves PPH phenotype and morphology is one of the first considerations for improving the efficacy of pre-clinical BAL devices (Naik *et al.*, 1996; Watts *et al.*, 1995). To this end, morphological characteristics of cultured porcine hepatocytes, on unmodified TCP were studied under four separate serum-free chemically-defined medium formulations. Inasmuch as this culture system eliminates the confounding variables introduced when using serum and / or biomatrix components, it may also reduce the aforementioned risks associated with use of these factors in BAL devices (Tsiaoussis *et* al., 2001; and Section 3.1).

A major limitation of our culture system, and most other conventional monolayer cultures (LeCluyse *et al.*, 1999) is that hepatocytes did not survive longer than one week on TCP, and had presumably undergone a rapid retro-differentiation. Some investigators have reported, notably in 3D porcine culture configurations, maintenance of long-term differentiated morphology and function for 18 days (DeBartolo *et al.*, 2000), and up to 7 weeks (Gerlach *et al.*, 1995). Whilst PPHs cultured in WE with 1% new born calf serum, maintained albumin and urea synthetic capacity similar to our cultures on TCP dishes, with or without collagen, for up to 19

days. This is clearly not achievable using our culture system on TCP, although the risk of genetic transformation or infection is reduced with short-term cultures.

The rationale for examining hepatocyte morphology and functional activity (Chapter 4) over a 6-day culture period in this study follows from the fact that most porcine-based BAL devices are designed to be operational within 2-4 days of seeding the bioreactor. (Flendrig *et al.*, 1997a; Gerlach *et al.*, 1994a; Kong *et al.*, 1996; Sheil *et al.*, 1996; Sheil *et al.*, 1998; Uchino *et al.*, 1991; Wang *et al.*, 1998). The majority of BAL systems utilise either or both a biomatrix component and serum-supplemented medium for cell support and nutrition. Porcine hepatocytes are inoculated, either extra- or intra-luminally, via synthetic hollow fibres of the bioreactor, onto a variety of substrata. The latter include: monolayer cultures on collagen type I (De Bartolo *et al.*, 2000), microcarriers (Kong *et al.*, 1996), gel-entrapment or alginate beads (Falasca *et* al., 2001; Nyberg *et al.*, 1993; Sielaff *et al.*, 1995a; Sielaff *et al.*, 1995b), Engelbreth-Holm Sarcoma (EHS) gel Natrix and Matrigel (Gerlach *et al.*, 1995). However, the influence of unknown variables, such as the purity and composition of the attachment substrates or heterologous serum, on cellular parameters of growth, function and morphology were not addressed.

These considerations prompted us to evaluate the effects of serum-free chemically-defined media on PPH morphology (and related biochemical parameters). Highly purified recombinant growth factor (L-EGF), insulin and dexamethasone were selected as agents to promote maintenance of PPH cultures. These supplements were chosen since they are considered to have the most marked effects on the morphology, function and survival of hepatocytes on simple substrata (Berry *et al.*, 1991b). Insulin enhances initial cell attachment, important for cells seeded onto TCP. Long-EGF, a synthetic analogue of endogenous EGF, with up to ten-times the mitogenic potency [Sigma Technical Service, personal communication], stimulates DNA synthesis, cell growth, amino acid transport and protein synthesis (Michalopoulos GK, 1990), as well as preservation of tissue-specific functions and hepatocyte morphology (Berry *et al.*, 1991b) acting in a synergistic fashion with insulin. The positive effects of EGF on

liver metabolism parallel those of insulin (Russell and Carver, 1998). Both hormones contribute to the preservation of hepatocyte morphology, survival and tissue-specific functions such as albumin synthesis. This is also true of dexamethasone, which in addition to supressing fibroblast growth, is also resistant to degradation compared to naturally occurring glucocorticoids (Berry *et al.*, 1991a). In addition dexamethasone also promotes retention of a relatively compact, polygonal cell shape and favours the formation of more bile-canalicular-like structures, at least for cultured rat hepatocytes (Berry *et al.*, 1991b; LeCluyse *et al.*, 1996).

It has been suggested however, that the beneficial effects educed by modification of defined media by addition of, for example, dexamethasone or low concentrations of DMSO, may be inapplicable for BAL designs because of systemic exposure of patients to these non-physiological media components (Allen *et al.*, 2001). Moreover, hepatocyte culture media are not approved for medical use. This may not be problematic considering that pre-clinical BAL systems will be flushed prior to connection to the patient's circulation. A complex hemofiltration solution (bicarbonate buffered, glucose, essential minerals) has been identified as suitable for this purpose (Flendrig *et al.*, 1998).

We have shown for the first time that, in the presence of different serum-free chemically-defined media formulations, exogenous attachment substrates or serum are superfluous for the culture of PPHs. High plating efficiencies (PE) and viability on tissue culture plastic can be maintained in the absence of serum or sophisticated substrate for attachment. PPHs have been shown to readily attached to TCP or to uncoated nonwoven polyester matrix material in Chamuleau's BAL device (Flendrig *et al.*, 1997a; Flendrig *et al.*, 1997b; te Velde *et al.*, 1995). To our knowledge, previous studies, including the latter, of PPH cultures in the context of BAL systems, have used serum-supplemented media. The use of non-autologous (bovine) serum may be inappropriate for BAL usage since it is heterogeneous in composition, promotes rapid cellular dedifferentiation and selective growth of non-parenchymal cells and may contain endotoxins (Berry *et al.*, 1991a) and potentially, zoonotic

entities (Enat *et al.*, 1984). Cell attachment or plating efficiencies based on TP measurements are defined as 'the TP content as a percentage of the initial value of the number of cells seeded into each culture dish' (Watt *et al.*, 1995; Gerlach *et al.*, 1994c), and are frequently used to assess both the quality of the initial isolate and subsequent cultures. PE on day 1 of culture (Figure 3.1), as measured by total cellular protein content, were significantly greater than both rat and sheep hepatocytes cultured in WE and M199, containing 5% serum (Watts *et al.*, 1995). However, computer aided image analysis showed quantitatively (Figure 3.13), that percentage confluency (analogous to plating or attachment efficiencies) to be significantly lower than day 1 TP based measurements, although the pattern of between media comparisons was similar. Moreover, this trend continued for HM-maintained cultures up to day 4. These data suggest that biochemical measurements of TP content may not alone be a reliable indicator of assessing PE or maintenance of cell culture confluency in the different media formulations. This may be due to the labile nature of cellular protein synthesis, reflecting variable TP content of cultured cells under certain conditions. On the other hand, the high TP content, translating into relatively high PE (compared with the image analysis data) could be a consequence of increased biomass residing in the discrete cell colonies observed in HM cultures (Figure 3.6), although this discrepancy was not observed for M1640 cultures, which showed similar gross morphology to the latter under light microscopy (see Figure 3.8) but with significantly higher % confluency.

Interestingly, te Velde *et al.*, (1995) demonstrated, by analysis of both DNA and TP content, identical day 1 PE of 76% for PPHs cultured in 10%FCS/WE medium on different biomatrices (including Matrigel, fibronectin, and collagen), compared with cells cultured on TCP. Morsiani *et* al., (1997) reported a 70% attachment efficiency of PPH onto microcarrier beads. These data correspond to a PE of ≈75% in HM cultures (Figure 3.1) on TCP, but are substantially lower than the other test media, suggesting neither serum, nor biomatrix, had influenced cell attachment in the other test media. Release of xenogenous proteins from Matrigel or EHS Natrix may anyway preclude their use in the BAL setting, despite some

demonstrable, enhancing effects on retention of *in vitro* liver-specific functions and culture longevity (Bhatia *et al.*, 1999; De Bartolo *et al.*, 2000). It is possible that the hormonal supplements (L-EGF, insulin and dexamathasone) in our defined culture system promote cell attachment through up-regulation of cell adhesion molecules or membrane stabilisation. Indeed, culturing hepatocytes as monolayers on tissue culture surfaces does allow recovery from the 'trauma' of isolation. During this respite period, cells can repair membranes, partially restore polarity and cell-cell interactions (Berry *et al.*, 1991c). Not surprisingly perhaps, environmental cues which enhance cellular repair mechanisms may be provided by a greater range of amino acids in complex media such as WE or M199 (see APPENDIX I). Originally developed to optimise the serum-free growth of hepatoma cells, M1640 is a relatively simple medium compared with WE or M199 and may explain its inability to maintain normal ultrastructure even at day 2, whereas HM is a proprietary formulation, based on Leibovitz L-15 formulation. The latter contains very high amino acid concentrations but does not contain important components such as proline, as well as aspartate, cystine and glutamate. Thus with wide variations in the amount and range of amino acids and other media componenets, it is not possible to delineate which factors are responsible for the observed differences in morphology between the test media with the present study design.

Image analysis (Figure 3.13) on the other hand imply that both WE and M199 maintained cultures are more efficient in terms of promoting the degree of confluency compared with HM and to a lesser extent, M1640 cells up to day 4. In fact, although somewhat subjective, light microscopic observations suggest that hepatocyte morphology was improved by day 2 of culture, as compared to day 1, particularly in both WE and M199 media (Figures 3.5 and 3.7; panels A-B, respectively). The near normal ultrastructure (Figures 3.5 and 3.7; panels C-F, respectively), high viability and total protein content (Figures 3.1-3.2) of these cells on day 2, as well as the image analysis data (Figure 3.13) lends support to the gross morphological observations and PE data.

Intracellular LDH activity has been shown to be proportional to the number of viable hepatocytes (Poullain *et al.*, 1992) whereas total protein content is a approximate correlate of cellular biomass with cell number (Gregory *et* al., 2000; Sharda *et al.*, 1996). In our study, viability remained high (range 80-90%) throughout the culture period (Figure 3.2). Again, day 2 cultures demonstrated significantly higher viabilities in WE and M199 than HM medium (Figures 3.1-3.2). Furthermore, our data may suggest an increase in cell numbers in cultures supported by M199 and WE, perhaps reflecting the greater concentration of amino acids, particularly proline, in both media, which stimulate cell growth (Houck and Michalopoulos, 1985; Michalopoulos GK, 1990; Mitaka, 1998; Berry *et al.*, 1991a). However, the correlation between TP content and cell number in PPHs cultures is questionable as mentioned, despite evidence of linearity for freshly isolated cells (Figure 3.1.1). Image analysis data (Figure 3.13) on the other hand, demonstrated, with the exception of HM, increases in % confluency in all test media cultures by day 2, and significant increases by day 4 compared with initial day 1 cultures. This suggests either cell proliferation and/or increased cell spreading had occurred, which correlates with the morphological observations for day 1 (Figure 3.4) versus day 2 cultures (Figures 3.5-3.8), where the gross morphology of day 2 cells appeared identical to day 4 cultures (not shown). In retrospect, it would have been useful to measure cell proliferation in the different test media, at different time points. Experiments confirming proliferation of the cultured cells, under these different culture conditions, could be made by quantifying DNA and labelling with tritiated thymidine, followed by scintillation counting. Indeed, hepatocytes suitable for BAL systems should ideally have both a well-differentiated *in vivo*-like phenotype and undergo controlled rounds of proliferation *in vitro* (Jauregui and Gann, 1991; Riordan *et al.*, 1998). Although functional activity is measured in Chapter 4, this combined data would give information on which culture condition provided the best balance between proliferation and the differentiated function of cells for BAL devices. As expected, the correlation between viability and functional activity is strong. In agreement with Wang *et al.*, (1998) we found that if hepatocyte viability fell below 60% functional activity

including albumin production, urea synthesis and P450 activity was severely attenuated (data not shown).

To overcome problems associated with subjective observations and bias in assessing gross cell culture morphology under light microscopy, and to increase accuracy, semi-automated computer-aided image analysis was used to quantitatively measure percentage confluency of each test culture, using the Image-Pro Plus™ software programme routinely used in the Department of Pathology (Dr C Bellamy, University of Edinburgh). A representative estimate of culture dish surface area covered by attached cells was made and quantified. In addition two independent, blinded investigators assessed the quality of cell culture morphology by the criteria outlined in Section 3.3.5.1. This purely subjective analysis ranked the quality of cultures on day 2 as: M199>WE>M1640>HM, whilst gross morphology of day 6 cultures had substantially deteriorated in all test media, with equal ranking. The image analysis method adopted here, proved simpler and more convenient, although is less informative, than nuclear counting and cellular DNA analysis. Measurement of the latter proving unreliable as measured by fluorimetry (data not shown), whereas the form of the PPH cultures, particularly in HM and M1640 (Figures 3,6 and 3.8), with piled up cells and overgrowth in other cultures made counting nuclei undependable. This form of image analysis is somewhat limited, since it only gives information on the extent of monolayer formation. Nonetheless, the healthy appearance in day 2 WE and M199 cultures of the monolayers thus formed (displaying a relatively compact, polygonal cell shape) complements the image analysis data as do the ultrastructural studies of the intracellular characteristics of PPHs under the different culture conditions.

Hepatocytes grown in WE (Figure 3.5) and M199 (Figure 3.7) media formulations, maintain and share most of the ultrastructural features of both fresh liver tissue and isolated hepatocytes (Figure 3.3), at least up to day 2 (Table 3.3). These observations, and such factors as consistent large round nuclei, are indicative of differentiated hepatocytes (Michalopoulos *et al.*, 2001). In addition hepatocytes

exhibit stereotypical gross morphology – distinct nuclei and nucleoli with well-demarcated refractile cell borders up to day 4 of culture (not shown). The bright, lucent rim surrounding each hepatocyte represents the presence of opposing membranes of bile canaliculi (Bader *et al.*, 1996; LeCluyse *et al.*, 1996), particularly in WE and M199 cultures, although bile canalicular-like structures were established only in TEM sections of WE-maintained cultures (Figure 3.5 and Table 3.3). However, these observations do not establish whether they are functional or not. Bile synthesis was confirmed in WE cultures day 2 cultures however, by detection of fluorescein diacetate metabolism using fluorescence microscopy (not shown). These findings suggest at least partial preservation of cellular polarity under defined conditions, despite the absence of serum or a biomatrix component. Such phenomenon has been demonstrated for rat hepatocytes cultured on collagen coated Permanox dishes in Chee's medium containing DMSO, dexamethasone and insulin (Arterburn *et* al., 1995). The authors concluded that these supplements, in concert with components of the culture medium, effectively 'bypassed' the need for biomatrices or serum.

Distinctive attributes of these media include their ability to preserve bile canaliculi-like structures whilst enhancing both the glycogen and RER protein synthetic machinery; the latter correlating with a significantly higher total protein content on day 2, than both HM and M1640 media, and a higher recorded albumin synthesis (Figure 4.9, page 4-29), although this could not be measured in HM. Taken together, these observations suggest that preservation of such morphological markers of differentiation and evidence of cellular polarity, reflects a potential for expression of normal *in vitro* functional diversity – desirable attributes required for the biological component of BAL systems.

In sharp contrast to the near normal phenotype expressed in hepatocytes grown in WE and M199 media, atypical gross morphology was evident in both HM and M1640 maintained cells up to day 4, most notably: the formation of discrete colonies (presumably of aggregated cells), the rather limited hepatocyte monolayer

formation and excessive cell spreading, and loss of delineating cell borders. Consistent with these findings, even at day 2, HM and M1640 hepatocyte cultures exhibited ultrastructural features of unhealthy cells including vacuolation and / or lipid deposition as well as fewer mitochondria. The relative frequencies of most cytoplasmic organelles (Table 3.3), was diminished in these media. Taken together, these findings reinforce the notion that different medium formulations can have differential effects on hepatocyte morphology, ultrastructure and possibly function. Moreover, the observed cell detachment, apoptosis, and probable necrosis of day 6 cells (Figures 3.9-3.12), may suggest release necro-inflammatory chemicals, such as certain cytokines, which are undesirable in the BAL setting. However, differentiated function, such as albumin synthesis, appeared unaffected by the deranged morphology.

Our findings make it clear that different serum-free chemically-defined media formulations allow maintenance of high viability hepatocyte cultures following high plating efficiencies, compatible with retention of functional activity, for up to 6 days. Furthermore, the type of medium formulation appears to modulate, to varying degrees, cell culture morphology, plating efficiency and viability *in vitro*. In particular, ultrastructural observations showed near normal morphology of subcellular organelles in both day 2 WE and M199 cultures, suggesting these hepatocytes retain an *in vivo*-like differentiated morphology. The preservation of intact and abundant subcellular organelles in these media such as mitochondria, with well preserved cristae and double membranes (Figures 3.5 and 3.7) reflects the potential of these organs to produce ATP; RER correlates with the maintained ability to synthesize proteins, including albumin (Chapter 4). These findings may be of use when considering the most favourable complex medium with which to support pre-clinical BAL devices. Despite the high viabilities evident in all test media on day 6, the morphological observations strongly favour these media over and above the other media used (see Figures 3.9-3.12). Future studies should address fundamental questions arising from this work: Which components of the test media account for the observed morphological variation? In the absence of exogenous attachment substrates, do cells

synthesize and secrete endogenous ECM? Do hepatocytes retain functional bile canaliculae, domain-specific proteins and polarity? Do cells proliferate under each test medium? What are the mechanisms responsible for the de-differentiation process? How do the cells respond in toxic FHF plasma, and can cytoprotective strategies be developed in this context? In the next chapter, the influence of these different culture conditions on the synthetic, detoxifying and metabolic capabilities of primary porcine hepatocytes is investigated.

Chapter 4

In Vitro Characterisation of Primary Porcine Hepatocyte Function

4.1 Introduction

Availability of primary human hepatocytes for cell-based approaches to treat acute liver failure (ALF) is severely restricted due to a shortage of donor organs. A corollary to this for experimental hepatocyte transplantation and bioartificial liver (BAL) therapies, is the possibility of using a variety of mammalian cells from pig, rabbit or rat species. However small mammals are impractical sources of cells to treat ALF due to insufficient yields. Indeed, the theoretical functional liver cell mass required for support is 20% of the whole liver, equivalent to approximately 20 billion hepatocytes (Nelson *et al.*, 2000; Newsome *et al.*, 2000; Plevris *et al.*, 1998).

As previously mentioned, primary porcine hepatocytes (PPHs) are the most appropriate biological component for BAL systems for treatment of ALF in terms of sufficient yield, viability and biocompatibility. PPHs exhibit differentiated function in culture and have a higher intrinsic metabolic activity compared to other mammalian hepatocytes (Behnia *et* al., 2000; Desille *et al.*, 1999; Donato *et al.*, 1999; Naik *et al.*, 1996). As demonstrated in Chapter 3, unlike other mammalian species, PPHs appear unique in that they do not require a substratum of exogenous ECM for initial attachment and survival, in agreement with recent reports (Gregory *et al.*, 2000; Pahernik *et al.*, 2001; te Velde *et al.*, 1995). We also have shown, that serum-free cultures of PPHs attach, survive and show ultrastructural features of differentiated hepatocytes, at least for short-term cultures, applicable to many current BAL devices. Hepatocyte morphology appeared to be influenced by the culture medium formulation, since ultrastructural examination of day 2 WE- and M199-maintained porcine hepatocyte cultures maintained features typical of metabolically active, differentiated liver cells, in contrast to both HM and RPMI 1640 cultures.

The influence of medium formulation on cultured cell functional activity can be significant. For instance, LeCluyse *et al.* (1999) showed that medium formulation and culture dish material had significantly greater effects on the induction of cytochrome P4502B by phenobarbital than either collagen or Matrigel™ sandwich cultures of rat hepatocytes. Watts *et al.*, (1995) found that Modified Earle's medium retained hepatic differentiated function, including total p450 (tP450) content and urea synthesis capacity, significantly better than either M199, Chee's media, or WE in rats. While studies from our laboratory have shown HM to be superior to WE in supporting tP450 biotransformation potential of cultured porcine hepatocytes (Keatch *et al.*, 2002).

Ideally, the primary requirement of a BAL system is the preservation of *in vivo*-like metabolic functions. Replacement of impaired liver functions on a temporary basis may sustain life by preventing and/or decreasing the progress of hepatic encephalopathy and/ or create conditions for native liver regeneration of functional tissue and full recovery (Gregory *et al.*, 2000; Jauregui *et al.*, 1995; Jauregui and Gann, 1991; Naik *et al.*, 1996). Whilst the precise metabolic functions required of hepatocytes to treat ALF are unknown, it is likely that a full repertoire of *in vivo*-like differentiated functions including synthetic, detoxifying and metabolic capabilities are prerequisites of xenogeneic hepatocytes in order to support the failing liver.

Key factors in achieving such *ex vivo* maintenance of differentiated PPH cultures are the most appropriate combination of biomatrix, hepatotrophic support and medium formulation. However, as mentioned, the use of serum-supplemented media or biomatrices to maintain retention of liver-specific functions in BAL devices for 2-4 days, may be unnecessary or even detrimental to cells.

Systematic investigations of the optimal medium requirements for PPH culture in BAL devices is lacking, probably due to the absence of standardisation and diversity of culture conditions used by different laboratories as well as the reliance on extrapolating data from rat hepatocyte studies to evaluating PPH culture systems.

Moreover, as mentioned, the type of medium formulation appears to modulate gross hepatocyte morphology, ultrastructure and possibly function.

The objective of this study was to assess the effects of different culture conditions on differentiated function of PPHs under fully defined conditions. Hepatocytes were cultured on biomatrix-free (unmodified) tissue culture plastic in four separate serum-free chemically-defined media formulations (WE, HM, M199 and M1640) containing equal amounts of hormonal supplements. Because synthetic, detoxifying and metabolic capabilities of *in vitro* hepatocyte culture are considered necessary to fulfil the hepatic replacement function required of the biological component of BAL systems, we measured the following markers of differentiation: (i) albumin production as an energy-requiring biosynthetic and secretory function, (ii) urea production from ammonium chloride as a measure of detoxifying capacity, (iii) galactose elimination to reflect the integrity of carbohydrate metabolism, and (iv) total cytochrome P450 content (tP450) as an indicator of biotransformation potential. Measurement of tP450 would give an overall perspective of the phase I potential of the hepatocytes under the different culture conditions using one assay.

Similar to the biochemical measurements of Chapter 3, this study will entail examination of multiple comparisons of biochemical functional activity. In order to define an index of global functional capacity, a scoring system (hepatocyte biological acitivity index; HBAI) was devised, to simplify comparisons, and as an integrated measure of overall functional capability. The biochemical data reported in Chapter 3 was used in the generation of the HBAI, whereas parallel morphological observations were used in the assessment of the comparative scores of the HBAI.

4.1.1 Aims

The specific aim of this study was to assess differential effects of separate, serum-free chemically-defined medium formulations on differentiated hepatic support functions of cultured porcine hepatocytes for future BAL devices.

4.2 Materials and Methods

4.2.1 Reagents

All reagents used were as detailed in Chapters 2 and 3 with the following additions: Ammonium chloride, D(+)-galactose, 3-N-morpholinopropanesulphonic acid (MOPS free acid) and MOPS Sodium salt were obtained from Sigma, St Louis, Mo, USA; Analar grade chemicals for albumin determination were obtained from Life Technologies (BDH Merck). Albumin blue 580 [2-chloro-3-(2,2-dicyanoethenyl)-2-cyclohexen-1-ylidene]methylpropanedinitrile potassium salt was from Molecular Probes (Cambridge Bioscience, UK). Galactose kits were from Roche Diagnostics Ltd. (UK).

4.2.2 Hepatocyte isolation

Hepatocytes were isolated from weanling piglets (<15kg) using our *ex vivo* collagenase perfusion method described in Chapter 2 (Nelson *et al.*, 2000).

4.2.3 Hepatocyte cultures

Hepatocytes were cultured as described in Chapter 3 (Section 3.3.3). Briefly, 10^7 viable cells were cultured for up to 6 days on 100mm tissue culture plastic (TCP) dishes in serum-free chemically-defined William's E (WE), Hepatocyte Medium (HM), Medium 199 (M199) and RPMI 1640 (M1640) media formulations. Unless indicated, media were changed on days 1, 2, and 4.

4.3 Biochemical and metabolic assessment

4.3.1 General description

For each test medium, hepatocytes were cultured on duplicate TCP dishes and evaluated for markers of differentiated biochemical function at the time points

indicated. On the day of isolation (day 0) and on culture days 2, 4 and 6, total cytochrome P450 (tP450) content and total cellular protein content (TP) of the cell lysates was measured. Plating efficiency was assessed by measuring TP of day 1 cultures (Section 3.4.3). Cell viability (lactate dehydrogenase (LDH) activity) was measured in Chapter 3 (Section 3.4.4). Samples of test culture media were analysed for albumin production and urea synthesis. In addition, both galactose elimination (GE) and urea synthesis rates (USR) were analysed following culture in test media at each time point, using HBSS as reference media with either D(+)-galactose or ammonium chloride challenge. Samples were stored at -70°C until analysis. This was performed in 10 separate isolations, unless indicated.

4.3.2 Total protein measurements

Total protein (TP) content was determined in fresh cell suspensions and for hepatocytes cultured in each medium on days 1, 2, 4 and 6 in duplicate culture dishes, as described in detail previously (Nelson *et al.*, 2000); see Chapter 2, Sections 2.3.7.1 and 2.3.7.2).

4.3.3 Urea synthesis rate and galactose elimination

4.3.3.1 Urea synthesis of PPHs in test media containing NH_4Cl

Urea synthesis rates were measured as described in detail in Chapter 2 (Nelson *et al.*, 2000). Briefly, on days 2, 4 and 6, duplicate cell culture dishes were washed 2x with HBSS (37°C) and incubated in 8ml of each test medium with 2 mmol/L NH_4Cl for 2 hours (Flendrig *et al.*, 1997a) in a humidified incubator at 37°C under an atmosphere of 95% air / 5% CO_2. For reference, media controls were treated under otherwise identical conditions except without cells.

Addendum A preliminary study for day 2 cultures (incubated overnight in each test medium without NH_4Cl), showed substantial differences in *basal* urea production for WE, HM, M199, and M1640 (67, 234, 79, and 173 nmol/h/ mg TP, respectively). Thus to permit a more standard methodology which avoids the potential confounding

factors of different constitution of the test media, such as the variable amino acid content, urea production was measured in HBSS containing NH_4Cl, on days 2, 4 and 6 of culture. This buffered solution does not contain amino acids.

4.3.3.2 Urea synthesis of PPHs in HBSS containing NH_4Cl

A pilot study was undertaken to confirm that urea production was linear over 2 hours in HBSS, using the same 2 mmol/L NH_4Cl concentration utilised in Chapter 2 (Section 2.3.8) for WE cultures. Briefly, cells were cultured in triplicate for 48 hours in each test medium, washed 2x in HBSS and incubated for 2 hours in HBSS reference medium containing 2 mmol/L NH_4Cl. 100µl samples were taken at 0, 30, 60, 90, and 120 minutes and assayed for urea (see Figure 4.2, page 4-16). Linear regression analysis confirmed that the urea production rate was linear.

Cells were then cultured in each test medium as described above (Section 4.2.3), and on days 2, 4, and 6, duplicate culture dishes of each test media were washed 2x in HBSS. Subsequently, cultures were incubated for 2 hours in HBSS containing 2 mmol/L NH_4Cl to determine urea production, which was corrected for endogenous urea production. Samples were taken at t_0 and t_2 hours and assayed for urea.

4.3.4 Calculation of urea concentration and urea synthesis rate

Calculations of urea concentration and the urea synthesis rate (USR) were determined as described in Chapter 2. Briefly, samples taken at the time points indicated were analysed using a modified colourimetric urea nitrogen kit (Sigma Diagnostics 535-B). The difference in absorbances (λ_{525} nm in a Pye Unicam spectrophotometer) for the chromogenic reaction was measured for each time point and both urea concentration and USR calculated. USR was expressed as nmol/hour/ mg TP. The coefficient of variation (CV) for this assay was 6% intra-assay CV and 8% inter-assay.

4.3.5 Galactose elimination

A galactose loading dose of 6 mmol/L was used for GE determination in HBSS reference medium of all cells pre-cultured in test media. This was because the galactose content of HM was found to be between 5-6 mmol/L. In addition, this is close to the value used clinically in liver function tests (Whitington, 1992), experimentally in BAL systems (Flendrig *et al.*, 1997a), and is close to linear up to galactose concentrations of 5-6 mmol/L (Figure 4.5, page 4-20). Finally, equimolar [galactose] allows valid, direct comparisons between the different test medium formulations.

Hepatocytes were cultured in each test media as described above (Section 4.2.3). On days 2, 4 and 6, duplicate cell culture dishes for each test medium were washed 2x with HBSS (37°C), and incubated in 8ml of HBSS containing 6 mmol/L D(+)-galactose for 2 hours in a humidified incubator at 37°C under an atmosphere of 95% air / 5% CO_2. Galactose elimination (GE) was determined in 0.5ml samples taken at t=0 and t=2 hours using a modified galactose kit. The difference in absorbances (λ_{340} nm) at each time point (before and after a 40 minute incubation with galactose dehydrogenase) enabled the galactose concentration to be calculated according to the manufacturers instructions. Cells were collected from these dishes and analysed for total protein content as described above. GE was expressed in nmol/hour/mg total protein. The intra-assay CV was 7% while the inter-assay CV was 10%.

4.3.6 Calculating USR and GE

The USR (Section 2.3.8.3) and GE were both corrected for total protein content and for pre- and post-incubation volumes for each culture dish according to the equations:

$$\mathbf{Rate_{USR} = C_2V_2\text{-}C_1V_1 / NT} \quad \text{(nmol/hour/ mg TP)}$$

and

$$\mathbf{Rate_{GE} = C_1V_1 - C_2V_2 / NT} \quad \text{(nmol/hour/ mg TP)}$$

where: C_1 is the initial concentration, V_1 is the initial volume prior to sampling, C_2 is the final concentration and V_2 is the final volume after sampling; **N** is the total protein content and **T** is the incubation time.

4.3.7 Total cellular cytochrome P450 levels

Total cellular P450 and total protein content were determined in fresh cell suspensions and for hepatocytes cultured in each medium on days 1, 2, 4 and 6 in duplicate culture dishes to assess cellular biotransformation potential as described in detail in Chapter 2 (Nelson *et al.*, 2000). Briefly, fresh or cultured hepatocyte samples were solubilised in ice-cold P450 buffer, sonicated and stored at –80°C until analysis. Total cytochrome P450 content was determined by carbon monoxide difference spectroscopy of the sodium hydrosulphite-reduced samples, using a dual-beam Kontron™ spectrophotometer. Results are expressed as pmol/mg protein (corrected for total cellular protein content as determined by the Bradford assay (Bradford, 1976). The intra-assay CV 7% while the inter-assay CV was 10%.

4.3.8 Albumin production detected using a fluorimetric albumin blue 580 dye-binding assay

The albumin concentration was determined in duplicate samples of culture supernatants taken on days 2, 4 and 6 using a fluorimetric albumin blue 580 (AB) dye-binding assay (Kessler *et al.*, 1997) optimised for measurement in cell culture supernatants. Cells were cultured as above and 1ml samples taken from duplicate cell culture dishes on days 2, 4 and 6 and stored at -80°C until measurement of albumin content. Quoted literature values for albumin concentrations in PPHs cultures are in the 20-40 μg/ml range (De Bartolo *et al.*, 2000; Gregory *et al.*, 2000); thus the ratio of volume of dye to that of albumin standard was chosen so that the fluorescence at 40 μg/ml of albumin was maximal.

4.3.8.1 Reagents

30 mg/L AB 580 dye (Mr = 306.8) stock was prepared by dissolving in 100% isopropanol. The concentration was measured spectrophotometrically in a Pye-Unicam spectrophotometer; absorbance at λ_{580} nm of a ten fold dilution of dye stock in isopropanol, with isopropanol as blank, was 1.0 ± 0.05 (Kessler *et al.*, 1997) (Fluorimeter range of absorbance units is 0-2.0). Dye stock was stored at 4°C in the dark until required. Working buffer (dye solution diluent) was prepared by dissolving 3.0 g MOPS free acid, 9.0 g of MOPS Sodium salt, 12.0 g sodium chloride and 1.0 g of EDTA disodium salt in 900 ml dH_2O / 100 ml isopropanol (pH 7.4). Working dye solution was prepared by diluting 5.0 ml of dye stock to a total volume of 100 ml with working buffer. This solution is photosensitive but stable for one month in the dark at 4°C.

4.3.8.2 Standard

Pig albumin (Sigma A1830) dissolved in calibrator diluent was used as the albumin standard and was prepared fresh for each assay run. Calibrator diluent was prepared by dissolving 2.7g KH_2PO_4, 0.9g K_2HPO_4, 4.5g of sodium chloride, 0.5g of EDTA disodium salt and 50 mg of pig gamma immunoglobulins (IgG; Sigma G2512) in 500 ml of dH_2O (pH 6.0) and stored at 4°C. Pig IgG was included as a stabilizer to prevent non-specific absorption of albumin to plastic surfaces.

4.3.8.3 Disposables and equipment

Polypropylene test tubes (5 ml; Sarstedt, FRG) were used for preparing standard and sample dilutions. The test was performed in 96 well microtitre plates (Dynatech, USA). Fluorescence was read using a fluorescent plate reader fitted with filters of bandwidth 20 nm for excitation at λ_{590} nm and 40 nm for emission at λ_{645} nm (Cytofluor 4000, Perseptive Biosystems, USA). The gain was set to 60 V.

4.3.8.4 Calibration

A standard curve of 0-40 μg/ml of pig albumin in calibrator diluent was prepared. 180 μl of each standard or test sample was added to duplicate wells of a microtitre plate. Samples (supernatants from pig hepatocytes cultured in each test media) were tested neat or diluted 1:4 in the appropriate culture medium. Media blanks (which had never been in contact with cells) were also included. Working dye solution (80 μl) was then added to all wells. The plate was then shaken for 30 s before reading the fluorescence. This was performed in 7 separate isolations. Albumin synthesis was expressed as μg/hour/mg total cellular protein.

4.3.8.5 Quality control

Culture medium (William's E, RPMI 1640 and Medium 199), spiked with pig albumin at 10 μg/ml and medium blanks were stored in aliquots at -80°C until analysis. The intra-assay CV 9% while the inter-assay CV was 11%.

4.4 Preliminary studies on immunostaining of albumin in culture supernatants

Since specific anti-pig albumin antibodies were not commercially available, preliminary experiments were performed to determine albumin concentrations. Firstly an immunoturbidimetric microalbumin kit, INCSTAR® (USA), was tried utilising an anti-human albumin antibody adapted for use on a COBAS FARA centrifugal analyser (Roche) and compared to an albumin standards calibration curve. Secondly, an attempt was made to develop an 'in-house' ELISA using an anti-human (sheep) polyclonal (Dako # A0001) coated to the plate and a second albumin anti-human (rabbit) albumin-HRP conjugated (Dako # P0356) antibody. Unfortunately, although minor signals were detected, both these assays were too insensitive for detecting μg amounts in culture supernatants (data not shown).

Albumin, with a molecular weight of ≈65000 Kda, was initially detected in cell culture supernatants by Western blotting using BioRad™ Protean Minigels, according to the manufactures instructions (based on the method of Laemmli *et* al., 1970). The first and second antibodies used are described below. To simplify the methodology for our experiments, a dot blot method was adopted, followed by densitometry (after addition of a chemiluminescent agent). This method is briefly described. Duplicate samples of culture supernatants were taken on days 2, 4 and 6 and 5µl spotted onto nitrocellulosestrips. This was repeated with a pig albumin standard [1 mg/ml] made up in WE medium, at a range of concentrations (0-100 µg/ml). The nitrocellulose strips were washed 3 x 5 minutes in 0.5 % (v/v) Tween-20 PBS solution, and incubated for 2 hours on a rotary shaker at room temperature (RT) with Pierce™ blocking buffer, to prevent non-specific binding. The first antibody (anti-human albumin (rabbit)) was titrated to 1:2000 in PBS containing 0.05 % Tween-20 solution with 3 % (w/v) dried milk (Marvel) and incubated for one hour (RT) on a rotary shaker. This was followed by 5 x 6 minute washing steps in the PBS 0.5 % Tween-20 solution. The second antibody (anti-rabbit IgG HRP-conjugated) was titrated to 1:20000 and incubated for one hour as above, and the washing steps repeated. Controls: i) albumin standard without the first antibody; and ii) test media (never seen cells) were similarly treated. A chemiluminescent agent (Supersignal, Pierce™) was added to the nitrocellulose strips (0.75 ml per strip) for 5 minutes, wrapped in cling-film and either exposed to photographic film (Kodak™ Omat Film) for 3-4 minutes or subject to densitometry using a BioRad™ (phosphoimager) image analysis system, according to the manufactures instructions.

4.5 Statistical analysis

For each parameter, multiple comparisons were made using ANOVA of:

1) Between-media evaluations on each day of culture, and
2) Between-day evaluations for each single medium formulation.

One-way single factor ANOVA (assuming equal variances) was performed followed by *Post Hoc* multiple comparisons tests of *least significant differences*, using the SPSS 9.0 statistical software package. The mean difference was considered significant at the 0.05 level. Results are expressed as mean±SEM (standard error mean of the mean) and the number n of experiments performed is indicated. Statistically relevant p values are quoted for the multiple comparisons of either or both 1) and 2) above.

4.6 Results

4.6.1 Cell isolation viability and yield

The hepatocytes were isolated using our *ex vivo* method described in detail in Chapter 2. For these experiments, cell viability was 87±5% with a yield of 2.2±0.8 x 10^{10} cells from 12±1 kg piglets (n=10).

4.6.2 Total cellular protein content

Total protein content was determined as outlined in Chapter 3 as a correction factor to normalize calculated urea and albumin synthesis rates as well as galactose elimination and total P450 values.

4.6.3 Urea synthesis

4.6.3.1 Urea synthesis in test media containing NH_4Cl

Between media comparisons of USR were made on each day of culture (Figure 4.1). Primary porcine hepatocytes cultured in RPMI 1640 medium on day 2 of culture showed significantly higher ($p<0.05$) conversion of ammonium chloride to urea (511±141 nmol/h/mg protein) compared to both WE medium and M199 (292±62; $p=0.044$ and 201±50; $p=0.015$, respectively). By day 4 of culture in RPMI 1640, the USR had further and significantly increased (608±102 nmol/h/mg protein) compared to WE (335±79; $p=0.01$), M199 (248±31; $p=0.001$) whereas a moderate increase was observed relative to HM (428±38; $p=0.078$). RPMI 1640 maintained a significantly higher USR capacity (847±249) over HM on day 6 (359±77; $p=0.031$) and a significantly greater ($p<0.05$) conversion rate than hepatocytes cultured in WE (448±90), or M199 (360±125). All other media comparisons and between day comparisons for each medium formulation were not significantly different at the 5% level. See *Addendum* in Section 4.3.3.1, page 4-5.

4.6.3.2 Urea production in NH_4Cl-stimulated PPHs cultured in HBSS

Figure 4.2 shows urea production as a function of time. This validates that urea production is linear for hepatocytes pre-cultured in each test medium and subsequently assayed in HBSS reference medium with 2mmol/L NH_4Cl. In the following experiments, USR was corrected for endogenous urea production (ie urea production in the absence of NH_4Cl).

Between media comparisons of USR were made on each day of culture (Figure 4.3). This data demonstrates that the urea synthesising capacity of day 2 WE, HM, and M199 pre-cultured cells were not significantly different at 104±11, 126±20, and 115±17 nmol/h/mg protein, respectively. Mean USR for M1640 cells (147±21) however, was significantly higher than WE pre-cultured cells. By day 4, the USR of HM pre-cultured cells was similar to M1640 grown cells (221±25 *vs* 176±31, respectively), although both WE and M199 pre-cultured cells, are significantly lower (93±14 *vs* 79±4, respectively; $p<0.01$) than the former, in their ability to convert ammonium to urea in HBSS reference medium. HM pre-cultured cells maintained a significantly higher USR (111±16) than all other test media on day 6. Between day comparisons for each pre-cultured test media reflected a statistically significant ($p<0.05$) increase in USR of day 4 HM cells compared with day2, and a moderate increase in M1640 cells, although the mean values of both were greater than either WE or M199 values. By day 6 USR was attenuated in WE, HM, M199 and M1640 pre-cultured cells (40±15, 111±16, 10±2, and 17±6 nmol/h/mg protein, respectively).

Figure 4.1 Urea Synthesis Rates of NH_4Cl-stimulated Primary Porcine Hepatocytes Cultured in Four Separate Chemically-Defined Media Formulations

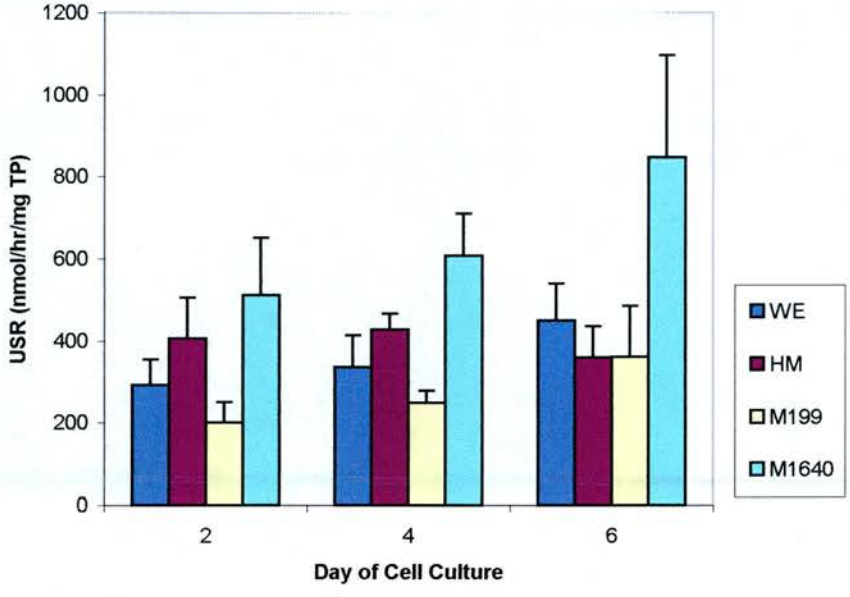

Figure 4.1 Urea synthesis rates (USR) of porcine hepatocytes cultured at 10^7 viable cells per 100mm dish in William's E, HM, M199 and M1640 chemically-defined media for up to 6 days. Following washing the cells twice with HBSS, 2mM NH_4Cl was added to each test medium and incubated for 2 hours on days 2, 4, or 6. USR was determined in media samples taken at t=0 and t=2 hours using a modified colourimetric urea nitrogen kit as described in *Materials and Methods*. Results are expressed as nmol/hour/ mg total protein. All values represent the means±SEM of nine experiments in duplicate.

Figure 4.2 Urea Production in HBSS / Ammonium Chloride-Stimulated Primary Porcine Hepatocytes Pre-Cultured for 2 days in Separate Serum-free Chemically-Defined Medium Formulations

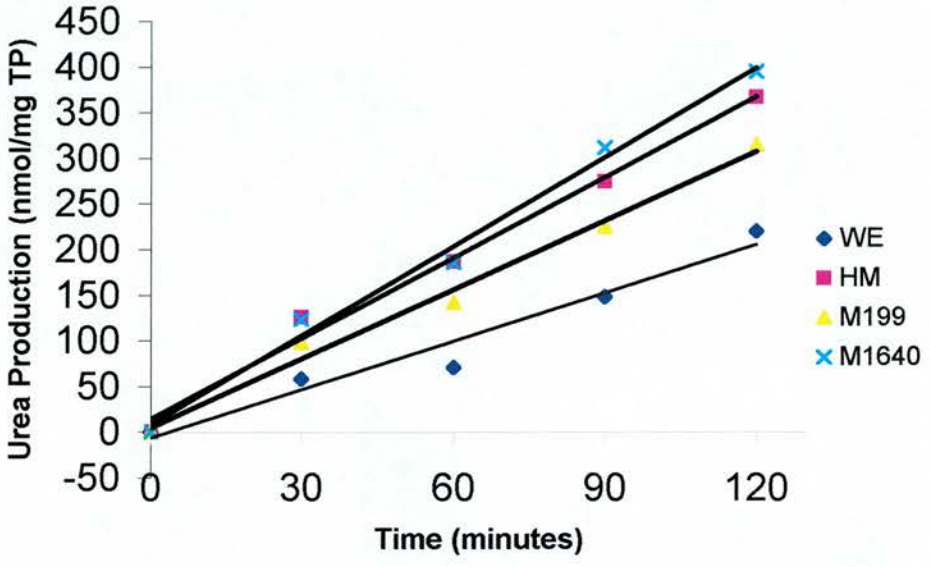

Figure 4.2 Urea production of ammonium chloride-stimulated porcine hepatocytes cultured for 2 hours in HBSS. Cells were pre-cultured in test media for 48 hours as described above (Figure 4.1). On day 2, triplicate culture dishes of each test media were washed 2x in HBSS and cultures incubated for 2 hours in 8ml HBSS reference medium containing 2mM NH_4Cl. 100μl samples were taken at 0, 30, 60, 90 and 120 minutes and urea production determined. Data points were fitted to linear regression curves using Microsoft Excel 2000 version 9.0. Results are expressed as nmol/mg total protein.

Figure 4.3 Urea Production in HBSS / Ammonium Chloride-Stimulated Primary Porcine Hepatocytes Pre-Cultured for up to 6 days days in Separate Serum-free Chemically-Defined Medium Formulations

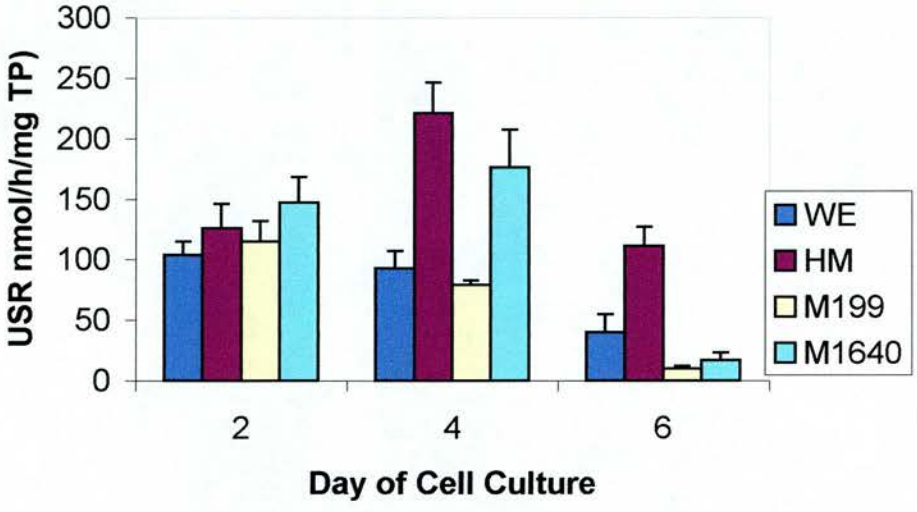

Figure 4.3 Urea production of ammonium chloride-stimulated porcine hepatocytes, cultured for 2 hours in HBSS reference medium. Cells were pre-cultured in each test media as described above (Figure 4.1). On days 2, 4, and 6, duplicate culture dishes of each test media were washed 2x in HBSS and cultures incubated for 2 hours in HBSS containing 2mM NH_4Cl. USR was determined in media samples taken at t=0 and t=2 hours and corrected for endogenous urea production, using a modified colourimetric urea nitrogen kit as described in *Materials and Methods*. Results are expressed as nmol/hour/mg total protein. All values represent the means±SEM of 3 experiments in duplicate.

4.6.4 Galactose elimination

Galactose elimination (GE) for PPHs cultured in HBSS reference medium was evaluated following spiking of cells (*pre-cultured* in each test media) with 6 mmol/L D(+)-galactose in HBSS. For each day of culture, between day comparisons of GE for each medium formulation were made (Figure 4.4; all mean±SEM, n=3). GE for WE, HM, M199 and RPMI 1640 on culture day 2 (420±66, 436±54, 416±33, 516±44 nmol/h/mg TP, respectively) was found to be significantly greater ($p<0.05$) in day 2 cultures compared with both day 4 (266±56, 298±78, 231±41, 277±101) and day 6 cultures (179±50, 225±69, 218±43, 250±74); although no significant difference was observed between day 4 and day 6. Results are expressed as nmol/hour/mg total protein. All between medium comparisons for each day of culture were not significantly different at the 5% level. Figures 4.5 show the relationship of GE as a function of [galactose] (see Discussion).

Figure 4.4 Galactose elimination in primary porcine hepatocytes cultured for up to 6 days in four serum-free chemically-defined media formulations

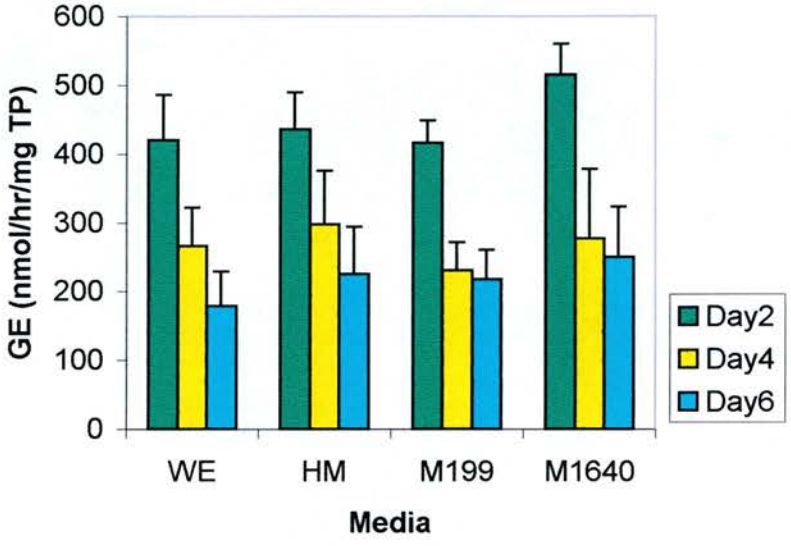

Figure 4.4 Galactose elimination (GE) in primary porcine hepatocytes cultured at 10^7 viable cells per 100mm dish in William's E, HM, M199 and M1640 chemically-defined media for up to 6 days. Duplicate cell cultures were washed 2x in HBSS, then 6mM D(+)-galactose in HBSS was added to culture dishes of each test media, and incubated for 2 hours on days 2, 4 and 6. GE was determined spectrophotometrically in media samples taken at t=0 and t=2 hours using a modified galactose kit, as described in Materials and Methods. Results are expressed as nmol/hour/ mg total protein. All values represent the means±SEM of 3 experiments in duplicate.

Figure 4.5 Michaelis-Menten representation of galactose elimination as a function of galactose concentration

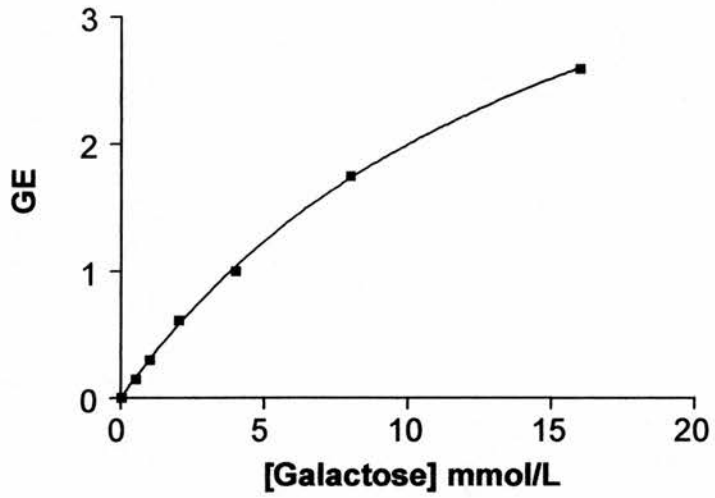

Figure 4.5 Galactose elimination (GE) as a function of galactose concentration. Primary porcine hepatocytes were incubated in duplicate with 0.5, 1, 2, 4, 8 or 16 mmol/L of galactose in William's medium E for 2 hours, as described above. The GE was calculated thus: GE = Initial [galactose] t_0 – final [galactose] t_2 / incubation time. GE is expressed as mmol/L/hour. The data was fitted to a hyperbolic curve using GraphPad Prism (version 1.03) software programme.

4.6.5 Total cytochrome P450 content

4.6.5.1 Between media comparisons for each day of cell culture

Between media evaluations of total cytochrome P450 content were made on each day of culture (Figure 4.6). Significant differences between cells cultured in each test media were not observed until culture days 4 and 6. tP450 content of HM medium grown hepatocytes on day 4 (36±3 pmol/ mg protein) was significantly higher ($p<0.05$) than both WE medium (24±3 pmol/ mg protein) and RPMI 1640 medium (25±5 pmol/ mg protein). The value of tP450 content was significantly lower in WE medium (17±1 pmol/mg protein) compared to HM (25±1 pmol/mg protein), M199 (28±1 pmol/mg protein; $p=0.026$), and RPMI 1640 (27±5 pmol/mg protein) cultured cells.

4.6.5.2 Between day comparisons of each medium formulation

For each medium formulation, between day comparisons of total cytochrome P450 content of freshly isolated (day 0) and cultured hepatocytes were analysed (Figure 4.7). There was a highly significant decrease ($p<0.001$) in tP450 content, from 120±37 pmol/mg protein for fresh cells, to ≈40±10 pmol/mg protein by day 2 of culture in all media formulations. Total cytochrome P450 content remained quite stable (≈30±3 pmol/mg protein) up to day 4. However, biotransformation potential had declined significantly ($p<0.05$), when comparing day 2 values (≈40±10 pmol/mg protein) with day 6 values in WE (17±1 pmol/ mg protein), and HM (25±1 pmol/mg protein) media formulations.

Figure 4.6 Total cytochrome P450 content in primary porcine hepatocytes cultured in four separate chemically-defined media formulations: Between-media evaluations on each day of culture

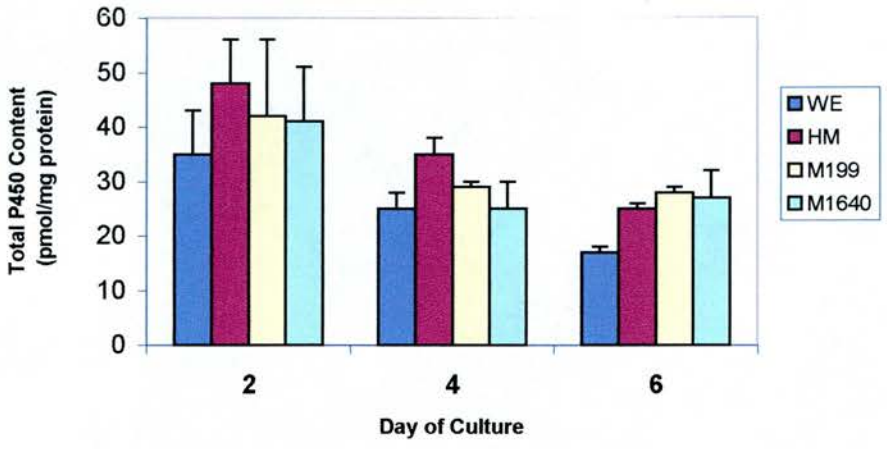

Figure 4.6 Total cytochrome P450 content of porcine hepatocytes cultured at 10^7 viable cells per 100mm dish in William's E, HM, M199 and M1640 chemically-defined media for up to 6 days. Cell cultures were scraped from dishes on days 2, 4 and 6 and total cytochrome P450 content determined by carbon monoxide difference spectroscopy of the sodium hydrosulphite reduced samples as described in *Materials and Methods*. Results are expressed as pmol/mg total protein. All values represent the means±SEM of three experiments in duplicate.

Figure 4.7 Total Cytochrome P450 Content in Primary Porcine Hepatocytes Cultured in Four Separate Chemically-Defined Media Formulations: Between day evaluations for each medium

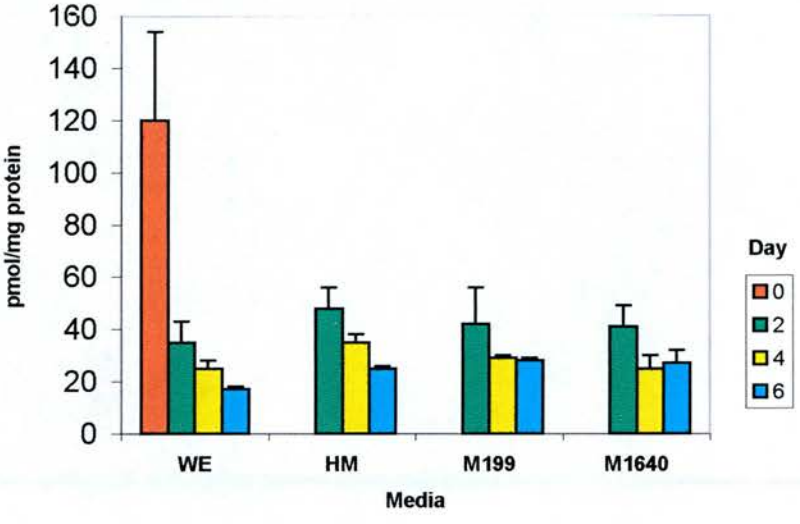

Figure 4.7 Total cytochrome P450 content of porcine hepatocytes cultured at 10^7 viable cells per 100mm dish in William's E, HM, M199 and M1640 chemically-defined media for up to 6 days. Total cytochrome P450 content in freshly isolated cells and cell cultures scraped from dishes on days 2, 4 and 6 was determined by carbon monoxide difference spectroscopy of the sodium hydrosulphite reduced samples as described in Chapter 2. Results are expressed as pmol/mg total protein. All values represent the means±SEM of three experiments in duplicate.

4.6.6 Determination of albumin concentration

The ratio of volume of dye to that of albumin standard was chosen so that the fluorescence at 40 μg/ml of albumin was maximal, based on previous literature (De Bartolo *et al.*, 2000; Gregory *et al.*, 2000). Using these conditions, the standard deviation of repeated sample blanks (calibrator diluent) was found to be 92 fluorescence units at a mean reading of 1660 unit. The limit of detection was defined as that test value which exceeds the blank value plus 3 standard deviations, giving a lower limit of detection at 3.5 μg/ml.

Fluorescence for the zero standard was substracted from the readings for the other standards prior to construction of the standard curve. The concentration (x) of albumin in the unknown samples was determined by measuring the fluorescence (y; in absorbance units) at λ_{580} nm and interpolating the unknown concentration, x from the albumin standard curve of the form, y = mx + c. Using Graphpad Prism v 1.8, these data were fitted to a linear regression curve (Figure 4.8).

Solving the equation, $\mathbf{y = mx + c}$ for concentration, x gives:

$$\mathbf{x = y - c / m}$$

Substituting the linear regression equation, $\mathbf{y = 346x + 0.9}$, gives;

$$\mathbf{x = (y - 0.9) / 346}$$

where:

y is the fluorescence absorbance value (arbitrary units)
m is the slope of the curve giving the unknown albumin concentration
x is the unknown value
c is the x-intercept

Figure 4.8 Representative Pig Albumin Standard Curve: A Plot of Fluorescence (Arbitrary Absorbance Units) at λ_{580} nm *Versus* [Albumin] (μg/ml)

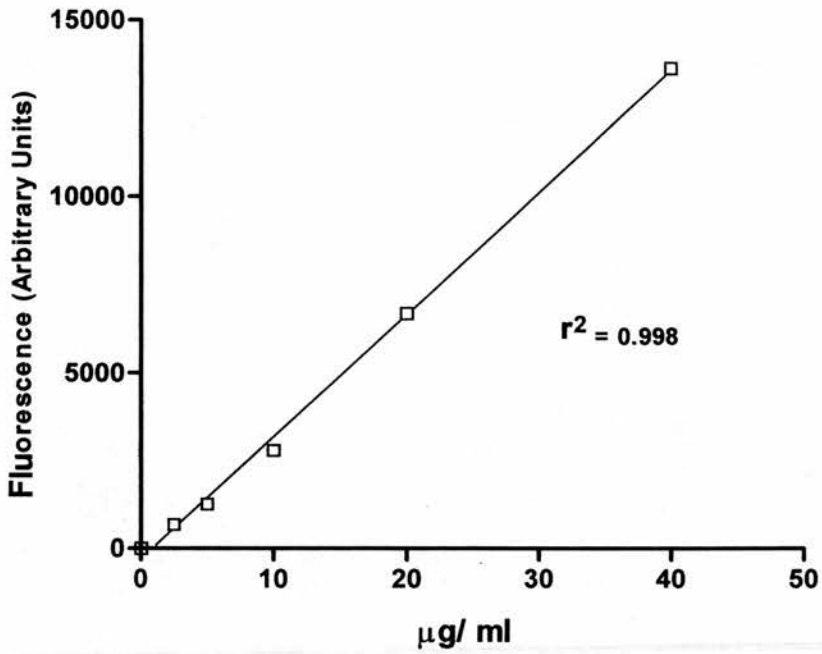

Figure 4.8 Pig albumin standard curve: 0-40 μg/ml of pig albumin in calibrator diluent was prepared; 180 μl of each standard or test sample was added to duplicate wells of a microtitre plate. Samples (test media from pig hepatocyte culture) were measured neat or diluted 1:4 in appropriate culture medium. Working dye solution (80 μl) was then added to all wells. The plate was then shaken for 30 s before reading the fluorescence. This was performed in 7 separate isolations. Albumin synthesis was expressed as μg/hour/mg total protein. Quality control: Culture medium (William's E, RPMI 1640 and Medium 199) were spiked with pig albumin at 10 μg/ml and stored in aliquots at -80°C.

Unknown test concentrations were calculated from the fluorescence readings after subtracting any background readings.

4.6.6.1 Quality control

Recovery experiments for pig albumin added to pig hepatocyte culture supernatants were performed. A recovery of 115 % of expected albumin was observed. Medium was spiked with albumin to concentrations of 2.5 and 20 μg/ml. However, if the total albumin exceeded 40 μg/ml, albumin recovery was increased to 120 %. Consequently, culture supernatants giving greater than 40 μg/ml were tested at a dilution of 1:4 in the same type of medium. Different test dilutions up to a maximum of 1:9 gave results within 5 % of the previous dilution.

The correlation coefficient ($\mathbf{r^2}$) for data fitted using the linear regression equation was 0.998 (Figure 4.8), demonstrating a unique fit that would reliably allow interpolation of unknown concentrations from the fluorescence data.

4.6.6.2 Assay performance with culture supernatants

Culture media alone gave background fluorescence readings which were subtracted from the values for test samples. Repeated testing of the QC samples gave a within batch and between batch coefficient of variation of 9 % at 10 μg/ml, within acceptable limits.

4.6.6.3 Albumin synthesis rates

For each medium formulation, between day comparisons were analysed (Figure 4.9). Albumin secretion by primary porcine hepatocytes cultures (n=7) remained stable up to day 4 (≈1.0-1.9 μg/h/ mg protein) but increased significantly thereafter up to day 6 of cell culture in RPMI 1640 medium (2.5±0.5 μg/h/ mg protein; p=0.024); with substantial increases to 2.3±0.5 μg/h/ mg protein observed in M199 (p=0.058) *versus*

2±0.4 μg/h/ mg protein in WE medium during the same culture period. All other between day comparisons for each medium and between media comparisons for each day of culture, were not significantly different at the 5% level. ASR could not be measured in HM due to very high background levels in this proprietary medium formulation.

4.6.6.5 Detection of albumin: Preliminary studies on immunostaining of albumin in culture supernatants

The presence of albumin was confirmed in each test medium by dot blot analysis (see Figure 4.10A and Section 4.4). As with the other methods briefly described in Section 4.4, densitometric analysis of samples was not reproducible or sensitive enough to detect μg amounts in culture supernatants (data not shown). However, the dot blots confirm that the cells produced albumin. Surprisingly, HM medium alone (in the absence of cells) contained significant amounts of albumin (Figure 4.4.3B). These findings led the development of the albumin blue 580 fluorimetric dye-binding assay (see Sections 4.3.9 and Section 4.6.6), in order to accurately quantify albumin synthesis.

Figure 4.9 Albumin Synthesis Rates in Primary Porcine Hepatocytes Cultured in Separate Chemically-Defined Media Formulations

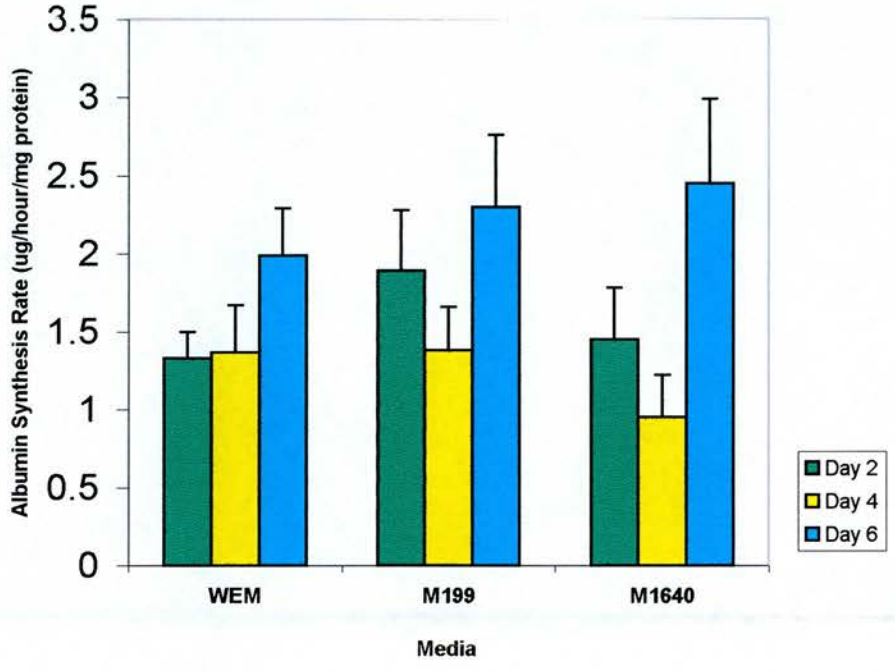

Figure 4.9 Albumin synthesis rates (ASR) of porcine hepatocytes seeded at 10^7 viable cells per 100mm dish in William's E, M199 and M1640 chemically-defined media for up to 6 days. Samples were taken on days 2, 4 and 6. and ASR determined for each media using fluorimetric analyses of albumin blue 580 dye binding to albumin as described in *Materials and Methods*. Results are expressed as μg/hour/ mg total protein. All values represent the means±SEM of 7 experiments in duplicate. Note that ASR was not measured in HM, due to very high background levels (5 % (w/v)) in this proprietary medium formulation.

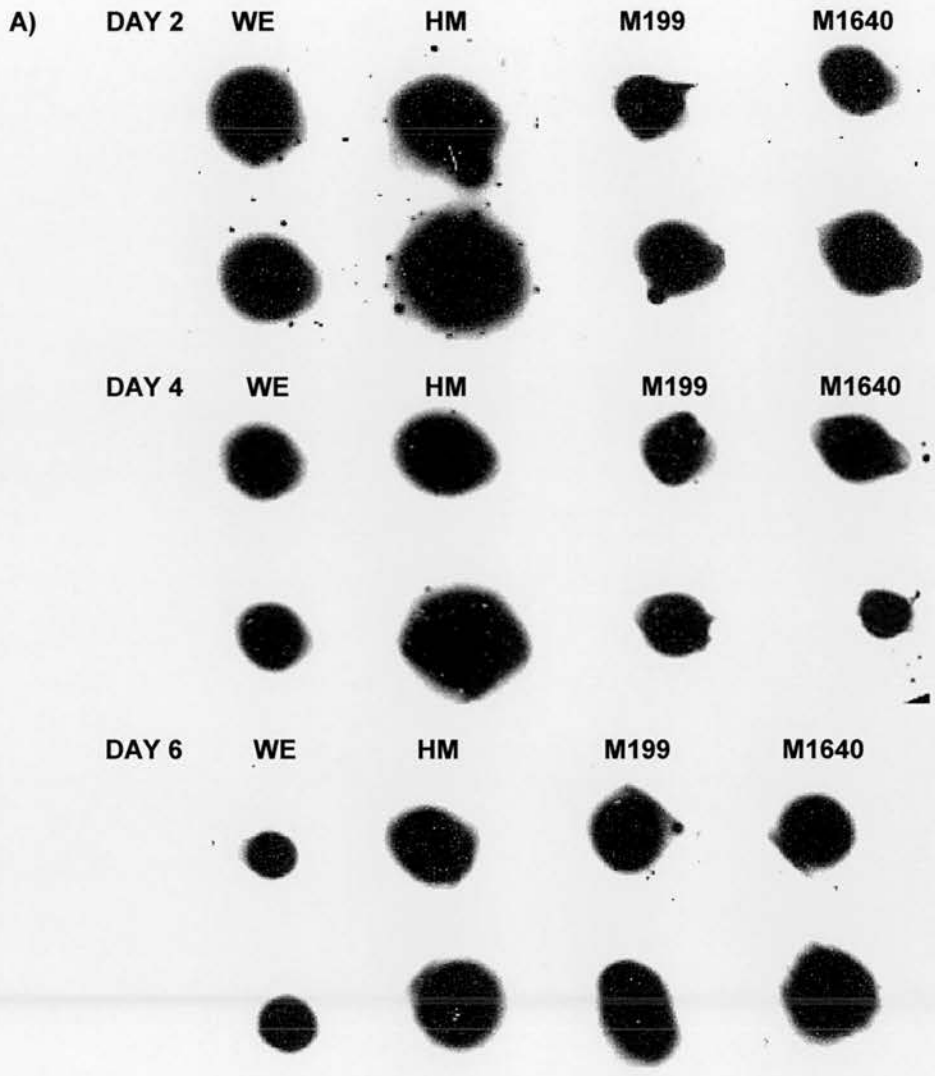

Figure 4.10 Dot Blot Analysis of Primary Porcine Hepatocytes Cultured in Separate Serum-free Chemically-defined Media Formulations Using Antiserum to Albumin

Albumin was detected in porcine hepatocyte cultures, initially seeded at 10^7 viable cells per 100mm dish in WE, HM, M199 and M1640 chemically-defined media, for up to 6 days. A) Duplicate samples of medium supernatant were taken on days 2, 4 and 6, and albumin determined for each (undiluted) medium sample using dot blot analyses (shown here as duplicate pairs of blots), as described in *Materials and Methods* (Section 4.4); B) As controls: i) Each (neat) medium formulation (HM also diluted 1/20 and 1/10), prior to exposure to PPHs, and ii) Purified pig albumin (Sigma A1830) at 0, 25, and 50 μg/ml, and 25 μg/ml without first antibody, were also subject to dot blot as above.

B) CONTROLS

i) MEDIA:	WE (neat)	HM (neat)	HM (1/20)	HM (1/10)	M199 (neat)	M1640 (neat)

ii) PIG ALBUMIN (μg/ml)	50	25	0	25 μg/ml (No first antibody)

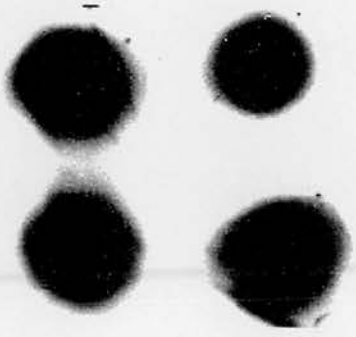

4.6.7 Assesment of overall performance of test media: The Hepatocyte Biological Activity Index (HBAI)

In order to define an index of global functional capacity, a scoring system was devised to simplify multiple comparisons and as an integrated measure of overall functional capability. Indeed, multiple comparisons of biochemical functional activity for 4 test media at 3 different time points cannot be analysed using conventional statistical software programmes. The following assumptions were made: (i) The hepatic-specific functions measured reflect some of the main synthetic, detoxification, and metabolic functions cited as prerequisite of their use in an idealised BAL device; (ii) The associated biochemical measurements of viability and attachment efficiency reflect cellular integrity in such a device; (iii) Scores were generated for each test medium at each time point, by assigning an equally weighted arbitary score of 0-10 points, for the mean values of each biochemical parameter determined from the data in Chapters 3 and 4. Albumun synthesis values were not included because it could not be determined in HM cultures.

Table 4.1 shows how comparative scores for this hepatocyte biological activity index (HBAI) were generated. The midpoint values approximate to a range of values reported in the literature (De Bartolo *et al.*, 2000; Donato *et al.*, 1999; Gregory *et al.*, 2000; Iwata *et* al., 1999; Keatch *et* al., 2002; Lazar *et* al., 1995a; Nelson *et al.*, 2000; Olsen *et al.*, 1997). USR data is derived from urea production in HBSS reference medium (Figure 4.3).

Following from this, Table 4.2 shows a summary of comparative scores; the rank order of test media accumulated over the 6 day culture period for each parameter and the overall ranking derived from the total score thus:

M199=HM>WE>M1640

The limitations of deriving these arbitrary values are discussed below.

Table 4.1: Hepatocyte Biological Activity Index (HBAI): Generation of Index

(See text for details).

Biochemical Parameters Liver Function Evaluated	USR (nmol/h/mg TP) Detoxification	GE (nmol/h/mg TP) Carbohydrate Metabolism	tP450 (pmol/mg TP) Biotransformation Potential	TP (mg) Attachment Efficiency	%LDH Viability
Arbitrary Assigned Score	RANGE				
0	<40	<50	<5	<1	<50
1	41-80	51-100	5-9	1.0-1.9	50-54
2	81-120	101-200	10-14	2.0-2.9	55-59
3	121-160	201-300	15-19	3.0-3.9	60-64
4	161-200	301-400	20-24	4.0-4.9	65-69
5	201-240	401-500	25-29	5.0-5.9	70-74
6	241-280	501-600	30-34	6.0-6.9	75-79
7	281-320	601-700	35-39	7.0-7.9	80-84
8	321-360	701-800	40-44	8.0-8.9	85-89
9	361-400	801-900	45-49	9.0-9.9	90-94
10	>400	>900	>49	>9.9	95-100

Table 4.2 Hepatocyte Biological Activity Index: Comparative Scores

Medium:	WE					HM					M199					M1640					Rank Order of Test Media
Culture day	1	2	4	6	ST	1	2	4	6	ST	1	2	4	6	ST	1	2	4	6	ST	
USR	-	2	2	0	4	-	3	5	2	10	-	2	1	0	3	-	3	4	0	7	HM > M1640>WE>M199
GE	-	5	3	2	10	-	5	3	3	11	-	5	3	3	11	-	6	3	3	12	M1640>HM=M199>WE
tP450	-	7	5	3	15	-	9	7	5	21	-	8	5	5	18	-	8	5	5	18	HM>M199=M1640>WE
TP	7	9	9	8	33	6	7	8	9	30	8	10	9	9	36	7	7	8	6	28	M199>WE>HM>M1640
%LDH	-	10	9	9	28	-	7	9	9	25	-	10	10	9	29	-	8	7	6	21	M199>WE>HM>M1640
Total Score/	7	33	28	22	**90**	6	31	32	28	**97**	8	35	28	26	**97**	7	32	27	20	**86**	OVERALL RANKING (from total score): M199=HM>WE>M1640
cumulative	7	40	68	90		6	37	69	97		8	43	71	97		7	39	66	86		

(See text for details).
ST : Sub-total

4.7 Discussion

Hepatocytes for therapeutic use in BAL devices should retain a full repertoire of synthetic, detoxifying, metabolic and excretory functions. To achieve this as yet elusive goal, many studies have focused on *in vitro* manipulation of the culture microenvironment, including modulation of ECM components, cocultures, and media composition (Allen *et al.*, 2001). In rat hepatocyte cultures, the use of a variety of hormonally-defined media formulations has improved hepatic-specific function, morphology and survival (LeCluyse *et al.*, 1996a). However, the optimal medium formulation required for effective support of primary porcine hepatocyte (PPH) culture in bioartificial liver (BAL) devices remains unclear. The importance of identifying a culture medium which optimises viability and differentiated function of PPHs *in vitro* is well recognised (Flendrig *et al.*, 1997a; Jauregui & Gann, 1991; Naik *et al.*, 1996; Sielaff *et al.*, 1995b), although no systematic studies have been undertaken. Direct comparisons of porcine hepatocyte culture conditions designed to study maintenance of hepatic-specific function are complicated by the number of culture variables and interdependence on such factors as substratum, medium formulation, and hormone supplementation. Moreover, comparisons are further complicated by the by the wide range of endpoints used to assess hepatic function. In fact, information on metabolic functions in PPHs is still very limited as compared with primary cultures of human and rat hepatocytes, which have been well characterised (Donato *et al.*, 1999; LeCluyse, 1996a).

The aim of this study was to examine *in vitro* conditions for maintenance of differentiated hepatic-specific functions of porcine hepatocytes under different culture conditions. Specifically, the effects of William's E, Hepatocyte Medium, M199 and RPMI 1640 serum-free chemically-defined medium formulations on synthetic, detoxification and metabolic parameters were assessed to determine which medium was best able to maintain hepatic support functions.

We have demonstrated that primary porcine hepatocytes can be cultured with high plating efficiency on biomatrix-free tissue culture plastic in different serum-free, chemically-defined media formulations whilst maintaining high viability (Chapters 2 and 3) and retention of hepatic-specific function for up to six days (Nelson *et al.*, 2000; Keatch *et al.*, 2002). The HBAI, as an integrated measure of overall functional capability, ranked the media as M199=HM>WE>M1640. The functional data for day 2, which is in the time frame for BAL device usage, showed that USR, ASR, tP450, and GE functions for test media, were up to 300%, 90%, 20%, and 50%, respectively, of *in vivo* values for human liver (Table 4.3). Medium 199 gave the highest mean values of plating efficiency, viability, and albumin synthesis rates (ASR) than the other media tested up to day 4, although the differences were not always statistically significant. By day 4 of culture, both M1640 and HM pre-cultured cells showed significantly greater urea synthesis rates (USR) than both WE and M199 maintained cells. There was a 66% decrease in total cytochrome P450 content (tP450) in 2-day-old cultures compared with fresh cells, whereas HM maintained cells preserved significantly higher day 4 tP450 levels than both WE and M1640 conditioned cells. Galactose elimination (GE) was significantly higher in day 2 cultures in all test media compared with both days 4 and 6 which then remained relatively stable thereafter. The albumin synthesis rate (ASR) tended to increase in all media up to day 6. Furthermore, parallel morphological studies indicated that different medium formulations modulate gross and ultrastructural morphology of hepatocyte cultures (Chapter 3). These findings may be of relevance when choosing an appropriate medium for porcine-based BAL devices, which require rapid attachment of high viability cells with significant ammonia detoxifying capacity whilst maintaining biotransformation potential and a diverse functional profile.

Table 4.3 Hepatic-specific functions of porcine hepatocyte cultures compared with monolayer cultures and *in vivo* data from several species

Monolayer: Day 2 cultures unless stated	**USR nmol/hr/ mg TP**	**ASR μg/hr/mg TP**	**Total P450 content (pmol/ mg TP)**	**GE nmol/hr/ mg TP**	***References / Comment***
Porcine	115 (basal)	0.7	205 (day 0)	ND	*Lazar 1995c; Sajiki 2000; Olsen 1997*
Porcine	30 (basal) 90 (2mM H_4Cl)	0.3 1.0 (d6) 2.1 (d10)	ND	ND	*Gregory 2000 (Dr P Gregory Pers Comm.)*
Porcine Porcine BAL	270 ND	0.034 0.08 (d21)	ND ND	ND 470 (d21)	*Koebe 1996* *Gerlach 1994*
Porcine Porcine BAL Porcine BAL	20 (10mM H_4Cl) 40 (10mM H_4Cl) ND	ND	ND	ND 25 45	*Flendrig 1997; Iwata 1999*
Human	145	0.25	60	ND	*Vilei 2001; Chesne 1993; Gomez-Lechon, 1990*
Sheep (Day 1 only assessed)	136 (d0 MEM) 51 (d1 WE) 70 (d1 WE) 135 (MEM)	ND	199 (day 0) 113 (d1 WE) 107 (d1 M199) 117 (MEM)	ND	*Watts 1995; Chee's-cultured Cells' non-viable*
Rat (10mM NH_4Cl)	216 (Day 0) 184 (MEM) 84 (WE) 84 (M199) 31 (Chee's)	ND	216 (day 0) 81 (MEM) 31 (WE) 49 (M199) 66 (Chee's)	ND	*Day 6 rat P450 levels unchanged*
Rat	103 (basal) 300 (3mM NH_4Cl)	2.2 (Day 0) 2.2	73 (day O) 40	ND	*Dich 1987; Weymouth's*
In vivo values (human liver) (pig liver) (rat liver)	 40 ND ND	 2.0 ND 2.4	 184* 204* 292*	 960 410 *(5mM gal)	*Iwata 1999; Lazar 1995c; Gomez-Lechon, 1990; Donato 1999 *(liver microsomes).*
Pig: WE HM M199 M1640	196 (Day 0) 104 126 115 147 (2mM NH_4Cl)	ND 1.4 ND 1.9 1.5	120 (Day 0) 35 48 42 41	ND 420 436 416 516 (6mM gal)	*Present data: USR / GE assays in HBSS reference medium*

Table 4.3 Hepatic-specific functions of porcine hepatocytes cultured in test media compared with monolayer cultures and *in vivo* data from different species. Since measured hepatocyte functions, culture conditions and duration vary greatly between research groups which makes direct comparisons difficult, each value represents the quoted mean values for day 2 measurements, unless stated, normalised to the total protein content (mg TP). *In vivo* values are shown for human, pig, and rat livers. The galactose and NH_4Cl loading doses' when cited in literature, are shown in parentheses. *Abbreviations*: ASR, albumin synthesis rate; BAL, bioartificial liver bioreactor; Gal, galactose; GE, galactose elimination; USR, urea synthesis rate; MEM, Modified Earle's Medium; Day 0 (fresh cellls); d1 (Day 1 cultures); ND, not determined in referenced study.

Previous studies

Much information is available on differentiated morphology, metabolic function and long-term survival of rat hepatocyte monolayer cultures. To achieve this, a substratum of liver-specific extracellular matrix (ECM), such as collagen, fibronectin or Matrigel is required. Serum is used in media or is required for the initial attachment phase and cells may be subsequently cultured in serum-free hormonally-defined medium (HDM) containing known concentrations of growth factors including epidermal growth factor (EGF), insulin and dexamethasone. Such conditions almost certainly provide the most physiologically appropriate *in vivo*-like environment currently available (Strain, 1994).

In contrast, far fewer studies have evaluated the influence of different media formulations on rat hepatic functional activity (Enat *et al.*, 1984; Gebhardt *et al.*, 1978; LeCluyse *et al.*, 1996; Mitaka, 1998; Watts *et al.*, 1995; Williams *et al.*, 1977), and no data is available for pigs. The data from functional studies of rat hepatocyte cultures has often been extrapolated to PPHs, which has important implications for porcine-based cell therapies since distinct species differences are known to exist, which may invalidate this approach. For example, cell proliferation studies have shown porcine hepatocytes to have a much greater proliferative potential than rat hepatocytes cultured on collagen in hormonally-defined medium (Joly *et al.*, 1997; Wegner *et al.*, 1992). As mentioned, PPHs do not require serum or an attachment substrate. The latter may however be required for long-term cultures. In addition, pig hepatocytes reproduced cytochrome P450-dependent oxidative metabolism of human hepatocytes to greater extent than either rat, rabbit or dog primary cells, or the HepG2 hepatoma cell line (Donato *et al.*, 1999). Finally, oxygen uptake rates, an important parameter in BAL design, were significantly higher for PPHs than rat hepatocyte monolayer cultures (Balis *et al.*, 1999).

These studies highlight the need for species-specific characterisation of hepatic cellular function to optimise performance for BAL systems.

Hepatic detoxification capacity

Total cytochrome P450 content

A major complication of ALF is hepatic encephalopathy. Contributory factors include ammonia toxicity, dysfunctional endogenous benzodiazipine-like substances and putative toxic compounds released from the injured liver, normally metabolised by the Cytochrome P450 system (Blei, 1997; Blei, 2000; Desille *et al.*, 1999; Jauregui and Gann, 1991; Naik *et al.*, 1996). As a result, many studies have focussed on both ammonia detoxification and P450 system biotransformation in PPHs. In agreement with previous observations in swine (Monshouwer *et al.*, 1998; Olsen *et al.*, 1997), our data shows that tP450 levels decreased substantially (55-65%) after 2 days in culture from 120 pmol/mg TP for freshly isolated cells to 40 pmol/mg TP in all media tested, remaining relatively stable for the remainder of the culture period (Figure 4.7). Total P450 content after 48 hours culture of rat, mouse, hamster and human hepatocytes, in media of 75% MEM/ 25% M199 with 10% FCS or WE or M199 with 5% FCS, was very similar to our values (Chesne *et al.*, 1993; Watts *et al.*, 1995). However, comparable studies with pig hepatocytes (Monshouwer *et al.*, 1998), cultured in WE with 4% FBS for 48 hours, showed double the mean tP450 levels (92 pmol/mg TP) of the serum-containing cultures above. This suggests that species differences might exist in retention of tP450 biotransformation potential under these conditions (Monshouwer *et al.*, 1998) and that there is a component(s) in serum which resulted in P450 induction, although this issue was not investigated. Factors such as age, sex, and strain of the animal can also influence the P450 activity and tP450 content (Prof JI Mason, University of Edinburgh, personal communication). The labile nature of total P450 may be explained by observed down-regulation of P450 mRNA transcripts triggered during the collagenase isolation process (Padgham *et al.*, 1993; Padgham and Paine, 1993). Total P450 measurements cannot easily be made in BAL devices due to restricted access during operation. The limitations of assessing P450 biotransformation of cultured porcine hepatocytes are discussed below.

In this study, tP450 levels have been measured as an indicator of the biotransformation potential of the hepatocytes. Previous reports (Mitaka, 1998; Nelson *et al.*, 2000; Keatch *et* al., 2002; Watts *et al.*, 1995) have used tP450 as a measure of highly differentiated hepatic function. The aim here was to assess, using carbon monoxide difference spectroscopy, both preservation of a wide range of P450 species and to demonstrate the totality of intact P450 enzymes in the pool using one assay. However, the values presented here merely gauge the xenobiotic metabolising activities of all phase I isoenzymes, where high levels of tP450 indicate enhanced global phase I metabolic capability (as in fresh hepatocytes). The decreased tP450 levels in subsequent cultures suggest a compromise of the phase I metabolising potential of the hepatocytes, in agreement with previous studies in swine (Donato *et al.*, 1999; Monshouwer *et al.*, 1998; Olsen *et al.*, 1997). Nevertheless, tP450 does not provide sufficient information on the type and specificity of phase I activities representative of particular P450 enzymes. Selection of the most appropriate functional assay is not straightforward. The metabolic conversion of 7-ethoxycoumarin to 7-hydroxycoumarin requires both phase I and II reactions and has been used as a functional assay for PPHs for BAL use (Naik *et al.*, 1996), whilst metabolism of diazepam has been used as an indicator of both P450 activity and cell viability (Jauregui and Gann, 1991). Use of the latter is based on the assumption that dysfunctional endogenous benzodiazipine-like substances are implicated in hepatic encephalopathy.

Alternatively, cells cultured in each test medium could be evaluated for cytochrome P450 regioselective testosterone metabolism. This has two main advantages over tP450 measurement alone: i) the metabolic profile is very similar to humans; ii) hydroxylated metabolites of testosterone (eg 6β, 15β; measured by HPLC) provide information on several P450 activities in a single assay. However, this approach, in common with other P450 activity assays, would reveal only a very limited repertoire of P450 species. Moreover, precisely which P450 species are required to be preserved to treat ALF remains elusive. Another complication in deciding on a suitable functional P450 activity assay is that some P450 isoforms are

lacking in certain species. For example, in pig hepatocyte cultures, the P450 2B related 7-pentoxy-resorufin *O*-depentylation activity, also involved in testosterone hydroxylation, was not detectable even after phenobarbital induction, a known inducer of this P450 isoform (Monshouwer *et al.*, 1998).

Interestingly, Monshouwer *et al.*, (1998) documented that the 50% reduction in tP450 content paralleled the decline in testosterone 6β-hydroxylase activity over 48 hours in PPH culture. Likewise, Donato *et al.*, (1999) correlated a decline in functional phase I (eg ECOD, EROD) and phase II activities in cultured hepatocytes of different species including pig and human with decreased tP450 levels. In fact, this study highlighted the lack of information on pig P450 isoenzymes involved in hepatic metabolism of a range of common substrates. Finally, due to the importance of phase II compounds in the detoxification process, it may be beneficial to measure, for example, cellular glutathione content in future comparative studies.

Urea synthesis

Detoxification of ammonia to urea is considered a prerequisite hepatic support function of BAL devices. Initial studies showed that cells cultured in each defined test medium maintained a highly efficient urea synthesising capacity (Figure 4.1), which was significantly higher than previously reported (De Bartolo *et al.*, 2000; Flendrig *et al.*, 1997a; Gregory *et al.*, 2000; Lazar *et al.*, 1995a; Lazar *et al.*, 1995b; te Velde *et al.*, 1995). In these experiments, cells were cultured in each test medium for 2, 4, or 6 days, and then assayed in the same medium containing 2 mmol/L NH_4Cl. In retrospect, although producing apparently high USR values, differences between the media could not be delineated because (a) the 'chronic' effect of the media *conditioning* the cells in culture may involve induction or repression of urea cycle enzymes (see Figure 1.6), and (b) the 'acute' effect of the assay medium may be due to differences in the amino acid concentrations of the test media (see APPENDIX I), and (c) a preliminary study for day 2 cultures (incubated overnight in each test medium without NH_4Cl), showed substantial differences in endogenous, basal urea

production for WE, HM, M199, and M1640 cultures (67, 234, 79, and 173 nmol/h/ mg TP, respectively).

Subsequent assays were modified to take account of these differential effects. Thus to permit a more standard methodology which avoids the potential confounding factors of different constitution of the test media (such as the variable amino acid content), cells were pre-cultured in test media and urea production measured in HBSS reference medium containing NH_4Cl on days 2, 4 and 6 of culture. This buffered solution does not contain amino acids. Figure 4.2 confirms that urea production was linear in cell cultures preconditioned in test media, and subsequently, assayed in HBSS reference medium containing 2 mmol/L NH_4Cl. The values obtained for each day of culture using this protocol, corrected for endogenous urea production, are shown in Figure 4.3. USR was significantly higher in HM- and M1640-conditioned cells up to day 4 compared with both WE and M199 cultures. USR values in all cultures conditioned in each test media up to this time point, were comparable with porcine, human, rat, and sheep hepatocytes under a variety of cultured conditions (Table 4.3), and 2-5 fold higher than endogenous urea production for human liver *in vivo*.

These findings support the idea that the ability of cultured pig hepatocytes to convert NH_4Cl to urea is in part, influenced by the test medium formulation in pre-culture. The ammonia concentration in liver cells is about 0.7 mM, about ten times the upper limit of normal in plasma, whereas at physiological pH, 99% is present as NH_4^+ (Ampola, 1994, Meijer, 1990). Considering values in FHF plasma are about 0.16 mM, depending on the aetiology (Demetriou & Rozga, 1998), the value of 2mM NH_4Cl used in our assays is somewhat validated. Under these culture conditions, the high circulating levels of ammonia, suggested to be involved in the development of cerebral oedema and herniation in FHF (Plevris *et al.*, 1998), could be lowered in a porcine-based BAL by compensating the function of the liver, and could, in theory, provide effective hepatic support and therapy for patients with FHF. In particular, both M1640- HM-preconditioned hepatocytes exhibited a greater urea synthesizing capacity than all other media (Figure 4.3) by day 4, and at least as efficiently as in

previous reports (Table 4.3), although, since measured hepatocyte functions, culture conditions and duration vary greatly between research groups, direct comparisons should be made with caution. Possible physiological reasons for the enhanced urea synthesis rates observed in these media are discussed later. USR was maintained at ≈120 nmol/h/mg TP in both M199 and WE conditioned cells on day 2. Considering that normal *in vivo* values for human liver are ≈40 nmol/h/mg TP, these conditions could potentially deliver BAL support functions, provided there was adequate cell mass. Hepatic detoxification is considered to assume a critical role in BAL systems. Whether sufficient P450 detoxification functions would be provided by the same critical mass of cells, is unknown at present, since different groups have used between 2-33 % of hepatic cell mass in their BAL designs.

The HM formulation is a modification of Leibovitz L-15, which contains supra-physiological concentrations of certain components, especially amino acids (APPENDIX I). *Conditioning* of cells in HM for 4 days probably allow increased cytosolic concentrations of amino acids by enhanced uptake via amino acid tansporters, which in turn may upregulate urea cycle enzyme expression. Indeed, a greater supply of amino acids and NH_4^+ to the hepatocytes increases urea flux, (1) through carbamoyl phosphate synthetase upregulation (Meijer *et al.*, 1990), and (2) by an increase in the supply of substrates (see Figure 1.6), via amino acid catabolism. Carbamoyl phosphate synthetase controls flux through the cycle and is the key regulatory enzyme in urea synthesis from ammonia (Meijer *et al.*, 1990). The high osmolarity of HM may compound these effects by enhancing anabolic reactions and enzyme expression, as well as amino acid uptake, so USR may approach maximum velocity.

This would not account for the observation of relatively high USR in M1640, compared with WE and M199 conditioned hepatocyte cultures. However, the most potent stimulator of ureogenesis, arginine (Ampola, 1994, Meijer, 1990) is present in supraphysiological but varying concentrations in the different media formulations. The high concentration of arginine in both M1640 and HM (4-10 fold greater than WE

and M199 test media; APPENDIX I) may account for the significantly higher urea synthesis rates in hepatocytes conditioned in these media.

It should be noted that L-15 medium was originally formulated for use in carbon dioxide free systems for support of cell lines. The extent to which this may affect, for example, pH homeostasis for HM cultured cells in particular, is unknown. However, since pH regulation may play an important role in a number of cellular processes such as glycolysis, cell volume, and urea synthesis (Strazzabosco and Boyer, 1996), monitoring and maintaining physiological pH to optimise culture conditions should be considered in future studies.

Our whole liver retrograde perfusion method may isolate parenchymal cells preferentially from the periportal region (Gumucio *et al.*, 1986; Kano *et al.*, 1998). Since all five enzymes of the urea cycle are located primarily in periportal hepatocytes (Meijer *et al.*, 1990), this may partly account for the augmented USR values observed in this study, compared with some other reports (Table 4.3), which use *in vivo* isolation procedures. In addition, unlike labile P450 enzymes, which are rapidly depleted in culture, expression of urea cycle enzymes are apparently more stable (Dunn *et al.*, 1991).

An important discrepancy in the urea synthesis data presented here is the lack of correlation with the ultrastructural observations of Chapter 3 (Section 3.5.3.2, page 3-22). Differences in hepatocyte morphology appeared to be influenced by the culture medium formulation, since ultrastructural examination of day 2 WE- and M199-maintained hepatocyte cultures illustrated that the features typical of metabolically active liver cells were maintained, in contrast to both HM and RPMI 1640 cultures. Since urea synthesis clearly requires functional and intact mitochondria, it suggests that alternative mechanisms account for the urea synthesis findings for HM and M1640 conditioned cells. Increased lactate concentrations (2mM) can stimulate urea synthesis from ammonia, at least in rat hepatocyte cultures (Berry *et al.*, 1991). The morphological appearance (Chapter 3) of M1640- and HM-conditioned cells

hepatocytes show progressive deterioration up to culture day 6 and relatively decreased viability compared with the other test media, perhaps reflecting an increase in lactate levels, with a concomitant increase in USR. However, other energy-requiring synthetic functions, such as albumin synthesis, were relatively well maintained in these media (see below).

Interestingly, our USR values were at least double those of PPHs grown on a variety of extracellular matrices (te Velde *et al.*, 1995), including Matrigel™ (50 nmol/h/ mg TP), considered the 'gold standard' attachment substrate with which to improve differentiated hepatic function. In addition, PPH cultured in a collagen gel-Matrigel sandwich configuration did not enhance CYP3A metabolic activity compared with collagen alone (Hosagrahara *et al.*, 2000). Moreover, (Gregory *et al.*, 2000) demonstrated that culturing porcine hepatocytes on collagen-coated surfaces or single or double collagen gel layers did not facilitate improved urea (or albumin) synthesis rates (Table 4.3). Furthermore, our values for albumin synthesis were 100 fold greater than those achieved using collagen gel entrapped PPHs cultured under serum-free conditions (Sielaff *et al.*, 1995a; Sielaff *et al.*, 1995b). This reinforces the notion that exogenous attachment substrates, notwithstanding the expense, may be unnecessary for porcine-based BAL devices.

Albumin synthesis

Albumin production by hepatocytes is not considered a primary function required of BAL systems since human albumin can be readily administered in the clinical setting of ALF (Gregory *et al.*, 2000; Plevris *et al.*, 1998; Riordan *et al.*, 1998; Tsiaoussis *et al.*, 2001). However albumin is a well established marker of hepatic-specific differentiation in culture and is the predominant product of hepatic protein synthesis representing a highly oxygen-dependent (aerobic), energy-requiring (ATP) biosynthetic function (Seifter and Englard, 1994). Furthermore albumin requires complex processing and packaging via the endoplasmic reticulum and Golgi membrane systems prior to secretion, processes which also require cellular energy.

Taken together, maintenance of albumin synthesis reflects well on both the capacity of the hepatocytes to synthesise and secrete proteins in general, acting as a surrogate marker of overall cell fitness.

Albumin production by PPHs was detected in test media using a novel, sensitive and reproducible method for detecting pig albumin in culture supernatants (fluorimetric albumin blue 580 dye binding assay). This method is much simpler, more expedient (samples can be analysed in under 2 hours) and convenient than ELISA, since there are no antibody incubation steps and the assay is based on a 96-well microtitre plate format, so enabling up to 40 duplicate samples to be assayed in one run. The presence of albumin was confirmed by dot blot analysis (Figure 4.4.3). A major drawback of our comparative study was the inability to measure endogenous albumin production in HM cultures due to the high background levels in this formulation. In retrospect, analysis for the presence or absence of albumin in the test media should have been undertaken, and a more appropriate alternative medium used in the study. However, conventional methods used for albumin detection in the initial phase of the study were too insensitive to measure μg quantities in culture supernatants (Figure 4.10).

Albumin production in WE, M199 and M1640 show good correlation with *in vivo* values of human and rat liver (Table 4.3 and Figure 4.9), although with a somewhat anomalous increase in ASR up to day 6 of culture, despite the observed deterioration in both gross morphology and ultrastructure noted in Chapter 3 at this time point. Gregory *et al.*, (2000) reported a similarly increasing trend in ASR throughout the culture period of PPHs cultured in WE/1% serum on plastic dishes, or as collagen sandwich cultures, from a relatively high initial ASR value, to values approaching *in vivo* production (Table 4.3). This phenomenon could be explained by the observation that, at least in rat hepatocytes, insulin and dexamethasone have a synergistic effect on ASR with an initial lag period of several days. Under defined serum-free conditions insulin initially stabilizes albumin mRNA whereas dexamethasone, after an extended time-lag, increases the transcription rate of the albumin gene in hepatocyte culture

(Grunnet *et al.*, 1988; Nawa *et al.*, 1986). It should be noted however that the influence of insulin, hydrocortisone, glucagons, and serum (of unknown hormonal and growth factor composition) were included as supplements in these media. The isolation process itself may account for the initial, relatively low albumin levels compared with that observed *in vivo*, since Dunn *et al.*, (1992) showed that collagenase digestion reduces the average polyribosome size for albumin mRNA translation within hepatocytes.

Between-media comparisons on each culture day did not reveal major differences. However, ASR in M1640-grown hepatocytes increased significantly between days 2 and 6. This could not be explained however by the influence of known stimulators of albumin synthesis (Doweiko and Nompleggi, 1991a; Doweiko and Nompleggi, 1991b) present in the test media. For example, potassium, which facilitates the release of albumin from the hepatocyte is identical in concentration in each medium. Moreover, although tryptophan enhances albumin synthesis, the lowest concentration was present in M1640, which paradoxically had the highest mean ASR value. Remarkably, the urea cycle and albumin synthetic machinery appear inextricably linked, the same amino acids stimulating both urea and albumin synthesis. In agreement with Oratz *et al.*, (1973) we have shown that urea synthesis rates and albumin appear to follow a similar pattern of expression on day 2 of culture (Figures 4.1 and 4.9, respectively).

Galactose elimination

Galactose elimination capacity is used as a quantitative liver function test to study functional hepatic mass (Baker, 1992). Unlike the caffeine clearance test, which requires expensive HPLC equipment, galactose levels in culture supernatants (or plasma) are easily measured using commercial kits requiring standard spectrophotometry. In humans, plasma [galactose] values are <0.28 mmol/L in adults, while the range for newborn infants is 0 to 1.11 mmol/L (Painter *et al.*, 1986). The ability of hepatocytes to metabolise galactose was tested to reflect the integrity of

carbohydrate metabolism in the BAL setting. A galactose loading dose of 6 mmol/L was used for GE determination in HBSS reference medium of all cells pre-cultured in test media, since this is close to the value used clinically in liver function tests (Whitington, 1992), experimentally in BAL systems (Flendrig *et al.*, 1997a), and is close to linear at [galactose] of 5-6 mmol/L over a range of concentrations (Figure 4.5). Finally, equimolar [galactose] loading dose allows valid, direct comparisons between the different test medium formulations, since HM contains 5-6 mmol/L galactose. The ability of the hepatocytes to uptake and metabolise galactose in each test medium was significantly higher for day 2 cultures (≈450 nmol/h/ mg protein) than days 4 and 6, but remained relatively stable (≈250 nmol/h/ mg protein) throughout the culture period (Figure 4.4). These findings are in agreement with Gerlach *et al.* (1994) although the GE was maintained at this level up today 21 of culture in their BAL device. This correlates with the *in vivo* GE capacity of pig liver (Table 4.3), and is 50% that of human liver under a 5mM loading dose of galactose. Moreover, our GE values are 10-20 fold higher than observed in the porcine-based BAL devices of Flendrig *et al.*, (1997a) and Iwata *et al.*, (1999). The latter study used DMEM/ 25% heparinised human blood, whereas the former used WE/ 10% FBS in a 3D culture configuration. Whether serum supplementation of the perfusion medium interferes with this facet of carbohydrate metabolism remains to be elucidated.

Thus, taken together with, for example the ASR data above, *in vitro* markers of functional activity of PPHs should be compared with documented *in vivo* levels, when considering the functional liver cell mass required of BAL systems.

The validity of the GE test in BAL setting remains controversial. Despite its relatively widespread use as global liver function test, *in vitro* and animal experiments suggested it is not a reliable indicator ((Demetriou & Rozga, 1998). However, the efficiency of galactose elimination in our study reflects both the presence of hexose uptake transporters in the hepatocyte cultures and the metabolic conversion suggests an intact Leloir pathway (Leloir, 1951; Figure 1.7). Although the mechanisms by which

different media formulations impact upon regulation of this facet of carbohydrate metabolism is unknown, culture age appears to be an important factor.

Overall performance of media formulations: The Hepatocyte Biological Activity Index (HBAI)

The definition of the most favourable conditions for PPH culture as determined by measurement of functional capability and identification of a variety of differentiation markers in optimal culture media is crucial for effective cell-based therapies (Sielaff *et al.*, 1995b). However, major drawbacks in testing the efficacy of the various BAL devices under development include the lack of an appropriate animal model of acetaminophen-induced ALF, discussed in detail in our recent review (Newsome *et al.*, 2000), and the absence of standardization for assessment of cell function between laboratories. This may be due to the variable usage of, for example, serum-free or serum-containing media formulations, biomatrices or culture system modalites.

Such diversity of approach and our limited information of the most important hepatocyte functions make direct comparisons between research groups very difficult. Moreover, since the pathophysiology underlying FHF is incomplete, precisely which hepatic support functions should be preserved in a BAL remains a challenge. Most investigators therefore evaluate BAL hepatocyte function empirically. It would seem reasonable to evaluate specific markers of differentiation that cover the spectrum of synthetic, detoxification and metabolic liver functions, since there is no single global marker to quantify liver function (Demetriou & Rozga, 1998).

It may therefore be useful to assess and weight all cell functions equally. To simplify comparisons, we proposed a 'hepatocyte biological activity index' (HBAI), which normalises each hepatic functional parameter with respect to an equally weighted scoring system (see Section 4.6.7 and Table 4.1). This would allow direct comparisons of any hepatocyte-based culture system, provided the same parameters were used to assess global function. The assumptions made in generating the HBAI

are outlined in Section 4.6.7, page 4-32. Using these criteria it is evident that both M199 and HM maintained cultures attained the highest HBAI cumulative score by day 6 (Table 4.2), ranking the media as follows: M199=HM>WE>M1640. However, the gross and ultrastructural morphological observations, and image analysis data presented in Chapter 3, suggest M199 and WE best preserves the *in vivo* characteristics of differentiated hepatocytes up to culture day 4, which is the time frame for current operational BAL usage, with high viability and attachment efficiency. Using this utility, HBAI scores for day 2, rank the media as M199>WE>M1640>HM, whereas the day 4 rankings were, M199>HM>WE>M199. The morphologica observations, combined with analysis of the HBAI scores, suggest that Medium 199 may be one of the most suitable synthetic media for preserving differentiated hepatic function and morphology, under serum-free chemically-defined conditions for BAL systems.

The HBAI utility presented here provides some measure of global functional activity of our hepatocyte culture system. There are however, some important caveats. Firstly, an accord would be necessary between BAL research centres, each requiring to adopt identical isolation, culture and assay procedures as presented in this thesis, as the overall quality of the hepatocytes are considered to be interdependent on these factors (Jauregui, 1991). The HBAI is based on certain empirical assumptions, and these arbitrary associations cannot take into account, *inter alia*, that some functions may be more important than others, or not even be a functional requirement, per se, for clinical BAL systems. For example, although albumin production is often cited as a marker of differentiated function, it is unlikely to play an important therapeutic role for patients with FHF (Gregory *et al.*, 2000). Equal weighting of each biochemical parameter may in itself distort the final score and outcome of the HBAI, since an important unmeasured function, or other factor, may be omitted, whereas random selection of chosen functions may introduce bias. For example, our data suggests that image analysis data of plating efficiencies may be more discriminatory than the biochemical measurements of total protein and LDH activity. Therefore, defining only biochemical measurements as the most important factors in the generation of the HBAI may be insufficient.

Also, if a given culture condition significantly enhanced a particular cell function, say, 10-fold, the scoring systems limited range would not take account of the relative improvement in function and would skew the final score. Use of only mean values and omission of SEM statistical data is also problematic. Furthermore, performance of hepatocytes in our culture system for example, does not guarantee the same functional efficacy in the BAL environment, since the cells may perform quite differently in the presence of FHF plasma. Indeed, recent studies have shown that exposure of ALF serum or plasma to hepatic cell lines has deleterious effects on important functional parameters including glutathione homeostasis and P450 activity (Shi *et al.*, 1998; McCloskey *et al.*, 2002). The HBAI may be useful then, in the more limited, unilateral context of assessing multiple comparisons.

Chapter 5

Morphology and Metabolic Function of Primary Porcine Hepatocytes Cultured in Simulated Microgravity

5.1 Introduction

Development of therapeutic applications for PPHs may benefit from a culture system expressing stable levels of liver-specific functions, which exhibit cellular polarity and morphology that closely resemble that found *in vivo*. In previous chapters, we have shown that although PPHs maintain relatively high metabolic activity and normal phenotype under a variety of culture conditions, cells have a limited life span suitable for BAL usage of only 2-4 days. One possible reason for this is that conventional hepatocyte (static) culture on 2-dimensional (2D) surfaces, such as plastic or collagen, disrupts cell shape and polarity, resulting in retrodifferentiation and loss of hepatic gene expression and function (Berthiaume *et al.*, 1996). Partial restoration of cell polarity and differentiated function (Michalopoulos *et al.*, 1999) is achieved using 3-dimensional (3D) matrices such as Matrigel™ or collagen gel sandwiches (Berthiaume *et al.*, 1996), in hormonally-defined medium (HDM).

Alternative strategies used to invoke 3D cell culture configurations, include the formation of porcine hepatocyte spheroids from cell suspensions using spinner flasks (Lazar *et al.*, 1995a; Lazar *et al.*, 1995c), conventional stirred fermentors (Unsworth and Lelkes, 1998) and the use of roller bottle culture (RBC) with microcarrier-attached hepatocytes (Jauregui *et al.*, 1997) or without synthetic support structures (Michalopoulos *et al.*, 2001). In the latter study, isolated rat hepatocytes and NPCs in collagen-coated RBCs, formed structured tissue-like formations bearing resemblance to hepatic histological organization. Hepatocyte aggregation in these systems, contributes to 3D cellular arrangements and enhanced cell-cell interactions, which have been reported to prolong and improve hepatocyte function *in vitro* compared with traditional 2D cultures (Auth and Ichihara, 1998; Lazar *et al.*, 1995a;

Lazar *et al.*, 1995b; Lazar *et al.*, 1995c). For example, a significant increase in albumin synthesis can be induced in engineered liver tissue by hepatocyte aggregation (Kim and Mooney, 1998; Parsons-Wingerter and Saltzman, 1993). In these dynamic culture modalities, however, physical forces of high shear stress, which damage the cells by fluid shear forces and rotationary impeller impacts, and gravity-induced sedimentation may hinder proper tissue-specific differentiation (Spaulding *et al.*, 1993; Unsworth and Lelkes, 1998).

Originally to offset the high shear forces of space shuttle launch and re-entry on biological tissues, NASA developed a novel rotary cell culture system (RCCS), which promotes growth of fastidious, delicate cells in a simulated microgravity environment. During space flight, cell suspensions experience microgravity forces of 10^{-4}-10^{-6} g, preferentially aggregate and yield higher cell densities than at 1 g (unit gravity) (Unsworth and Lelkes, 1998). Human liver, cartilage, bone marrow, skin explants and various cell lines and carcinomas have been successfully cultured in the RCCS into macroscopic, differentiated, tissue-like 3D constructs (Becker *et al.*, 1993; Goodwin *et al.*, 1993; Jessup *et al.*, 1993; Spaulding *et al.*, 1993). This is facilitated by a simulated microgravity environment (10^{-2}g), which promotes randomised angular gravitational vectors on the growing aggregate thus creating a freefall (quasi-stationary) rotation of the cell aggregate(s) around a horizontal axis within the vessel. The resultant efficient low-shear mass transfer of nutrients and waste products with high oxygenation, promotes close apposition (spatial co-location) of single cell suspensions resulting in the formation of microgravity-induced, 3D cell formations.

Preferential aggregation in microgravity may not only enhance cell-cell interactions, differentiated function and cell polarity, but may well induce tissue-specific up-regulation of cell adhesion molecules, extracellular matrix (ECM) proteins and their respective integrin receptors (Unsworth and Lelkes, 1998). ECM geometry in concert with adhesive cell-cell and cell-ECM interactions, modulate and maintain structural and differentiated functional features of hepatocytes *in vivo*, such as expression of cell surface adhesion molecules, albumin production and urea synthesis

(Berthiaume *et al.*, 1996; Bhatia *et al.*, 1999). Such regulatory effects of ECM, are often mediated by integrins, which comprise a large family of cell surface receptors that attach cells to ECM proteins and mediate mechanical and chemical signals arising from ECM. For example, the most abundant hepatocyte integrin, the fibronectin receptor, $\alpha_5\beta_1$, is thought to be involved in the coordinated control of cell shape, growth and survival, important for the establishment and maintenance of tissue architecture (Giancotti and Ruoslahti, 1999; Stamatoglou *et al.*, 1990; Stamatoglou and Hughes, 1994). Indeed, antibodies blocking the binding of β1-integrin subunits to collagen, in collagen-sandwiched hepatocyte cultures, resulted in significant alterations in hepatic morphogenesis, cell polarity and differentiated function (Moghe *et al.*, 1997). Using time-lapse microscopy, Peshwa *et al.*, (1996), revealed that cell movement and reorganization were involved in spheroid formation, implicating a mechanistic role for integrins. In fact, integrin bridging between cellular cytoskeleton (CSK) and ECM components allows cells to exert force on their environment, critical for many cellular processes including efficient cell movement (Holly *et al.*, 2000). Moreover it has been suggested that cell surface adhesion molecules such as integrins act as mechanoreceptors, which might sense the microgravity environment and alter ECM mechanics, cell shape and cytoskeletal organisation and thus tissue-specific function (Ingber, 1999; Ingber, 1997). Integrins likely play an important role in the differentiation of the epithelial and endothelial cell populations of the liver (Couvelard *et al.*, 1998). The present study was designed to investigate the feasibility of using the RCCS to culture PPHs in a simulated microgravity environment to maintain 3D aggregate culture formations and differentiated function for an extended period of time.

5.2 Aims

Using biochemical, histological, ultrastructural and immunocytochemistry studies, we sought to identify whether spheroid aggregate formation in the unique environment of simulated microgravity, maintained stable, liver-specific metabolic capacity and characteristic hepatic morphology for an extended period. The expression of integrin

α5, as a marker of hepatic differentiation and structural integrity, was investigated and the findings compared with conventional static cultures.

5.3 Materials and methods

5.3.1 Reagents

All reagents used were as detailed in previous chapters, with the following additions: Primary antibody: polyclonal anti-integrin α5 (raised in goat) from Insight Biotechnology (Middlesex, UK). The secondary antibody, indodicarbocyanine, Cy3™-conjugated donkey anti-goat IgG and normal donkey serum (NDS; 60 mg/ml) were supplied by Jackson Immunoresearch (West Grove, PA, USA). Fluorescein diacetate was obtained from Sigma.

5.3.2 Hepatocyte isolation

Hepatocytes were isolated from weanling piglets (<15kg) using our *ex vivo* collagenase perfusion method described in Chapter 2 (Nelson *et al.*, 2000).

5.3.3 Hepatocyte cultures

5.3.3.1 Static cultures

For immuno-staining cells were cultured for up to 6 days on Lab-Tek™ glass chamber slides in serum-free chemically-defined William's E (WE) Medium. To verify cell viability, a spheroid sample cultured for 12 days in serum-free chemically-defined WE medium in the RCCS-HARV, was dispersed by gentle pipetting and transferred to TCP dishes and cultured for 2 days in the same medium. Otherwise, hepatocytes were cultured as described in Chapter 2.

5.3.3.2 Hepatocyte culture in simulated microgravity: The rotary cell culture system-high aspect ratio vessel (RCCS-HARV)

Microgravity conditions were simulated using two RCCS-HARV configurations: 1) 55 ml capacity single station RCCS-HARV (Figure 5.1) and 2) 10 ml capacity, four station RCCS-HARV (Figure 5.2).

Preliminary work: In order to optimise, empirically, the consistent formation of cell aggregates in microgravity, cells were seeded (day 0) in the 10 ml capacity HARVs (Cellon-Sarl, Luxembourg) at densities of 0.25, 0.5, 1.0 or $2x10^6$ viable cells per ml of serum-free, chemically-defined William's Medium E at 37°C. Seeding densities of $1x10^6$ viable cells per ml gave the most consistent simulated microgravity culture of aggregates in freefall rotation as defined above (Section 5.1), and were used for all subsequent experiments.

The HARV was connected to the horizontally rotating axle of the RCCS, which pumped incubator gas via a central aperture, across a silicon rubber, semi-permeable gas exchange membrane within the HARV. The RCCS-HARV assembly was placed in a humidified incubator under a 95% air: 5% CO_2 atmosphere. Next day (day 1), aggregated cells were allowed to sediment, the HARV aspirated, and pre-warmed, fresh medium added, which was subsequently changed every 2 days. The optimal rotational speed of the HARV was determined by adjusting the RCCS rotational speed such that the aggregate(s) maintained a freefall, quasi-stationary orbit within the culture vessel. The rotational speed varied according to both aggregate size and the corresponding sedimentation coefficient. However, by day 6 of culture, rotational speed was set between 10-15 rpm. For changes of supplemented William's E medium a 0.5 cm fill port was used using a suction aspirator. Medium was replenished on days 1 and 2, and every 2 days thereafter. When changing the medium, the cells were covered by a small amount of medium to minimise cell damage. Media samples were taken at the time points indicated via a syringe attached to one of the luer-lock syringe ports and stored at -80°C until analysis.

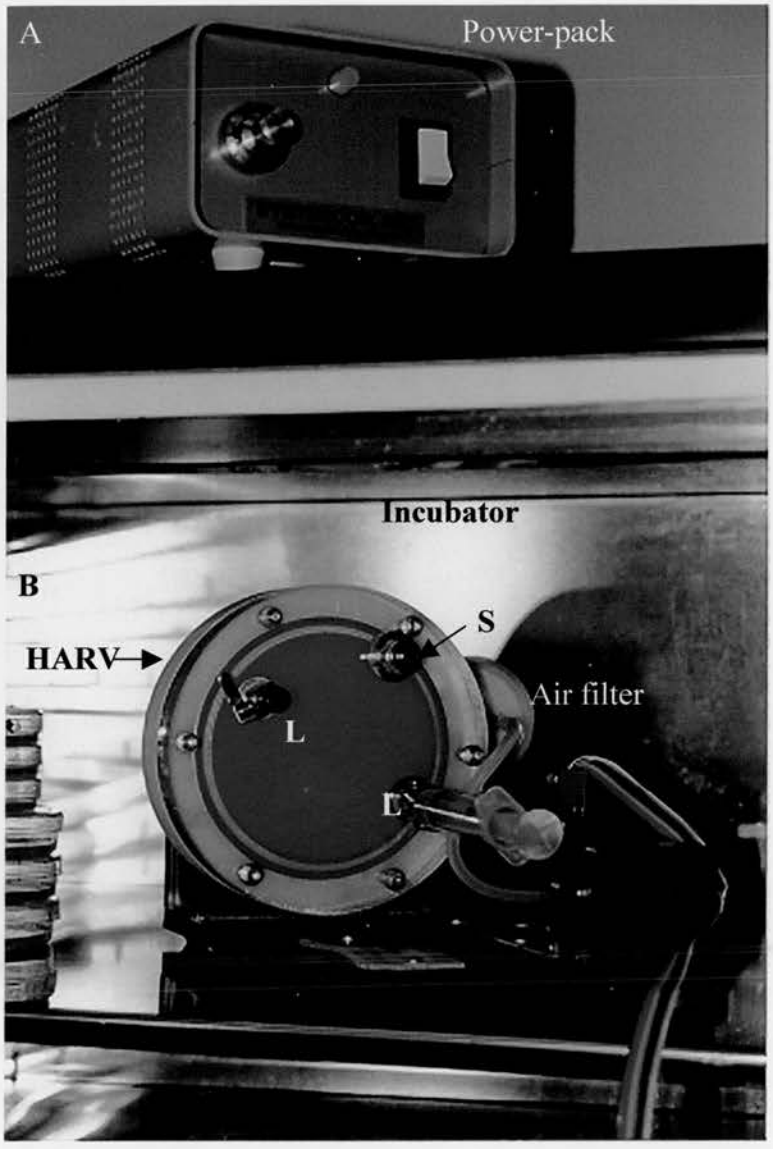

Figure 5.1 The single station high aspect ration vessel (HARV) and rotary cell culture system (RCCS) set-up.

The power-pack (A) drives the HARV (B) around a horizontal axis which provides a simulated microgravity environment for the culture of cell suspensions (see text for details). Medium is replenished via the sample port (S) and samples taken via luer locks (L, L') and attached syringe (at L').

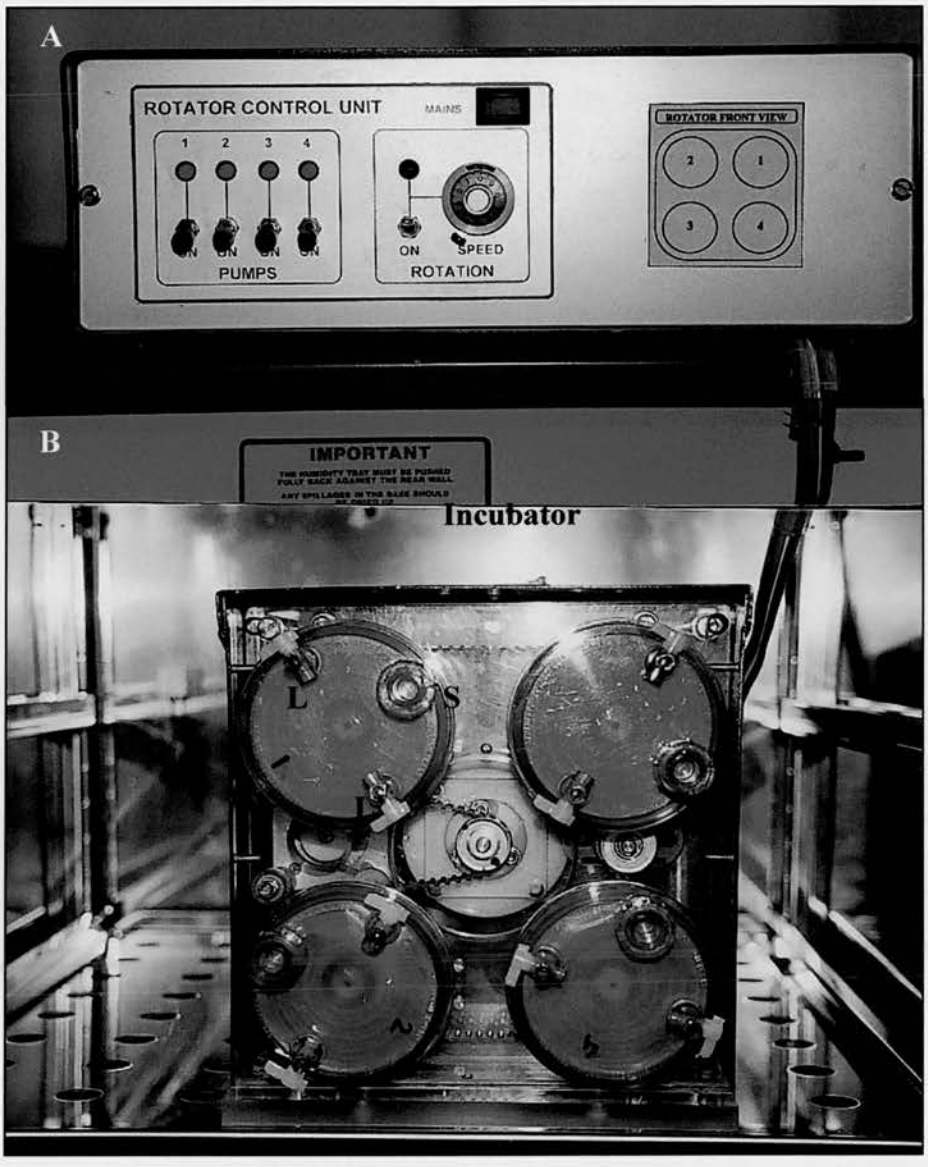

Figure 5.2 The four-station high aspect ration vessels (HARVs) and rotary cell culture system (RCCS) set-up

The power-pack (A, rotator control unit) drives the 4 HARVs (B) around a horizontal axis, via a pully/belt arrangement, which provides a simulated microgravity environment for the culture of cell suspensions (see text for details). Medium is replenished via the sample port (S) and samples taken via luer locks (L, L') where syringes can be attached. Incubator air is pumped through the central shaft of each HARV. Gas dissolves in the medium and induction of air bubbles is eliminated, so minimizing fluid shear stresses.

5.3.4 Functional parameters

5.3.4.1 Urea synthesis rate and galactose elimination

Freshly isolated hepatocytes (day 0) were inoculated into the 4-station, 10 ml capacity HARV at a density of 10^6 cells/ ml in supplemented WE medium containing 2mmol/ L NH_4Cl, and rotated at 10 revolutions per minute, in a humidified incubator at 37°C under an atmosphere of 95% air / 5% CO_2. The ammonium chloride challenge was repeated on culture days 2, 6 and 12; after washing the cells with pre-warmed HBSS. To allow comparisons with static cultures, galactose elimination (GE) was assayed by addition of 6 mmol/L D(+)-galactose in HBSS at these time points. The urea synthesis rate (USR) and GE were determined in t=0 samples (assay medium which had never been in contact with cells) and at t=2 hours of incubation, using modified commercial kits, as described in Chapters 2 and 4.

5.3.4.2 Albumin production

The albumin concentration in HARV cultures was determined using the fluorimetric albumin blue 580 dye-binding assay detailed in Chapter 4, Section 4.3.9. Cells were cultured as above and 1 ml samples taken from duplicate HARVs on days 2 (24 hours post medium change), 6 and 12 (48 hours post medium change) and stored at -80°C until analysis of albumin synthesis.

5.3.5 Morphology

5.3.5.1 Histology of cell aggregates

On days 2, 6, and 12 for HARV-grown aggregates, cell samples were removed and fixed in 3 % formaldehyde / 0.1M cacodylate buffer. The fixative was aspirated and the cells washed with PBS; cell aggregates were resuspended in 100 µl of molten agarose for ease of handling. Histological staining was performed using hematoxylin and eosin (H&E) to identify hepatocyte nuclei and cytoplasm, respectively. Periodic

Acid Schiff (PAS) reagent was used to detect the presence of glycogen, whereas silver nitrate stain was used to identify collagen. Subsequent sample processing and staining was performed using standard techniques. Morphology was recorded by photomicrography using an inverted microscope (Zeiss, Germany) under transmitted light, for each culture modality at each time point.

5.3.5.2 Scanning electron microscopy

Freshly isolated hepatocytes and cell aggregates taken from the HARV-RCCS on days 6 and 12 were washed in HBSS buffer and subject to low-speed centrifugation (20 g) for 5 minutes. Cell samples were fixed in 3 % gluteraldehyde in 0.1M sodium cacodylate buffer (SCB) at pH 7.4 for at least 3 hours. Following washing in 0.1M SCB, samples were post-fixed with 1 % osmium tetroxide in 0.1M SCB for 2 hours and washed in distilled water. Following dehydration in a graded series of acetone (50, 70, 90, and 100 % (3 times)), cells were subject to critical point drying with CO_2 in a Poleron E3000 SII critical point dryer. For conductive coating, samples were sputter-coated with 20nm gold / palladium (60/40) in an Emscope sputter coater (Cohen, 1979; Echlin, 1975; Hayat, 1970; Sabatini *et al.*, 1963). Finally cell aggregates were viewed in a Philips 505 scanning electron microscope (SEM).

5.3.5.3 Transmission electron microscopy

Cell aggregates taken from the HARV-RCCS on days 6 and 12 were washed in HBSS buffer and subject to low-speed centrifugation (20 g) for 5 minutes. Cell samples were fixed in 3 % gluteraldehyde in 0.1M SCB and processed as described in Chapter 3, Section 3.3.6.

5.3.5.4 Acridine orange fluorescent dye staining

To assess cell viability, fresh HARV-cultured cell aggregate samples were taken on day 12 and 100 μM acridine orange in WE medium added for 2 minutes at room

temperature (RT). Viable (apple green nuclei) and non-viable cells (yellow / orange nuclei) were visualised using confocal microscopy (see below) and photographed.

5.3.6 Confocal microscopy

The following protocol was modified from Stamatoglou *et al.*, (1990). Adherent cultures on Lab-Tek™ glass chamber slides or aggregate samples from the HARV at the time points indicated above, were fixed in formal saline (4% formaldehyde / 4% paraformaldehyde) / 0.4M sucrose) for 2 hours at room temperature and then washed in PBS with 0.5 % Triton-X for 30 minutes. RCCS aggregates were transferred to 1.5 ml eppendorf tubes for three cycles of 20 minute washes with 1% donkey serum albumin (DSA) in PBS on a Spiramix roller bottle tray. For static cultures, slides were similarly treated and gently shaken on an orbital shaker. Titration of the polyclonal anti-α5 integrin (goat) primary antibody resulted in an optimal concentration of 1:20 for indirect immuno-fluorescence. 50 µl of primary antibody were added to samples for 1 hour at RT. After the primary antibody incubation, the cells were washed in PBS 3x for 20 minutes before addition of the secondary antibody. The Cy3™-conjugated donkey anti-goat IgG secondary antibody was used at a dilution of 1:20 (in 1 % DSA / PBS), 50 µl added and incubated for 20 minutes at RT. Unbound antibody was removed by three 20 minute washes with 1% NDS in PBS. RCCS aggregate samples were mounted in 50:50 glycerol:PBS in wells made by strips of coverslip on standard glass slides. The wells were sealed with nail-varnish to prevent leakage. The Lab-Tek™ glass chamber slide cultures were mounted in 50:50 glycerol:PBS and covered with a glass coverslip and sealed as above. Cells were viewed using a Leica TCSNT confocal microscope system (Heidelberg, Germany) with a 10x objective lens or a 63x water-corrected lens with the Argon-Krypton laser set at λ_{568} nm. Images were recorded on computer and stored on CD for future analysis. As controls: 1) Negative controls: cells were treated as above except that the primary antibodies were omitted; 2) Positive controls: fresh human and pig liver samples were homogenised in SDS / PBS and dot blot analysis was performed of cell lysates using the above primary antibody and an HRP-conjugated donkey anti goat IgG secondary revealing high

(human) and moderate (pig) levels of cross-reactivity (performed courtesy of Drs K Humphreys and AF Howie, Dept of Clinical Biochemistry, University of Edinburgh).

5.3.7 Fluorescein diacetate metabolism of cultured porcine hepatocytes

Fluorescein diacetate (FDA) metabolism of day 12 cultures was analysed to assess bile canalicular function. 80µl FDA was added for 30 minutes in a 10 ml capacity RCCS placed in a CO_2 incubator at 37°C, according to Mitaka *et al.*, 1999. Cells were subsequently rinsed 3x with warm PBS following brief centrifugation at low speed (25g), placed on glass microscope slides and photographed using a Leitz Wetzlar Ortholux II fluorescent microscope with a 25x water immersion lense.

5.3.8 Statistics

Results are expressed as mean ± standard error of the mean. Student's t-test was used to compare means of different groups. A p value of < 0.05 was taken as significant (two tailed test of significance).

5.4 Results

5.4.1 Cell isolation viability and yield

The hepatocytes were isolated using our *ex vivo* method described in detail in Chapter 2. For these experiments, cell viability was 87±5% with a yield of 2.2±0.8 x 10^{10} cells from 12±1 kg piglets (n=10).

5.4.2 Biochemical measures of functional activity in HARV cultures

5.4.2.1 Urea synthesis rate, galactose elimination and albumin synthesis rates

Figure 5.3 shows that urea synthesis rates (USR) were significantly higher ($p<0.05$) in fresh cell cultures (162±40 nmol/hr/ 10^6 cells seeded) compared to both day 2 (61±14; $p<0.01$) and day 12 (85±20; $p<0.05$), although not significantly greater than day 6

HARV cultures (108±38). HARV cultured cells showed enhanced, although not statistically significant, conversion of ammonia to urea on day 6 (108±38) compared to day 2 (61±14) cultures and plateaued at this level until day 12 (85±20). USR values for cells grown in simulated microgravity were approximately one fifth of the values obtained for static, WE maintained cultures (Chapter 4; Figure 4.1) at each time point, although the latter became non-viable after one week of culture, following detachment from TCP dishes.

Figure 5.4 demonstrates that HARV-grown cells had similar day 2 (483±44 nmol/hr/ 10^6 cells) galactose elimination (GE) capacity as observed for corresponding static cultures (420±66), assuming TP content of 10^6 cells ≈1mg (Chapter 3). The mean GE value of HARV cultures remained higher than static cultures up to day 6 (317±57 *vs* 179±50 %, respectively) and plateaued until termination of the experiment on day 12. However, GE levels were significantly lower ($p<0.05$) in both day 6 and day 12 (277±33) HARV cultures compared with day 2.

Albumin synthesis rates (ASR) displayed a similar upward trend (Figure 5.5) compared with static cultures (Chapter 4; Figure 4.4.2) for the duration of the respective experiments. Although the ASR values in HARV cultures on days 2 and 6 of culture were approximately half the values for of comparable static cultures, HARV environment maintained stable cellular secretion of albumin up to day 12 at 1.4±0.4 μg/hr/ 10^6 seeded cells (Figure 5.5).

Figure 5.3 Urea synthesis rates in primary porcine hepatocytes cultured for up to 12 days in the HARV-RCCS simulated microgravity environment

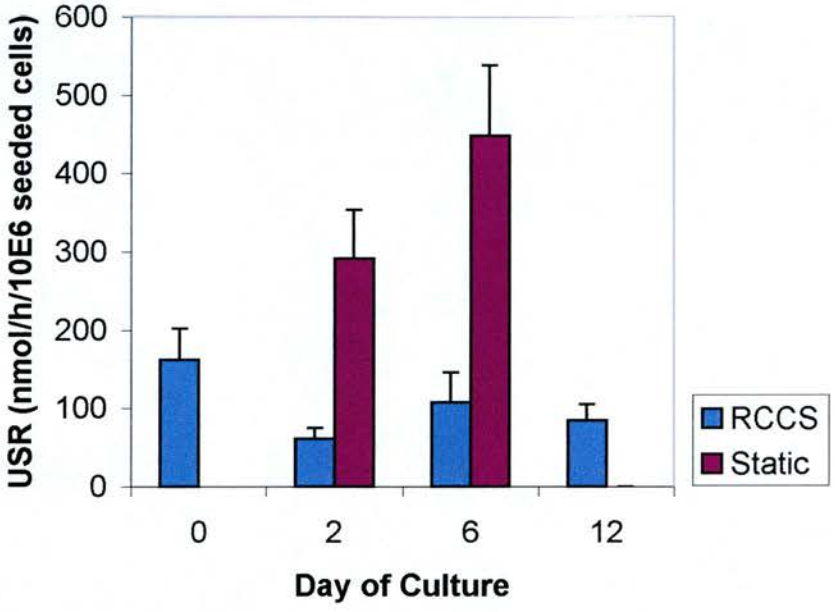

Figure 5.3 Urea synthesis rate (USR) was measured in primary porcine hepatocytes cultured at 10^7 viable cells per 10 ml HARV in William's E chemically-defined medium for up to 12 days in simulated microgravity. 2mM NH_4Cl was added to culture vessels and incubated for 2 hours on days 0, 2, 4, 6 and 12. USR was determined in media samples taken at t=0 and t=2 hours using a modified colourimetric urea nitrogen kit as described in *Materials and Methods*. Results are expressed as nmol/hour/ 10^6 seeded cells. USR is significantly higher in fresh cell cultures compared to day 2 ($p<0.01$) and day 12 ($p<0.05$) All values represent the means±SEM of 3 experiments in duplicate. Student's t-test was used to compare means of different groups. A p value of < 0.05 was taken as significant (two tailed test of significance).

Figure 5.4 Galactose elimination of primary porcine hepatocytes cultured for up to 12 days in the HARV-RCCS simulated microgravity environment

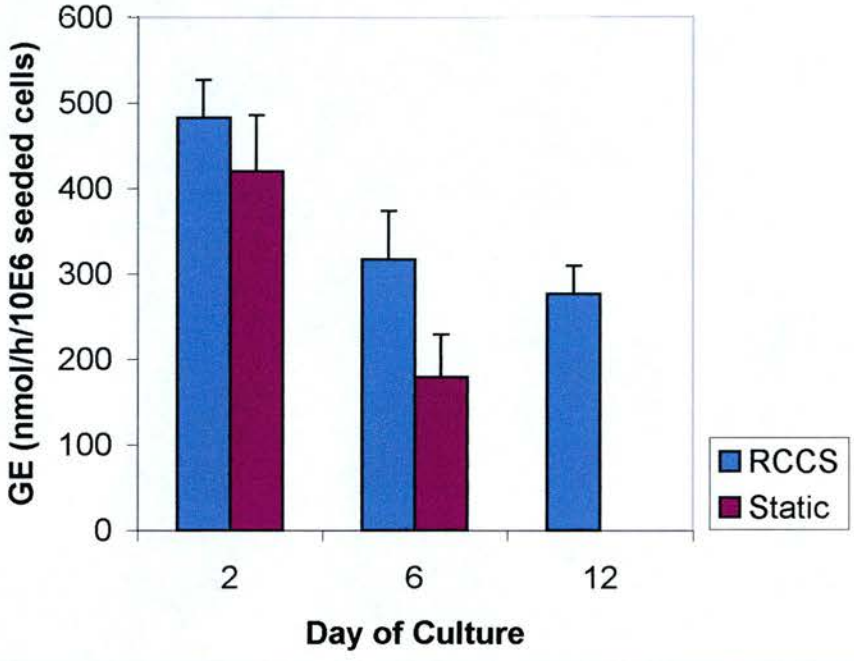

Figure 5.4 Galactose elimination (GE) of primary porcine hepatocytes pre-cultured at 10^7 viable cells per 10 ml HARV in William's E chemically-defined media for up to 12 days in simulated microgravity. 6mM D(+)-galactose was subsequently added to HBSS and incubated for 2 hours on days 2, 6 and 12. and GE determined as described in Materials and Methods. Results are expressed as nmol/hr/ 10^6 cells. All values represent the means±SEM of 3 experiments in duplicate. GE is significantly higher in day 2 cultures compared with both day 6 and day 12 cultures ($p<0.05$). Student's t-test was used to compare means of different groups. A p value of < 0.05 was taken as significant (two tailed test of significance).

Figure 5.5 Albumin synthesis rates of primary porcine hepatocytes cultured for up to 12 days in the HARV-RCCS simulated microgravity environment

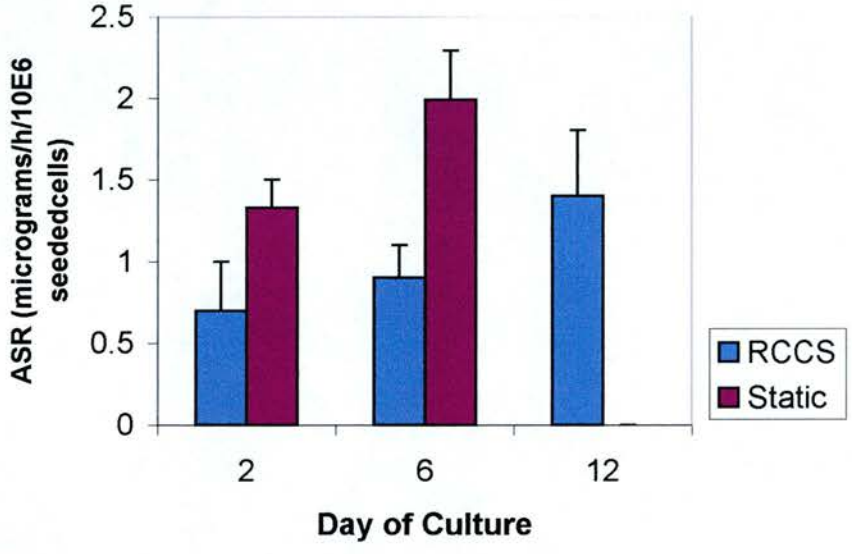

Figure 5.5 Albumin synthesis rates (ASR) of primary porcine hepatocytes cultured at 10^7 viable cells per 10 ml HARV in William's E chemically-defined medium for up to 12 days in simulated microgravity. Samples were taken on days 2 (24 hours post medium change), 6 and 12 (48 hours post medium change) and stored at -80°C until analysis of ASR, determined by fluorimetric analysis of albumin blue 580 dye binding to albumin as described in *Materials and Methods* (Chapter 4, Section 4.3.9). Results are expressed as μg/hour/ 10^6 seeded cells. All values represent the means±SEM of 3 experiments in duplicate. ASR is significantly higher in day 12 cultures compared with day 2 cultures ($p<0.05$). All values represent the means±SEM of 3 experiments in duplicate. Student's t-test was used to compare means of different groups. A p value of < 0.05 was taken as significant (two tailed test of significance).

5.4.3 Morphology of freshly isolated primary porcine hepatocytes and HARV cultured hepatocytes in simulated microgravity

5.4.3.1 Histology

Figure 5.6 shows both freshly isolated hepatocytes (panel A) and day 6 HARV grown aggregate sections (panels B-C) stained with periodic acid schiff (PAS) glycogen stain and counterstained with H&E. The eosinophilic cytoplasm of fresh hepatocytes is stained pink and nuclei are darkly stained. A feature of the fresh cell suspension is the presence of numerous small clusters of hepatocytes as seen in Chapter 2 (Figure 2.3). Panel B in Figure 5.6 shows a transverse section of a HARV aggregate with a distinctive rim of PAS-positive hepatocytes, 8-10 cells in depth, which circumscribes a core of dying cells, although the cells in the core region had eosinophilic cytoplasm in both day 12 (Figure 5.7) and day 6 cultures (not shown). The size of the whole aggregate was estimated to be 4-5 mm in diameter. At higher magnification (Figure 5.6, panel C) some of the cells in the core appear apoptotic as evidenced by condensed nuclei and some cells were necrotic as shown by cell fragmentation. In contrast, the rim of PAS-positive cells appears viable in that the nuclei of individual cells are large and round with prominent nucleoli with discrete eosinophilic staining of the cytoplasm up to day 12 (Figure 5.7). The histology of the HARV cultured aggregates is maintained up to day 12 (Figure 5.8). However, staining for collagen / reticulin fibres using empiric silver nitrate impregnation of aggregate sections proved negative.

5.4.3.2 Scanning electron microscopy

Figure 5.9 shows that, following low speed centrifugation, single cells and 5-20 cell clusters, typical of freshly isolated primary porcine hepatocytes, appear as a densely packed arrangement at both low (Panel A) and higher magnification (Panel B). Numerous microvilli are present on the surface of the hepatocytes, which display a spherical shape upon isolation. By day 6 of culture in simulated microgravity (Figure 5.10), rounded hepatocytes, organized as tight clusters, are clearly distributed on the aggregate surface suggesting extensive cell-cell contacts. Microvilli are still evident on

the surface of hepatocytes (Panel A). At low magnification (Figure 5.11, Panel A) the aggregate is organized as an ellipsoidal, compact cellular structure, although with more loosely associated rounded parenchymal and, presumably, nonparenchymal cells present on the aggregate surface. At higher magnification, the smooth appearance on the aggregate surface (Panel B, open arrow) may be indicative of the compact morphology. Again, microvilli are present on the surface of hepatocytes (closed arrows in panel B).

5.4.3.3 Transmission electron microscopy

Transmission electron microscopy of some sections of HARV-RCCS cultured hepatic aggregates show ultrastructural features of fresh liver tissue (see Chapter 3, Figure 3.3) up to day 12. It should be noted that hepatocytes exhibiting these features are probably cell formations derived from the rim of (viable) PAS-positive cells which circumscribe the core of necrotic/apoptotic cells observed above (Figures 5.6 and 5.8). In fact, most of the TEM sections we observed revealed non-viable, damaged hepatocytes (not shown). After 6 days in culture (Figure 5.12, Panel A) a binucleate hepatocyte retains characteristic ultrastructural features including prominent round nuclei and nucleoli, abundant mitochondria and granular endoplasmic reticulum (ER); interspersed between the mitochondria are numerous dense glycogen particles. Panel B shows several hepatocytes whose borders are separated by canaliculi-like channels with distinguishing microvillous processes; at higher magnification (Panel C) part of the nucleus is shown in close proximity to granular endoplasmic reticulum, adjacent mitochondria and electron dense glycogen particles. At day 12 cells show bile canaliculi-like channels with characteristic microvillous processes between several juxtaposed polygonal hepatocytes (Panel A of Figure 5.13). Ultrastructural features of fresh liver tissue are evident although there is an asymmetric cytoplasmic distribution of granular endoplasmic reticulum, mitochondria and other organelles; interspersed between the mitochondria are numerous electron dense glycogen particles. At higher magnification (Panel B), ultrastructural features observed in day 6 cultures are maintained.

Figure 5.6 Morphology of both freshly isolated primary porcine hepatocytes and cells cultured for 6 days in the HARV-RCCS simulated microgravity environment

Representative photographs showing morphology of fresh primary porcine hepatocytes (A, x100; scale bar 100μm) and of histological sections of PPH aggregates cultured for 6 days in serum-free chemically-defined WE medium in the HARV (B, x50; scale bar 100μm) and corresponding higher magnification photographs of HARV cultures (C, x200; scale bar 50μ). Cell samples (B-C) were stained with periodic acid Schiff glycogen stain and all samples were counter-stained with haematoxylin. **Panel A** shows fresh cell suspension just prior to inoculation into the HARV with eosinophilic cytoplasm and distinct nuclei present; **Panels B and C** Part of a HARV cultured cell aggregate is shown with a distinctive PAS-positive rim of apparently viable cells (arrows, v-v' in panels B and C), some 8-10 cells in depth with large round nuclei (N; panel C); a necrotic / apoptotic core (n) is apparent particularly at higher magnification (Panel C) as evidenced by condensed nuclei (open arrows), and cell degeneration. The area (a), devoid of cells in panel B, is probably an artifact of the fixation process.

A

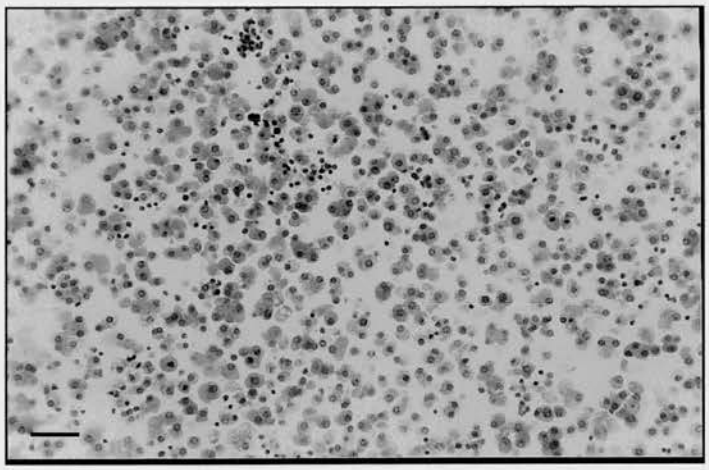

B

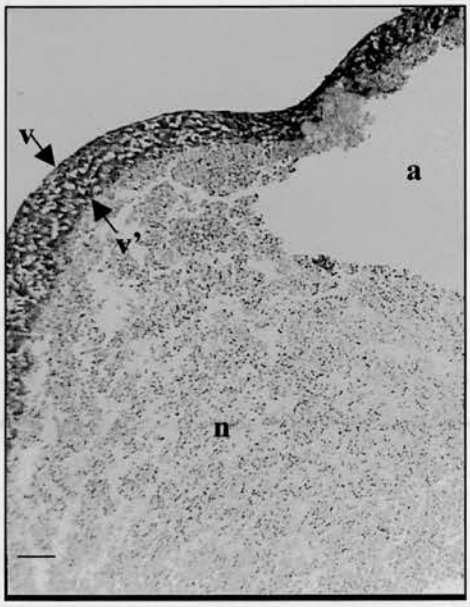

C

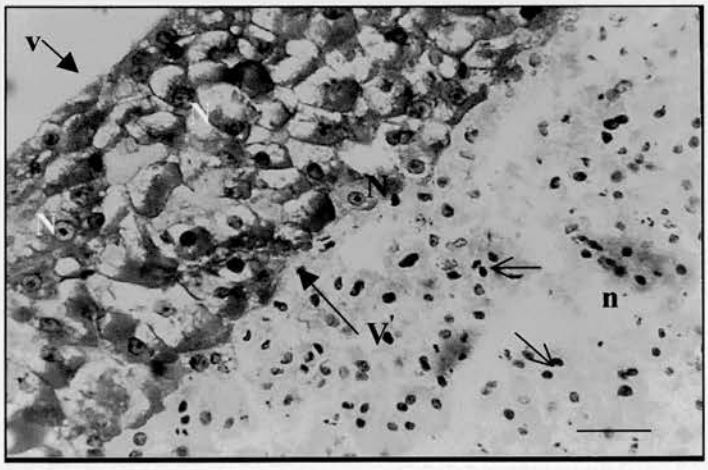

A

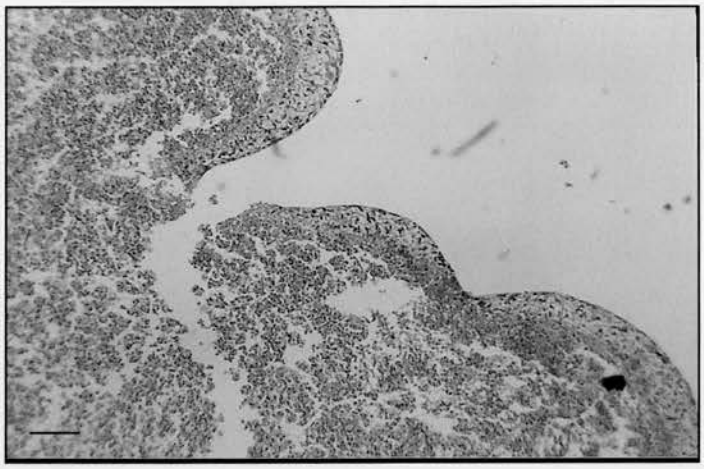

B

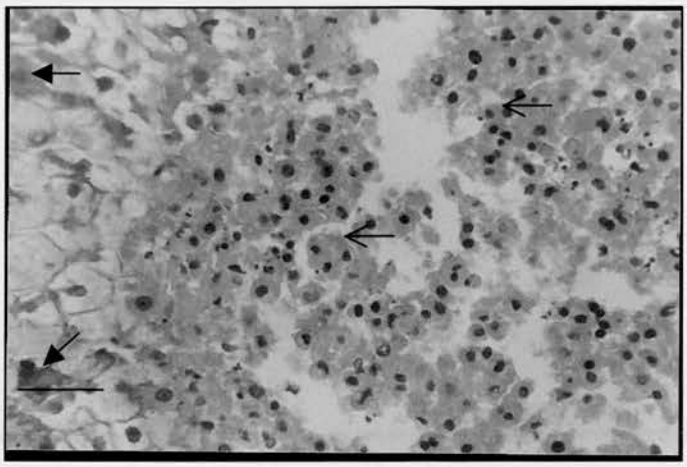

Figure 5.7 Morphology of primary porcine hepatocytes cultured for 12 days in the HARV-RCCS simulated microgravity environment

Representative photographs showing overall morphology and histology of PPH aggregates cultured for 12 days in serum-free chemically-defined WE medium in the HARV (A, x50; scale bar 200μ) and corresponding higher magnification photographs of HARV cultures (B, x200; scale bar 50μ). Cells were stained with haematoxylin (nuclear) and eosin (cytoplasmic) stains. Note that the cytoplasm of the inner core of cells is eosinophilic in both images and condensed nuclei are evident in panel B (open arrows); whereas only discrete eosin staining of the rim of PAS positive cells (see Figure 5.6) with large round nuclei is observed here (closed arrows).

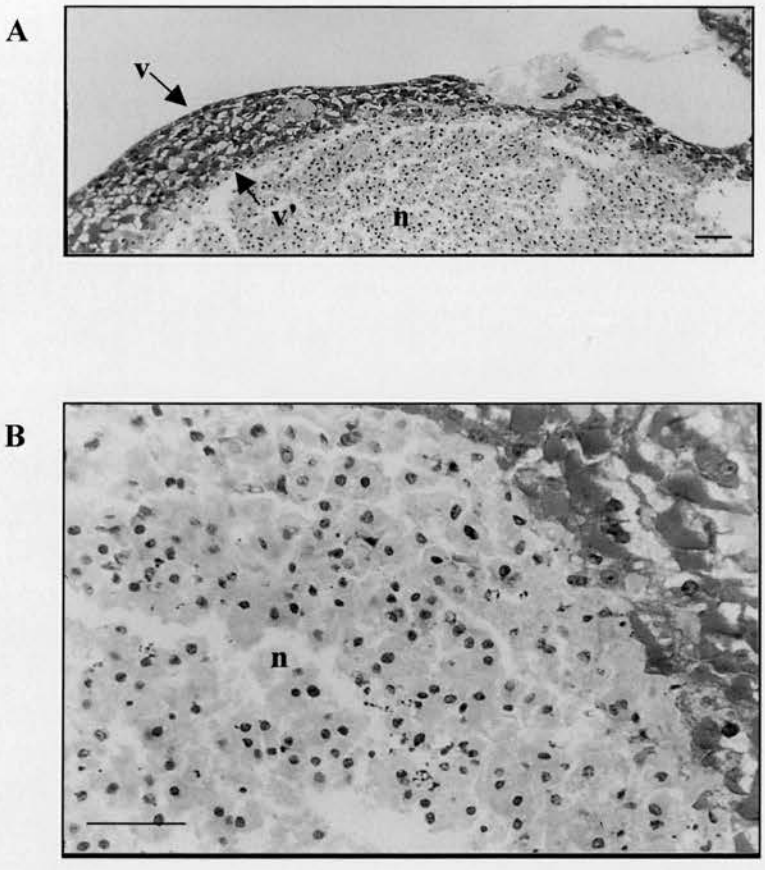

Figure 5.8 Morphology of isolated primary porcine hepatocytes cultured for 12 days in the HARV-RCCS simulated microgravity environment

Representative photographs showing morphology of primary porcine hepatocytes aggregates cultured for 12 days in serum-free chemically-defined WE medium in the HARV (A, x50; scale bar 100μ) and corresponding higher magnification photographs of HARV cultures (B, x200; scale bar 50μ). Cells were stained with periodic acid Schiff glycogen stain and counter-stained with haematoxylin. Morphology of 12 day old HARV cultures is very similar to that seen on day 6 (see Figure 5.6). Note the rim of PAS positive hepatocytes in Panel A (v-v') and Panel B (upper right) with a central core of dying cells (n) evident in both sections.

A

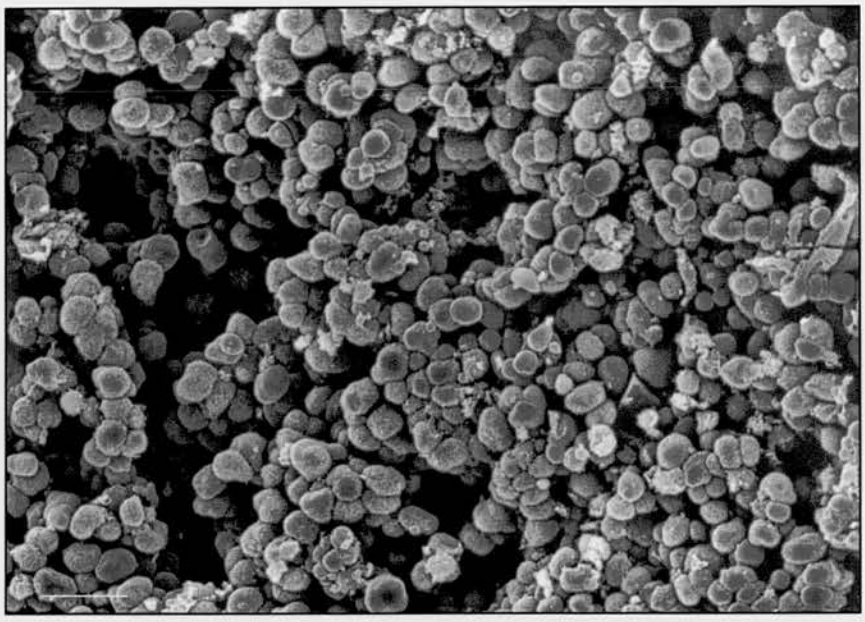

B

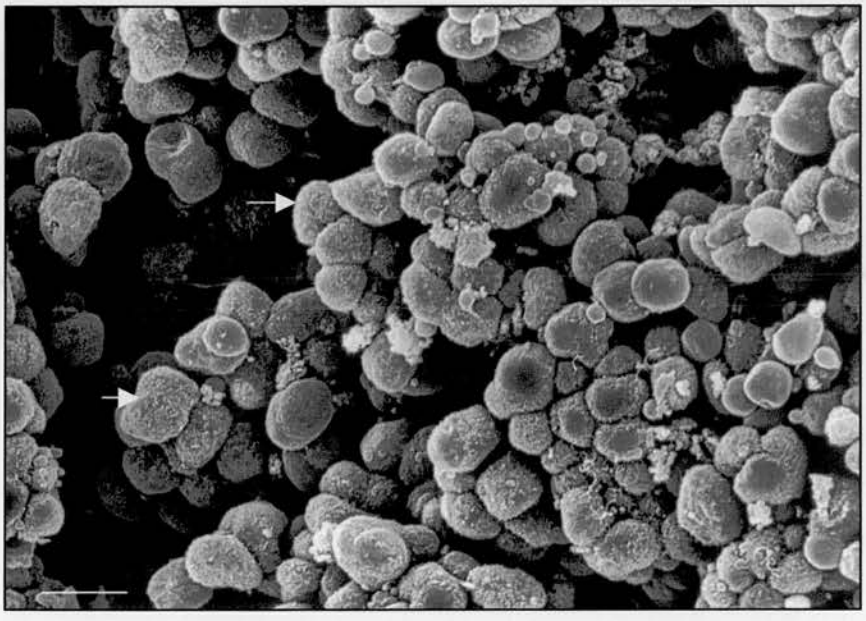

Figure 5.9 Scanning electron micrographs of freshly isolated primary porcine hepatocytes. Following low speed centrifugation, single cells and 5-20 cell clusters appeared as a densely packed arrangement at both low (**Panel A**; x250; scale bar 50μm) and higher magnification (**Panel B**; x460; scale bar 25μm). Note the presence of numerous microvilli on the surface of hepatocytes, arrows in panel B. Cells were processed as detailed in *Materials and Methods*, Section 5.3.5.3.

A

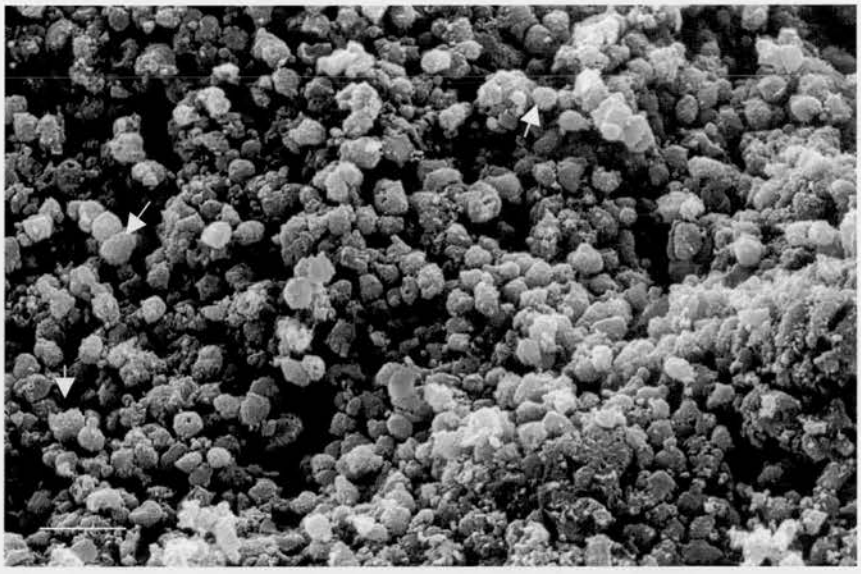

B

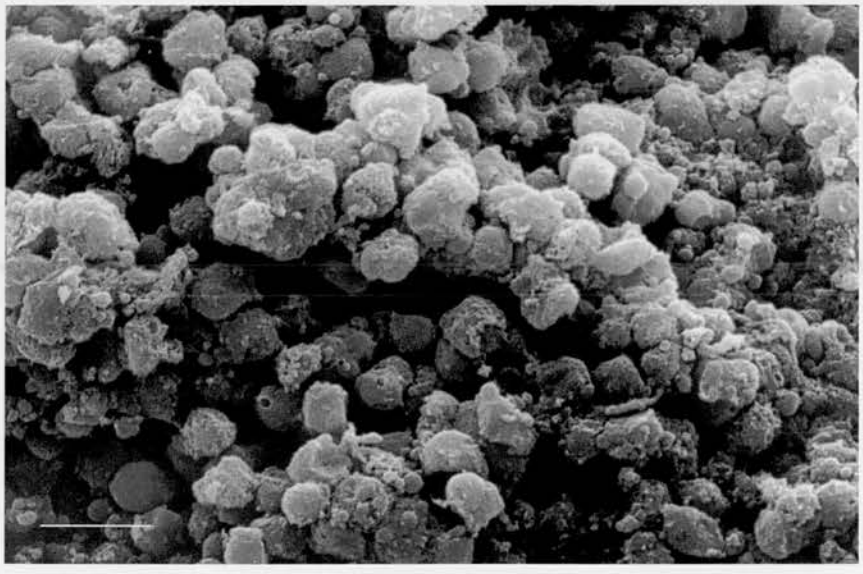

Figure 5.10 Scanning electron micrographs of primary porcine hepatocytes cultured for 6 days in simulated microgravity. Panel A (x200; scale bar 100μm) shows rounded hepatocytes organized as tight clusters suggesting extensive cell-cell contacts and at higher magnification (Panel B; x400; scale bar 50μm). Note the presence of microvilli on the surface of hepatocytes (closed arrows in Panel A). Cells were processed as detailed in *Materials and Methods*, Section 5.3.5.3.

Figure 5.11 Scanning electron micrographs of primary porcine hepatocytes cultured for 12 days in simulated microgravity.

Panel A (x150; scale bar 100μm) shows a tightly packed arrangement of cells organized as an ellipsoidal, compact structure with more loosely associated rounded parenchymal and presumably, nonparenchymal cells present on the aggregate surface. At higher magnification (**Panel B**; x520; scale bar 50μm), the smooth appearance on the aggregate surface (open arrow) may be indicative of the compact morphology. Note the presence of microvilli on the surface of hepatocytes, closed arrows in panel B. Cells were cultured and processed as detailed in *Materials and Methods*, Section 5.3.5.3.

A

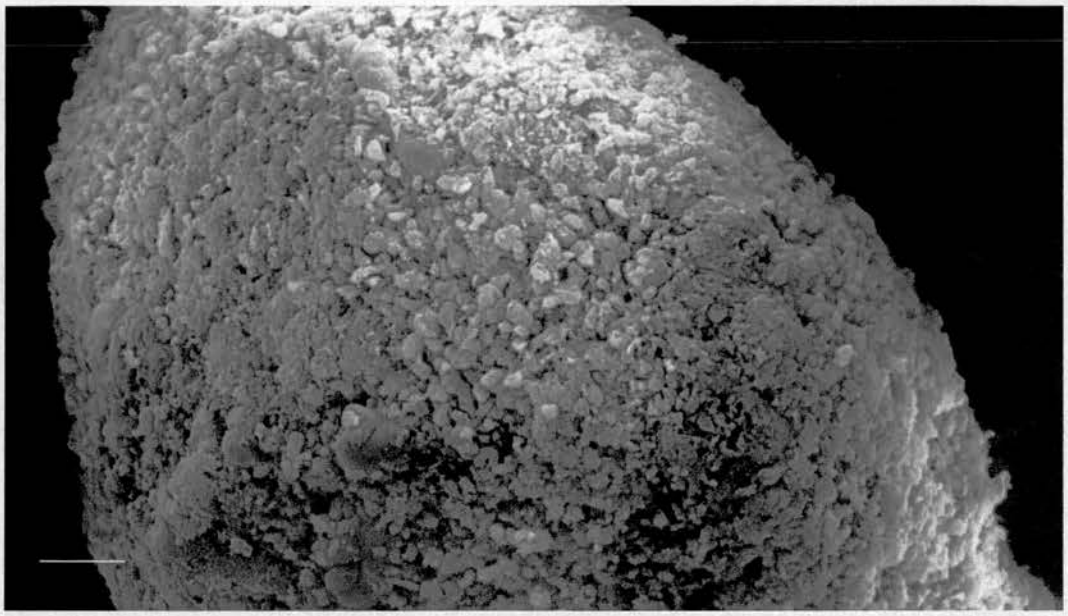

B

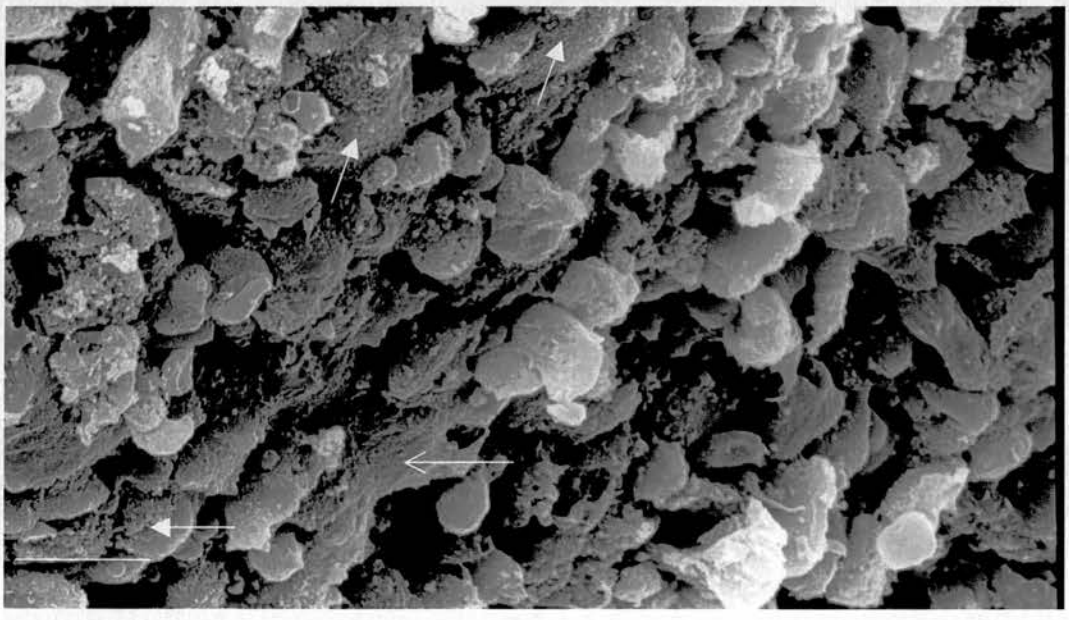

Figure 5.12 Transmission electron microscopy of primary porcine hepatocytes cultured for 6 days in simulated microgravity

Panel A (x8000) shows a binucleate hepatocyte with prominent round nuclei (N) with nucleoli, abundant mitochondria (Mt) and granular endoplasmic reticulum (ger); interspersed between the mitochondria are numerous electron dense glycogen particles (G). **Panel B** (x6300) shows several hepatocytes whose borders are separated by canaliculi-like channels (Bc) with characteristic microvillous processes (m) and prominent granular endoplasmic reticulum present in the cytoplasm. Panel C (x45000) shows part of a nucleus (top left) in close proximity to granular endoplasmic reticulum, adjacent mitochondria and glycogen particles. Cells were cultured and processed as detailed in *Materials and Methods*, Section 5.3.5.3.

A

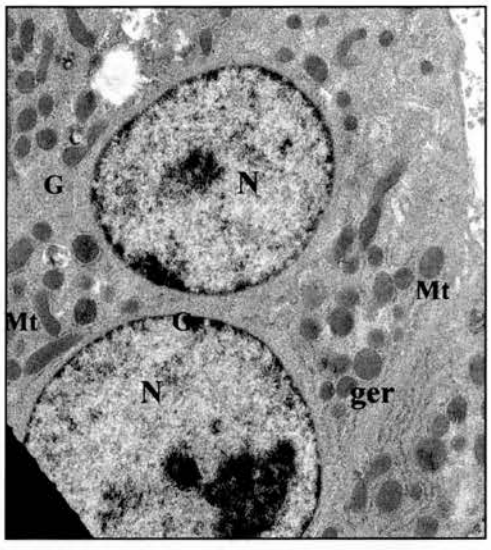

B

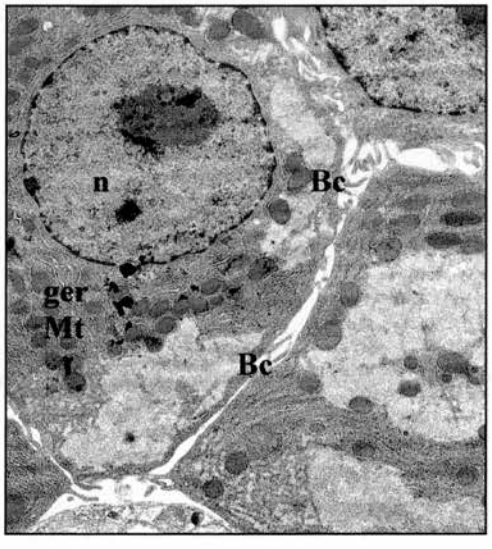

C

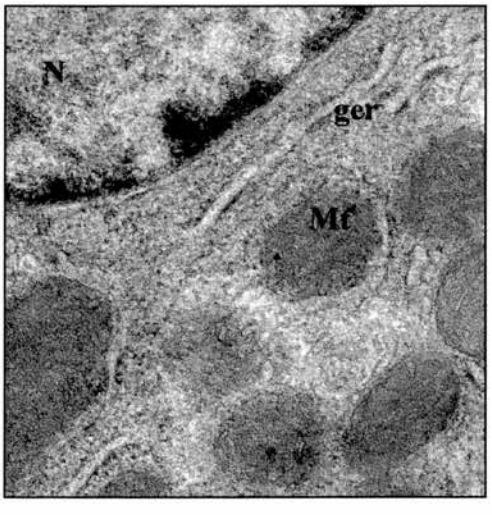

Figure 5.13 Transmission electron microscopy of primary porcine hepatocytes cultured for 12 days in simulated microgravity

Panel A (x1800) shows bile canaliculi-like channels (Bc) with characteristic microvillous processes between several juxtaposed polygonal hepatocytes. Ultrastructural features of fresh liver tissue are evident although there is an asymmetric cytoplasmic distribution of granular endoplasmic reticulum, mitochondria (Mt) and other organelles; interspersed between the mitochondria are numerous electron dense glycogen particles. A possible nonparenchymal cell (npc) is resident in the center right of this image. **Panel B** (x17000) shows part of the hepatocyte nucleus (lower left) in close proximity to mitochondria and lysosomes and adjacent glycogen particles. High magnification image (**Panel C**, x75000) of a bile-canaliculus showing microvillous processes and adjacent Golgi apparatus (Ga). Cells were cultured and processed as detailed in *Materials and Methods*, Section 5.3.5.3.

A

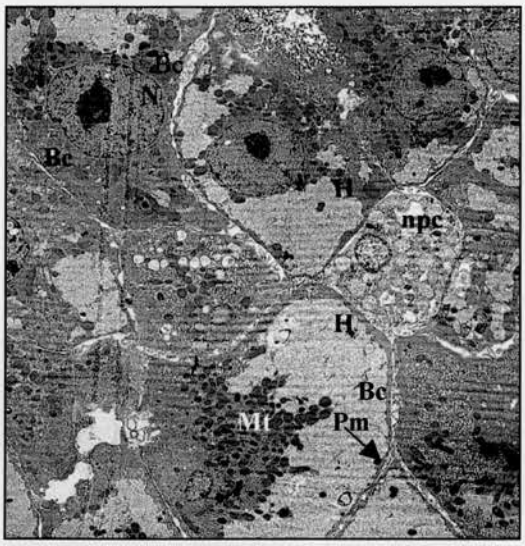

B

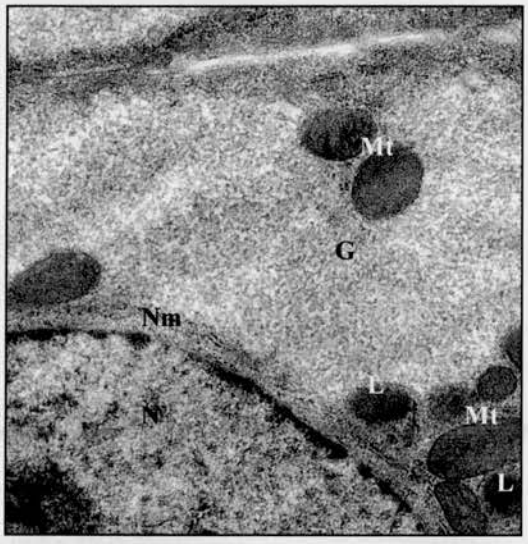

C

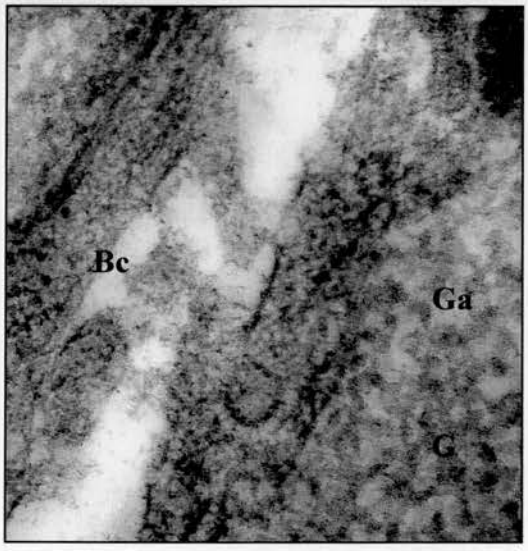

5.4.3.4 Spheroidal viability: Fluorescent acridine orange viability staining of primary porcine hepatocytes cultured for 12 days in the HARV-RCCS simulated microgravity environment

Figure 5.14 shows a small cell aggregate (broken off from a larger aggregate during the staining process), which has stained apple green with the fluorescent dye, acridine orange, characteristic of viable cells *in vitro*; non-viable cells are stained orange-yellow. This demonstrates that at least the outer layer of HARV cultured cellular aggregates, remain viable up to culture day 12 in simulated microgravity. To verify cell viability by cell attachment to TCP dishes, a spheroid sample cultured for 12 days in serum-free chemically-defined WE medium in the RCCS-HARV, was dispersed by gentle pipetting and transferred to TCP dishes and cultured for 2 days in the same medium. Figure 5.19 shows a fragment of the spheroid (green asterisk), which readily attached to the dish surface and formed hepatocyte monolayers, radiating from the cell aggregate base (white arrows) after 2 days of culture (x100; scale bar 50μm).

5.4.4 Laser Scanning Confocal Imaging Microscopy: Expression of integrin α5 in fresh, static culture and simulated microgravity HARV-RCCS cultured primary porcine hepatocytes

5.4.4.1 Expression of integrin α5 in freshly isolated primary porcine hepatocytes

Figure 5.15 shows the expression of the extracellular matrix counter receptor, integrin α5, on both a single hepatocyte (panel A) and on a hepatocyte doublet (panel B). Hepatocytes were placed in fixative and processed for indirect immuno-fluorescent staining only 2 hours following the initial isolation step (Chapter 2, Section 2.3.4) suggesting cell surface integrins are not degraded in this time frame. Noteworthy is the distinct clustering pattern of integrin α5, reminiscent of the configuration adopted at focal adhesion complexes in native liver *in vivo*.

5.4.4.2 Expression of integrin alpha 5 in day 2 static primary porcine hepatocyte cultures

Figure 5.16 demonstrates that integrin α5 cell surface receptors are retained in static cultures at least up to culture day 2. However, by day 6, integrin expression was not detected (not shown).

5.4.4.3 Expression of integrin alpha 5 in day 12 primary porcine hepatocyte aggregates cultured in the HARV-RCCS simulated microgravity environment

Figure 5.17 shows small cell aggregates (broken off from a larger aggregates during the staining process), which have stained positive for integrin α5. Panels A-C: Under low magnification (x100; scale bar 200 μm), strong staining of integrin α5 (white open arrows) is evident in a tight spheroidal aggregate, A; panel B shows the corresponding light image of A; whereas C is an enlargement of a region of A (dotted green box). Panels D-E: Note the appearance of integrin 'hotspots' (white closed arrows) on the surfaces of aggregated cells under higher magnification (x630; scale bar 50 μm), D, and the corresponding enlarged region of D (dotted green box), shown in E.

5.4.5 Fluorescein diacetate metabolism of of primary porcine hepatocytes cultured for 12 days in the HARV-RCCS simulated microgravity environment

Figure 5.18 shows 2 small cell aggregates (broken off from a larger spheroid during preparation). Strong staining of the compact spheroid surface is evident with little demarcation between individual adjacent cells. Hepatocyte nuclei (orange asterisks) are just visible in cells on the aggregate periphery.

Figure 5.14 Laser scanning confocal image: Fluorescent acridine orange viability staining of primary porcine hepatocytes cultured for 12 days in the HARV-RCCS simulated microgravity environment

Laser scanning confocal image (x100) showing staining of viable (apple green) and non-viable (diffuse orange-yellow) hepatocyte aggregates cultured in the HARV-RCCS under conditions of simulated microgravity. Cell aggregates were stained with 100μM of the fluorescent dye, acridine orange (scale bar 100 μm). Cells were cultured and processed as described in *Materials and Methods*.

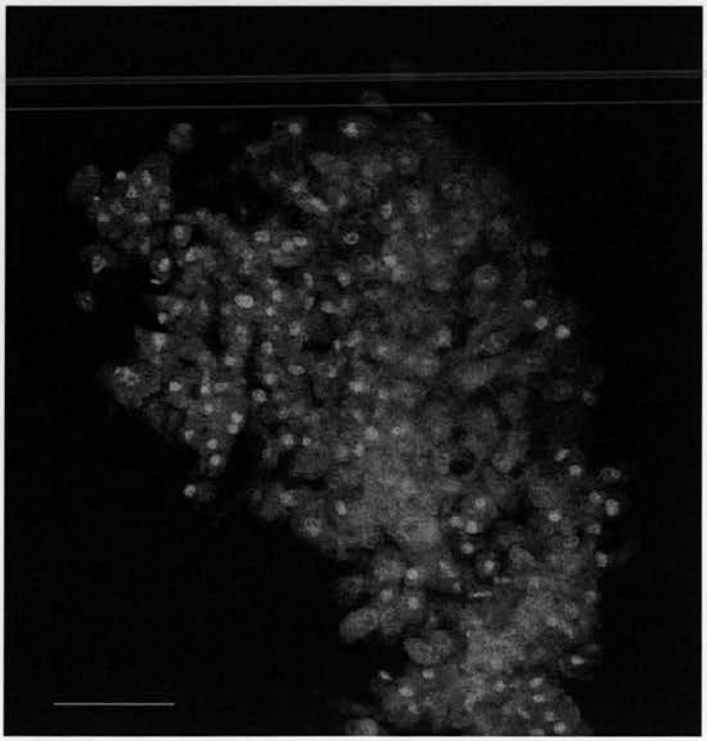

Figure 5.13 Integrin alpha 5 expression in freshly isolated primary porcine hepatocytes (x630)

Panel A: Laser scanning confocal image showing red fluorescent staining of the cell surface extracellular matrix counter-receptor, integrin $\alpha 5$ on a single hepatocyte. Note the clusters of integrins apparent on the cell surface (scale bars 25 μm). **Panel B** Confocal image of a hepatocyte doublet showing a similar clustering pattern of integrin $\alpha 5$ expression. Cells were cultured and processed as described in *Materials and Methods*.

A

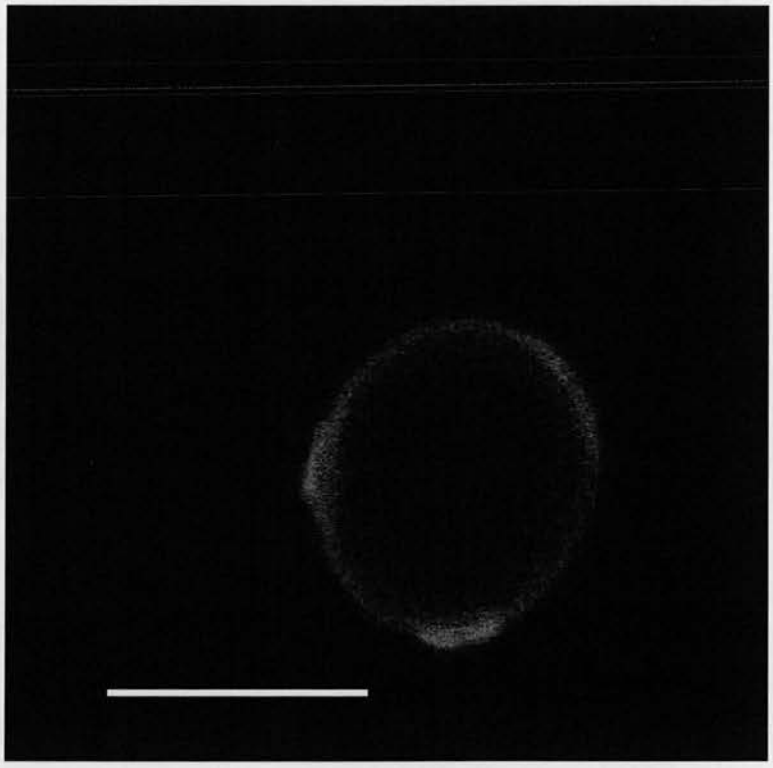

B

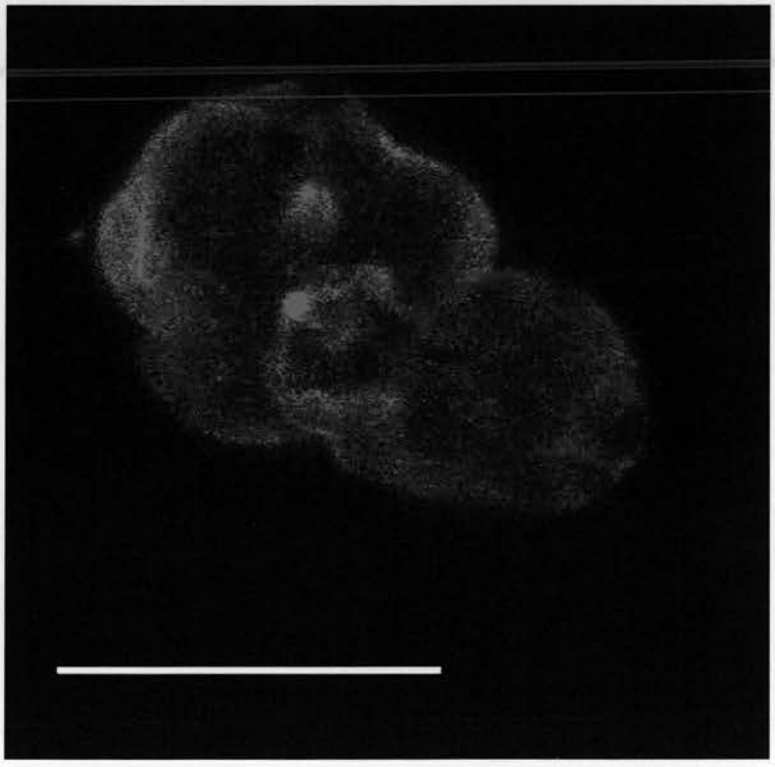

Figure 5.16 Integrin alpha 5 expression in primary porcine hepatocytes on day 2 of static culture (x100)

Panel A: Representative transmitted light image showing gross morphology of 2 day old primary porcine hepatocyte cultures in serum-free chemically-defined WE medium (scale bar 100μ). **Panel B** is the corresponding laser scanning confocal image showing red fluorescent staining of the cell surface extracellular matrix counter-receptor, integrin α5 (scale bar 100μ). Cells were cultured and processed as described in *Materials and Methods*. Note that integrin α5 expression was not detected in day 6 static cultures (not shown).

A

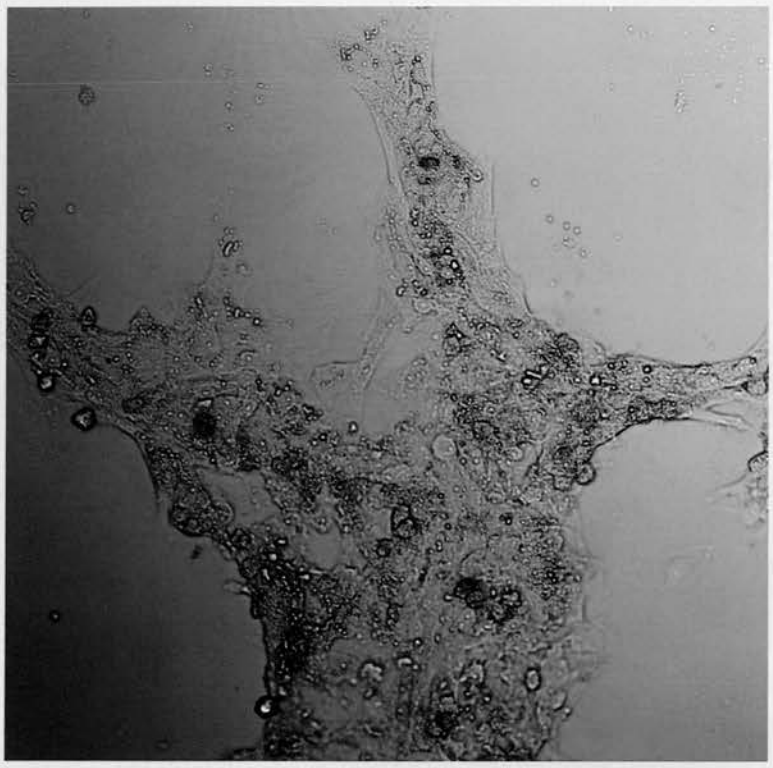

B

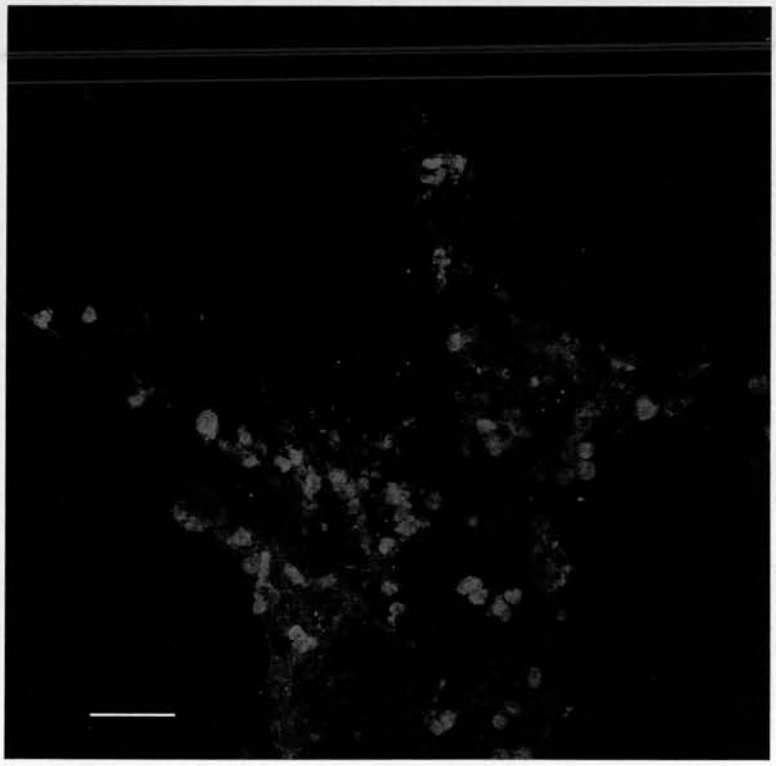

Figure 5.17 Confocal imaging of primary porcine hepatocyte aggregates cultured for 12 days in the HARV-RCCS simulated microgravity environment showing integrin alpha 5 expression

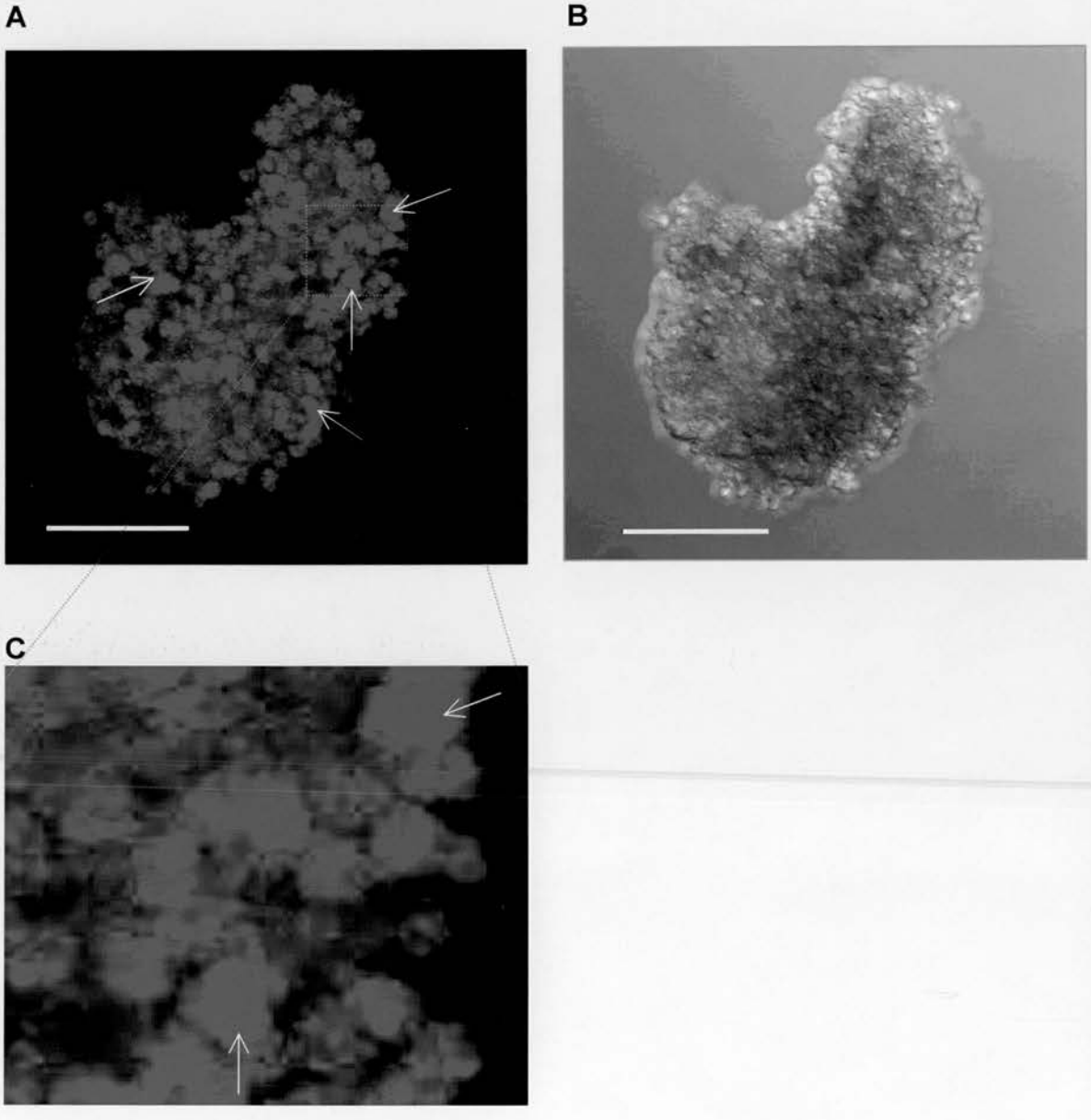

Laser scanning confocal images showing red fluorescent staining of the cell surface extracellular matrix counter-receptor, integrin $\alpha 5$ on aggregates of hepatocytes cultured in the HARV-RCCS under conditions of simulated microgravity. **Panels A-C** Under low magnification (x100; scale bar 200 μm), strong staining of integrin $\alpha 5$ (white open arrows) is evident in a tight spheroidal aggregate, A; panel B shows the corresponding light image of A; whereas C is an enlargement of a region of A (dotted green box).

D

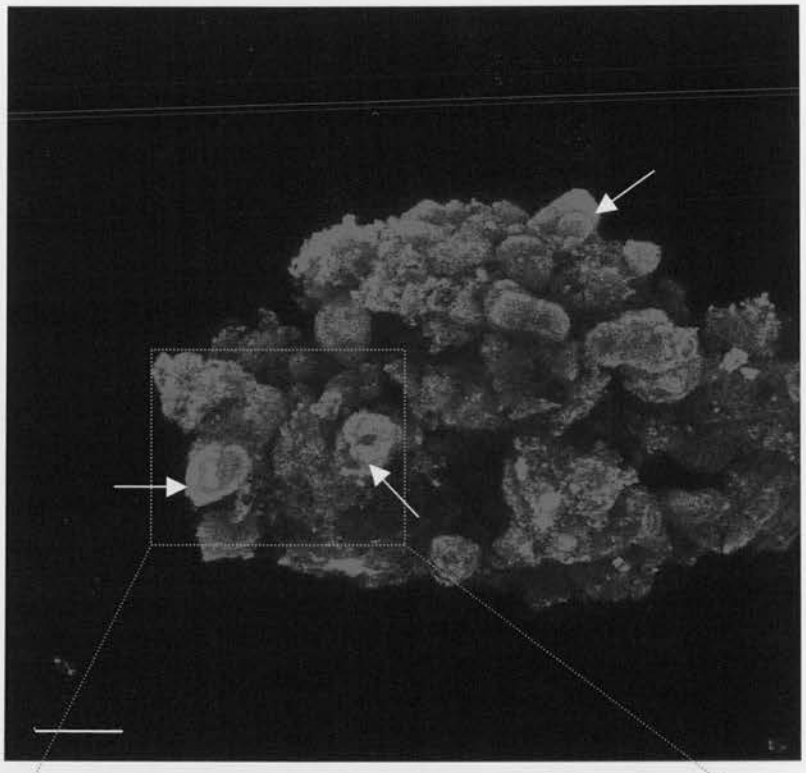

E

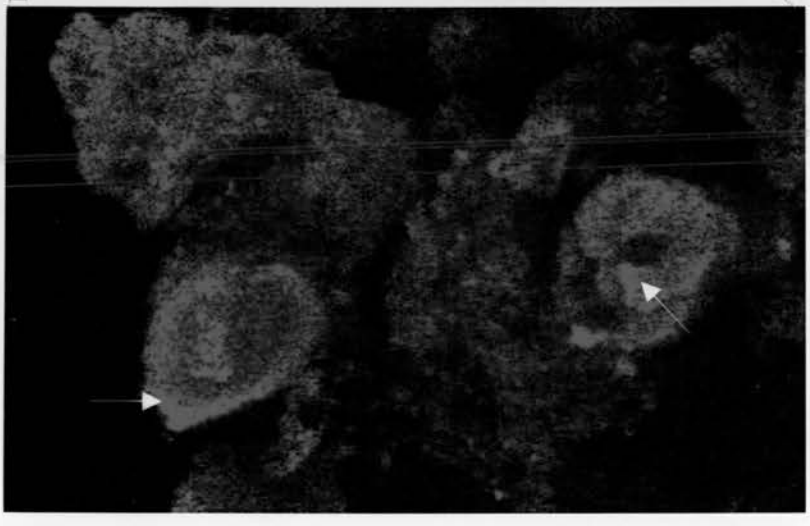

Panels D-E Note the appearance of integrin 'hotspots' (white closed arrows) on the surfaces of aggregated cells under higher magnification (x630; scale bar 50 μm), D, and the corresponding enlarged region of D (dotted green box), shown in E. Cells were cultured and processed as described in *Materials and Methods*.

Figure 5.18 Fluorescent micrograph of day 12 primary porcine hepatocyte organoids cultured in a simulated microgravity environment in the presence of fluorescein diacetate as a marker of bile canalicular function

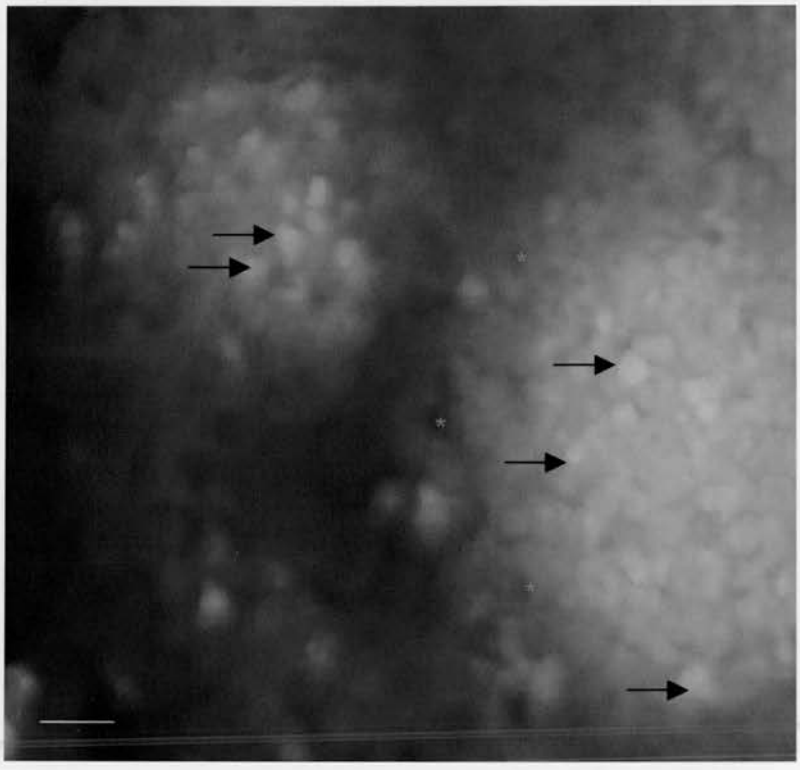

Representative fluorescent micrograph showing fluorescein diacetate (FDA) metabolism of primary porcine hepatocyte spheroid cultures to assess bile canalicular function (x50; scale bar 50 μm). A small cell aggregate, broken off from a larger aggregate during the staining process was incubated with 80μl FDA was for 30 minutes in a 10 ml capacity RCCS placed in a CO_2 incubator at 37°C. Cells were subsequently rinsed 3x with warm PBS and photographed using a Leitz Wetzlar Ortholux II fluorescent microscope with a 25x water immersion lens. FDA is actively taken up across bile canalicular membranes and, following deacetylation, the bright green fluorescent product (black arrows) is formed, so confirming the presence of functional bile canaliculae. Strong staining of the compact spheroid surface is evident with little demarcation between individual, adjacent cells. Hepatocyte nuclei (orange asterisks) are just visible in cells on the aggregate periphery.

Figure 5.19 Morphology of primary porcine hepatocytes pre-cultured for 12 days in the HARV-RCCS simulated microgravity environment and then for 2 days on tissue culture plastic to verify spheroid viability

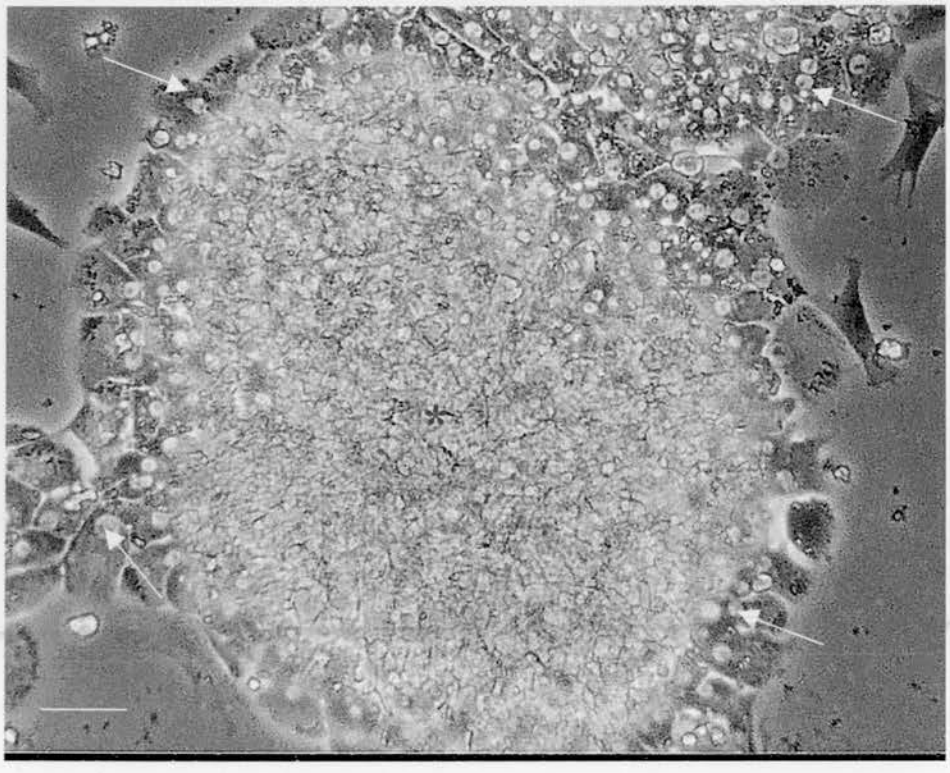

Figure 5.19 A spheroid sample cultured for 12 days in serum-free chemically-defined WE medium in the HARV was dispersed by gentle pipetting and transferred to TCP dishes and cultured for 2 days in the same medium (x100; scale bar 50μ). Fragments of the spheroid (asterisk) readily attached to the dish surface and formed hepatocyte monolayers radiating from the cell aggregate base (white arrows) after 2 days of culture.

5.5 Discussion

Hepatocytes cultured in unit gravity *in vitro* are limited in their capacity to exhibit normal functional and morphological characteristics of native liver. Therapeutic applications, including bioartificial liver devices and xenogeneic hepatocyte transplantation strategies, would benefit from improved *in vitro* performance of PPHs. It has been widely reported that the improved *ex* vivo maintenance of viability and differentiated functions of hepatocytes is correlated with the cell-cell contacts and more ordered cytoarchitecture of cell aggregates, compared with flattened, static monolayer cultures (Allen *et al.*, 2001; Michalopoulos *et al.*, 2001; Selden *et al.*, 1999; Strain & Neuberger, 2002). In the latter, the 2-dimensional environment and rigid substrata alters gene expression and attenuates differentiation. To address these issues, a large number of liver cell culture techniques have been developed to promote cell organisation with the ultimate aim of simulating *in vivo* conditions. These techniques include gel entrapment, 3D culture on microcarriers or in spinner flasks, nonwoven fabrics in bioreactors, 3D hollow-fibre membrane networks, and coculture with NPCs with or without extracellular matrix (ECM) proteins. Simulated microgravity cultures are hypothesized to support differentiation of cells through provision of three-dimensionality, low shear and turbulence, and cospatial relation of dissimilar cell types coupled with high mass transfer and oxygenation capabilities (Hammond *et al.*, 2000). Recently, RCCS spheroid cultures of human hepatocytes were shown to retain both ultrastructural characteristics of hepatic tissue-like structures and albumin mRNA expression for up to 60 days (Khaoustov *et al.*, 1999). The shortage of human liver tissue, however precludes their use in large-scale clinical BAL devices. Therefore PPHs are used in most current systems (Strain & Nueberger, 2001). However, there is no information on liver-specific function and morphology of PPH spheroids cultured in simulated microgravity, which may improve the *ex vivo* maintenance of PPHs for future therapeutic applications.

In conventional 3D culture using Matrigel™, Michalopoulos *et al.* (1999) suggested integrin mediated reorganization of cell-ECM and cell-cell interactions were involved

in hepatocyte differentiation. However, Matrigel use in pre-clinical BAL devices or other therapeutic applications is not desirable due to the potential risks of murine and / or tumourigenic proteins entering the patients circulation and is cost-limiting. As mentioned, the microgravity environment may promote tissue-specific up-regulation of cell adhesion molecules, ECM proteins and their respective integrin receptors (Unsworth and Lelkes, 1998).

Given the importance of these factors in the expression of liver-specific functions and histological architecture (Auth and Ichihara, 1998; Giancotti and Ruoslahti, 1999; Lazar *et al.*, 1995a; Lazar *et al.*, 1995b, Michalopoulos *et al.*, 1999; Michalopoulos *et al.*, 2001), the aim of this study was to ascertain whether a simulated microgravity environment, would promote aggregate formation, maintain hepatocyte-specific function and be accompanied by more *in vivo*-like morphological characteristics than is possible using conventional culture methods.

The results of albumin and urea synthesis as well as galactose elimination, indicate that the HARV-RCCS microgravity spheroid cultures retained extended, liver-specific functions compared with static cultures, for a pre-determined period of 12 days. Morphological and ultrastructural features, characteristic of differentiated 3D hepatocyte cultures, were observed including bile canalicula-like structures, capable of fluorescein diacetate (FDA) metabolism and expression of integrin α5. However, histological evaluation alone could not confirm the presence of collagen matrix, whereas large aggregates typically formed a rim of viable cells, which display only partial restitution of 3D *in vivo*-like hepatic architecture, circumscribing a core of non-viable cells. Khaoustov *et al.* (1999) observed similar histological phenomena with a pure population of primary human hepatocytes cultured for up to 60 days in a RCCS microgravity environment. Under these conditions, spheroids would not be suitable for use in BAL devices. Further study is required to enhance the viable cell population, phenotype, polarity and thus functional activity of such liver constructs.

The vast majority of studies into spheroid culture systems have been undertaken with rat liver cells (Hamamoto *et al.*, 1998; Ijima *et al.*, 1998; Kawaguchi *et al.*, 1992; Koide *et al.*, 1989; Koide *et al.*, 1990; Landry *et al.*, 1985; Matsushita *et al.*, 1991; Peshwa *et al.*, 1996; Sakaguchi *et al.*, 1991; Wu *et al.*, 1999; Yuasa *et al.*, 1993). Increasingly, the importance of studying spheroid formation, morphology and function using PPHs for use in BAL systems is recognized (Ijima *et al.*, 1998; Lazar *et al.*, 1995b; Lazar *et al.*, 1995a; Naruse *et al.*, 1996b; Naruse *et al.*, 1996a; Sajiki *et al.*, 2000; Sakai *et al.*, 1996c; Sakai *et al.*, 1996a; Sakai *et al.*, 1996b; Sakai *et al.*, 1999). In contrast, no information is available for these cells grown in the unique environment of simulated microgravity.

Unlike single cell rat isolates, PPHs naturally form small clusters of 5-20 cells even after comprehensive collagenase digestion of the liver matrix. Intuitively, this property of PPHs might be a beneficial attribute for the formation and study of spheroid cultures. Indeed, freshly isolated PPHs seeded directly into different bioreactor designs are maintained as quasi, 3 dimensional culture configurations in several BAL devices, with reportedly improved biological performance (Bader *et al.*, 2000; De Bartolo *et al.*, 2000; Iwata *et al.*, 1999; Kong *et al.*, 1996). Using a different approach, Naruse *et al.*, (1996b), pre-cultured PPHs as spheroids for 24 hours in spinner flasks and found 3D cellular formations to be functionally superior to single cell suspensions immobilized in a non-woven fabric BAL module. Other culture systems have utilised PPH spheroid cultures (Auth and Ichihara, 1998). PPH spheroids cultured in defined medium, either entrapped in collagen gel or inert alginate beads, result in cell-cell contacts which appear to enhance differentiated function including albumin and urea synthesis, as well as P450 biotransformation and glucuronidation activity, in comparison with monolayer and dispersed suspension cultures (Lazar *et al.*, 1995a; Lazar *et al.*, 1995b; Wu *et al.*, 1999). Maintenance of such cell-cell contacts, as occurs in spheroid cultures, may well contribute to the enhanced differentiated cell function observed (Bhatia *et al.*, 1999).

Porcine liver cells, with a mean viability of 87 %, inoculated into the HARV-RCCS, formed several cellular aggregates approximately 2-5 mm in diameter within 24-48 hours and were successfully maintained in culture for a preset period of 12 days. This contrasts with the 5-day culture period required to form spheroid cultures using spinner flasks in unit gravity (Lazar *et al.*, 1995c). Scanning electron microscopy showed a tightly packed arrangement of cells organized as compact spheroidal or ellipsoidal (see Figure 5.11) structures, often with more loosely associated rounded parenchymal cells present on the aggregate surface (Figures 5.10-5.11). Interestingly, Boonstra (1999) demonstrated that EGF-induced cell rounding, an actin mediated process, was enhanced under simulated microgravity conditions.

Both our study and that of Khaoustov *et al* (1999) mentioned above, used chemically-defined medium containing EGF, insulin and dexamethasone. Studies have demonstrated that both were essential supplements for successful formation of floating rat hepatocyte spheroids cultures (Kawaguchi *et al.*, 1992; Yuasa *et al.*, 1993). In contrast, Hsiao *et* al., (1999) demonstrated that serum promotes disassembly of rat hepatocyte spheroids cultured in spinner vessels. Using our defined William's E medium formulation, we have shown that PPHs cultured under simulated microgravity conditions retain galactose elimination capacity, comparable with the static cultures studied in Chapter 4, although both albumin and urea synthesis levels, are only 50% and 20%, respectively of static values. However, on a per (viable) cell basis, the RCCS cultures may exceed the static values (see below). Importantly, unlike the latter cultures, functionality was maintained in the microgravity spheroids up to day 12. Histological evaluation of aggregate transverse sections showed consistent formation, up to the termination of the experiment on day 12, of cohesive 3D structures reminiscent of poorly organized hepatic architecture with some hepatocytes arranged in cord-like structures (Figures 5.6 and 5.8), although these were predominantly in the non-viable cell core. The latter was bounded by a viable perimeter of glycogen positive cells, about 8-10 cells deep. Recently, Michalopoulos *et al.* (2001) showed that isolated hepatocytes and NPCs in collagen-coated RBCs formed structured histological formations bearing resemblance to characteristic

hepatic histological organization. Hepatocyte growth factor (HGF), EGF, and dexamethasone were required for complete histological organisation and phenotypic maturation of the tissue construct, although functional studies were omitted. Interestingly, Hamilton *et* al., (2001) found the HM medium formulation superior to WE for spheroid formation, and for the maintenance of ultrastructure and albumin production. The findings of this work and our own histological observations (see below) and functional data, emphasise the need for additional studies focusing on the hepatotrophic requirements for building reproducible tissue structures.

Table 5.1 summarises hepatic-specific function and compares our data for porcine hepatocytes cultured as 3-dimensional spheroids in microgravity with other culture systems in unit gravity. Since measured hepatocyte functions, culture conditions and duration vary greatly between research groups which make direct comparisons difficult, values quoted are for day 6 measurements only, normalised to the number of cells initially seeded. The biochemical data in our study, is normalised (per million cells) to the number of cells initially seeded in the RCCS. This is because the aggregates were required for morphological analysis at the end of each experiment and destructive biochemical assays, such as total protein (or indeed LDH and cytochrome tP450 levels) measurements, could not be made. This is an obvious drawback in RCCS studies and is compounded by the limited number of (HARVs) culture vessels available using this set-up.

Lazar *et al.* (1995c) cultured PPHs as spheroids using standard spinner flasks in serum-free WE containing similar levels of EGF, insulin and dexamethasone as our study, and reported *basal* USR of ≈170 nmol/hr/ 10^6 seeded cells at day 6 which declined to ≈70 nmol/hr/ 10^6 cells by day 12; ASR was maintained at ≈2 μg/hr/ 10^6 cells up to culture day 20. In agreement with others (Dr P Gregory, Organogenesis USA, personal communication), we found that ammonium chloride-stimulated assays produce about 3x more urea than in the basal state (not shown). The higher basal functional values of normal gravity spheroid cultures of Lazar, and enhanced ASR, suggest smaller spheroids in unit gravity cultures are functionally more efficient than

Table 5.1 Hepatic-specific functions of 3-dimensional porcine hepatocyte cultures compared with monolayer cultures and *in vivo* data

Modality: Day 6 cultures	USR nmol/hr/10^6 cells	ASR μg/hr/10^6 cells	GE nmol/hr/10^6 cells	References
Spheroid (SF) Monolayer	170 (basal) 70 (basal)	2.1 0.6	ND ND	Lazar *et* al., 1995c
Spheroid (CE) Dispersed cells	140 (basal) 70 (basal)	2.1 0.6	ND ND	Lazar *et* al., 1995c
Spheroid (BAL) Spheroid (SF)	200 (1mM NH_4Cl) 100 (1mM NH_4Cl)	6.0 4.2	ND ND	Naruse *et* al., 1996a
Cell Aggregates (NWP biomatrix)	270 (basal)	0.6	ND	Pahernik *et* al., 2001
Spheroids (SF) Spheroids (CE) Monolayer	ND ND ND	0.7 0.4 0.3	ND ND ND	Sakai *et* al., 1996a
Cell Aggregates (BAL)	ND	ND	45 (35mM galactose)	Iwata *et al.*, 1999
In vivo values (human liver) (pig liver)	 40 ND	 2.0 ND	 960 410 (5mM galactose)	Iwata *et al.*, 1999; Lazar *et* al., 1995c; Gomez-Lechon, *et al.*, 1990
Spheroid: RCCS Monolayer	108 448	0.8 2.0	317 179 (6mM galactose)	Present data:

Hepatic-specific functions of porcine hepatocytes cultured as 3-dimensional spheroids in unit- or micro-gravity, as small cell aggregates or collagen-entrapment cultures, compared with monolayer cultures and *in vivo* data. Since measured hepatocyte functions, culture conditions and duration vary greatly between research groups which makes direct comparisons difficult, each value represents the quoted mean values for day 6 measurements, normalised to the number of cells initially seeded. *In vivo* values are shown for human and pig livers. The galactose and NH_4Cl loading doses' are shown in parentheses. *Abbreviations*: ASR, albumin synthesis rate; BAL, bioartificial liver bioreactor; CE, collagen-entrapment; GE, galactose elimination; ND, not determined in referenced study; NWP, nonwoven polyurethane biomatrices in petri dishes; RCCS, rotary cell culture system microgravity cultures; SF, spinner flasks; USR, urea synthesis rate.

much larger RCCS spheroid cultures (see Figures 5.3 and 5.5). Moreover, the BAL module of Naruse *et al.* (1996a), mentioned above, showed significantly higher albumin and urea production than RCCS cultures despite using only half the NH_4Cl concentration in the latter assay, as was used in our cultures (see Figure 2.5). Finally, the functionality of monolayer cultures (Chapter 4) was, apart from galactose elimination capacity, significantly more efficient than microgravity cultures. Taken together, the RCCS modality does not appear to confer significant advantage over more conventional spheroid culture systems in terms of hepatic-specific function. Metabolic activity was nevertheless retained in microgravity cultured cells up to day 12, whereas static cultures had expired after one week in culture on tissue culture plastic. Functionality of the viable cell population, calculated on a per cell basis, may however be more efficient in the RCCS (see below). Also, recent work in our laboratory showed sustained metabolic activity of RCCS cultured cells for a predetermined period of 21 days (Dabos *et al.*, 2001). Glucose metabolism, glutamine synthesis and ketogenesis were assessed using ^1H nuclear magnetic resonance spectroscopy of the culture medium. After an initial 10-day period of acclimatisation cell aggregates formed in the RCCS-HARV switched from the anaerobic to the more efficient aerobic pattern of metabolism, which was exhibited until the experiments were terminated. Further experiments require to be undertaken to assess the impact of these data on hepatic-specific function, as well as in determining the prospective longevity of cells maintained in this culture system.

The majority of viable hepatocytes most likely reside in the outer rim of aggregates (Figures 5.6, 5.8 and 5.14), probably as a consequence of mass transfer constraints. To estimate the fractional volume of viable cells in the aggregate rim, two diameters (x, y) at right angles to each other were measured for both the external boundary of viable cells (giving, Total Volume of Spheroid) and for the inner boundary of viable cells (giving, Volume of Necrotic Core) for typical histological preparations of aggregates (2-5 mm in diameter), using an eyepiece graticule in an inverted microscope.

The volume of the spheroid ($V_{spheroid}$) was calculated as:

$$V_{spheroid} = \frac{4}{3}\pi \cdot \left(\frac{\sqrt{xy}}{2}\right)^3$$

The Percentage Volume Fraction (PVF) was calculated as:

$$PVF = \frac{\text{(Total Volume of Spheroid – Volume of Necrotic Core)}}{\text{Total Volume of Spheroid.}} \times 100$$

The PVF or proportion of viable cells within an aggregate was calculated as approximately 5 %. Since these viable cells comprise roughly $1/20^{th}$ of the total number of cells within an aggregate (see Figure 5.6, panel B), the actual value for urea synthesis and the other functional measurements on a per cell basis may be considerably greater than the values measured (see Figures 5.3-5.5). However, four to five aggregates were often observed in the HARV culture vessels, so reducing the functional (per cell) value. Also, smaller aggregates frequently rafted together, forming a macroscopic ensemble of loosely attached aggregates. Upon sampling and processing for subsequent morphological analysis however, this large assembly broke up into smaller aggregates, so making a precise determination of the number of 'autonomous' spheroids difficult.

The histological observations presented in our study highlight a significant limitation of culturing relatively large cellular aggregates under simulated microgravity conditions. Mass transfer kinetics of oxygen and other nutrients is limited to <200 μm across multi-cell layers (Kim and Mooney, 1998; McClelland and Coger, 2000), comparable to the thickness of the viable cell rim in our spheroid aggregates. Although RCCS microgravity cultures permit formation of much larger 3D structures than appears to be possible using conventional spheroid culture systems, the downside is that cells located beyond the 200 μm threshold depth, as observed in our study, do

show evidence of hypoxia-induced cellular necrosis and apoptosis (Mueller-klieser, 1997; Riva *et al.*, 1998). These results are in conflict with the assertion of a high mass transfer and oxygenation capacity of the HARV-RCCS modality (Spaulding *et al.*, 1993; Unsworth and Lelkes, 1998). In comparison though, spheroid formation in unit gravity achieve a range of spheroid sizes of 50-160 μm in diameter, containing ≈100 cells, which exhibit good viability throughout the 3D structure (Lazar *et al.*, 1995c; Sakai *et al.*, 1996a). These studies make it clear that other environmental cues are certainly required to improve the efficacy of the RCCS (discussed below).

A seeming advantage of the microgravity environment over conventional culture systems in unit gravity is that the 'freefall fluid orbit' of the aggregates facilitates growth in all directions, since no single gravity vector dictates the direction of growth. Assuming an average diameter of 25μm for a porcine hepatocyte and cell compaction in a 5 mm diameter spherical aggregate as evidenced histologically, the total number of cells per spheroid may be up to $8x10^6$, with in the order of $4x10^5$ viable cells. Considering the inoculum was 10^7 cells per HARV and several aggregates were often observed, one may speculate whether cell proliferation occurs in the viable cell population under these conditions. Indeed, day 10 RCCS cultures were positive for the Ki67 proliferation marker (not shown). Interestingly, Yuasa *et* al., (1993) showed that rat hepatocytes remained in the quiescent, G_o phase of the cell cycle, conducive to more differentiated morphology and function compared with subsequent culture of the spheroids in monolayer in which they flattened, spread and entered G_1 with concomitant reduction in albumin synthesis. We observed similar morphological phenomena when spheroid fragments were transferred to TCP dishes (Figure 5.19). Defining the conditions for expansion of the cell population whilst maintaining differentiated function, remains a major challenge in tissue engineering and would be an important factor in future studies which seek to optimise spheroid culture systems.

Mass transfer constraints are a common problem with BAL design configurations. For example, in the hepatocyte gel-entrapment bioreactor module of Nyberg *et al.*, (1993), where cell suspensions are inoculated intraluminally within

hollow fibre membranes, both oxygen uptake rates and cell viability (<50 %) decreased with increasing gel depth (Balis *et al.*, 1999). Similary, Hu *et al.*, (1997) reported decreased cell viability when the hollow-fibres in the bioreactor, which were similar in scale to Nyberg's study, incorporated hepatocyte spheroids.

Morphological analysis revealed some conflicting results. Aside from the histological observations, transmission electron microscopy (TEM) analysis, presumably of samples derived from the rim of viable hepatocytes, showed some ultrastructural characteristics of polarized epithelial cells. Intact cytoplasmic organellar structures and glycogen granules are features reminiscent of fresh liver tissue (see also Chapter 3, Figure 3.3). An asymmetric distribution of organelles was sometimes observed however, which may be a consequence of the centrifugal force on the cells. Further evidence of cell polarity in the viable cell population comes from both the ability of these cells to metabolise FDA (Figure5.18) and the expression of the cell adhesion receptor, integrin α5 (Figure 5.17). The latter is considered to be important in morphogenesis and maintenance of tissue architecture (Giancotti and Ruoslahti, 1999; van der Flier and Sonnenberg, 2001). Integrin receptors are normally present in the sinusoidal or basal domain *in vivo* where they recognize fibronectin (integrin α5), and other ECM components including laminin, collagen and proteoglycans (Desmet *et al.*, 1994). FDA metabolism was demonstrated in day 12 spheroids (Figure 5.18) by the intense green fluorescent staining of the apical (bile canalicular) domain, although it was difficult to distinguish individual cells in the multicellular aggregate fragment. These findings are in agreement with Absu-Absi *et al.*, (2002) and Yumoto *et al.* (1996) who have demonstrated structural and functional bile canalicula in rat hepatocyte spheroids. Uptake and metabolism of FDA is considered a good marker of functional polarity and canalicular function (Strain, 1999), however excretion into the bile canalicular-like channels could not be resolved. The intensity of fluorescence has been shown also to correlate with cell viability and hepatic-specific function (Nyberg *et al.*, 1993). As suggested by Mitaka *et al.*, (1999), the lack of a normal drainage system for bile caused retention of fluorescence and the observed dilatation (Figure 5.18). Further immunocytochemical studies are required

to confirm cellular polarity, as in the study of Absu-Absi *et al.*, (2002), using domain-specific probes, for example to confirm the presence of the apical-specific protein dipeptidylpeptidase (DPPIV), and E-cadherins in the lateral domain, important in cell-cell interactions. Bit Plane 3D Imaging software could also allow three dimensional reconstruction of (0.4μm) optical sections of confocal stacked images, to assess the precise topology of structural proteins involved in maintenance of polarity and cell-cell, cell-matrix interactions. For example, if no porcine antibody or cDNA probes were available, a fluorogenic substrate of DPPIV, Ala-Pro-cresyl violet, could be utilised since DPPIV cleaves the substrate at the proline residue releasing the fluorescent cresyl violet molecule, which may be detected using confocal imaging.

Most of the TEM sections we observed however, revealed non-viable, damaged hepatocytes (not shown) probably originating from the aggregate core. Khaoustov *et al.*, (1999) observed similar histological phenomena and suggested that the aggregate's core was composed mainly of necrotic and apoptotic cells. We observed condensed nuclei and loss of integrity of hepatocyte borders in support of these findings (Figures 5.6 and 5.8), although the cytoplasm of many core hepatocytes was found to be eosinophilic (Figures 5.7), suggesting mitochondria and cytoplasmic proteins may still be present (Junqueira, 1977).

To confirm the viability of aggregates we cultured samples taken at days 6 and 12 (Figure 5.19) from the HARV-RCCS onto tissue culture plastic and observed attachment and formation of hepatocyte monolayers radiating from the cell aggregate base which detached from the dish surface after one week, as observed for static cultures (Chapter 3). In addition, acridine orange fluorescent staining of 12 day old HARV-RCCS cultured aggregates confirmed viability, at least of the outer, 10 cell deep PAS positive layer of cells (Figure 5.14).

Given the importance of the ECM, via integrins, in modulating hepatic cell migration, differentiation and polarity (Selden *et al.*, 1999), reticular staining of spheroid sections was performed but did not confirm the presence of collagen matrix.

However, immunocytochemical studies have revealed that the 'reticulin fibres' demonstrated by empiric silver impregnation correspond to collagen types I and III (Desmet, 1994). ECM deposition by spheroid cultures has been demonstrated. Interestingly, spheroid cultures of rat liver cells described by Landry *et al.*, (1985) and Tong *et al.*, (1990) observed, using immunostaining techniques, the formation of a thin layer of NPCs encapsulating the spheroid and deposition of ECM containing fibronectin, laminin and collagen delineating the entire spheroidal structure (LeCluyse *et al.*, 1996). The presence of type IV collagen or other components of the ECM in PPH microgravity spheroid needs to be clarified, as soon as suitable antibody or cDNA probes become commercially available.

Primary porcine hepatocytes express the extracellular matrix (fibronectin) counter receptor, integrin α5, in freshly isolated cells (Figure 15), static cultures up to day 2 (Figure 16) but not day 6, while it is expressed in the HARV-RCCS to day 12 (Figure 17). The static WE-maintained cultures ability to express integrin α5 correlated with ultrastructural indicators of differentiated function (see Chapter 3, Figure 3.5), both of which were lost by day 6. Thus, simulated microgravity conditions appear to support expression of this integrin class, which may also provide indirect evidence for the presence of its counter-receptor, fibronectin. Integrin α5 is part of the fibronectin receptor heterodimer, $\alpha_5\beta_1$, transmembrane cell surface receptor. We hypothesized that expression of integrin α5 is important in simulated microgravity culture, since it is intimately involved in the coordinated control, along with various growth factors including EGF, of cell shape, growth, movement and survival, important for the establishment and maintenance of tissue architecture (Giancotti and Ruoslahti, 1999). This control is achieved by the congress of integrin clusters. In essence, upon binding of cellular integrins to matrix proteins, assembly of these components takes place in association with cytoskeletal (CSK) and adaptor proteins, forming focal adhesion complexes (Berman and Kozlova, 2000) (Figure 5.20). The ECM-integrin-CSK axis thus formed permits bi-directional integrin signalling allowing mechanical and biochemical signal transduction and the appropriate physiological response to ensue.

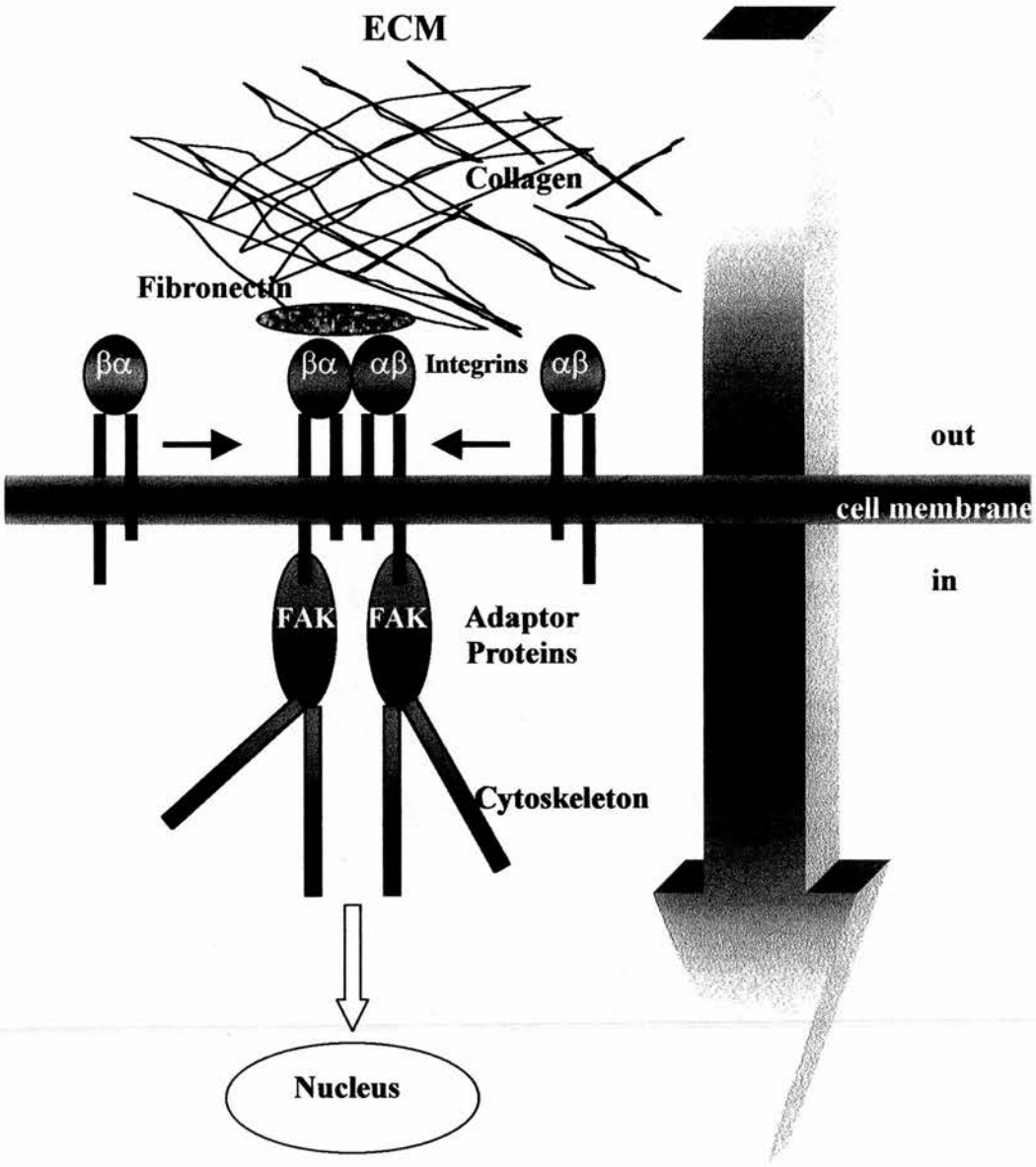

Figure 5.20 The ECM-Integrin-Cytoskeletal Axis (large 3D-arrow). Binding of ECM components, such as fibronectin, to integrin receptors (αβ heterodimers) promotes integrin clustering (closed arrows) forming supramolecular complexes called focal adhesion sites, comprised of adaptor proteins such as focal adhesion kinases (FAK), which are associated with cytoskeletal elements (eg B-tubulin and/or actin). Activation of the intracellular signalling pathways can activate cell regulatory processes such as nuclear gene expression (open arrow), cell attachment, movement, and survival (Figure adapted from; Giancotti and Ruoslahti, 1999; Holly *et al.*, 2000;Sastry and Burridge, 2000).

It is suggested that the ECM-integrin-CSK axis is, in effect, 'hard-wired' for mechanotransduction (Ingber, 1999; Ingber, 1997). Demonstrating the presence of this signal transduction axis in simulated microgravity cultured aggregates, may provide evidence of the role of focal adhesion complexes in cellular sensing of the microgravity environment.

In preliminary studies, we attempted to demonstrate the presence of key components of this axis using immuno-fluorescent staining and confocal microscopy. We used speculative antibodies (ie not specific, pig antisera) directed against fibronectin, integrins α5 and α3, B-tubulin, and focal adhesion kinase as representative of the ECM, integrin, cytoskeletal, and signal transduction elements, respectively. Following single, double or triple immuno-fluorescent staining and confocal microscopy analysis, only integrin α5 stained positive in RCCS-grown cell aggregates. Indeed, only integrin α5 showed cross-reactivity following dot blotting (Section 5.3.6). Clarification of the presence of these components would require in-house development of specific anti-porcine antibodies.

As mentioned, Peshwa *et al.*, (1996), demonstrated that cell movement and reorganization were involved in spheroid formation, implicating a mechanistic role for integrins. Given that PPHs readily attach to plastic culture surfaces without exogenous matrix proteins and that the fibronectin counter receptor, integrin α5 is expressed in RCCS cultures and day 2 static WE cultures, may suggest that PPHs (or 'contaminating' NPCs) can synthesize fibronectin locally, although this could not be confirmed by immunostaining. In fact, rat and human hepatocytes, which have an absolute requirement for exogenous matrix proteins for attachment, can synthesize and secrete cellular fibronectin *in vitro* (Christiansen *et al.*, 1988; Odenthal *et al.*, 1992).

Deposition of fibronectin may be beneficial in promoting 3D cytoarchitecture. Sanchez *et al.*, (2000) demonstrated that this matrix protein facilitated the formation of liver plate-like structures and expression of liver-specific genes in foetal rat

hepatocytes suggesting fibronectin partakes in polarization of hepatic tissue. Furthermore, the $\alpha_5\beta_1$ integrin, induces expression of the anti-apoptotic protein Bcl-2 (Giancotti and Ruoslahti, 1999), protecting cells from apoptosis from a variety of cell stresses. Of course, further studies are required to identify the presence of fibronectin or other components of both ECM and corresponding focal adhesion complexes, using western immunoblotting or confocal microscopy. Unfortunately, specific antibodies directed against porcine-derived cellular components are not commercially available at present.

The findings presented here recommend that many improvements are required to prove the microgravity spheroid cultures beneficial for clinical BAL use. Utilising strategies which have been employed to improve the hepatic culture environment in both unit gravity and microgravity, it may be possible to reduce the relative size of the necrotic core, improve overall viability and metabolic function of 3D cell aggregates cultured in simulated microgravity. While the present study provides some evidence in the viable cell population of rather poorly organized hepatic proto-tissues in RCCS-grown aggregates, they clearly do not recapitulate the phenotypic diversity of parental tissues. Important components are absent, including the correct ratio of parenchymal cells (PC) to non-parenchymal (NPC) cells, tissue-specific autologous matrices and vascularization of the engineered tissue. Heterotypic coculture between PC and NPC cells in conventional cultures, provide for cell-cell interactions which have been demonstrated to preserve liver-specific functions and phenotype *in vitro* (Bader *et al.*, 1996; Bhatia *et al.*, 1998b; Bhatia *et al.*, 1998a; Bhatia *et al.*, 1999; Duray *et al.*, 1997; Gerlach *et al.*, 1995; Glicklis *et al.*, 2000; Yuasa *et al.*, 1993). For example, Michalopoulos *et al.*, (1999) used roller bottles to maintain phenotypically stable 3D cultures of a mixture of rat PC (hepatocytes) and a 'contaminating' NPC population of 5 % which attached to collagen coated polystyrene beads. Expression of both albumin and cytochrome P450 species, and structures reminiscent of hepatic architecture, such as formation of hepatocyte guided plates, was retained for up to 2 months. However, we found that attachment of PPHs using identical microcarrier beads and a similar PC:NPC ratio as in the former study, was very poor in the HARV-

RCCS (data not shown). Mitaka *et al.*, (1999) on the other hand, cultured a 50 % NPC:PC (containing both small and mature rat hepatocytes) mix of rat hepatic cells on collagen coated static culture dishes which showed proliferation, synthesis of ECM proteins and formed 3D colonies of acinar-like structures.

In the context of simulated microgravity cultures, provision of the necessary cues for organotypic reconstruction of native liver is a formidable task, requiring, amongst other considerations, a systematic assessment of the precise ratio of PC:NPC cells which may optimise phenotypic and functional stability as well as defining the most favourable biochemical environment of both the culture medium and biomatrix components. Coculture of rat or porcine hepatocytes with murine 3T3 cells have been shown to induce the highest levels of albumin production by hepatocytes (4.2 to 15 μg/h/ 10^6 cells (Bhatia *et al.*, 1999; Gregory *et al.*, 2001). However, the latter study by Gregory *et al.*, (2001) found no effect on urea synthesis or P450 activity compared with standard control cultures.

Primary human liver cells (PHLC) cocultured with an NPC fraction (containing fibroblasts, Kupffer cells, endothelial cells and bile duct epithlelial cells) under simulated microgravity conditions formed 3D liver tissue-like structures with a markedly reduced non-viable core of cells compared to homotypic hepatocyte cultures (Khaoustov *et al.*, 1999; Yoffe *et al.*, 1999). However, neither the PC:NPC ratio nor functional activity of the spheroids were documented. The quality of PHLC cocultures was further enhanced by the use of polyglycolic acid (PGA), a non-toxic biodegradable synthetic polymer scaffold, resulting in more efficient cell assembly, much larger viable cell aggregates of up to 3 cm with, albeit limited, formation of nascent vascular 'sprouts'. Scaffolding is considered to be a critical component in tissue engineering since it provides 3D cues for cell seeding, migration, growth, and morphogenesis (Sundback and Vacanti, 2000).

Due to the inherent limits of nutrient diffusion mentioned above, vascularization of engineered tissue seems critical for the formation and maintenance

of large cellular constructs to facilitate metabolic transport of oxygen and nutrients and removal of waste products (Kim and Mooney, 1998; Unsworth and Lelkes, 1998). This could be achieved in the microgravity bioreactor by incorporating the appropriate levels of angiogenic factors such as vascular endothelial factor, hyaluronidase, and migration stimulating factor (Prof. SL Schor, University of Dundee, personal communicatin), as well as sinusoidal endothelial cells and bioengineered tubular scaffolds with which to form such blood vessel conduits, perhaps incorporated into the PGA scaffolds mentioned above.

Delineation of the optimal conditions under simulated microgravity, necessary for the *in vitro* replication of *in vivo* liver architecture, phenotype and function remains a major challenge. Preliminary results using the HARV-RCCS modality suggest determination of the appropriate seeding density, coculture ratios and interactions, matrix component(s) and angiogenic factors, alluded to above, will allow appropriate design criteria for more efficient BAL devices. In engineering terms scale-up of the RCCS utility for provision of adequate cell mass is not problematic (Synthecon, Technical Services), whereas incorporation of optimised spheroids into current BAL devices is feasible (Allen *et al.*, 2001) Ultimately, success in this endeavour would result in bioreactors that require less hepatocellular mass, have reduced costs and extend the effective lifetime of these devices.

Chapter 6

Concluding Remarks

6.1 Bioartificial liver devices

Bioartificial liver support systems incorporating primary porcine hepatocytes are a promising modality with which to treat acute liver failure. Many BAL device configurations are under development around the world. In fact, clinical trials are already underway, using the HepatAssist 2000 developed by Circe Biomedical (Watanabe *et al.*, 1997). However, despite the use of PPHs as the principal xenogeneic source for BAL devices, published data characterising both porcine hepatocyte biochemical functionality and morphology under defined culture conditions is very limited. Moreover, it is difficult to make direct comparisons of bioreactor efficacy because each research group uses different culture media and supplements, biomatrices and bioreactor design configurations to maintain cell function *in vitro*. Given that the pathophysiology of acute liver failure is not well defined, clinically effective PPH-based BAL designs should maintain a range of differentiated hepatic support functions. Notwithstanding this, many issues relating to optimisation of bioreactor device configuration to maximize hepatocyte function remain unresolved. The ability to maximize porcine hepatic support functions would contribute significantly to the development of ergonomic BAL designs, which provide the required cell mass for optimal performance. The work presented in this thesis addresses some of these issues.

6.2 Thesis aims

The principal aims of this thesis were to develop a high viability, high yield, reproducible *ex vivo* method for obtaining PPHs and to characterise different PPH culture conditions, under defined conditions, using functional and morphological criteria for use in BAL devices.

6.3 Summary of experimental results

In this study, our method provides a high viability, high yield and rapid isolation technique, which is easy to perform in a standard research laboratory. Outcome is similar to most *in vivo* protocols reported, although improved yield and viabilities are attainable with the latter. Nevertheless, the method obviates the need for relatively complex, *in vivo* surgical techniques and facilities, which are time-consuming and require highly trained, licensed personnel. Cells can be deployed in a variety of *in vitro* liver model systems in under two hours, whilst maintaining viability and hepatocyte functionality. In this study, yield, viability and function of isolated hepatocytes compare favourably with results obtained using *in vivo* techniques.

Primary porcine hepatocytes were cultured in separate medium formulations (commonly used in BAL systems) with serum-free, chemically-defined supplements. It was demonstrated that high plating efficiencies and viability on biomatrix-free (unmodified) tissue culture plastic can be maintained in the absence of serum or sophisticated substrate for attachment, up to day 6. Image analysis data proved more discriminatory, in assessment of cell attachment efficiencies, than assessment of total protein, or viability using LDH activity. Cellular biomass, compatible with retention of functional activity, is maintained up to culture day 6. Hepatocytes maintained in M199 and WE media formulations preserve ultrastructural and gross morphological features of healthy cells up to culture day 4. In contrast, HM- and M1640-grown hepatocytes, exhibit features of damaged or unhealthy cells even on day 2. Morphological observations suggest that 6 day old hepatocyte cultures may not be compatible for use in cell based therapies. Thus, selection of the most appropriate medium formulation may be a significant factor in experimental liver culture systems, as it appears to modulate gross hepatocyte morphology, ultrastructure and possibly function.

In this culture environment, hepatocytes show variable effects on functional activity depending on the medium formulation and / or culture age. The HBAI utility for multiple comparisons, reinforced by morphological observations, ranked the

media on day 2 as: M199>WE>M1640>HM, with M199 retaining primacy up to day 6. The gross and ultrastructural morphological observations, and image analysis data presented in Chapter 3, suggest M199 best preserves characteristics of differentiated hepatocytes *in vivo* up to culture day 4, which is the time frame for current operational BAL usage, with high attachment efficiency. Using this utility, it is concluded that Medium 199 may be one of the most suitable synthetic media for culturing PPHs under serum-free chemically-defined conditions for BAL systems. The HBAI presented here provides some measure of global functional activity of our hepatocyte culture system, with important caveats. The HBAI may be only useful in the limited context of assessing multiple comparisons.

The functional data for day 2, which is in the time frame for BAL device implementation, showed that USR, ASR, tP450, and GE functions for test media, were up to 300%, 90%, 20%, and 50%, respectively, of *in vivo* values for human liver. Medium 199 gave the highest mean values of plating efficiency, viability, and albumin synthesis rates than the other media tested up to day 4, although the differences were not always statistically significant. By day 4 of culture, both M1640 and HM pre-cultured cells showed significantly greater urea synthesis rates than both WE and M199 maintained cells. There was a 66% decrease in total cytochrome P450 content in 2-day-old cultures compared with fresh cells, whereas HM maintained cells preserved significantly higher day 4 tP450 levels than both WE and M1640 conditioned cells. Galactose elimination (GE) was significantly higher in day 2 cultures in all test media compared with both days 4 and 6, which then remained relatively stable thereafter. The albumin synthesis rate tended to increase in all media up to day 6. Furthermore, parallel morphological studies indicated that different medium formulations modulate gross and ultrastructural morphology of hepatocyte cultures. These findings may be of relevance when choosing an appropriate medium for porcine-based BAL devices, which require rapid attachment of high viability cells with significant ammonia detoxifying capacity, whilst maintaining biotransformation potential and a diverse functional profile.

Cells cultured in the HARV-RCCS, simulated microgravity environment, formed cellular aggregates approximately 2-5 mm in diameter within 24-48 hours

and were successfully maintained in culture for a preset period of 12 days. The HARV-RCCS modality retains stable, liver-specific synthetic, detoxification and metabolic functions of PPHs over a 12 day culture period. Morphological and ultrastructural features characteristic of 3D hepatocyte cultures were observed throughout the culture period. The presence of bile canalicular-like structures, and integrin α5expression, suggest the viable cell population maintained a differentiated, 3D cytoarchitecture with evidence of polarity. Under these conditions, large aggregates formed a rim of viable cells circumscribing a core of non-viable cells, which displayed only partial restitution of *in vivo* hepatic architecture. Further study is required to enhance the viable cell population, phenotype, polarity and thus functional activity of such liver constructs, for future therapeutic use.

6.4 Future work and perspectives

From a practical point of view, rapid deployment of freshly isolated PPHs into a BAL device would be the ideal scenario, since these cells are superior to cultured hepatocytes both metabolically and in terms of differentiated function (Guillouzo *et al.*, 1997). Microcarrier-attached PPHs, obtained using an *in vivo* procedure and cryopreserved, have been used in BAL devices (inoculated with 5×10^9 cells) to treat FHF (Demetriou, 1998; Rozga *et al.*, 1993a; Watanabe *et al.*, 1997). However, since cryopreservation of large numbers of high viability PPHs for on-demand usage has, historically, proven difficult (Darr and Hubel, 1997; Strain, 1994), the fact that our simplified procedure takes less than 2 hours from animal sacrifice to the isolation of purified cells, and could accommodate any scaled-up BAL currently under development, is highly advantageous.

Although freshly isolated cells showed high viability, improvements in this technique are desirable to achieve optimal BAL function. Wang *et al.*, (2000) investigated 21 multivariables including pig body and liver weight, collagenase digestion times, a range of concentrations of Na^+ and Cl^-, as well as pH in perfusates. Viabilities >90% and increased P450IA1 activity were consistently achieved by strictly controlling the Na^+ and Cl^- perfusate concentrations. Further refinement of

the isolation technique, ongoing in our laboratory, using digitonin-collagenase perfusion, can allow differential isolation of perivenous and periportal hepatocytes for use in studies of heterogeneous hepatocyte function pertaining to BAL and other applications, including hepatocyte transplantation.

Further work is required to establish precisely how long PPHs should be cultured in a bioreactor for optimal BAL support. Flendrig *et al.*, (1998b) demonstrated that prolonging culture recovery time of freshly seeded PPHs from 14 to 38 hours improved cell performance and BAL efficacy. Unger *et al.*, (2000) concluded that hepatocyte nutrition with WE medium during this 'standby' period, influenced the metabolic functional profile and efficacy of their bioreactor, when compared with human plasma-perfused cells. It is assumed hepatocytes undergo a 'consolidation phase' during the first 24-48 hours of culture, whereby cells can repair membranes, partially restore polarity and cell-cell interactions (Berry *et al.*, 1991c), and undergo proliferation (Wegner *et al.*, 1992). The morphological observations and functional data presented here suggest cells are most suitable for application in BAL systems between days 2 and 4 of culture.

Related to this, is the question of the duration of BAL therapy. How long are hepatocytes able to function effectively in their optimised state, in the presence of 'toxic' human plasma? Most PPH-based BAL devices are designed to be operational for 4-8 hours of perfusion with heterologous plasma (Stefanovich *et al.*, 1996; Demetriou *et al.*, 1998). Follow-up studies should be undertaken to assess PPH performance in 'toxic' human plasma within this timeframe and beyond. Uchino *et al.*, (1991) reported that pig hepatocytes cultured for 3 days in human ALF plasma maintained gluconeogenesis and ureogenesis equal to that of cells cultured in normal human plasma or Leibovitz medium. However, Kawazoe *et al.*, (1999) showed that the viability of PPHs cultured in normal human plasma decreased to 37%, while albumin synthesis was one third of that in DMEM controls. Moreover, nafamostat mesilate, a protease inhibitor, had a favourable effect on these parameters. Washizu *et al.*, (2000) found that amino acid supplementation improves cell-specific functions of rat hepatocytes exposed to human plasma. Elucidation of the potentially toxic

effects of ALF plasma and mechanisms of cells death may allow for BAL cytoprotective strategies to be developed.

Clearly, a systematic study of PPH attachment efficiency and function on the many and varied hollow-fibre biomembrane materials used in BAL devices is warranted. In terms of the biological component of BAL systems, there is evidence that isolated hepatocytes arranged into multi-cellular formations, establish cell-cell and cell-matrix contacts which result in improved differentiation and liver-specific function, when compared with single cell culture monolayers (Ben-Ze'ev *et al.*, 1988; Bhatia *et al.*, 1999; Khaoustov *et al.*, 1999). Indeed Gerlach *et al.*, (1995) have demonstrated that PPHs readily attached to uncoated hollow fibre membranes constructed of polypropylene, a synthetic material similar to that used in TCP dish manufacture. Formation of cell aggregates may be achieved by culturing cells in a simulated microgravity environment (Dabos *et* al., 2001; Khaoustov *et al.*, 1999; Yoffe *et al.*, 1999) or as hepatospheroids on Primaria™ dishes (Koide *et al.*, 1990), providing an *in vivo*-like liver micro-architecture promoting maintenance of viability and differentiated functions. The use of serum-supplemented medium in this context is controversial. Hsiao *et al.*, (1999) demonstrated foetal bovine serum caused disassembly of hepatospheroids and a decrease in cytochrome P450 1A/2 activity. On the other hand, Sakai *et al* (Sakai *et al.*, 1996a; Sakai *et al.*, 1996b) showed that culturing spheroids in suspension within rotating dishes or entrapped in collagen gel in 100% porcine or human plasma could enhance ammonia detoxification compared to conventional monolayer cultures. The use of bio-degradable scaffolds (see below) optimised for cell-cell, cell-matrix geometry and heterogeneous functional activity promises to be a major advance in promoting and sustaining vital differentiated function required of a liver support device (Glicklis *et al.*, 2000).

The precise reasons for the observed marked differences in morphology and function up to culture day 4 between different media formulations are unclear. An explanation proposed for this pattern may lie in the individual medium compositions. Medium 199, and to a lesser extent WE, are media formulations which contain a greater range of constituents (including inorganic salts, vitamins, cofactors and

amino acids) with which to support hepatocyte culture compared with the other test media. Although the hormone levels are the same for each test medium, a greater pool of amino acids, in the presence of insulin, may enhance utilisation of this pool and favour anabolic protein metabolism (Berry *et al.*, 1991a). This could influence cell attachment, membrane integrity and survival as well as favouring better preservation of cell ultrastructure and hence differentiated functions. These effects may be synergistic, acting in concert with the other hormonal supplements, dexamethasone and L-EGF. Another possibility is that a broader spectrum of amino acid concentrations are a requirement of the high density cultures used in our experiments. High cell density, not only delays the loss of some differentiated functions, but may well lead to a relatively more cuboidal, less flattened cell shape (Ben-Ze'ev *et al.*, 1988; Berry *et al.*, 1991a). Hepatocytes with this topology display ultrastructural characteristics of both cell aggregates and liver cells *in situ* (Berry *et al.*, 1991b; Gerlach *et al.*, 1995; Sajiki *et al.*, 2000), as do both M199 and WE maintained cultures described here (see Figures 3.3, 3.5 and 3.7). Of course, other hepatocyte culture media are commercially available and routinely used including: DMEM, Chee's, and Modified Earl's Medium. (Berry *et al.*, 199b, 1991d). Testing all media formulations and all combinations with the numerous, potentially beneficial supplements available, would require a major research undertaking.

In Chapters 3 and 4, it was shown that PPHs readily attached to biomatrix-free TCP whilst maintaining viability and functional activity, as well as morphological characteristics of differentiated cells up to day 4 of culture, at least in WE and M199. Considering the wealth of evidence in other species, particularly rat, it would be prudent to assess whether autologous ECM might enhance these criteria of hepatic support functions for BAL systems. Equally, tissue engineered PPH culture systems may allow for functional living tissue to be fabricated using hepatocytes and NPCs seeded on highly porous, synthetic, biodegradable polymer scaffolds, and permanently implanted to restore hepatic function (Sundback and Vacanti, 2000). Important liver functions cannot be enabled by use of purified, homotypic hepatocyte cultures (Busse *et al.*, 1999; Bhatia *et al.*, 1999). Potential benefits of NPC inclusion in cocultures (discussed below) include bile excretion and

the phagocytic function of Kupffer cells. However, the possibility of antigenicity from the NPC coculture fraction should not be underestimated (Demetriou, 1998a), and needs to be investigated further.

Since the liver serves as the primary site of detoxification of an enormous range of natural, synthetic, and toxic substances in the systemic circulation, any BAL system must be capable of dealing with this complex metabolism. Parallel diminution in tP450 levels (Chapter 4) and functional activity is observed in swine and other mammals (Donato *et al.*, 1999; LeCluyse *et al.*, 1996; Monshouwer *et al.*, 1998; Olsen *et al.*, 1997). Determination of tP450 by CO-binding capacity does not distinguish between the many P450 isoforms. Species differences in xenobiotic metabolism are also well recognised (LeCluyse *et al.*, 1996). Future studies would characterise a much wider spectrum of porcine P450 species utilising both 'speculative' antibody homologues or, ideally, pure anti-porcine antibodies could be developed via protein purification through expression vectors, as the pig genome project unfolds (Professor JI Mason, Personal Communication). Moreover, as the requirements of BAL system detoxification are more clearly identified, P450 enzyme induction could be tailored accordingly.

Hepatocye functional activity can be augmented *in vitro*. Cytochrome P450 isoenzymes can be induced using a variety of inducers including phenobarbital or dexamethasone. This results in both increased tP450 content and P450-mediated enzyme activities including testosterone hydroxylation, caffeine demethylation, and induction of the pig CYP3A4 isoform, an important inducible enzyme involved in the metabolism of many drugs in humans (Desille *et al.*, 1999; Li *et al.*, 1995; Monshouwer *et al.*, 1998; Olsen *et al.*, 1997). Suprisingly, few intervention strategies have been designed to manipulate pig liver *in vivo* or *in vitro*, in order to *condition* cells which may enhance bioreactor efficacy. Porcine xenobiotic metabolism could be further characterised by establishing whether *in vivo* and/or *in vitro* intervention with high dose dexamethasone or phenobarbital enhances hepatic Phase I and II isoenzyme expression and function *in vitro* under defined conditions. In our culture system, use of the P450 inducer, dexamethasone could be confounding when

assessing either tP450 or functional activity, since, precisely which individual enzymes are present in pig liver, or are modulated by induction remains unclear.

Alternative approaches to enhance the hepatic culture environment should also be investigated. Supplementation of optimal media with DMSO (combined with dexamethasone) or retinoic acid, can maintain or re-establish hepatocyte culture morphology, differentiated morphology and function (Arterburn *et al.*, 1995; Mitaka *et al.*, 1998; Falasca *et al.*, 1998) Nicotinamide could also be used to maintain the capability of cell growth (Mitaka *et al.*, 1998), required during the attachment and growth phase for pre-clinical BAL devices.

Culture of hepatocytes as hepatospheroids offers great potential for improving culture longevity, morphology and function. In retrospect, parallel spinner flask or roller bottle cultures, using cells from the same pig isolation, would have permitted a more direct comparison of differences in biochemical functionality and morphology between RCCS-grown and conventional rotational cultures in unit gravity. If we consider that the sinusoidal surface of liver is about 150 m^2 and current dialysers offer an exchange surface of 0.5-2 m^2 (Busse et al., 1999), and their are inherent limits to nutrient diffusion, vascularization of engineered tissue appears a critical step. The formation and maintenance of large, vascularized cellular constructs, would facilitate metabolic transport of oxygen and nutrients and removal of waste products (Kim and Mooney, 1998; Sundback and Vacanti, 2000; Unsworth and Lelkes, 1998). This could be achieved in the microgravity bioreactor by incorporating the appropriate levels of angiogenic factors, sinusoidal endothelial cells and bioengineered tubular scaffolds with which to form such blood vessel conduits, perhaps incorporated into PGA scaffolds.

6.4.1 Potential disadvantages of xenogeneic cells in bioartifcial liver devices

Immunogenicity, zoonoses and biocompatibility are potential disadvantages of xenogeneic cells for therapeutic use (Tsiaoussis *et al.*, 2001):

Immunogenicity: Pre-formed IgM antibodies against porcine hepatocytes have been reported in almost 7% of the healthy population leading to hyper-acute rejection in xenogeneic organ transplantation. Consequently immuno-isolation using semi-permeable hollow-fibre membranes with 100 KDa molecular weight cut-off, have been incorporated into many systems to prevent extensive porcine hepatocyte necrosis and consequent flux of necro-inflammatory chemicals back into the patient. The membranes may also protect against possible immunological compounds escaping from xenogeneic tissue into the patient's circulation, although despite their usage elevated titers of anti-pig IgM and IgG xeno-antibodies (primarily against A-Gal epitope on pig hepatocytes) have been found following two or more treatments with porcine- based BAL systems indicating that host exposure to porcine antigens still occurs. The promising developments of transgenic animals with knock-outs for Gal-epitope, and addition of nafamostat mesilate (a synthetic serine protease inhibitor of complement with cytoprotective properties) to BAL systems, may mitigate the problem of hyperacute rejection and human serum cytotoxicity (Kawazoe *et al.*, 1999) As yet, no adverse immunological reactions have been reported with repeated usage of these systems over a prolonged period of several days, but this may be due to the fact that patients with ALF are relatively immunosuppressed and are unable to mount significant immune responses.

Zoonoses: Standard health screening protocols are available to ensure that animals are free of various pathogens. Of greater importance is the issue of Porcine Endogenous Retroviruses (PERVs), which are incorporated into the porcine genome itself. At present, it has not proven possible to remove PERVs from such hepatocytes. There is no evidence to indicate any pathogenic role of PERVs in pigs, but there has been concern that this may not be the case if human cells become infected. Consequently, experiments have focused on transmission of PERVs to

human cells and possible pathological sequelae. Demonstration that PERV particles can be transmitted from porcine to human cells appear to confirm this. However, a series of large studies has subsequently not demonstrated any evidence for the transmission of viable virus with replicative potential. The distinction between 'simple' uptake of viral particles and the successful migration of PERVs and potential adverse effects is of paramount importance in combating difficulties that may arise. Whilst there is therefore no evidence of successful transmission of active PERV from pig to human or even evidence of pathogenicity the issue is far from resolved. Some countries have consequently implemented xenotransplantation moratoria before permitting the usage of xenogeneic tissue. Ongoing studies are in place to develop PERV-free pigs, although the possibility of transmitting hitherto unknown zoonotic (or human) viruses will always remain a concern.

Biocompatibility: Whilst porcine hepatocytes may detoxify human toxins there are concerns that products from different species such as coagulation factors, albumin, growth factors and cytokines may not exert a similar biological response in humans. It is worth noting however that porcine tissue, such as heart valves, pancreas transplants and insulin have been used to good effect in human diseases for many years now.

6.4.2 Key logistical and technical considerations

There are still key logistical and technical issues to be resolved in terms of the ready availability of PPHs for on-demand usage, cryopreservation of cells, and the critical functional liver cell mass required for effective support. Ongoing hepatocyte culture within the bioreactor has the disadvantage of high costs (labour, materials and time), as well as the limited 'shelf-life' of the hepatocytes. Several bioreactors would have to be maintained concurrently if, for example the 6-hour multiple treatment regime was adopted. Quality control tests of biochemical functionality and microbial screening would be limited also. Cryopreserved liver cells would have obvious advantages. However, despite their use in the HepatAssist™ device, there is evidence that upon thawing, only 50 % of cells attach

to plastic (compared to 80-90 % for freshly isolated cells (Chapter 3)), suggesting compromised function (Darr and Hubel, 1998; Loretz *et al.*, 1989). Further advances in freezing protocols and optimisation of function, post-thaw, are required (Tsiaoussis *et al.*, 2001). The critical cell mass for effective BAL support is not known. Current estimates from clinical studies of partial hepatectomy and treatment of animal models of ALF with BAL systems (Busse *et al.*, 1999; Demetriou, 1998; Tsiaoussiss *et al.*, 2001) suggest 20-40 % is required, corresponding to about 150 to 300 g of liver tissue for a 70 kg patient. Of the three bioartificial liver support systems for which clinical data are available (see Table 6.1), there are also significant differences in the number of cells used to load the bioreactor (6 $x10^9$ to $100x10^9$) which corresponds to 2-33% of normal liver mass (Sundback and Vacanti, 2000). Specifically, the HepatAssist BAL device (Rozga *et al.*, 1993a) contains approximately $6x10^9$ cryopreserved porcine hepatocytes (30g; 2% of normal hepatocyte mass), whilst the ELAD (Sussman *et al.*, 1994) contains $40x10^9$ transformed C3A cells (200g; 15% of normal hepatocyte mass). A more complex device (Gerlach *et al.*, 1994b) contains $100x10^9$ porcine hepatocytes (500g; 33% of normal hepatocyte mass). Other devices which are at a developmental stage contain similar numbers of hepatocytes, for example, Bader's bioreactor (DeBartolo *et al.*, 2000) contains $10x10^9$ porcine hepatocytes.

Table 6-1 Critical Hepatic Cell Mass for BAL Systems

BAL System	Cell Type	No. of Cells	Weight (g)	Liver Mass (%)	Phase of Development
[1]HepatAssist	Porcine	6×10^9	30	2	Clinical
[2]ELAD	C3A	40×10^9	200	15	Clinical
[3]Gerlach	Porcine	100×10^9	500	33	Clinical
[4]Bader	Porcine	10×10^9	50	3.3	Experimental

Notes: The number of hepatocytes varies significantly from as low as 2% to 33%. The Percentage of liver cell mass is derived from a value of a human liver of 1.5 kg. References: [1]Rozga *et al.*, (1993a); [2]Sussman *et al.*, 1994; [3]Gerlach *et al.*, 1994b; [4]DeBartolo *et al.*, 2000.

Human hepatocytes are considered the ideal cellular component to fulfil hepatic support functions for BAL systems. However, the growing disparity between the numbers of donor organs and patients requiring OLT precludes their use in this setting. The development of genetically-engineered immortalized human cell lines, with fully differentiated normal hepatic support functions, would alleviate both the logistical constraints and disadvantages associated with using xenogeneic cell sources. As an alternative to tumour-derived lines such as C3A or HepG2, mentioned previously, reversibly immortalized cell lines have been developed. For example, the NKNT-3 line, has been heralded as a breakthrough for hepatocyte transplantation. Produced by retroviral transfection of normal primary human hepatocytes with the Simian Virus 40 large T antigen, NKNT-3 cells have been shown to express key genes of liver metabolism and produced significant biochemical and clinical improvements in 90 % hepatectomy rats when infused into the spleen (Kobayashi *et al.*, 2000). The utility of this and other cell lines under development are exciting prospects for the field of BAL support.

The work presented in this thesis provides information on the use of primary porcine hepatocytes as a model culture system for functional and morphological characterisation under fully-defined conditions, appropriate for BAL support systems. Evidence has been presented that media formulation can have significant modulatory effects on hepatocyte morphology and function, which may impact upon bioreactor efficacy. Also, a simulated microgravity environment was investigated as a novel system to study the cytoarchitecture and biochemical functionality of three-dimensional liver cell cultures over an extended period of time. These findings could be important in highlighting the need for both species-specific characterisation of porcine hepatocytes, and the ongoing requirement for a more comprehensive approach to culture optimisation for BAL applications. Several areas where progress needs to be made have been outlined above. Refinements of existing technology and the rapid advancements in the new areas of tissue engineering and stem cell biology suggest the promise of clinically effective BAL support will become realised.

APPENDIX I

Amino–acid composition of the four media used. HM is a modification based on Leibovitz L-15 medium with identical amino acid concentrations (Sigma Technical Service).

	WE (g/L)	**L–15 (g/L)**	**M199 (g/L)**	**M1640 (g/L)**
Alanine	0.09	**0.45**	0.05	–
Arginine	0.05	**0.5**	0.07	**0.2**
Asparagine	0.02	**0.25**	–	0.05
Aspartate	0.03	–	0.06	0.02
Cysteine	0.04	**0.12**	0.00011	–
Cystine	0.02	–	0.026	0.0652
Glutamate	0.0445	–	0.1336	0.02
Glutamine	–	–	–	0.3
Glycine	0.05	**0.2**	0.05	0.01
Histidine	0.015	**0.25**	0.02188	0.015
Hydroxy–proline	–	–	0.01	0.02
Isoleucine	0.05	**0.25**	0.04	0.05
Leucine	0.075	**0.125**	0.12	0.05
Lysine	0.08746	0.075	0.07	0.04
Methionine	0.015	**0.15**	0.03	0.015
Phenylalanine	0.025	**0.25**	0.05	0.015
Proline	0.03	–	**0.04**	0.02
Serine	0.01	**0.2**	0.05	0.03
Threonine	0.04	**0.6**	0.06	0.02
Tryptophan	0.01	0.02	0.02	0.005
Tyrosine	0.05045	**0.3**	0.05766	0.02883
Valine	0.05	**0.2**	0.05	0.02

Bibliography

Abouna GM, Boehmig HG, Serrou B, Amemiya H, Martineau G. Long-term hepatic support by intermittent multi-species liver perfusions. Lancet 1970;2:391-396.

Abu-Absi SF, Friend JR, Hansen LK, Hu WS. Structural polarity and functional bile canaliculi in rat hepatocyte spheroids. Exp Cell Res 2002; 274(1):56-67.

Albrecht J, Jones EA. Hepatic encephalopathy: molecular mechanisms underlying the clinical syndrome. J Neurol Sci 1999;170:138-146.

Alpini G, Phillips JO, Vroman B, LaRusso NF. Recent advances in the isolation of liver cells. HEPATOLOGY 1994; 20(2):494-514.

Ampola MG. The Urea Cycle. In: Arias IMBLFN and et al, eds. The Liver: Biology and Pathobiology. 3 ed. New York: Raven press Ltd., 1994:365-377.

Arterburn LM, Zurlo J, Yager JD, Overton RM, Heifetz AH. A morphological study of differentiated hepatocytes in vitro. HEPATOLOGY 1995;22:175-187.

Auth MKH, Ichihara A. Hepatocyte co-culture, three-dimensional culture models and the extracellular matrix. In: Strain AJ and Diehl AM, eds. Liver Growth and Repair. 1 ed. London: Chapman & Hall, 1998:465-481.

Bader A, De Bartolo L, Haverich A. High level benzodiazepine and ammonia clearance by flat membrane bioreactors with porcine liver cells. J Biotechnol 2000;81:95-105.

Bader A, Knop E, Boker K, Fruhauf N, Schuttler W, Oldhafer K, Burkhard R, Pichlmayr R, Sewing KF. A novel bioreactor design for in vitro reconstruction of in vivo liver characteristics. Artif Organs 1995a;19:368-374.

Bader A, Knop E, Fruhauf N, Crome O, Boker K, Christians U, Oldhafer K, Ringe B, Pichlmayr R, Sewing KF. Reconstruction of liver tissue in vitro: geometry of characteristic flat bed, hollow fiber, and spouted bed bioreactors with reference to the in vivo liver. Artif Organs 1995b;19:941-950.

Bader A, Knop E, Kern A, Boker K, Fruhauf N, Crome O, Esselmann H, Pape C, Kempka G, Sewing KF. 3-D coculture of hepatic sinusoidal cells with primary hepatocytes- design of an organotypical model. Exp Cell Res 1996;226:223-233.

Baker AL. Liver Chemistry Tests. In: Kaplowitz N, ed. Liver and Biliary Diseases. 1 ed. Baltimore: Williams & Wilkins, 1992:182-194.

Balis UJ, Behnia K, Dwarakanath B, Bhatia SN, Sullivan SJ, Yarmush ML, Toner M. Oxygen consumption characteristics of porcine hepatocytes. Metab Eng 1999;1:49-62.

Baserga R. Measuring parameters of growth. In: Studzinski GP, ed. Cell growth and apoptosis. 1st ed. Oxford: Oxford University Press, 1995:1-5.

Becker JL, Prewett TL, Spaulding GF, Goodwin TJ. Three-dimensional growth and differentiation of ovarian tumor cell line in high aspect rotating-wall vessel: morphologic and embryologic considerations. J Cell Biochem 1993;51:283-289.

Behnia K, Bhatia S, Jastromb N, Balis U, Sullivan S, Yarmush M, Toner M. Xenobiotic metabolism by cultured primary porcine hepatocytes. Tissue Eng 2000;6:467-479.

Ben-Ze'ev A, Robinson G, Bucher NLR, Farmer SR. Cell-cell and cell-matrix interactions differentially regulate the expression of hepatic and cytoskeletal genes in primary cultures of rat hepatocytes. Proc Natl Acad Sci USA 1988;85:2161-2165.

Berman AE, Kozlova NI. Integrins: structure and functions. Membr Cell Biol 2000;13:207-244.

Berry MN, Edwards AM, Barritt GJ. Biochemical properties. In: Berry MN, Edwards AM, and Barritt GJ, eds. Isolated hepatocytes: Preparation, properties and application. Amsterdam: Elsevier Science, 1991d:121-178.

Berry MN, Edwards AM, Barritt GJ. Hepatocyte isolation for primary culture and methods for non-adherent culture. In: Berry MN, Edwards AM, and Barritt GJ, eds. Isolated hepatocytes: Preparation, properties and application. Amsterdam: Elsevier Science, 1991c:237-263.

Berry MN, Edwards AM, Barritt GJ. Microscopy of Isolated Hepatocytes. In: Berry MN, Edwards AM, and Barritt GJ, eds. Isolated hepatocytes: Preparation, properties and application. Amsterdam: Elsevier Science, 1991a:99-121.

Berry MN, Edwards AM, Barritt GJ. Monolayer culture of hepatocytes. In: Berry MN, Edwards AM, and Barritt GJ, eds. Isolated hepatocytes: Preparation, properties and application. Amsterdam: Elsevier Science, 1991b:265-354.

Berry MN, Grivell AR, Grivell MB, Phillips JW. Isolated hepatocytes--past, present and future. Cell Biol Toxicol 1997;13:223-233.

Berthiaume F, Moghe PV, Toner M, Yarmush ML. Effect of extracellular matrix topology on cell structure, function, and physiological responsiveness: hepatocytes cultured in a sandwich configuration. FASEB J 1996;10:1471-1484.

Bhatia SN, Balis UJ, Yarmush ML, Toner M. Effect of cell-cell interactions in preservation of cellular phenotype: cocultivation of hepatocytes and nonparenchymal cells. FASEB J 1999;13:1883-1900.

Bhatia SN, Balis UJ, Yarmush ML, Toner M. Microfabrication of hepatocyte/fibroblast co-cultures: role of homotypic cell interactions. Biotechnol Prog 1998b;14:378-387.

Bhatia SN, Balis UJ, Yarmush ML, Toner M. Probing heterotypic cell interactions: hepatocyte function in microfabricated co-cultures. J Biomater Sci Polym Ed 1998a;9:1137-1160.

Blei AT. Brain edema and intracranial hypertension: a focus for the use of liver support systems. Artif Organs 1997;21:1182-1184.

Blei AT. Medical therapy of brain edema in fulminant hepatic failure. HEPATOLOGY 2000;32:666-669.

Boonstra J. Growth factor-induced signal transduction in adherent mammalian cells is sensitive to gravity. FASEB J 1999;13 Suppl:S35-S42.

Bradford MM. A rapid and sensitive method for the quantitation of microgram quantities of protein utilising the principle of protein-dye binding. Anal Biochem 1976;72:248-254.

Burkitt HG, Young B, Heath JW. Liver and pancreas. In: Burkitt HG, Young B, and Heath JW, eds. Wheater's Functional Histology: A Text and Colour Atlas. 3 ed. Churchill Livingston, 1993:271-287.

Busse B, Smith MD, Gerlach JC. Treatment of acute liver failure: hybrid liver support. A critical overview. Langenbecks Arch Surg 1999 Dec;384(6):588-99
Cao S, Esquivel CO, Keeffe EB. New approaches to supporting the failing liver. Annu Rev Med 1998;49:85-94.

Chen SC, Hewitt WR, Watanabe FD, Eguchi S, Kahaku E, Middleton Y, Rozga J, Demetriou AA. Clinical experience with a porcine hepatocyte-based liver support system. Int J Artif Organs 1996;19:664-669.

Chen SC, Mullon C, Kahaku E, Watanabe F, Hewitt W, Eguchi S, Middleton Y, Arkadopoulos N, Rozga J, Solomon B, Demetriou AA. Treatment of severe liver failure with a bioartificial liver. Ann N Y Acad Sci 1997;831:350-360.

Chesne C, Guyomard C, Fautrel A, Poullain M-G, Fremond B, De Petrillo G, Guillouzo A. Viability and Function in Primary Culture of Adult Hepatocytes from Various Animal Species and Human Beings after Cryopreservation. HEPATOLOGY 1993;18:406-414.

Christiansen BS, Ingerslev J, Heickendorff L, Petersen CM. Human hepatocytes in culture synthesize and secrete fibronectin. Scand J Clin Lab Invest 1988;48:685-690.

Clayton DF, Darnell JE. Changes in liver-specific compared to common gene transcription during primary culture of mouse hepatocytes. Mol Cell Biol 1983;3:1552-1561.

Clement B, Desille M, Fremond B, Campion JP, Guguen-Guillouzo C, Bourel M, Guillouzo A. [Hepatocytes in cell therapy]. Transfus Clin Biol 1998;5:80-87.

Clemmesen JO, Larsen FS, Kondrup J, Hansen BA, Ott P. Cerebral herniation in patients with acute liver failure is correlated with arterial ammonia concentration. HEPATOLOGY 1999;29:648-653.

Cohen AL. Critical point drying principles and procedures. Scanning Electron Microscopy 1979;303-323.

Dabos KJ, Nelson LJ, Bradnock TJ, Parkinson JA, Sadler IH, Hayes PC, Plevris JN. The simulated microgravity environment maintains key metabolic functions and promotes aggregation of primary porcine hepatocytes. Biochemica et Biophysica Acta 2001;251:1-12.

Darr TB, Hubel A. Freezing characteristics of isolated pig and human hepatocytes. Cell Transplantation 1997;6:173-183.

De Bartolo L, Jarosch-Von Schweder G, Haverich A, Bader A. A novel full-scale flat membrane bioreactor utilizing porcine hepatocytes: cell viability and tissue-specific functions. Biotechnol Prog 2000;16:102-108.

Demetriou AA and Rozga J. Artificial liver support. In: Strain AJ and Diehl AM, eds. Liver Growth and Repair. 1st ed. London: Chapman & Hall [Thomson Science], 1998:627-652.

Demetriou AA. Support of the acutely failing liver: state of the art. Ann Surg 1998a; 228:14-15.

Desille M, Corcos L, L'Helgoualc'h A, Fremond B, Campion JP, Guillouzo A, Clement B. Detoxifying activity in pig livers and hepatocytes intended for xenotherapy. Transplantation 1999;68:1437-1443.

Desmet VJ. Organizational Principles. In: Arias IM *et al.*, eds. The Liver: Biology and Pathobiology. 3 ed. New York: Raven press Ltd., 1994:3-14.

Dixit V. Development of a bioartificial liver using isolated hepatocytes. Artificial Organs 1994;18:371-384.

Donato MT, Castell JV, Gomez-Lechon MJ. Characterization of drug metabolizing activities in pig hepatocytes for use in bioartificial liver devices: comparison with other hepatic cellular models. J Hepatol 1999;31:542-549.

Donato MT, Castell JV, Gomez-Lechon MJ. Characterization of drug metabolizing activities in pig hepatocytes for use in bioartificial liver devices: comparison with other hepatic cellular models. J Hepatol 1999;31:542-549.

Donini A, Corno S, Lavaroni S, Pellerito R, Bigi L, Pasqualotto A, Belvedere O, Crivellato E, Degrassi A, Bresadola F. Ex vivo preparation of porcine hepatocytes for use if bioartificial hepatic support systems. Transplantation Proceedings 1997;29:1948-1949.

Doweiko JP, Nompleggi DJ. Role of albumin in human physiology and pathophysiology. JPEN J Parenter Enteral Nutr 1991b;15:207-211.

Doweiko JP, Nompleggi DJ. The role of albumin in human physiology and pathophysiology, Part III: Albumin and disease states. JPEN J Parenter Enteral Nutr 1991a;15:476-483.

Dunn JC, Tompkins RG, Yarmush ML. Hepatocytes in collagen sandwich: evidence for transcriptional and translational regulation. J Cell Biol 1992;116:1043-1053.

Dunn JC, Tompkins RG, Yarmush ML. Long-term in vitro function of adult hepatocytes in a collagen sandwich configuration. Biotechnol Prog 1991;7:237-245.

Duray PH, Hatfill SJ, Pellis NR. Tissue Culture in Microgravity Paul H. Duray, Steven J. Hatfill, and Neal R. Pellis in the May/June 1997 issue of *Science & Medicine* (pp 46-55). Science & Medicine 1997;46-55.

Echlin P. Sputter coating techniques for scanning electron microscopy; *1975 IIpp217-224.* Scanning Electron Microscopy 1975;217-224.

Eiseman B, Liem DS, Raffucci F. Heterologous liver perfusion in treatment of hepatic failure. Ann Surg 1965;162:329-345.

Ellis AJ, Hughes RD, Wendon JA, Dunne J, Langley PG, Kelly JH, Gislason GT, Sussman NL, Williams R. Pilot-controlled trial of the extracorporeal liver assist device in acute liver failure. HEPATOLOGY 1996;24:1446-1451.

Ellis AJ, Sussman NL, Kelly JH, Williams R. Acute liver failure. In: Lee WM and Williams R, eds. Cliical experience with an extracorporeal liver assist device. Cambridge: Cambridge University Press, 1997:255-265.

Enat R, Jefferson DM, Ruiz-Opazo N, Gatmaitan Z, Leinwand LA, Reid LM. Hepatocyte proliferation in vitro: its dependence on the use of serum- free hormonally defined medium and substrata of extracellular matrix. Proc Natl Acad Sci U S A 1984;81:1411-1415.

Enosawa S, Suzuki S, Kakefuda T, Amemiya H. Examination of 7-ethoxycoumarin deethylation and ammonia removal activities in 31 hepatocyte cell lines. Cell Transplant 1996;5:S39-S40.

Falasca L, Favale A, Serafino A, Ara C, Conti Devirgiliis L. The effect of retinoic acid on the re-establishment of differentiated hepatocyte phenotype in primary culture. Cell Tissue Res 1998;Aug;293(2):337-47.

Falasca, L, Miccheli,A, Sartori E, Tomassini A, Devirgiliis LC. Hepatocytes entrapped in alginate beads and cultured in a bioreactor: rapid repolarization and reconstitution of adhesion areas. Cells Tissues Organs 2001;168;126-136.

Fan G, Steer CJ. Cellular Biology of the Normal Liver. In: O'Grady JG, Lake JR, and Howdle PD, eds. Comprehensive Clinical Hepatology. 1st ed. London: Harcourt, 2000:2.1-2.22.

Finlayson N. The liver: anatomy, physiology, liver biopsy and congenital disorders. In: Shearman DJC, Finlayson N, Canilleri MC eds. Diseases of the gastrointestinal tract and liver. 3rd ed. Edinburgh: Churchill Livingston, 1997:707-734.

Flendrig LM, Calise F, Di Florio E, Mancini A, Ceriello A, Santaniello W, Mezza E, Sicoli F, Belleza G, Bracco A, Cozzolino S, Scala D, Mazzone M, Fattore M, Gonzales E, Chamuleau RA. Significantly improved survival time in pigs with complete liver ischemia treated with a novel bioartificial liver. Int J Artif Organs 1999;22:701-709.

Flendrig LM, la Soe JW, Jorning GG, Steenbeek A, Karlsen OT, Bovee WM, Ladiges NC, te Velde AA, Chamuleau RA. In vitro evaluation of a novel bioreactor based on an

integral oxygenator and a spirally wound nonwoven polyester matrix for hepatocyte culture as small aggregates. J Hepatol 1997a;26:1379-1392.

Flendrig LM, Maas MA, Daalhuisen J, Ladiges NC, la Soe JW, te Velde AA, Chamuleau RA. Does the extend of the culture time of primary hepatocytes in a bioreactor affect the treatment efficacy of a bioartificial liver? Int J Artif Organs 1998b;21:542-547.

Flendrig LM, Sommeijer D, Ladiges NC, te Velde AA, Maas MA, Jorning GG, Daalhuisen J, Chamuleau RA. Commercially available media for flushing extracorporeal bioartificial liver systems prior to connection to the patient's circulation: an in vitro comparative study in two and three dimensional porcine hepatocyte cultures. Int J Artif Organs 1998a;21:467-472.

Flendrig LM, te Velde AA, Chamuleau RA. Semipermeable hollow fiber membranes in hepatocyte bioreactors: a prerequisite for a successful bioartificial liver? Artif Organs 1997b;21:1177-1181.

Folkman J, Moscona A. Role of cell shape in growth control. Nature 1978;273:345-349.

Fremond B, Joly A, Desille M, Desjardins JF, Campion JP, Clement B. Cell-based therapy for acute liver failure: The extracorporeal bioartificial liver. Cell Biology and Toxicology 1996;12:325-329.

Gebhardt R, Bellemann P, Mecke D. Metabolic and enzymatic characteristics of adult rat liver parenchymal cells in non-proliferating primary monolayer cultures. Exp Cell Res 1978;112:431-441.

Gerlach J, Brombacher J, Smith M, Neuhaus P. High yield hepatocyte isolation from pig livers for investigation of hybrid liver support systems: influence of collagenase concentration and body weight. Journal of Surgical Research 1996a;62:85-89.

Gerlach J, Encke J, Hole O, Courtney JM, Neuhaus P. Hepatocyte culture between three dimensional arranged biomatrix-coated independent artificial capillary systems and sinusoidal endothelial cell coculture compartments. Int J Artificial Organs 1994a;17:306.

Gerlach J, Kloppel K, Schauwecker HH, Tauber R, Muller C, Bucherl ES. Use of hepatocytes in adhesion and suspension cultures for liver support bioreactors. Int J Artif Organs 1989;12:788-792.

Gerlach J, Kloppel K, Stoll P, Vienken J, Muller C. Gas supply across membranes in bioreactors for hepatocyte culture. Artif Organs 1990;14:328-333.

Gerlach J, Trost T, Ryan CJ, Meisler M, Hole O, Muller C, Neuhaus P. Hybrid liver support system in a short term application on hepatectomized pigs. Int J Artificial Organs 1994b;17:549-553.

Gerlach J, Zeimer R, Neuhaus P. Fulminant liver failure: relevance of extracorporeal hybrid liver support systems. Int J Artificial Organs 1996b;19:7-13.

Gerlach JC, Brombacher J, Klóppel K, Schnoy N, Neuhaus P. Comparison of four methods for mass hepatocyte isolation from pig and human livers. Transplantation 1994c;57:1318-1322.

Gerlach JC, Encke J, Hole O, Muller C, Ryan CJ, Neuhaus P. Bioreactor for a larger scale hepatocyte in vitro perfusion. Transplantation 1994; 58(9):984-988.

Gerlach JC, Schnoy N, Encke J, Smith MD, Muller C, Neuhaus P. Improved hepatocyte in vitro maintenance in a culture model with woven multicompartment capillary systems: Electron microscopy studies. HEPATOLOGY 1995;22:546-552.

Giancotti FG, Ruoslahti E. Integrin signaling. Science 1999;285:1028-1032.

Glicklis R, Shapiro L, Agbaria R, Merchuk JC, Cohen S. Hepatocyte behavior within three-dimensional porous alginate scaffolds. Biotechnol Bioeng 2000;67:344-353.

Gomez-Lechon MJ, Lopez P, Donato T, Montoya A, Larrauri A, Gimenez P et al. Culture of human hepatocytes from small surgical liver biopsies. Biochemical characterization and comparison with in vivo. In Vitro Cell Dev Biol 1990; 26(1):67-74.

Goodwin TJ, Prewett TL, Wolf DA, Spaulding GF. Reduced shear stress: a major component in the ability of mammalian tissues to form three-dimensional assemblies in simulated microgravity. J Cell Biochem 1993;51:301-311.

Goulet F, Normand C, Morin O. Cellular interactions promote tissue-specific function, biomatrix deposition and junctional communication of primary cultured hepatocytes. HEPATOLOGY 1988;8:1010-1018.

Gregory PG, Connolly CK, Toner M, Sullivan SJ. In vitro characterization of porcine epatocyte function. Cell Transplant 2000;9:1-10.

Gregory PG, Connolly CK, Gillis BE, Sullivan SJ. The effect of coculture with nonparenchymal cells on porcine hepatocyte function. Cell Transplant 2001;10(8);731-738.

Grunnet N, Vind C, Dich J. Synergistic effect of insulin and glucocorticoid on albumin secretion in cultured hepatocytes. Acta Physiol Scand 1988;133:593-594.

Guillouzo A, Morel F, Langouet S, Maheo K, Rissel M. Use of hepatocyte cultures for the study of hepatotoxic compounds. J Hepatology 1997;26:73-80.

Gumucio JJ, May M, Dvorak C, Chianale J, Massey V. The isolation of functionally heterogeneous hepatocytes of the proximal and distal half of the liver acinus in the rat. HEPATOLOGY 1986;6:932-944.

Gumucio JJ. Structural Organization of the Liver and Function of the Hepatic Acinus. In: Kaplowitz N, ed. Liver and Biliary Diseases. 1 ed. Baltimore: Williams & Wilkins, 1992:2-17.

Ham AW. The Digestive System. In: Ham AW, ed. Histology. 2 ed. Philadelphia: Lippincott Co., 1953:532-552.

Hamamoto R, Yamada K, Kamihira M, Iijima S. Differentiation and Proliferation of Primary Rat Hepatocytes Cultured as Spheroids. J Biochem 1998;124:972-979.

Hamilton GA, Westmorel C, George AE. Effects of medium composition on the morphology and function of rat hepatocytes cultured as spheroids and monolayers. In Vitro Cell Dev Biol Anim 2001; 37(10):656-667.

Hargreaves T. Anatomy of the Liver. In: Hargreaves T, ed. The Liver and Bile Metabolism. 1 ed. New York: Meredith Corporation, 1968:1-38.

Hayat MA. Principles and Techniques of Electron Microscopy. Vol. 1 ed. New York: Van Nostrand Reinhold Company., 1970.

Heneine W, Tibell A, Switzer WM, Sandstrom P, Rosales GV, Mathews A, et al. No evidence of infection with porcine endogenous retrovirus in recipients of porcine islet-cell xenografts. Lancet 1998;352:695-9.

Hoofnagle JH, Carithers RL, Shapiro C, Ascher N. Fulminant hepatic failure: summary of a workshop. HEPATOLOGY 1995;21:240-252.

Horslen SP, Hammel JM, Fristoe LW, Kangas JA, Collier DS, Sudan DL, Langnas AN, Dixon RS, Prentice ED, Shaw BW, Fox IJ. Extracorporeal liver perfusion using human and pig livers for acute liver failure. Transplantation 2000;70:1472-1478.

Hosagrahara VP, Hansen LK, Beilman GJ, Remmel RP. Evaluation of the effect of culture matrices on induction of CYP3A isoforms in cultured porcine hepatocytes. Chem Biol Interact 2000;127:91-106.

Houck KA, Michalopoulos G. Proline is required for the stimulation of DNA synthesis in hepatocyte cultures by EGF. In Vitro Cell Dev Biol 1985;21:121-124.

Hsiao CC, Wu JR, Wu FJ, Ko WJ, Remmel RP, Hu WS. Receding cytochrome P450 activity in disassembling hepatocyte spheroids. Tissue Eng 1999;5:207-221.

Hu W-S, Friend JR, Wu FJ, Peshwa MV, Lazar A, Nyberg SL, Remmel RP, Cerra FB. Development of a bioartificial liver employing xenogeneic hepatocytes. Cytotechnology 1997;23:29-38.

Hubbard Al, Barr VA, Scott LJ. Hepatocyte Surface Plarity. In: Arias IMBLFN and et al, eds. The Liver: Biology and Pathobiology. 3 ed. New York: Raven press Ltd., 1994:189-213.

Hughes RD, Williams R. Assessment of bioartificial liver support in acute liver failure. Int J Artificial Organs 1996;19:3-6.

Ijima H, Nakazawa K, Mizumoto H, Matsushita T, Funatsu K. Formation of a spherical multicellular aggregate (spheroid) of animal cells in the pores of polyurethane foam as a cell culture substratum and its application to a hybrid artificial liver. J Biomater Sci Polym Ed 1998;9:765-778.

Ingber D. How cells (might) sense microgravity. FASEB J 1999;13 Suppl:S3-15.

Ingber DE. Tensegrity: the architectural basis of cellular mechanotransduction. Annu Rev Physiol 1997;59:575-599.

Iwata H, Sajiki T, Maeda H, Park YG, Zhu B, Satoh S, Uesugi T, Ikai I, Yamaoka Y, Ikada Y. In vitro evaluation of metabolic functions of a bioartificial liver. ASAIO J 1999;45:299-306.

Jauregui H, Hayner NT, Driscoll J, Williams-Holland R, Lipsky MH, Galletti PM. Trypan blue uptake and lactate dehydrogenase in adult rat hepatocytes - freshly isolated cells, cell suspensions, and primary monolayer cultures. In Vitro 1981;17:1100-1110.

Jauregui HO, Gann KL. Mammalian hepatocytes as a foundation for treatment in human liver failure. J Cell Biochemistry 1991;45:359-365.

Jauregui HO, McMillan PN, Driscoll J, Naik S. Attachment and long term survival of adult rat hepatocytes in primary monolayer cultures: comparison of different substrata and tissue culture media formulations. In Vitro Cell Dev Biol 1986;22:13-22.

Jauregui HO, Naik S, Santangini H, Trenkler DM, Mullon CJP. The use of microcarrier-roller bottle culture for large-scale production of porcine hepatocytes. Tissue Engineering 1997;3:17-25.

Jauregui HO, Trenkler DM, Naik S, Santangini H, Press P, Muller TE, Solomon BA. In vivo evaluation of a hollow fibre liver assist device. HEPATOLOGY 1995;21:460-469.

Jessup JM, Goodwin TJ, Spaulding G. Prospects for use of microgravity-based bioreactors to study three- dimensional host-tumor interactions in human neoplasia. J Cell Biochem 1993;51:290-300.

Joly A, Desjardins JF, Fremond B, Desille M, Campion JP, Malledant Y, Lebreton Y, Semana G, Edwards-Levy F, Levy M-C, Clement B. Survival, proliferation, and functions of porcine hepatocytes encapsulated in coated algenate beads: A step towards a reliable bioartificial liver. Transplantation 1997;63:795-803.

Jones EA, Schafer DF. Hepatic encephalopathy: a neurochemical disorder. Prog Liver Dis 1986;8:525-540.

Junqueira LC. Glands associated with the Digestive Tract. In: Junqueira LCCJCA, ed. Basic Histology. 2 ed. California: Lange Medical Publications, 1977:315-329.

Kano J, Tokiwa T, Zhou X, Kodama M. Colonial growth and differentiation of epithelial cells derived from abattoir adult porcine livers. J Gastroenterol Hepatol 1998;13 Suppl:S62-S69.

Kawaguchi M, Koide N, Sakaguchi K, Shinji T, Tsuji T. Combination of epidermal growth factor and insulin is required for multicellular spheroid formation of rat hepatocytes in primary culture. Acta Med Okayama 1992;46:195-201.

Kawazoe Y, Eguchi S, Sugiyama N, Yuzawa H, Kawashita Y, Fujioka H, Kanematsu T. Protective effect of nafamostat mesilate on injury of porcine hepatocytes by human plasma. Cell Transplant 1999;8:419-425.

Keatch SA, Nelson LJ, Mason JI, Hayes PC, Plevris JP. Cytochrome P450 content of primary porcine hepatocyte ccultures with various media formulations for use in bioartificial liver devices. J Art Org;5;(1);2002.

Kessler MA, Meinitzer A, Wolfbeis OS. Albumin blue 580 fluorescence assay for albumin. Anal Biochem 1997;248:180-182.

Khaoustov VI, Darlington GJ, Soriano HE, Krishnan B, Risin D, Pellis NR, Yoffe B. Induction of three-dimensional assembly of human liver cells by simulated microgravity. In Vitro Cell Dev Biol Anim 1999;35:501-509.

Kim B-S, Mooney DJ. Development of biocompatible synthetic extracellular matrices for tissue engineering. TIBTECH 1998;16:224-230.

Kobayashi N, Noguchi H, Watanabe T, Matsumura T, Totsugawa T, Fujiwara T, Westerman K, Leboulch P, Fox IJ, Tanaka N. Establishment of a tightly regulated human cell line for the development of hepatocyte transplantation. Hum Cell 2000;13:7-13.

Koebe HG, Schildberg FW. Isolation of porcine hepatocytes from slaughterhouse organs. Int J Artificial Organs 1996;19:53-60.

Koide N, Sakaguchi K, Koide Y, Asano K, Kawaguchi M, Matsushima H, Takenami T, Shinji T, Mori M, Tsuji T. Formation of multicellular spheroids composed of adult rat hepatocytes in dishes with positively charged surfaces and under other nonadherent environments. Exp Cell Res 1990;186:227-235.

Koide N, Shinji T, Tanabe T, Asano K, Kawaguchi M, Sakaguchi K, Koide Y, Mori M, Tsuji T. Continued high albumin production by multicellular spheroids of adult rat hepatocytes formed in the presence of liver-derived proteoglycans. Biochem Biophys Res Commun 1989;161:385-391.

Kong LB, Chen S, Demetriou AA, Rozga J. Matrix-induced liver cell aggregates (MILCA) for bioartificial liver use. Int J Artif Organs 1996;19:72-78.

Kreamer BL, Staecker JL, Sawada N, Sattler GL, Hsia MT, Pitot HC. Use of a low-speed, iso-density percoll centrifugation method to increase the viability of isolated rat hepatocyte preparations. In Vitro Cell Dev Biol 1986; 22(4):201-211.

Laemmli UK. Cleavage of structural proteins during the assembly of the head of bacteriophage T4. Nature 1970;227:680-685.

Landry J, Bernier D, Ouellet C, Goyette R, Marceau N. Spheroidal aggregate culture of rat liver cells: histotypic reorganization, biomatrix deposition, and maintenance of functional activities. J Cell Biol 1985;101:914-923.

Lazar A, Mann HJ, Remmel RP, Shatford RA, Cerra FB, Hu WS. Extended liver-specific functions of porcine hepatocyte spheroids entrapped in collagen gel. In Vitro Cell Dev Biol Anim 1995b;31:340-346.

Lazar A, Peshwa MV, Wu FJ, Chi CM, Cerra FB, Hu WS. Formation of porcine hepatocyte spheroids for use in a bioartificial liver. Cell Transplant 1995a;4:259-268.

LeCluyse E, Bullock P, Madan A, Carroll K, Parkinson A. Influence of extracellular matrix overlay and medium formulation on the induction of cytochrome P-450 2B enzymes in primary cultures of rat hepatocytes. Drug Metab Dispos 1999;27:909-915.

LeCluyse EL, Bullock P, Parkinson A. Strategies for restoration and maintenance of normal hepatic structure and function in long-term cultures of rat hepatocytes. Advanced Drug Delivery Reviews 1996b;22:186.

LeCluyse EL, Bullock PL, Parkinson A, Hochman JH. Cultured rat hepatocytes. Pharm Biotechnol 1996a;8:121-159.

Leloir LF. The enzymatic transformation of uridine diphosphate glucose into a galactose derivative. Arch Biochem Biophys 1951;33:186.

LeTissier P, Stoye JP, Takeuchi Y, Patience C, Weiss RA. Two sets of human-tropic pig retroviruses. Nature 1997;389:681-2.
Li AP, Kaminski DL, Rasmussen A. Substrates of human hepatic cytochrome P450 3A4. Toxicology 1995;104:1-8.

Liu J, Pan J, Naik S, Santangini H, Trenkler D, Thompson N, Rifai A, Chowdhury JR, Jauregui HO. Characterization and evaluation of detoxification functions of a nontumorigenic immortalized porcine hepatocyte cell line (HepLiu). Cell Transplant 1999;8:219-232.

Loretz LJ, Li AP, Flye MW, Wilson AG. Optimization of cryopreservation procedures for rat and human hepatocytes. Xenobiotica 1989 May;19(5):489-98.

Maddrey WC. Bioartificial liver in the treatment of hepatic failure. 49-55. 2000. Dallas, Amercian Association for the Study of Liver Disease. Critical care issues in livertransplantation. Plevak, D. and Seef, LRef Type: Conference Proceeding

Maher JJ. The extracellular matrix in liver regeneration. In: Strain AJ and Diehl AM, eds. Liver Growth and Repair. 1 ed. London: Chapman & Hall, 1998:451-464.

Marsh DC, Hjelmhaug JA, Vreugdenhil PK, Kerr JA, Rice MJ, Belzer FO, Southard JH. Hypothermic preservation of hepatocytes. III. Effects of resuspension media of viability after up to 7 days of storage. HEPATOLOGY 1991;13:500-508.

Martin U, Keissig V, Blusch JH, Haverich A, von der Helm K, Herden T, Steinhoff G. Expression of pig endogenous retrovirus by primary porcine endothelial cells and infection of human cells. Lancet 1998;352:692-694.

Matsumoto K, Nakamura T. Heparin functions as a hepatotrophic factor by inducing production of hepatocyte growth factor. Biochem Biophys Res Commun 1996; 227(2):455-461.

Matsushita T, Ijima H, Koide N, Funatsu K. High albumin production by multicellular spheroids of adult rat hepatocytes formed in the pores of polyurethane foam. Appl Microbiol Biotechnol 1991;36:324-326.

McClelland RE, Coger RN. Use of micropathways to improve oxygen transport in a hepatic system. J Biomech Eng 2000;122:268-273.

McCloskey P, Tootle R, Selden C, Larsen F, Roberts E, Hodgson HJ. Modulation of hepatocyte function in an immortalized human hepatocyte cell line following exposure to liver-failure plasma. Artif Organs 2002; 26(4):340-348.

Meijer AJ, Lamers WH, Chamuleau RA. Nitrogen metabolism and ornithine cycle function. Physiol Rev 1990;70:701-748.

Meijer AJ, Boon L, van Woerkom GM. Control by pH of ureogenesis in isolated hepatocytes. Contrib Nephrol 1988; 63:167-170.

Michalopoulos GK, Bowen WC, Zajac VF, Beer-Stolz D, Watkins S, Kostrubsky V, Strom SC. Morphogenetic events in mixed cultures of rat hepatocytes and nonparenchymal cells maintained in biological matrices in the presence of hepatocyte growth factor and epidermal growth factor. HEPATOLOGY 1999;29:90-100.

Michalopoulos GK, Bowen WC, Mule K, Stolz DB. Histological organization in hepatocyte organoid cultures. Am J Pathol 2001; 159(5):1877-1887.
Michalopoulos GK. Liver regenaration: molecular mechanisms of growth control. FASEB J 1990;4:176-187.

Mitaka T, Sato F, Mizuguchi T, Yokono T, Mochizuki Y. Reconstruction of hepatic organoid by rat small hepatocytes and hepatic nonparenchymal cells. HEPATOLOGY 1999;29:111-125.

Mitaka T. The current status of primary hepatocyte culture. Int J Exp Pathol 1998;79:393-409.

Moghe PV, Berthiaume F, Ezzell RM, Toner M, Tompkins RG, Yarmush ML. Culture matrix configuration and composition in the maintenance of hepatocyte polarity and function. Biomaterials 1996; 17(3):373-385.

Monshouwer M, van't Klooster GAE, Nijmeijer SM, Witkamp RF, Van Miert A. Characterization of cytochrome P450 isoenzymes in primary cultures of pig hepatocytes. Toxicology In Vitro 1998;12:715-723.

Morsiani E, Pazzi P, Moscioni AD, Rozga J, Azzena G, Demetriou AA. In vitro morphological and functional characterization of isolated porcine hepatocytes for extracorporeal liver support: bile acid uptake and conjugation. J Surg Res 1998;79:54-60.

Moseley RH. Function of the normal liver. In: O'Grady JG, Lake JR, and Howdle PD, eds. Comprehensive Clinical Hepatology. 1 ed. London: Harcourt, 2000:3.1-3.16.

Moshage H, Yap SH. Primary cultures of human hepatocytes: a unique system for studies in toxicology, virology, parasitology and liver pathophysiology in man. J Hepatol 1992;15:404-413.

Mueller-klieser W. Three-dimensional cell cultures: from molecular mechanisms to clinical applications. Am J Physiol [Cell Physiol] 1997;273:C1109-C1123.

Naik S, Trenkler D, Santangini H, Pan J, Jauregui HO. Isolation and culture of porcine hepatocytes for artificial liver support. Cell Transplant 1996;5:107-115.

Naruse K, Sakai Y, Nagashima I, Jiang GX, Muto T. Development of a new bioartificial liver module filled with porcine hepatocytes immobilized on non-woven fabric. Int J Artificial Organs 1996a;19:347-352.

Naruse K, Sakai Y, Nagashima I, Jiang GX, Suzuki M, Muto T. Comparisons of porcine hepatocyte spheroids and single hepatocytes in the non-woven fabric bioartificial liver module. Int J Artif Organs 1996a;19:605-609.

Naruse K, Sakai Y, Nagashima I, Jiang GX, Suzuki M, Muto T. Development of a new bioartificial liver module filled with porcine hepatocytes immobilized on non-woven fabric. Int J Artif Organs 1996b;19:347-352.

Nawa K, Nakamura T, Kumatori A, Noda C, Ichihara A. Glucocorticoid-dependent expression of the albumin gene in adult rat hepatocytes. J Biol Chem 1986;261:16883-16888.

Nelson LJ, Newsome PN, Howie AF, Hadoke PW, Dabos KJ, Walker SW, Hayes PC, Plevris JN. An improved ex vivo method of primary porcine hepatocyte isolation for use in bioartificial liver systems [In Process Citation]. Eur J Gastroenterol Hepatol 2000;12:923-930.

Neuberger J, Finlayson N. Drugs and Toxins. In: Shearman DJC, Finlayson N, Canilleri MC, and Surgical Editor C, eds. Diseases of the gastrointestinal tract and liver. 3rd ed. Edinburgh: Churchill Livingston, 1997:837-860.

Newsome PN, Plevris JN, Nelson LJ, Hayes PC. Animal models of fulminant hepatic failure: a critical evaluation. Liver Transpl 2000;6:21-31.

Nyberg SL, Remmel RP, Mann HJ, Peshwa MV, Hu W-S, Cerra FB. Primary hepatocytes outperform Hep G2 cells as the source of biotransformation functions in a bioartificial liver. Annals of Surgery 1994;220:59-67.

Nyberg SL, Shirabe K, Peshwa MV, Sielaff TD, Crotty PL, Mann HJ, Remmel RP, Payne WD, Hu W-S, Cerra FB. Extracorporeal application of a gel-entrapment, bioartificial liver: demonstraton of drug metabolism and other biochemical functions. Cell Transplantation 1993;2:441-452.

Odenthal M, Neubauer K, Baralle FE, Peters H, Meyer zum Buschenfelde KH, Ramadori G. Rat hepatocytes in primary culture synthesize and secrete cellular fibronectin. Exp Cell Res 1992;203:289-296.

Olsen AK, Hansen KT, Friis C. Pig hepatocytes as an in vitro model to study the regulation of human CYP3A4: prediction of drug-drug interactions with 17 alpha-ethynylestradiol. Chem Biol Interact 1997;107:93-108.

Omura T, Sato R. The carbone monoxide binding pigment of liver microsomes I : Evidence for its hemoprotein nature. J Biol Chem 1964;239:2370-2378.

Oratz M, Schreiber SS, Rothschild MA. Study of albumin synthesis in relation to urea synthesis. Gastroenterology 1973;65:647-650.

Padgham CR, Boyle CC, Wang XJ, Raleigh SM, Wright MC, Paine AJ. Alteration of transcription factor mRNAs during the isolation and culture of rat hepatocytes suggests the activation of a proliferative mode underlies their de-differentiation. Biochem Biophys Res Commun 1993;197:599-605.

Padgham CR, Paine AJ. Altered expression of cytochrome P-450 mRNAs, and potentially of other transcripts encoding key hepatic functions, are triggered during the isolation of rat hepatocytes. Biochem J 1993;289 (Pt 3):621-624.

Painter PC, Cope JY, Smith JL. Appendix. In: Burtis CA and Ashwood EA, eds. Tietz Textbook of Clinical Chemistry. 2nd ed. Philadelphia: Saunders, 1986:2189.

Palade GE. A study of fixation for electron microscope. Journal of Experimental Medicine 1952;95:297.

Paradis K, Langford G, Long Z, Heneine W, Sandstrom P, Switzer WM, et al. Search for cross-species transmission of porcine endogenous retrovirus in patients treated with living pig tissue. Science 1999;285:1236-1241.

Parsons-Wingerter PA, Saltzman WM. Growth versus function in the three-dimensional culture of single and aggregated hepatocytes within collagen gels. Biotechnol Prog 1993;9:600-607.

Patience C, Patton GS, Takeuchi Y, Weiss RA, McClure MO, Rydberg L, et al. No evidence of pig DNA or retroviral infection in patients with short-term extracorporeal connection to pig kidneys. Lancet 1998;352:699-701.

Percy-Robb IW, Finlayson N. Clinical chemistry of liver disease. In: Shearman DJC, Finlayson N, Canilleri MC, and Surgical Editor C, eds. Diseases of the gastrointestinal tract and liver. 3rd ed. Edinburgh: Churchill Livingston, 1997:735-762.

Peshwa MV, Wu FJ, Sharp HL, Cerra FB, Hu WS. Mechanistics of formation and ultrastructural evaluation of hepatocyte spheroids. In Vitro Cell Dev Biol Anim 1996;32:197-203.

Plevris JN, Schina M, Hayes PC. Review article: the management of acute liver failure. Aliment Pharmacol Ther 1998;12:405-418.

Portmann BC. Anatomy of the Normal Liver. In: O'Grady JG, Lake JR, and Howdle PD, eds. Comprehensive Clinical Hepatology. 1 ed. London: Harcourt, 2000:1.1-1.14.

Poullain M-G, Fautrel A, Guyomard C, Chesne C, Grislain L, Guillouzo A. Viability and primary culture of rat hepatocytes after hypothermic preservation: the superiority of the Leibovitz medium over the University of Wisconsin solution for cold storage. HEPATOLOGY 1992;15:97-106.

Rappaport M. The microcirculatory acinar concept of normal and pathological hepatic structure. Beitr Pathol 1976;157:215-243.

Record CO. Neurochemistry of hepatic encephalopathy. GUT 1991;32:1261-1263.

Reid LM, Jefferson DM. Culturing hepatocytes and other differentiated cells. HEPATOLOGY 1984;4:548-559.

Rhodin JAG. Liver and Pancreas. In: Rhodin JAG, ed. Histology: A Text and Atlas. 1 ed. Oxford: Oxford University Press, 1974:580-594.

Riordan SM, Skouteris GG, Williams R. Metabolic activity and clinical efficacy of animal and human hepatocytes in bioartificial support systems for acute liver failure. Int J Artif Organs 1998;21:312-318.

Riva C, Chauvin C, Pison C, Leverve X. Cellular physiology and molecular events in hypoxia-induced apoptosis. Anticancer Res 1998;18:4729-4736.

Rothschild MA, Oratz M, Schreiber SS. Albumin metabolism. Gastroenterology 1973;64:324-337.

Rozga J, Holzman MD, Ro M-S, Griffin DW, Neuzil DF, Giorgio T, Moscioni AD, Demetriou AA. Development of a hybrid bioartificial liver. Annals of Surgery 1993a;217:502-511.

Rozga J, Williams F, Ro M-S, Giorgio T, Backfish G, Moscioni AD, Hakim R, Demetriou AA. Development of a bioartificial liver: Properties and function of a hollow fibre module innoculated with liver cells. HEPATOLOGY 1993b;17:258-265.

Russell WE, Carver RS. the EGF/TGFα family of growth factor and their receptors. In: Strain AJ and Diehl AM, eds. Liver Growth and Repair. 1st ed. London: Chapman & Hall [Thomson Science], 1998:185-218.

Sabatini DD, Bensch K, Barrentl RJ. Cytochemistry and electron microscopy: the preservation of cellular ultrastructure and enzymic activity by aldehyde fixation. Journal of Cell Biology 1963;17:58.

Sack. Pig Abdomen. In: Sack WO, ed. Essentials of Pig Anatomy:Pig Anatomy and Atlas. Ithaca, NY: Veterinary Textbooks, 1982:30-32.

Sajiki T, Iwata H, Paek HJ, Tosha T, Fujita S, Ueda Y, Park YG, Zhu B, Satoh S, Ikai I, Yamaoka Y, Ikada Y. Morphologic studies of hepatocytes entrapped in hollow fibers of a bioartificial liver. ASAIO J 2000;46:49-55.

Sakaguchi K, Koide N, Asano K, Takabatake H, Matsushima H, Takenami T, Ono R, Sasaki S, Mori M, Koide Y. Promotion of spheroid assembly of adult rat hepatocytes by

some factor(s) present in the initial 6-hour conditioned medium of the primary culture. Pathobiology 1991;59:351-356.

Sakai Y, Naruse K, Nagashima I, Muto T, Suzuki M. A new bioartificial liver using porcine hepatocyte spheroids in high- cell-density suspension perfusion culture: in vitro performance in synthesized culture medium and in 100% human plasma. Cell Transplant 1999;8:531-541.

Sakai Y, Naruse K, Nagashima I, Muto T, Suzuki M. Functional stability of porcine hepatocyte spheroids in various culture systems under 100% porcine and human plasma conditions. Artif Organs 1996c;20:56-60.

Sakai Y, Naruse K, Nagashima I, Muto T, Suzuki M. In vitro function of porcine hepatocyte spheroids in 100% human plasma. Cell Transplant 1996b;5:S41-S43.

Sakai Y, Naruse K, Nagashima I, Muto T, Suzuki M. Large-scale preparation and function of porcine hepatocyte spheroids. Int J Artif Organs 1996a;19:294-301.

Sanchez A, Alvarez AM, Pagan R, Roncero C, Vilaro S, Benito M, Fabregat I. Fibronectin regulates morphology, cell organization and gene expression of rat fetal hepatocytes in primary culture. J Hepatol 2000;32:242-250.

Sanders SW, Dukes GE, Jr., Gray P, Tolman KG. Toxicity of heparin in isolated rat hepatocytes. Biochem Pharmacol 1984; 33(14):2223-2226.

Seifter S, Englard S. Energy Metabolism. In: Arias IMBLFNeal, ed. The Liver: Biology and Pathobiology. 3 ed. New York: Raven press Ltd., 1994:323-364.

Selden C, Khalil M, Hodgson HJ. What keeps hepatocytes on the straight and narrow? Maintaining differentiated function in the liver. GUT 1999; 44(4):443-446.

Sharda N, Trenkler T, Santangini H, Pan J, Jauregui HO. Isolation and culture of porcine hepatocytes for artificial liver support. Cell Transplantation 1996;5:107-115.

Shatford RA, Nyberg SL, Meier SJ, White JG, Payne WD, Wei-Shou Hu, Cerra FB. Hepatocyte function in a hollow fibre bioreactor: A potential bioartificial liver. Journal of Surgical Research 1992;53:549-557.

Sheil AG, Sun J, Mears DC, Waring M, Woodman K, Johnston B, Horvat M, Watson J, Koutalistras N, Wang L. Positive biochemical effects of a bioartificial liver support system (BALSS) in a porcine fulminant hepatic failure (FHF) model. Int J Artif Organs 1998;21:43-48.

Sheil AG, Sun J, Mears DC, Waring M, Woodman K, Johnston B, Horvat M, Watson KJ, Koutalistras N, Wang LS. Preclinical trial of a bioartificial liver support system in a porcine fulminant hepatic failure model. Aust N Z J Surg 1996;66:547-552.

Sielaff TD, Hu MY, Amiot B, Rollins MD, Rao S, McGuire B, Bloomer JR, Hu W-S, Cerra FB. Gel-entrapment bioartificial liver therapy in galactosamine hepatitis. Journal of Surgical Research 1995a;59:179-184.

Sielaff TD, Hu MY, Rao S, Groehler K, Olson D, Mann HJ, Remmel RP, Shatford RA, Hu W-S, Cerra FB. A technique for porcine hepatocyte harvest and description of differentiated functions in static culture. Transplantation 1995b;59:1459-1463.

Skett P, Bayliss M. Time for a consistent approach to preparing and culturing hepatocytes? Xenobiotica 1996;26:1-7.

Smith MD, Airdrie I, Cairns D, Courtney JM, Cousins RB, Ekevall E, Grant MH, Gaylor JDS. Characterisation of a hybrid artificial liver bioreactor with integral membrane oxygenation. Artificial Organs 1997b;21:531.

Smith MD, Airdrie I, Cairns D, Cousins RB, Ekevall E, Gaylor JDS. A novel hybrid artificial liver with integral membrane oxygenation: Theory and initial *in vitro* evaluation. Cell Biology and Toxicology 1996;p56.

Smith MD, Cairns D, Veitch R, Cousins RB, Gaylor JDS. Analysis of oxygen transfer in hollow fibre hepatocyte bioreactors. Artificial Organs 1997a;21:531.

Spaulding GF, Jessup JM, Goodwin TJ. Advances in cellular construction. J Cell Biochem 1993;51:249-251.

Stamatoglou SC, Hughes RC. Cell adhesion molecules in liver function and pattern formation. FASEB J 1994;8:420-427.

Stamatoglou SC, Sullivan KH, Johansson S, Bayley PM, Burdett ID, Hughes RC. Localization of two fibronectin-binding glycoproteins in rat liver and primary hepatocytes. Co-distribution in vitro of integrin (alpha 5 beta 1) and non-integrin (AGp110) receptors in cell-substratum adhesion sites. J Cell Sci 1990;97 (Pt 4):595-606.

Stange J, Mitzner S, Strauss M, Fischer U, Lindemann S, Peters M, Holtz M, Drewelow B, Schmidt R. Primary or established liver cells for a bioartificial liver? Comparison of metabolic features. ASAIO 1995;41:M310-M315.

Strain AJ. Isolated hepatocytes: use in experimental and clinical hepatology. [Leading article - Hepatology series]. GUT 1994;34:433-436.

Strain AJ. Ex vivo liver cell morphogenesis: one step nearer to the bioartificial liver? HEPATOLOGY 1999; 29(1):288-290.

Strain AJ, Neuberger JM. A bioartificial liver--state of the art. Science 2002; 295(5557):1005-1009.

Strazzabosco M, Boyer JL. Regulation of intracellular pH the hepatocyte: Mechanisms and physiological implications. J Hepatology 1996; 24(-):631-644.

Sundback CA,.Vacanti JP. Alternatives to liver transplantation: from hepatocyte transplantation to tissue-engineered organs [editorial; comment]. *Gastroenterology* 2000;118:438-42.

Sussman NL, Chong MG, Koussayer T, He D, Shang TA, Whisennand HH, Kelly JH. Reversal of fulminant hepatic failure using an extracorporeal liver assist device. HEPATOLOGY 1992;16:60-65.

Sussman NL, Gislason GT, Conlin CA, Kelly JH. The Hepatix extracorporeal liver assist device: Initial clinical experience. Artif Organs 1994;18;390-396.

te Velde AA, Ladiges NC, Flendrig LM, Chamuleau RA. Functional activity of isolated pig hepatocytes attached to different extracellular matrix substrates. Implication for application of pig hepatocytes in a bioartificial liver. J Hepatol 1995;23:184-192.

Tong JZ, Bernard O, Alvarez F. Long-term culture of rat liver cell spheroids in hormonally defined media. Exp Cell Res 1990;189:87-92.

Tsiaoussis J, Newsome PN, Nelson LJ, Hayes PC, Plevris JN. Which hepatocyte will it be? Hepatocyte choice for bioartificial liver support systems. Liver Transpl 2001;7:2-10.

Turner NA, Pitot HC. Dependence of the induction of cytochrome P-450 by phenobarbital in primary cultures of adult rat hepatocytes on the composition of the culture medium. Biochem Pharmacol 1989;38:2247-2251.

Uchino J, Matsue H, Takahashi M, Nakajima Y, Matsushita M, Hamada T, Hashimura E. A hybrid artificial liver system: Function of cultured monolayer pig hepatocytes in plasma from hepatic failure patients. ASAIO Trans 1991;37:M337-M338.

Uchino J, Matsue H, Takahashi M, Nakajima Y, Matsushita M, Hamada T, Hashimura E. A hybrid artificial liver system: Function of cultured monolayer pig hepatocytes in plasma from hepatic failure patients. ASAIO Trans 1991;37:M337-M338.

Unger JK, Catapano G, Horn NA, Schroers A, Gerlach JC, Rossaint R. Comparative analysis of metabolism of me. Int J Artif Organs 2000;23:104-110.

Unsworth BR, Lelkes PI. Growing tissues in microgravity. Nature Medicine 1998;4:901-907.

van der FA, Sonnenberg A. Function and interactions of integrins. Cell Tissue Res 2001; 305(3):285-298.

Vilei MT, Granato A, Ferraresso C, Neri D, Carraro P, Gerunda G et al. Comparison of pig, human and rat hepatocytes as a source of liver specific metabolic functions in culture systems--implications for use in bioartificial liver devices. Int J Artif Organs 2001; 24(6):392-396.

Voet DVJG. Amino Acid Metabolism. In: Voet DVJG, ed. Biochemistry. 1 ed. New York: John Wiley & Sons Inc., 1995:727-784.

Wang L, Sun J, Li L, Mears D, Horvat M, Sheil AG. Comparison of porcine hepatocytes with human hepatoma (C3A) cells for use in a bioartificial liver support system. Cell Transplant 1998;7:459-468.

Wang L, Sun J, Wang C, Woodman K, Li L, Wu L, Harbour C, Johnston B, Shi L, Horvat M, Koutalistras N, Luo X, Watson J, Sheil AG. Analysis of multivariables during porcine liver digestion to improve hepatocyte yield and viability for use in bioartificial liver support systems. Cell Transplant 2000 May-Jun;9(3):329-36

Waring MA, Sun J, Woodman K, Mears DC, Johnston B, Jung SE, Horvat M, Koutalistras N, Watson KJ, Sheil AG. Metabolic aspects of cultured hepatocytes for use in a bioartificial liver support system. Transplant Proc 1995;27:3572-3573.

Washizu J, Chan C, Berthiaume F, Tompkins RG, Toner M, Yarmush ML. Amino acid supplementation improves cell-specific functions of the rat hepatocytes exposed to human plasma. Tissue Eng 2000;6:497-504.

Watanabe FD, Mullon CJ, Hewitt WR, Arkadopoulos N, Kahaku E, Eguchi S, Khalili T, Arnaout W, Shackleton CR, Rozga J, Solomon B, Demetriou AA. Clinical experience with a bioartificial liver in the treatment of severe liver failure. A phase I clinical trial. Ann Surg 1997;225:484-491.

Watts P, Smith MD, Edwards I, Zammit V, Brown V, Grant MH. The influence of medium composition on the maintenance pf cytochrome P-450, glutathione content and urea synthesis: a comparison of rat and sheep primary hepatocyte cultures. J Hepatology 1995;23:605-612.

Wegner H, Schareck W, Bayer-Helms H, Gebhardt R. Different proliferative potential of rat and pig hepatocytes in pure primary culture and coculture. European Journal of Cell Biology 1992;58:411-417.

Whitington PF. Metabolic liver diseases of childhood. In: Kaplowitz N, ed. Liver and Biliary Diseases. 1 ed. Baltimore: Williams & Wilkins, 1992:456-478.

Williams GM, Bermudez E, Scaramuzzino D. Rat hepatocyte primary cell cultures. III. Improved dissociation and attachment techniques and the enhancement of survival by culture medium. In Vitro 1977;13:809-817.

Winkler K, Henriksen JH, Tygstrup N. Hepatic, renal, and total body galactose elimination in the pig. Am J Physiol 1993;265:G9-14.

Wolf CF, Munkelt BE. Bilirubin conjugation by an artificial liver composed of cultured cells and synthetic capillaries. Trans Am Soc Artif Intern Organs 1975;21:16-27.

Wu FJ, Friend JR, Remmel RP, Cerra FB, Hu WS. Enhanced cytochrome P450 IA1 activity of self-assembled rat hepatocyte spheroids. Cell Transplant 1999;8:233-246.

Yoffe B, Darlington GJ, Soriano HE, Krishnan B, Risin D, Pellis NR, Khaoustov VI. Cultures of human liver cells in simulated microgravity environment. Adv Space Res 1999;24:829-836.

Yuasa C, Tomita Y, Shono M, Ishimura K, Ichihara A. Importance of cell aggregation for expression of liver functions and regeneration demonstrated with primary cultured hepatocytes. Journal of Cellular Physiology 1993;156:522-530.

Yumoto AU, Watanabe S, Hirose M, Kitamura T, Yamaguchi Y, Sato N. Structural and functional features of bile canaliculi in adult rat hepatocyte spheroids. Liver 1996; 16(1):61-66.

Zeidl-Engelhart E, Rabes HM. Variant protein patterns in hepatomas and transformed liver cell lines as determined by high resolution two-dimensional gel electrophoresis (2DE). Carcinogenesis 1992;13:1177-1183.

Full publications

1. **Nelson LJ** *et al* An improved ex vivo method of primary porcine hepatocyte isolation for use in bioartificial liver systems. Eur J Gastroenterol Hepatol. 2000 Aug;12(8):923-30.
2. Tsiaoussis J, Newsome PN, **Nelson LJ** *et al.* Which hepatocyte will it be? Hepatocyte choice for bioartificial liver support systems. Liver Transpl. 2001 Jan;7(1):2-10.
3. Newsome P **Nelson LJ** *et al* Animal models of fulminant hepatic failure: a critical evaluation. Liver Transpl. 2000 Jan;6(1):21-31.
4. Dabos KD, **Nelson LJ** *et al* The rotary cell culture system is a favourable environment and preserves key metabolic functions of cultivated porcine hepatocytes long term. Biochimica Biophysica Acta [In Press].
5. **Nelson L J**, Newsome P N, Howie A F, Srirangalingam S, Beldon I, Walker S W, Hayes P C, Plevris J N. Culture medium formulation modulates morphology and biochemical function of primary porcine hepatocytes *in vitro*. ***[Manuscript in preparation].***

Abstracts published: *[Those presented at national or international conferences]*

1. **Nelson L J**, Newsome P N, Howie A F, Srirangalingam S, Beldon I, Walker S W, Hayes P C, Plevris J N. Primary porcine hepatocytes cultured in serum-free chemically-defined media formulations retain significant liver-specific functional parameters suitable for bioartificial liver devices. Hepatology 2000;32 No.4, Pt 2:400A. ***[AASLD, Dallas 2000, USA]***

2. **Nelson LJ**, Sharma N, Tsiaoussis J, et al. Morphological and functional characteristics of 3D poricine hepatospheroids cultured in a rotary cell culture system (RCCS) compared to conventional 2D static culture. HEPATOLOGY 32: (4) 463A-463A Part 2 OCT 2000

3. **Nelson LJ**, Newsome PN, Mitchell S, et al. Transmission electron microscopy reveals differential effects on ultrastructure of primary porcine hepatocytes cultured in serum-free chemically defined media formulations. HEPATOLOGY 32: (4) 463A-463A Part 2 OCT 2000.

4. Dabos KJ, Parkinson JA, **Nelson LJ**, et al. The rotary cell culture system is a favourable environment that preserves key metabolic functions of cultured porcine hepatocytes long-term. GUT 46: A62-A62 Suppl. 2 APR 2000. ***[Birmingham, UK 2000]***

5. Dabos J N, Plevris J N, Parkinson J A, **Nelson L J**, Hewage C H, Sadler I H, Hayes P C. Effect of cryopreservation on primary porcine hepatocytes metabolism. GUT 1999;44(1): A60 Suppl. 1 APR 1999. ***[Birmingham, UK 2000]***

6. Bradnock T J, **Nelson L J**, Sharp L, Ross J, Hayes P C. Expression of integrin alpha-3, alpha-5 and beta-tubulin is prolonged in porcine hepatocytes cultured in simulated microgravity. HEPATOLOGY 1999;30(4):325A. ***[AASLD, Dallas 1999, USA]***

7. **Nelson LJ**, Plevris JN, Dabos KJ, et al. An improved *ex vivo* method for rapid deployment of high yield high viability primary porcine hepatocytes for *in vitro* culture systems. HEPATOLOGY 28: (4), 623A-623A, Part2, Suppl.S; OCT 1998.

8. **Nelson LJ**, Plevris JN, Dabos KJ, et al. Assessment of porcine hepatic function in different hormonally-defined media. HEPATOLOGY 28: (4) 624A-624A Part 2 Suppl. S OCT 1998

9. Dabos K J, **Nelson L J**, Plevris J N, Dollinger M M, Hewage C, Sadler I H, Hayes P C. Microgravity environment in a rotary cell culture system (RCCS) promotes cell aggregation and maintains differentiation and proliferation of primary porcine hepatocytes. GUT 1998;42 (suppl 1):A26.

10. **Nelson L J**, Plevris J N, Dragomirov B, Howie A F, Schina M, Hayes P C. A comparison between a rotary cell culture system (RCCS) and a hollow fibre haemodialyzer cartridge (HDC) with a standard static culture system (SSCS) using primary porcine hepatocytes. Gut 1997;41(suppl 3):A254. ***[Royal College of Physicians, Edinburgh 1997]***

An improved *ex vivo* method of primary porcine hepatocyte isolation for use in bioartificial liver systems

Leonard J. Nelson[a], Philip N. Newsome[a], A. Forbes Howie[b], Patrick W. F. Hadoke[a], Konstantinos J. Dabos[a], Simon W. Walker[b], Peter C. Hayes[a] and John N. Plevris[a]

Introduction **Primary porcine hepatocytes are commonly used in bioartificial liver devices and for *in vitro* studies of hepatocyte function. Although *in vivo* isolation of porcine hepatocytes can give high yield and viability, such methods are time-consuming and expensive, requiring specialist surgical facilities.**

Aim **To develop a simple, low-cost, high viability, high yield, reproducible *ex vivo* method for obtaining functional porcine hepatocytes for use in bioartificial liver systems.**

Methods **Weanling piglets (12 kg) were killed with pentobarbitone sodium, the infra-hepatic inferior vena cava was clamped and the supra-hepatic inferior vena cava cannulated. The whole liver was retrogradely perfused *in situ* with cold saline and excised, followed by an *ex vivo* open-loop and re-circulating perfusion method (at 37°C) in five steps. The liver was disrupted, sequentially filtered in washing buffer, purified by centrifugation and resuspended in Williams E medium. Viability and cell number were assessed using trypan blue exclusion. The cells were subsequently cultured in serum-free chemically-defined medium and function was assessed.**

Results **The time interval from when the animals were killed to the final cell wash was 105 ± 5 min ($n = 20$). Cell viability was 85 ± 6% with a yield of (2.4 ± 0.5) × 10^{10} from 12 ± 1 kg piglets using 0.03% (w/v) collagenase ($n = 20$). Hepatocytes from all isolations were successfully plated and grown in monolayer culture. In freshly isolated hepatocytes (day 0) total protein content (TP) was 1.2 ± 0.1 mg/10^6 cells ($n = 5$) and 1.2 ± 0.3 mg/10^6 cells ($n = 5$) for day 2 monolayer cultures, corresponding to approximately 9 × 10^6 hepatocytes per dish. The percentage of total LDH released into the medium was 13 ± 4% for day 0 and 8 ± 4% at day 2; conversely, intracellular LDH activities were 87 ± 4% and 92 ± 4% of the total, respectively. The urea synthesis rate was 196 ± 36 nmol/h/mg total protein at day 0 ($n = 5$) and 292 ± 62 nmol/h/mg protein ($n = 9$) at day 2. The total P450 content was 99 ± 11 pmol/mg total protein for fresh cells ($n = 5$) and maintained at 89 ± 35 pmol/mg total protein in day 2 cultures.**

Conclusions **This *ex vivo* method provides a high viability, high yield, cost-effective and rapid technique for isolating functional porcine hepatocytes with high plating efficiency, which compares favourably with results obtained using complex *in vivo* techniques. *Eur J Gastroenterol Hepatol* 12:923–930 © 2000 Lippincott Williams & Wilkins**

European Journal of Gastroenterology & Hepatology 2000, 12:923–930

Keywords: bioartificial liver, function, hepatocytes, isolation, porcine

[a]Liver Cell Biology Laboratory, Dept of Medicine and [b]Dept of Clinical Biochemistry, University of Edinburgh, Edinburgh, UK

Correspondence to Leonard J. Nelson, Liver Cell Biology Laboratory, University of Edinburgh Dept of Medicine, The Royal Infirmary, 1 Lauriston Place, Edinburgh EH3 9YW, UK
Tel: +44 (0)131 536 2264; fax: +44 (0)131 229 2948;
e-mail: L.Nelson@ed.ac.uk

Received 13 June 1999 **Revised** 14 July 1999
Accepted 15 February 2000

Introduction

There is an increasing demand for hepatocytes for use in studies of gene therapy, hepato-toxicology, hepatocyte transplantation and incorporation into bioartificial liver (BAL) devices for treatment of fulminant hepatic failure (FHF) [1,2]. Immortalized human hepatocyte cell lines, such as Hep G2, can theoretically provide an unlimited resource for use in BAL systems [3], but problems associated with possible transfer of tumorigenic proteins to the patient via the BAL, and the dedifferentiated metabolic profile of such cells, have limited the use of cell lines in BAL devices [4–7].

Inadequate yields from rat livers and other small mammals prohibits direct scale-up to clinical BAL application. Hepatocyte viability from standard rat liver perfusions is similar to that obtained from pigs [8] but yields of 10^8 hepatocytes are not sufficient to be incorporated into a scaled-up clinical device for use in humans. Since primary human hepatocytes are not readily available [7] and large yields of functional hepatocytes are required for a clinically effective BAL, primary porcine hepatocytes (PPHs) are the cells of choice for most BAL devices. They have similar physiology and metabolic functions to human hepato-

cytes, differentiated function and can be obtained with good viability and yield [4,5,9–13,29].

Conventional *in vivo* isolation of PPHs involves antegrade perfusion of the portal vein, sometimes in combination with perfusion of the hepatic artery. However, although producing excellent cell viability and yield, this technique requires large perfusion volumes and high collagenase costs with increased perfusion times [12–18]. Moreover, *in vivo* techniques involve anaesthetic maintenance regimens and extensive surgical facilities requiring expert licensed personnel. These requirements may preclude many laboratories from obtaining and utilizing the considerable research potential of porcine hepatocytes.

Ex vivo isolation of PPHs from livers of abattoir origin can attain acceptable viabilities [19,20] but with several disadvantages, including insufficient yield for BAL devices, availability and locality constraints of the abattoir source, high collagenase costs and potential infection problems with abattoir-derived organisms.

The aim of this study was to develop a rapid, low-cost, high viability, high yield and reproducible *ex vivo* method for obtaining functional primary hepatocytes from whole livers of weanling piglets for use in BAL systems.

Fig. 1

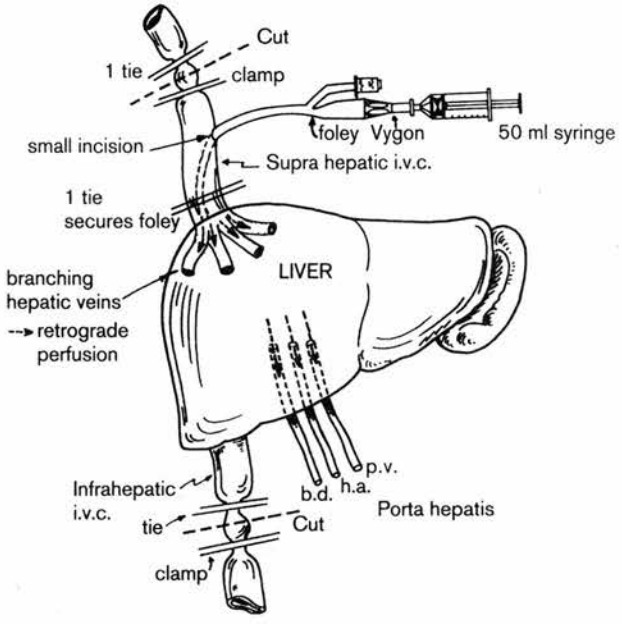

Diagram showing the Foley catheter assembly in the supra-hepatic inferior vena cava (i.v.c.) and positioning of tie clamps for retrograde perfusion of whole piglet liver (not to scale). Perfusate enters the liver through the supra-hepatic i.v.c., while clamping the infra-hepatic i.v.c. shunts the perfusate to exit via the porta hepatis; (h.a.) hepatic artery, (b.d.) bile duct, (p.v.) portal vein. Broken lines with arrow heads depict the direction of retrograde perfusion.

Materials and methods

Animals

The animals were treated in accordance with UK Home Office Guidelines (Scientific Procedures Act, 1986). Following euthanasia, all procedures were performed post-mortem. Piglets (Large White; < 15 kg) were obtained from the Roslin Institute (Roslin, UK) on the day of isolation and maintained on standard feed and water *ad libitum* up to the time when they were killed. Animals were anaesthetized with 30 mg/kg body weight of pentobarbitone sodium via the auricular vein and then killed with an i.v. bolus dose of 150 mg/kg body weight. The abdominal cavity and lower chest were opened with a midline incision exposing the viscera and the supra-hepatic IVC was clamped just below the heart, cannulated with a Foley catheter and secured with a ligature. The infra-hepatic IVC was also clamped (Fig. 1).

Reagents

Type IV collagenase (from *Clostridium histolyticum*), ethylene glycol-bis[β-aminoethyl ether]-*N,N,N',N'*-tetraacetic acid (EGTA), *N*-2-hydroxyethylpiperazine-*N'*-2-ethanesulfonic acid (HEPES), albumin (Fraction V), long epidermal growth factor (L-EGF), Triton X-100 and Williams E (WE) medium were obtained from Sigma (St Louis, MO, USA); and penicillin–streptomycin, gentamicin, fungizone (Amphotericin), L-glutamine, phosphate-buffered saline (PBS, pH 7.4) and Hanks' Balanced Salt Solution (HBSS; Ca and Mg free, pH 7.4), supplied by Gibco (Paisley, UK), were of cell culture grade. Analar grade chemicals for the perfusion solutions and P450 buffer were obtained from Life Technologies (BDH Merck). Other reagents were: dexamethasone (David Bull Labs, England), aprotinin (Trasylol™, Bayer) and porcine insulin (Pork Velosulin™, Novo Nordisk, Denmark).

Perfusion and washing buffers

A stock solution (stock PB) was prepared, consisting of 2 l of perfusion buffer (PB) containing 154 mmol/l NaCl, 5.6 mmol/l KCl, 5 mmol/l glucose, 25 mmol/l $NaHCO_3$ and 20 mmol/l HEPES, made up with distilled H_2O, adjusted to pH 7.4 and sterile filtered.

Solution PB1 consisted of 500 ml stock PB supplemented with 1 mmol/l EGTA, 20 mg dexamethasone and 1.4 mg aprotinin. Solution PB2 contained 500 ml stock PB with 1 mmol/l EGTA. Solution PB3 contained 100 ml PB stock alone. Solution PB4 was 500 ml stock PB with 5 mmol/l $CaCl_2$ and 0.03–0.05% (w/v) Type IV collagenase. Solution PB5 was 200 ml Williams E medium only. Two litres of washing buffer (WB) containing 120 mmol/l NaCl, 6.2 mmol/l KCl, 0.9 mmol/

$CaCl_2$, 10 mmol/l HEPES and 0.2% (w/v) albumin, as made up with distilled H_2O, adjusted to pH 7.4 d sterile filtered [19]. All equipment was sterilized by toclaving.

rfusion steps

he liver was retro-gradely perfused *in situ* with 250 ml BS at 4 °C, via the Foley catheter which was coupled a Vygon™ connector and 50 ml syringe with luer cks (Fig. 1). The whole liver was excised and subse-iently exsanguinated with a further 250 ml of PBS, nfirmed by a clear perfusate emerging from the porta patis (leaving the Foley assembly and infra-hepatic C clamp in place), rinsed with PBS, placed in a lythene bag with 200 ml PBS on ice, and transported the laboratory.

e-warmed perfusion buffers (PB1–4) were saturated th 95% O_2/5% CO_2 and the liver was transferred to a inless-steel bowl and placed in a 37 °C water bath. rfusion was either open loop (non-re-circulated; PB 3, PB5) or closed loop (re-circulated; PB4). The liver s sequentially perfused via the Foley catheter con-cted to a peristaltic pump (Watson–Marlow, USA) at 65 ml/min via silastic tubing thus: PB1 (8 min), 32 (8 min), PB3 (2 min), PB4 (16 min) and PB5 at C (3 min). Perfusate was removed following steps 31 and PB2.

patocyte isolation

llowing perfusion the whole liver was dissected ptically with sharp scissors into pieces of approx. m^3 and the disrupted tissue placed in an orbital aker at moderate speed for 5 min at 37 °C in the sence of PB4 and PB5. The resulting cell suspen-n was transferred to a laminar flow hood and quentially filtered through a stainless-steel collander d meshes of grid sizes 200, then 150 and then 0 μm into collection bottles placed on ice. Collage-se activity was neutralized by adding 500 ml WB at C (containing 0.2% albumin) to the filtered suspen-n to achieve a final volume of 1200 ml. The parench-al cell fraction was allowed to sediment on ice and non-parenchymal fraction aspirated. The hepato-es were then washed using three centrifuge–wash les at 25 *g* (4 °C) for 5 min. Finally, the hepatocyte lets were resuspended in Williams E medium at C. Cell number and viability were initially deter-ned by the trypan blue exclusion test using a ubauer cytometer. Aliquots of fresh cell suspension re analysed for total protein content, total cyto-ome P450 content, lactate dehydrogenase (LDH) ivity and for urea synthesis rate following ammo-m chloride challenge.

patocyte cultures

lls were seeded at a density of 8×10^6 viable cells per 90 mm culture dish (Dow Corning, USA) in 8 ml WE medium at 37 °C. The culture medium consisted of serum-free, chemically-defined Williams E media (WE+) supplemented with 50 ng/ml L-EGF, 10 μg/ml porcine insulin, 1 μmol/l dexamethasone, 2 mmol/l L-glutamine, 50 mg/ml gentamicin, 50 mg/ml penicillin–streptomycin and 2.5 μg/ml fungizone. The culture dishes were shaken gently to aid dispersal of cells for attachment and placed in a humidified incubator under a 95% air:5% CO_2 atmosphere. For the initial cell attachment phase, the incubator was gassed with 30% O_2/5% CO_2 for 2 h [21]. Next day (day 1), the culture dishes were aspirated and fresh WE+ medium was added.

Assays

On the day of isolation (day 0) and on day 2, total protein (TP) content, LDH activity, urea synthesis rate (USR) and total cytochrome P450 content of the cells were measured. The above assays were performed in at least five separate isolations.

Treatment of fresh cell suspension for total protein and LDH measurements

On day 0, 10 ml (5×10^7) fresh cell suspension in WE medium was centrifuged at 25 *g* (4 °C) for 5 min and 1-ml samples of the supernatant taken (F1 fraction) and stored at −70 °C until analysis of extracellular LDH activity. The cell pellet was resuspended in 10 ml 0.25% Triton X-100 in HBSS and frozen to −70 °C, thawed, centrifuged at 200 *g* (4 °C) for 5 min and 1-ml samples of supernatant (F2 fraction) taken as above for analysis of cytosolic LDH and total protein (TP). TP was analysed using the Bradford assay [22,30] modified for a COBAS FARA multi-analyser (Roche Diagnostics); results are expressed as mg protein/10^6 cells. LDH activity was determined in the F1 and F2 fractions by following the rate at which NADH is converted to NAD^+ at λ_{340} nm in the presence of pyruvate (Sigma Diagnostics LDH kit DG1340-K) using the COBAS FARA. The percentage of total extracellular LDH released into the medium is calculated as follows: %LDH = (F1/F1 + F2) × 100 whereas the percentage of total cellular (cytosolic) LDH = 100 − (F1/F1 + F2) × 100. The coefficient of variation of this assay was less than 5%.

Treatment of day 2 monolayer cell cultures for total protein and LDH [23,24] measurements

On day 2, 1-ml samples of medium (F1 fraction) were taken from duplicate dishes and stored at −70 °C until analysis for extracellular LDH. The medium was then aspirated completely, the cell monolayer washed twice with HBSS (4 °C) and 5 ml 0.25% Triton-X 100 in HBSS added. Dishes were freeze–thawed and cells scraped from the dish using a pastette. Residual cells were rinsed from the dish with 5 ml HBSS, added to

the lysed cell homogenate and centrifuged at 200 *g* (4 °C) for 5 min, and 2 × 1-ml samples of supernatant (F2 fraction) were stored at −70 °C until analysis for TP and LDH activity (as above).

Treatment of fresh cell suspension and day 2 monolayer cultures for total cellular P450 levels [27,28]

On day 0, 2×10^7 freshly isolated cells in WE medium were centrifuged at 25 *g* (4 °C) for 5 min and the supernatant was aspirated; 2 ml of ice-cold P450 buffer [28] (containing 0.1 M sodium phosphate buffer pH 7.6 (87 ml 0.2 M Na_2HPO_4 + 13 ml 0.2 M NaH_2PO_4), 0.02% Nonidet P-40, 20% glycerol, 1 mM EGTA and 1 mM dithiothreitol) was added to the cell pellet and the crude suspension homogenized using seven strokes of a Teflon–glass Dounce homogenizer and stored at −70 °C until analysis. Day 2 monolayer cultures were washed twice with HBSS (4 °C) and 2 ml P450 buffer was added; the crude homogenate was collected and treated as above. Following assay of the TP content as above, both fresh and cultured cells were diluted with P450 buffer to 4 mg protein/ml and 1 ml of sample was placed into each of two 1-cm quartz glass sample and reference cuvettes; 1 mg sodium hydrosulphite was added to both cuvettes; 2 min later the sample cuvette was bubbled for 20 s with 99% pure CO gas. The P450 content was assessed by carbon monoxide-difference spectroscopy [27] of the sodium hydrosulphite-reduced samples using a Kontron dual beam spectrophotometer scanning between λ_{400} and λ_{500} nm. The difference in absorbance between λ_{450} and λ_{490} nm was recorded using an extinction coefficient, $E = 91$ mM cm^{-1} to calculate the P450 concentration thus: [P450] = Absorbance/E. Results are expressed as pmol/mg protein (corrected for total cellular protein content). The coefficient of variation for this assay was less than 7%.

Urea synthesis rate

Freshly isolated hepatocytes (day 0) were inoculated at a density of 8×10^7 in 55 ml WE+ medium with 2 mmol/l NH_4Cl, into a rotary cell culture vessel (high aspect ratio vessel; Cellon–Sarl, Luxembourg) and rotated at 10 revolutions per minute for 2 h in a humidified incubator at 37 °C under an atmosphere of 95% air/5% CO_2. The urea synthesis rate (USR) was determined in 0.5 ml samples taken at t = 0 and t = 2 h using a modified colorimetric urea nitrogen kit (Sigma kit 535-B). The difference in absorbances for the chromogenic reaction was measured at each time point at λ_{525} nm in a Pye Unicam spectrophotometer and USR calculated. Cells were collected and analysed for total protein content as above. The coefficient of variation for this assay was less than 5%.

On day 2, duplicate cell culture dishes were washed twice with HBSS (37 °C) and incubated in 8 ml WE+ with 2 mmol/l NH_4Cl for 2 h at 37 °C as above. The USR was determined as above and corrected for total protein content for each culture modality.

Morphology

Morphology was assessed using a Zeiss inverted microscope (Zeiss, Germany) under phase-contrast on both day 0 and day 2 of culture. Photomicrographs recorded hepatocytes in suspension and monolayer culture. Hepatocyte purity was determined by cytospin (× 200 *g*, 5 min) of 5×10^5 freshly isolated cells and staining with haematoxylin + eosin/periodic acid Schiff (PAS), followed by counting cells in three separate fields for three separate isolations.

Statistics

Results are expressed as mean ± standard error. Student's *t*-test was used to compare means of different groups. A P value of <0.05 was taken as significant (two-tailed test of significance).

Results

The time intervals from when the animals were killed to the initial PBS flush and PBS flush to cold storage were 12 ± 4 and 16 ± 6 min respectively. Transport time to the laboratory was 12 ± 3 min, while hepatocyte isolation time (PB1 to final cell wash) was 65 ± 6 min ($n = 20$). Total isolation time (from the time the animals were killed to final cell wash) was 105 ± 5 min ($n = 20$).

The common Large White strain of pig (<15 kg; costing $25 each) was used in the hepatocyte isolation experiments. A reduction of the collagenase concentration ($200 per g) from 0.05 to 0.03% (w/v) produced a five-fold increase in cell yield (Table 1), and significantly reduced the cost of the isolation.

Table 1 **Hepatocyte isolation from whole livers of weanling piglets showing the influence of collagenase concentration on cell viability and yield**

Cell isolation group	Body weight (kg)	Collagenase % (w/v)	% Viability	Yield ($\times 10^{10}$)
1 ($n = 5$)	12.8 ± 1.3	0.05	82 ± 9	0.43 ± 0.22
2 ($n = 5$)	14.1 ± 0.6	0.04	76 ± 6	0.70 ± 0.20
3 ($n = 20$)	12 ± 1	0.03	85 ± 6	2.4 ± 0.5

Results are expressed as mean ± standard error. The number, *n*, of hepatocyte isolations performed is in parentheses.

Cell viability was 85 ± 6% with a yield of (2.4 ± 0.5) × 10^{10} cells from 12 ± 1 kg piglets using 0.03% (w/v) collagenase ($n = 20$; Table 1). Hepatocytes from all isolations were successfully plated and grown in monolayer culture. Microbiological sensitivity tests of cell cultures showed no evidence of infection.

In freshly isolated hepatocytes ($n = 5$) (day 0) total protein content (TP) was 1.2 ± 0.1 mg/10^6 cells and 1.17 ± 0.27 mg/10^6 cells for day 2 monolayer cultures, corresponding to approximately 9 × 10^6 hepatocytes per dish (Table 2). The percentage of total LDH released into the medium was 13 ± 4% for day 0 and 8 ± 4% at day 2; conversely, intracellular LDH activities were 87 ± 4% and 92 ± 4% of total, respectively.

Urea synthesis rate was 196 ± 36 nmol/h/mg of protein at day 0 ($n = 5$) and significantly increased to 292 ± 62 nmol/h/mg of protein ($n = 9$) at day 2 ($P < 0.01$, Table 2).

Total P450 content was 99 ± 11 pmol/mg of protein for fresh cells ($n = 5$) and maintained at 89 ± 35 pmol/ mg of protein in day 2 cultures.

The cell suspension was composed of single cells and small aggregates of between five and 20 cells showing bright cytoplasm, sharply defined borders, commonly with round or polygonal shape and little physical damage (blebbing) under phase contrast microscopy (Fig. 2a). In monolayer culture, hepatocytes showed a flattened morphology with typical trabecular arrangement, sharp refractile borders and dark cytoplasm with a pronounced nucleus often with two or more nucleoli. Bi-nucleated hepatocytes were also present (Fig. 2b). Hepatocyte purity for day 0 cells was 95 ± 3% ($n = 3$) (Fig. 2c). PAS staining revealed a high hepatocyte glycogen content (not shown).

Discussion

Hepatocyte based BAL systems as used in the treatment of liver failure require large numbers of viable hepatocytes that have preserved synthetic, metabolic and detoxifying functions. The most common source for such cells has been porcine liver tissue. Whilst several methods have been described for isolating porcine hepatocytes, there have been technical problems which have restricted their use. These include the requirements of prolonged anaesthesia and surgical expertise with *in vivo* techniques and low yield in current *ex vivo* techniques [1,4,5,11–17,21,31]. Our aim was to establish a simple, time- and cost-effective method to isolate PPHs with a high yield and viability.

Comparative yields and viabilities of differing methods of PPH isolation are outlined in Table 3. With a mean cell viability of 85% and a viable cell yield of 2.4 × 10^{10}corresponding to 10^8 cells/g wet weight liver, our data compare favourably with *in vivo* techniques [1,5,11–16] and outperform yields obtained using comparable *ex vivo* isolation methods by an order of magnitude [19,20]. The theoretical functional liver mass required for a clinically effective BAL is between 20 and 40% of total liver mass corresponding to approximately (20–40) × 10^9 hepatocytes [1,5,15,16,26,32,33], which is obtainable using our *ex vivo* method.

The hepatocytes show good morphology in both suspension and day 2 cultures (Fig. 2a and b) and have high intracellular LDH activity (Table 2), indicating high viability and preservation of membrane integrity [23,24]. Microscopic analysis of fresh cell suspensions shows a tendency of the hepatocytes to aggregate into small clusters of 5–20 cells (Fig. 2a). This may be advantageous for cells expediently seeded into a bioartificial liver device. Indeed, there is evidence that isolated hepatocytes arranged into multi-cellular formation establish cell–cell and cell–matrix contacts which result in improved differentiation and liver-specific function, when compared with single cell culture monolayers [25,37,38]. It is thought that formation of

Table 2 Biochemical parameters of freshly isolated hepatocytes (day 0) and day 2 hepatocyte monolayer cultures ($n = 5$)

Biochemical parameter	Fresh cells (day 0)	Cultured cells (day 2)	*P*-value
% LDH in medium (F1)	13 ± 4	8 ± 4	NS
% LDH retained in cells (F2)	87 ± 4	92 ± 4	NS
Total protein (mg/10^6 cells)	1.2 ± 0.10	1.17 ± 0.27	NS
Urea synthesis rate (nmol h^{-1}/mg protein)	196 ± 36	292 ± 62 ($n = 9$)	< 0.01
Total P450 (pmol/mg protein)	99 ± 11	89 ± 35	NS

Cell viability was assessed as a function of percentage total lactate dehydrogenase (LDH) released into the medium (F1) and retained as cytosolic LDH (F2); total protein (TP) approximates to cell number and urea synthesis rate (USR) to detoxification capacity; total P450 content indicates cellular bio-transformatory potential. Results are means (± standard error) from at least five separate hepatocyte isolations measured in duplicate for each parameter.

Fig. 2

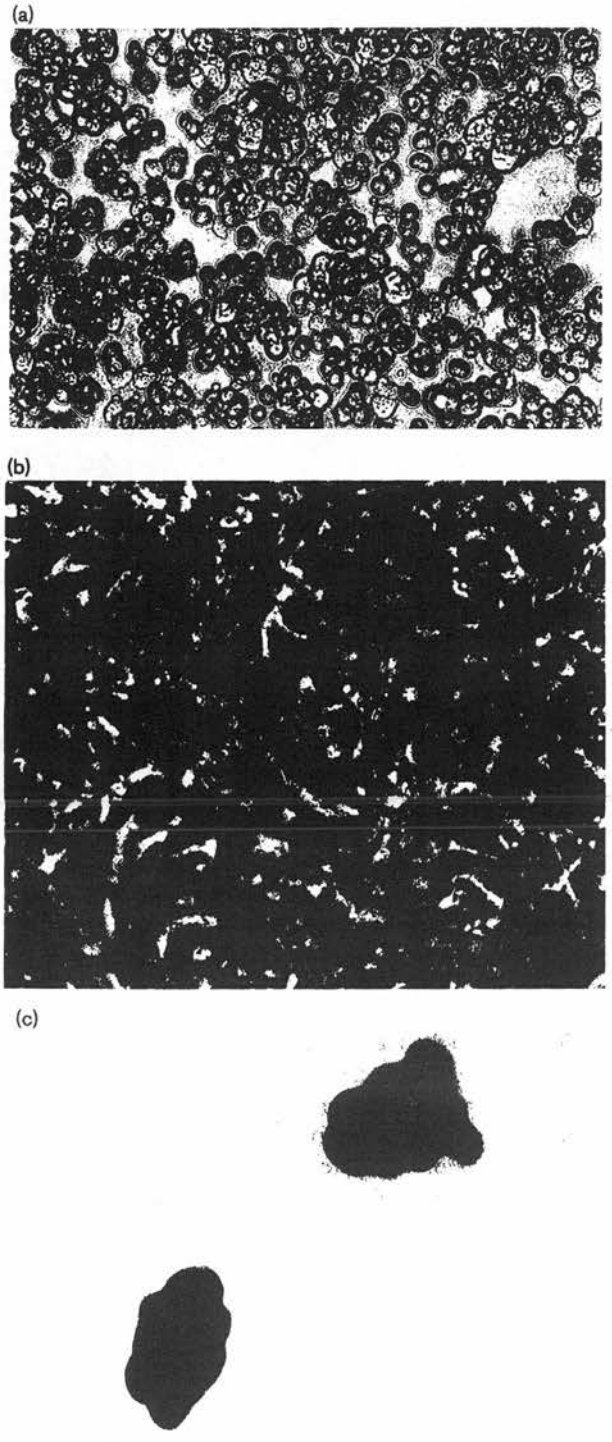

(a) Freshly isolated porcine hepatocyte suspension following the final washing step. Under phase contrast microscopy, hepatocytes show bright cytoplasm, sharply defined borders with round or polygonal shape and little physical damage (blebbing). Original magnification × 200. (b) Hepatocytes in confluent monolayer culture show a flattened morphology with typical trabecular arrangement, sharp refractile borders and dark cytoplasm with pronounced nucleus often with two or more nucleoli. (c) Haematoxylin + eosin staining showing a pure hepatocyte population.

cell aggregates may provide an *in vivo*-like liver micro-architecture promoting maintenance of viability and differentiated functions [5,17,39–41].

For hepatocyte cultures, we used serum-free, chemically-defined medium containing long-EGF and insulin. Porcine hepatocytes cultured this way showed much greater growth potential than rat hepatocytes cultured under the same conditions [37]. Indeed density-dependent inhibition of cell growth was less pronounced with the porcine hepatocytes even after reaching confluency [42,43]. Morphologically, we have observed overgrowth of pig hepatocytes even after reaching confluence on day 2 and up to day 6 (not shown). This may be important in terms of maintaining differentiated, multi-cellular formations in BAL devices as discussed above.

The hepatocytes isolated by our method showed a high level of ammonia detoxification (Table 2). Ammonia is a putative neurotoxin in the development of hepatic encephalopathy and brain oedema in FHF, so NH_3 detoxification is considered essential for an effective BAL device in clinical usage [4,21,35,43]. In addition, we have shown that these cells retain P450 activity and thus maintain a significant metabolic bio-transformation potential (Table 2). Although cellular P450 content is known to decline with culture age in most species, it can be enhanced by modulating culture conditions [28] or by administration of phenobarbital prior to cell isolation. Recently, pig hepatocytes have been shown to outperform both rodent and dog hepatocytes in maintenance of phase 1 and phase 2 activities, whilst high metabolic similarities were found between pig and human hepatocytes [29]. These attributes of pig hepatocytes support their use as the cells of choice for the biological component of BAL devices.

The main factors we have adopted for the successful *ex vivo* isolation of porcine hepatocytes, without compromising yield and viability are as follows:

1. The use of weanling piglets with a mean body weight of 12 kg. Viability and yield have been shown to decline with increasing pig weight (Table 3) [36], possibly as a result of increased fibrous tissue content in the more mature pig liver.
2. Retrograde perfusion via the large supra-hepatic IVC allows easy access to the liver (Fig. 1) and rapid removal of blood following the initial *in situ* flush with PBS.
3. Reduced collagenase concentrations to 0.03% (w/v) thereby minimizing cost (Table 1).
4. Reduced perfusion volumes and time.
5. Use of a simple, cheap liver storage solution (PBS).
6. Perfusion with cooled hepatocyte medium (Williams E) as a cytoprotectant (after the collagenase re-

Table 3 Comparative data of various techniques employed to isolate primary porcine hepatocytes with high yield and viability

Method	Mean yield	Mean viability	Body weight (kg)	% Collagenase (w/v)	References
In vivo	10^{10}–10^{11}	70–95	5–40	0.05–1.0	[1], [5], [13–18], [21], [36]
Ex vivo 1	2×10^9	84	35–115	0.05	[19], [20]
Ex vivo 2	3×10^8	71	60	0.05	unpublished data
Ex vivo 3	$> 2 \times 10^{10}$	85	12	0.03	present method

circulation step) prior to disruption and mechanical handling of the digested liver [14].

7. Avoidance of Percoll™ purification [19,20] to enhance viability (by up to 10%) as it is known to reduce yield by 40–50%.

Furthermore the whole procedure can be performed in approximately 2 h, a benefit which may be of importance in the provision of an on-demand supply of hepatocytes for a BAL device. Such cells are, at present, only available on demand by thawing supplies of cryopreserved cells. This situation is not ideal given the loss of metabolic function seen in cryopreserved hepatocytes [34,35].

In conclusion, our method provides a simple, high viability, high yield, rapid isolation technique which is easy to perform in a standard research laboratory. Cells can be deployed in a variety of *in vitro* liver model systems in less than 2 h, whilst maintaining viability and hepatocyte functionality.

Acknowledgement

This work was supported by a BIOMED 2 grant (R33267) from the European Community.

References

1 Demetriou AA, Rozga J. Artificial liver support. In: *Liver Growth and Repair*, 1st edn. Strain AJ, Diehl AM (editors). London: Chapman & Hall; 1998. pp. 636–640.
2 Guillouzo A, Morel F, Langouet S, Maheo K, Rissel M. Use of hepatocyte cultures for the study of hepatotoxic compounds. *J Hepatology* 1997; **26**:73–80.
3 Sussman NL, Chong MG, Koussayer T, He D, Shang TA, Whisennand HH, *et al.* Reversal of fulminant hepatic failure using an extra-corporeal liver assist device. *Hepatology* 1992; **16**:60–65.
4 Jauregui HO, Gann KL. Mammalian hepatocytes as a foundation for treatment in human liver failure. *J Cell Biochem* 1991; **45**:359–365.
5 Jauregui HO, Naik S, Santangini H, Trenkler DM, Mullon CJP. The use of microcarrier-roller bottle culture for large-scale production of porcine hepatocytes. *Tissue Engineering* 1997; **3**:17–25.
6 Nyberg SL, Remmel RP, Mann HJ, Peshwa MV, Hu W, Cerra FB. Primary hepatocytes outperform Hep G2 cells as the source of biotransformation functions in a bioartificial liver. *Ann Surg* 1994; **220**:59–67.
7 Plevris JN, Schina M, Hayes PC. Review article: the management of acute liver failure. *Aliment Pharmacol Ther* 1998; **12**:405–418.
8 Nyberg SL, Shirabe K, Peshwa MV, Sielaff TD, Crotty PL, Mann HJ, *et al.* Extracorporeal application of a gel-entrapment, bioartificial liver: demonstration of drug metabolism and other biochemical functions. *Cell Transplantation* 1993; **2**:441–452.
9 Gerlach J, Trost T, Ryan CJ, Meisler M, Hole O, Muller C, *et al.* Hybrid liver support system in a short term application on hepatectomized pigs. *Int J Artificial Organs* 1994; **17**:549–553.
10 Gerlach J, Zeimer R, Neuhaus P. Fulminant liver failure: relevance of extracorporeal hybrid liver support systems. *Int J Artificial Organs* 1996; **19**:7–13.
11 Clement B, Desille M, Fremond B, Campion JP, Guguen-Guillouzo C, Bourel M, *et al.* Hepatocytes and cell therapy. *Transfusion Clinique et Biologique* 1998; **5**:80–87.
12 Sheil AGR, Sun J, Mears DC, Waring M, Woodman K, Johnston B, *et al.* Positive biochemical effects of a bioartificial liver support system (BALSS) in a porcine model of fulminant hepatic failure (FHF). *Int J Artificial Organs* 1998; **21**:43–48.
13 Dixit V. Development of a bioartificial liver using isolated hepatocytes. *Artificial Organs* 1994; **18**:371–384.
14 Gerlach JC, Brombacher J, Klöppel K, Schnoy N, Neuhaus P. Comparison of four methods for mass hepatocyte isolation from pig and human livers. *Transplantation* 1994; **57**:1318–1322.
15 Fremond B, Joly A, Desille M, Desjardins JF, Campion JP, Clement B. Cell-based therapy for acute liver failure: the extracorporeal bioartificial liver. *Cell Biol Toxicol* 1996; **12**:325–329.
16 Sielaff TD, Hu MY, Rao S, Groehler K, Olson D, Mann HJ, *et al.* A technique for porcine hepatocyte harvest and description of differentiated functions in static culture. *Transplantation* 1995; **59**:1459–1463.
17 Flendrig LM, la Soe JW, Jorning GGA, Steenbeek A, Karlsen OT, Bovee WMMJ, *et al.* *In vitro* evaluation of a novel bioreactor based on an integral oxygenator and spirally wound nonwoven polyester matrix for hepatocyte culture as small aggregates. *J Hepatology* 1997; **26**:1379–1392.
18 Hu W, Friend JR, Wu FJ, Peshwa MV, Lazar A, Nyberg SL, *et al.* Development of a bioartificial liver employing xenogeneic hepatocytes. *Cytotechnology* 1997; **23**:29–38.
19 Koebe HG, Schildberg FW. Isolation of porcine hepatocytes from slaughterhouse organs. *Int J Artificial Organs* 1996; **19**:53–60.
20 Donini A, Corno S, Lavaroni S, Pellerito R, Bigi L, Pasqualotto A, *et al.* *Ex vivo* preparation of porcine hepatocytes for use in bioartificial hepatic support systems. *Transplantation Proceedings* 1997; **29**:1948–1949.
21 Sharda N, Trenkler T, Santangini H, Pan J, Jauregui HO. Isolation and culture of porcine hepatocytes for artificial liver support. *Cell Transplantation* 1996; **5**:107–115.
22 Bradford MM. A rapid and sensitive method for the quantitation of microgram quantities of protein utilising the principle of protein–dye binding. *Anal Biochem* 1976; **72**:248–254.
23 Marsh DC, Hjelmhaug JA, Vreugdenhil PK, Kerr JA, Rice MJ, Belzer FO, *et al.* Hypothermic preservation of hepatocytes III; effects of re-suspension media on viability after up to 7 days of storage. *Hepatology* 1991; **13**:500–508.
24 Poullain M, Fautrel A, Guyomard C, Chesne C, Grislain L, Guillouzo A. Viability and primary culture of rat hepatocytes after hypothermic preservation; the superiority of the Leibovitz medium over the University of Wisconsin solution for cold storage. *Hepatology* 1992; **15**:97–106.
25 Naruse K, Sakai Y, Nagashima I, Jiang GX, Muto T. Development of a new bioartificial liver module filled with porcine hepatocytes immobilized on non-woven fabric. *Int J Artificial Organs* 1996; **19**:347–352.
26 Jauregui HO, Trenkler DM, Naik S, Santangini H, Press P, Muller TE, *et al.* *In vivo* evaluation of a hollow fibre liver assist device. *Hepatology* 1995; **21**:460–469.
27 Omura T, Sato R. The carbon monoxide binding pigment of liver microsomes I: Evidence for its hemoprotein nature. *J Biol Chem* 1964; **239**:2370–2378.
28 Watts P, Smith MD, Edwards I, Zammit V, Brown V, Grant H. The influence of medium composition on the maintenance of cytochrome P-450, glutathione content and urea synthesis: a comparison of rat and sheep primary hepatocyte cultures. *J Hepatology* 1995; **23**:605–612.
29 Donato MT, Castell JV, Gomez-Lechon MJ. Characterization of drug metabolizing activities in pig hepatocytes for use in bioartificial liver devices:

comparison with other hepatic cellular models. *J Hepatology* 1999; **31**:542–549.

30 Baserga R. Measuring parameters of growth. In: *Cell Growth and Apoptosis*, 1st edn. Studzinski GP (editor). Oxford: Oxford University Press; 1995. pp. 1–4.

31 Joly A, Desjardins JF, Fremond B, Desille M, Campion JP, Malledant Y, *et al.* Survival, proliferation, and functions of porcine hepatocytes encapsulated in coated alginate beads; a step towards a reliable bioartificial liver. *Transplantation* 1997; **63**:795–803.

32 Watanabe FD, Shackleton CR, Cohen SM, Goldman DE, Arnaout WS, Hewitt W, *et al.* Treatment of acetaminophen-induced fulminant hepatic failure with a bioartificial liver. *Transplantation Proceedings* 1997; **29**:487–488.

33 Rozga J, Holzman MD, Ro M-S, Griffin DW, Neuzil DF, Giorgio T, *et al.* Development of a hybrid bioartificial liver. *Ann Surg* 1993; **217**:502–511.

34 Darr TB, Hubel A. Freezing characteristics of isolated pig and human hepatocytes. *Cell Transplantation* 1997; **6**:173–183.

35 Strain AJ. Isolated hepatocytes; use in experimental and clinical hepatology. *Gut* 1994; **34**:433–436.

36 Gerlach J, Brombacher J, Smith M, Neuhaus P. High yield hepatocyte isolation from pig livers for investigation of hybrid liver support systems: influence of collagenase concentration and body weight. *J Surg Res* 1996; **62**:85–89.

37 Wegner H, Schareck W, Bayer-Helms H, Gebhardt R. Different proliferative potential of rat and pig hepatocytes in pure primary culture and co-culture. *Eur J Cell Biol* 1992; **58**:411–417.

38 Loyer P, Cariou S, Glaise D, Bilodeau M, Baffet G, Guguen-Guillouzo C. Growth factor dependence of progression through G_1 and S phases of adult rat hepatocytes *in vitro*; evidence of a mitogen restriction point in mid-late G_1. *J Biol Chem* 1996; **271**:11484–11492.

39 Ben-Ze'ev A, Robinson G, Bucher NLR, Farmer SR. Cell–cell and cell–matrix interactions differentially regulate the expression of hepatic and cytoskeletal genes in primary cultures of rat hepatocytes. *Proc Natl Acad Sci USA* 1988; **85**:2161–2165.

40 Lazar A, Peshwa MV, Wu FJ, Chi C, Cerra FB, Hu W. Formation of porcine hepatocyte spheroids for use in a bioartificial liver. *Cell Transplantation* 1995; **4**:259–268.

41 Gerlach J, Encke J, Hole O, Courtney JM, Neuhaus P. Hepatocyte culture between three dimensional arranged biomatrix-coated independent artificial capillary systems and sinusoidal endothelial cell co-culture compartments. *Int J Artificial Organs* 1994; **17**:306.

42 Yuasa C, Tomita Y, Shono M, Ishimura K, Ichihara A. Importance of cell aggregation for expression of liver functions and regeneration demonstrated with primary cultured hepatocytes. *J Cellular Physiol* 1993; **156**:522–530.

43 Hughes RD, Williams R. Assessment of bioartificial liver support in acute liver failure. *Int J Artificial Organs* 1996; **19**:3–6.

Which Hepatocyte Will It Be? Hepatocyte Choice for Bioartificial Liver Support Systems

John Tsiaoussis, Philip Noel Newsome, Leonard Joseph Nelson, Peter Clive Hayes, and John Nicholas Plevris

Liver failure, notwithstanding advances in medical management, remains a cause of considerable morbidity and mortality in the developed world. Although bioartificial liver (BAL) support systems offer the potential of significant therapeutic benefit for such patients, many issues relating to their use are still to be resolved. In this review, these issues are examined in terms of the functions required, the cells of choice in such a system, and the most appropriate environment to optimize the function of such cells. The major functions identified to date for a BAL are ammonia detoxification and biotransformation of toxic compounds, although this somewhat belies the complexity of the functions required. Two practical choices for cell type within such a system are xenogenic hepatocytes and immortalized human hepatocyte lines. Both these choices have drawbacks, such as the transmission of zoonoses and malignant infiltration, respectively. Finally, improvements in culture conditions, such as supplemented media, biodegradable scaffolds, and coculture, offer the possibility of prolonging the differentiated function of hepatocytes in a BAL. (*Liver Transpl 2001;7:2-10.*)

The development of nonbiological systems to support critically ill patients with acute liver failure (ALF) that incorporate plasmapheresis,[1] charcoal hemoperfusion,[2] and ultrafiltration techniques[3] has not had a significant impact on survival. Consequently, hepatocyte-based biological systems have attracted intense interest worldwide but have also generated most of the controversy. Uncertainty exists about the most suitable biological component and the risk for zoonoses and immune rejection in the host. In addition, the optimization of culture conditions and thus metabolic function of the biological component have not been systematically studied, although continuing improvements in these areas have rendered this therapeutic avenue in ALF more promising. To compound matters, the question of which aspects of hepatocyte metabolism in an artificial liver are required to sustain life and promote recovery remains largely unanswered, further limiting development. In this review, the biological substrate of such systems is critically examined and insights are provided into the ideal system.

From the Department of Internal Medicine, Liver Unit, Royal Infirmary of Edinburgh, Edinburgh, Scotland.

Address reprint requests to Philip Noel Newsome, MD, MRCP, Department of Internal Medicine, Royal Infirmary of Edinburgh, Edinburgh, Scotland EH3 9YW. Telephone: 0044-131-536-2245; FAX: 0044-131-229-2948; E-mail: p.newsome@ed.ac.uk

1527-6465/01/0701-0013$3.00/0

doi:10.1053/jlts.2001.20845

Essential Metabolic Functions

A major cause of death in ALF is hepatic coma, but because of controversy about its exact cause, it is unclear which specific hepatocyte functions are required in a bioartificial liver (BAL) system. The theories of the pathogenesis of hepatic coma in ALF are not discussed here except to list those most widely accepted.[4] These include ammonia accumulation (with depletion of brain glutamate),[5,6] endogenous benzodiazepine accumulation (leading to neural inhibition through γ-aminobutyric acid type A–receptor activation),[7,8] and generation of false neurotransmitters from gut-derived amines (again leading to neural inhibition).[9]

Thus, removal of nitrogenous waste and the ability to perform a number of biotransformatory functions with regard to ammonia metabolism can be considered important functions of a BAL. Removal of nitrogenous waste can occur through 3 main pathways: (1) incorporation of ammonia into the urea cycle, (2) conversion of ammonia into glutamine, and (3) conversion of ammonia into glutamate. Consequently, urea cycle enzyme activities must be well maintained in a BAL system to facilitate the elimination of ammonia.[10] The biotransforming properties of hepatocytes can be divided into phase I (oxidation by P-450 enzymes) and phase II (conjugation with glutathione, glucuronidation, and sulfation) activities. Appropriate laboratory tests (Table 1) can be used for the relevant enzymes to ensure that their levels are suitably maintained.[10]

Other functions, such as gluconeogenesis, albumin synthesis, and coagulation factor synthesis, are valuable, but not of paramount importance because most can be administered exogenously without the need for a BAL.

Table 1. BAL Quality Control

	Test	Required Criteria
Cellular appearance and number	Cell number	$>15 \times 10^9$/BAL
	Viability (Trypan blue elimination)	>75% viable*
Infection	Sterility (bacterial)	<5 CFU/mL
	Sterility (fungal)	<5 CFU/mL
	Mycoplasma	Negative
	Endotoxin limulus assay	Negative
Metabolic function	Galactose elimination	>30 μg/h/million cells†
	Urea synthesis	>5 μg/h/million cells† (or 0.083 μmol)
	Lidocaine metabolism	>50 μg/h/million cells†

NOTE. Suggested checks to be performed before using a BAL in a clinical treatment.
* This figure reflects the realistic cellular viabilities that can be obtained after hepatocyte isolation.[86]
† These values represent the metabolic function that can be obtained from a BAL system that contains healthy hepatocytes.[87,88] Due to uncertainty about the desired function of BAL systems, it is not clear whether these values are sufficient or even required.

Choice of Cells

Human Hepatocytes

Although on first inspection, human hepatocytes may appear to be the natural cellular choice for an artificial liver system, further scrutiny shows many difficulties. One of their major drawbacks, their relative scarcity, is further compounded by the competing demands of whole-organ liver transplantation and, to a lesser extent, hepatocyte transplantation. In addition, the lack of a regular supply of human tissue makes it difficult to plan for its appropriate clinical use. Attempts to overcome this difficulty by maintaining long-term cultures of hepatocytes have been hindered by both cost and the rapid loss of differentiated metabolic function.[11,12] As with whole-organ transplantation, immune rejection is also a problem, although hyperacute rejection, which often applies in xenotransplantation, is generally not seen.[13] Finally, the use of human hepatocytes isolated from liver tissue from partial hepatectomy and/or hepatocellular carcinoma surgery has raised concerns about the transmission of malignancy or infection to the patient. Consequently, human hepatocytes have not been widely used in artificial livers, and attention has turned to immortalized human hepatocyte lines or xenogenic hepatocytes.

Human Hepatocyte Cell Lines

Immortalized human hepatocyte cell lines can provide an unlimited resource for BAL systems,[14,15] although concerns exist about their metabolic function and the transmission of immortalized cells or tumorigenic products to the patient's circulation.[16] This concern is heightened by the knowledge that patients with liver failure are immunocompromised for long periods of their lifetime, either acutely or posttransplantation, thus decreasing their ability to remove such malignant cells from the circulation. However, this still remains a theoretical concern because no evidence exists of transmission in trials performed to date.[17]

The 2 basic types of human hepatocyte lines are those derived from human tumors[18,19] and those created by immortalizing human hepatocytes.[20-22]

Tumor-derived line. One of the most developed BAL systems currently under trial, the ELAD system[23,24] (VITAGEN Inc, La Jolla, CA), uses the C3A cell line, a clonal derivative of the hepatoblastoma-based HepG2 cell line, which is reported to have a more highly differentiated hepatic phenotype than the HepG2 line.[25] Metabolic studies of the C3A line have shown greater levels of such synthetic function as albumin and alpha-fetoprotein production, as well as nitrogen-metabolizing activity similar to that of perfused rat livers.[26] However, compared with primary porcine hepatocytes, the C3A cell line has lower levels of P-450 IA1 activity, ammonia removal, and amino-acid metabolism.[19] Increasing evidence shows that continuous human liver cell lines derived from liver cancers may not conserve all aspects of drug metabolism found in normal cells, further limiting their efficacy.[27]

Immortalized cell lines. Human hepatocyte lines derived from normal liver and immortalized by coculture with rat epithelial cells, such as HH01, HH02, HH09, and HH25[21] cells, show viability in continuous culture for several years and express a spectrum of differentiated hepatocyte functions. This admixture of nonhuman

and human cells may prove to be a disadvantage in subsequent clinical application.

Attempts to develop new transfected cell lines with decreased malignant potential include the OUMS-29[20] and HepZ.[28] The OUMS-29 is derived from human fetal hepatocytes transfected with the pSV3neo plasmid and contains the genes encoding simian virus 40 large T antigen (SV40T) and neomycin phosphotransferase. The OUMS-29 cells express genes of many liver-specific functions, including albumin, asialoglycoprotein receptor, glutamine synthetase, glutathione-*S*-transferase-*p*, and human blood coagulation factor X.[20] Injected into 90% hepatectomy rats, these cells resulted in significant clinical improvement in terms of blood ammonia level, hepatic encephalopathy grade, and survival.[20] Furthermore, preliminary data with the OUMS-29 line did not show tumorigenic features when transplanted into athymic nude mice[29] compared with the HepG2 line, which caused multiple tumor nodules within 2 weeks of infusion into similar mice.[15] Although reassuring that OUMS-29 cells may not represent as important a malignant risk as HepG2 cells, there still remains concern about the use of irreversibly immortalized cells in immunosuppressed patients.

The recent development of a reversibly immortalized cell line, NKNT-3,[22] has been heralded as a breakthrough for hepatocyte transplantation. The NKNT-3 line is produced by the retroviral transfection of normal primary human hepatocytes with SV40T flanked by LoxP recombination targets. In addition, there is concurrent expression of a protein fusion (Hygro-TK) that confers cellular sensitivity to ganciclovir. The NKNT-3 line can be successfully remortalized by transduction with a replication-deficient recombinant adenovirus that expresses the Cre recombinase, which permanently excises both the SV40T and Hygro-TK genes by acting at the LoxP recombination targets. Although the immortalized (nonreverted NKNT-3) line maintains expression of key genes of liver metabolism (glutamine synthetase, hepatic bilirubin-uridine diphosphate-glucoronyltransferase, and glutathione-*S*-transferase-*p*), the levels of expression increase dramatically after excision of the SV40T gene, and albumin and human blood coagulation factor X messenger RNA were only detected after the SV40T gene had been removed. Nevertheless, both forms of NKNT-3 produced significant biochemical and clinical improvement in 90% hepatectomy rats when infused into the spleen.[22] To further mitigate against the transmission of malignancy, this line remains sensitive to ganciclovir, which, together with the host immune response, should remove such cells from the patient's circulation when needed. Although the investigators present data that describe the successful removal of such cells from the rat model, more work is required to confirm that this line can be used for hepatocyte transplantation. Nonetheless, for the purposes of BAL systems, this line offers the possibility of treating and then removing cells that have escaped from the BAL into the patient's circulation.

Xenogenic Hepatocytes

Because of the previously mentioned concerns about metabolic function and/or malignant risk with immortalized cell lines, xenogenic hepatocytes have been widely used in BAL systems.[30] Although rat hepatocytes are metabolically active, the relatively small size of the animal has made it difficult to obtain a sufficiently high yield to load a BAL system for use in human liver failure. Conversely, porcine hepatocytes have remarkably similar physiological characteristics and metabolic functions to human hepatocytes, with high expression of mixed-function oxidases (cytochrome P-450 system) that are essential for detoxification of chemicals found in liver failure,[31] as well as relative size compatibility with humans.[32,33] Although considerable expertise has been gained in the use of xenogenic hepatocyte-driven BALs, as with immortalized hepatocyte lines, serious concerns exist about their use. Xenogenic cells have the following 3 main recognized disadvantages.

Immunogenicity. Preformed immunoglobulin M (IgM) antibodies against porcine hepatocytes have been reported in almost 7% of the healthy population,[34] leading to hyperacute rejection in xenogenic organ transplantation. Consequently, immunoisolation using semipermeable membranes has been incorporated into many systems to prevent extensive porcine hepatocyte necrosis and the consequent flux of necroinflammatory chemicals back into the patient. The membranes also might protect against possible immunologic compounds escaping from xenogenic tissue into the patient's circulation. However, despite their use, elevated titers of antipig IgM and IgG xenoantibodies (primarily against A-Gal epitope on pig hepatocytes) have been found after 2 or more treatments with porcine-based BAL systems, indicating that host exposure to porcine antigens still occurs.[35,36] The promising development of animals with knockouts for Gal-epitope may mitigate the problem of hyperacute rejection, although this has yet to be achieved in the pig and may cause further problems with porcine endogenous retroviral (PERV) transmission, described next. To date, no adverse immunologic reactions have been reported with repeated use of these systems over a prolonged period of several days, possibly because patients with ALF are relatively

immunosuppressed and are unable to mount significant immune responses.[37]

Zoonoses. Standard health-screening protocols are available to ensure that animals are free of various pathogens. Of greater importance is the issue of such ubiquitous organisms as PERVs,[38,39] which at present are not removable from such hepatocytes. Although there is no evidence to date to indicate a pathogenic role of PERVs in pigs or other species, much concern remains about cross-species transmission of these viruses. Consequently, experiments have focused on the possible transmission of PERVs to human cells and the study of the subsequent events. Although PERV particles can be transmitted from porcine to human cells when cocultured in vitro,[17,39] only recently has evidence come to light that indicates the transmitted virus has the potential to replicate in its new host. Coculture of the human kidney epithelial cell (U293) with either PK-15 or pig islets showed that the U293 line was positive for PERV *pol* DNA after 18 and 28 days of culture.[40] However, in the context of BAL treatment, coculture is not the most suitable comparison, and Nyberg et al[41] showed that exposure of human HEK 293 cells with fulminant serum incubated with porcine hepatocytes does not lead to PERV infection. Although it is known that some cells escape from a BAL and enter the patient's circulation, inclusion of a 150-nm mesh bioreactor membrane reduces PERV infectivity by 100,000-fold.[42]

Of greater concern is the finding that pancreatic islet transplantation into severe combined immunodeficiency (SCID) mice causes widespread infection with PERV, showing for the first time evidence of in vivo transmission.[40] Although a large study of human recipients of porcine tissue and/or BAL treatments did not show evidence of transmission, this may reflect several important differences between the 2 reports. Although some of the human recipients were immunosuppressed, it is unlikely they were as suppressed as SCID mice. In addition, mice do not have natural immunity against galactose α(1-3)-galactose terminal sugars.[43] Significantly, the majority of immunosuppressed human recipients did not show long-term survival and function of their grafts, raising concerns about long-term safety of xenografts.[40] Consequently, many countries have implemented xenotransplantation moratoria before permitting the further use of xenogenic tissue. Ongoing studies are in place to develop PERV-free pigs,[44] although the possibility of transmitting as yet unknown viruses will always remain a potential concern.

Biocompatibility. Although porcine hepatocytes may detoxify human toxins, there are concerns that products from different species, such as coagulation factors or albumin, may not exert a similar biological response in humans,[13] although porcine tissues, such as pancreas transplants and/or insulin, have been used to good effect in human diseases.

Critical Cell Mass

Animal studies have suggested between 20% and 40% of host liver mass is required for effective support (Table 1), which would correspond to approximately 150 to 300 g of liver tissue for a 70-kg patient (3 to 6 $\times$ 10^{10} hepatocytes).[45] Animal models have shown that as little as 2% of normal liver mass reduced the levels of transforming growth factor-β1, an inhibitor of hepatic regeneration.[46] Of the 3 BAL support systems for which clinical data are available (Table 2), significant differences exist in the number of cells used to load the bioreactor (6×10^9 to 1×10^{11}), which corresponds to 2% to 33% of normal liver mass.[47] Specifically, the BAL device, HepatAssist, contains approximately 6×10^9 cryopreserved porcine hepatocytes (30 g; 2% of normal hepatocyte mass),[48] whereas the ELAD contains 4×10^{10} transformed C3A cells (200 g; 15% of normal hepatocyte mass).[49] A more complex device, Gerlach's device contains 1×10^{11} porcine hepatocytes

Table 2. Critical Cell Mass of BAL Systems

BAL System	Cell Type	No. of Cells	Weight (g)	Liver Mass (%)	Phase of Development
HepatAssist[89] (Circe Biomedical Inc, Lexington, MA)	Porcine	6×10^9	30	2	Clinical
ELAD[49]	C3A line	4×10^{10}	200	15	Clinical
Gerlach[90] (University of Berlin, Berlin, Germany)	Porcine	1×10^{11}	500	33	Clinical
Bader[51]	Porcine	1×10^{10}	50	3.3	Experimental

NOTE. The number of hepatocytes in the BAL systems varies significantly from as low as 2% to 33%. The percentage of liver mass is derived from a value of a human liver of 1.5 kg.

(500 g; 33% of normal hepatocyte mass).[50] Other devices at a developmental stage contain similar numbers of hepatocytes; for example, Bader's bioreactor contains 1×10^{10} porcine hepatocytes.[51]

Modulation of Function

With a view to augmenting the function of the hepatocyte load in BALs, other approaches to enhance the culture environment have been undertaken. The main strategies used to enhance performance in vitro are (1) media supplementation, (2) use of biomatrices, (3) preferential cell isolation, (4) novel culture modalities, and (5) cocultures.

Media Supplementation

Culture media containing nonautologous serum introduce unknown factors, such as selective cytoinhibitors, bacterial endotoxins, and lipids, that may contribute to the observed cytostatic and cytotoxic effects of serum.[52] Serum has been shown to inhibit the expression of differentiated liver-specific functions and be selective for the growth of nonparenchymal cells.[53] For these reasons, the use of serum-free chemically defined media with potent mitogenic supplements is preferred. Such supplements include long-epidermal growth factor, a synthetic recombinant analogue of endogenous epidermal growth factor that has stimulatory effects on DNA synthesis, cell growth, amino acid transport, and protein synthesis.[54] Insulin has been shown to enhance initial cell attachment and may be important for seeding cells onto tissue culture plastic or BAL hollow-fiber membranes. Both hormones contribute to the preservation of hepatocyte morphological characteristics, survival, and such tissue-specific functions as albumin synthesis. This is also true of dexamethasone, which stimulates protein synthesis and suppresses fibroblast growth.[53]

Biomatrices

Engelbreth-Holm-Sarcoma gel (Matrigel; Becton Dickinson & Co, Franklin Lakes, NJ)[55-58] and collagen gel sandwiches[59] have been shown to maintain differentiated function and improve cellular polarity of rat hepatocytes.[60] Matrigel, unlike collagen gels acquired from nontumor sources, is a laminin-rich protein obtained from Engelbreth-Holm-Sarcoma cells. Thus, a theoretical concern exists about the transmission of tumor particles from Matrigel biomatrices, although this has not been shown to date.[58] Uniquely, porcine hepatocytes appear able to maintain these functions without the aid of exogenous substrates.[61,62] For these reasons, the use of biomatrices to enhance liver-specific functions in BAL devices remains controversial.

Maintenance and enhancement of the biological component of BAL systems without resort to a biomatrix environment is theoretically achievable. The peroxisome proliferators, methylclofenapate and nafenopin, as well as phenobarbital barbiturate, can induce DNA synthesis and provide a survival signal for cultured rat hepatocytes by suppressing apoptotic cell death.[63] However, such pharmacological interventions are largely experimental at present.

Preferential Cell Isolation

Preferential zonal isolation of hepatocytes using the digitonin/collagenase perfusion technique can be used to isolate periportal or perivenous hepatocytes that have differing metabolic profiles. Both urea synthesis and glutathione replenishment capacities are enhanced in the periportal (acinar zone 1) region, whereas P-450 activity is greater in the perivenous areas. Thus, the potential exists to load a BAL selectively with zone 3 hepatocytes to augment P-450 function and improve biotransformation, although there is no evidence to suggest that such cells can function optimally in isolation.[64-66]

Novel Culture Modalities

Formation of hepatospheroids using a rotary cell culture system (inducing a simulated microgravity environment), roller bottles, or nonadherent positively charged surfaces may facilitate the development of cell-cell cell-matrix interactions, thus promoting cellular polarity and enhanced differentiated function. Again, such modalities are at an experimental stage, and their applicability remains to be confirmed.[67-72]

Hepatocyte Coculture With Nonparenchymal Cells

The number of required hepatocytes may be reduced if their function can be enhanced by coculturing hepatocytes with such nonparenchymal cells as fibroblasts. The murine embryonic fibroblast cell line, 3T3-J2, can induce a 3- to 15-fold increase in albumin secretion per rat hepatocyte,[68] thus decreasing the need for a large number of hepatocytes. The optimum ratio of nonparenchymal to parenchymal cells in cocultures has been studied, and it appears that a ratio near 6:1 maximizes the effectiveness of nonparenchymal cells.[68] BALs incorporating nonparenchymal cells with a biodegradable polymer scaffold obtained impressive results in terms of both survival and function of hepatocytes.[73]

The possibility of further antigenicity from the coculture cells should not be underestimated[74] and needs to be investigated further. When the HHY4[75] cell line was encapsulated in 1% alginate, cytochrome P-450 1A1 activity increased 3- to 4-fold compared with monolayer cultures, and urea production was detected for the first time.[76] Currently, this approach remains very promising, and further studies will determine their future role in BALs.

Availability

The ready availability of hepatocytes to load a bioreactor at short notice has been a major issue in the development of BAL support systems for the treatment of patients with ALF. Different approaches to this problem have been adopted.

Ongoing Hepatocyte Culture Within the Bioreactor

This has the disadvantage of high costs and a limited shelf life because of rapid deterioration of the biological function of the hepatocytes. Although groups[77] have claimed that improved bioreactor design may be important in maintaining viability and metabolic activity, even with these improved bioreactor configurations, cells are unlikely to maintain significant function beyond 3 weeks.[11] Another approach is to identify the optimum medium for culturing hepatocytes before and during seeding of a BAL, an area that requires further work, although it is unclear which metabolic function is of most value. Regular microbial screening could be incorporated into such a system.

Fresh Isolation of Hepatocytes From Readily Available Sources and Loading the Bioreactor as Required

This approach requires a team to be on standby on a 24-hour basis to be able to prepare a bioreactor but has the advantage of using fresh cells near the peak of their metabolic activity. Given that patients often present with ALF before requiring treatment, there may be adequate time for bedding hepatocytes into a BAL to ensure optimal function.

Cryopreservation of Hepatocytes

This has been explored as a means of maintaining their ready availability and is an approach adopted by the HepatAssist system, currently under clinical evaluation (phase III multicenter trial).[48] This system uses porcine hepatocytes that are attached to dextran microcarriers and cryopreserved. In general, the viability of primary porcine hepatocytes after cryopreservation is decreased by 10% to 25%,[78,79] although Percoll (Pharmacia, Uppsala, Sweden) separation can remove these dead cells before their use in BAL systems. There is concern that simple measures of viability may be inadequate; however, in testing, the true health and function of cryopreserved hepatocytes and, consequently, cell attachment to plastic has been suggested as a more accurate marker of such functions. Only 50% of cells retain their ability to attach on plastic after thawing,[80] confirming that the metabolic function and/or health of these hepatocytes deteriorates at a greater extent than suspected by simple measurement of viability. Work has therefore focused on ways of improving the functionality of cryopreserved cells by changing the cryopreservative solutions and the freezing protocols. Dimethyl sulfoxide reduces ice formation and osmotic changes during freezing by interacting electrostatically with phospholipid membranes[81] and is considered the most suitable cryoprotectant.[82] Several cryopreservation protocols have been used, such as slow-freezing protocols, quick-freezing protocols, and stepwise protocols.[83,84] To date, computer-controlled stepwise freezing with rapid thawing has given the most satisfactory results.[82] A high cellular energy status has been recognized as an important factor in maintaining sufficient metabolic function during cryopreservation; therefore, isolated hepatocytes have been incubated in a well-oxygenated buffer containing 15 mmol/L of glucose for 30 minutes at 37°C before freezing process, with improvement in postthawing results.[85]

Although cryopreservation has much to offer for the use of primary hepatocyte-based BAL therapy, further advances are required to optimize the function of the cryopreserved hepatocytes.

Conclusion

Extensive progress has been made in the field of hepatocyte biology for BAL systems over the past 10 years, but many questions remain. Although such functions as ammonia detoxification and compound biotransformation are important for BAL efficacy, additional functions required for the treatment of liver failure remain unclear. This is primarily because of uncertainty about the pathological processes underlying ALF, which must be explored further if BAL advances are to be made. When choosing the hepatocyte for use in a BAL system, it is important to be aware that a balance of risks exists. The practical choices are xenogenic (porcine) hepatocytes or transformed human hepatocyte lines. Although

porcine hepatocytes confer greater biological functions, there is the unknown risk for PERV transmission. However, transformed human lines offer slightly poorer biological function, with the risk for malignant infiltration. Increasingly, a body of literature suggests that transformed lines are becoming safer in this respect, and their biological function appears to improve with each successive development. Consequently, both cell types have been used in human trials with no major ill effects to date. To complicate decision making further, the possibility of using human hepatocytes derived from human adult and/or embryonic stem cells has been added to the list of possibilities. Of equal importance will be developments in the housing and culture of cells within the reactor to maintain these cells at their optimal function. When considering the use of BALs, whichever cell type they contain, it is imperative that their suggested risks are balanced with the urgency of the clinical condition. A patient with ALF who requires treatment with a BAL is seriously ill and still has a depressingly high mortality rate without liver transplantation.

References

1. Kondrup J, Almdal T, Vilstrup H, Tygstrup N. High volume plasma exchange in fulminant hepatic failure. Int J Artif Organs 1992;15:669-676.
2. Ash SR. Hemodiabsorption in the treatment of acute hepatic failure. ASAIO J 1994;40:80-82.
3. Matsubara S, Okabe K, Ouchi K, Miyazaki Y, Yajima Y, Suzuki H, et al. Continuous removal of middle molecules by hemofiltration in patients with acute liver failure. Crit Care Med 1990; 18:1331-1338.
4. Blei AT. Brain edema and portasystemic encephalopathy. Liver Transpl 2000;6:S14-S20.
5. Clemmesen JO, Larsen FS, Kondrup J, Hansen BA, Ott P. Cerebral herniation in patients with acute liver failure is correlated with arterial ammonia concentration. Hepatology 1999; 29:648-653.
6. Record CO. Neurochemistry of hepatic encephalopathy. Gut 1991;32:1261-1263.
7. Albrecht J, Jones EA. Hepatic encephalopathy: Molecular mechanisms underlying the clinical syndrome. J Neurol Sci 1999;170: 138-146.
8. Jones EA, Schafer DF. Hepatic encephalopathy: A neurochemical disorder. Prog Liver Dis 1986;8:525-540.
9. Fischer JE, Baldessarini RJ. False neurotransmitters and hepatic failure. Lancet 1971;2:75-80.
10. Hawker F. The liver—Anatomy, physiology and biochemistry. In: Hawker F (ed). The liver. London: Saunders, 1993:1-43.
11. Guzelian PS, Bissell DM, Meyer UA. Drug metabolism in adult rat hepatocytes in primary monolayer culture. Gastroenterology 1977;72:1232-1239.
12. Sherratt AJ, Damani LA. Activities of cytosolic and microsomal drug oxidases of rat hepatocytes in primary culture. Drug Metab Dispos 1989;17:20-25.
13. Candinas D, Adams DH. Xenotransplantation: Postponed by a millennium? Q J Med 2000;93:63-66.
14. Sussman NL, Kelly JH. Artificial liver: A forthcoming attraction. Hepatology 1993;17:1163-1164.
15. Sussman NL, Kelly JH. Improved liver function following treatment with an extracorporeal liver assist device. Artif Organs 1993;17:27-30.
16. Zeindl-Eberhart E, Rabes HM. Variant protein patterns in hepatomas and transformed liver cell lines as determined by high resolution two-dimensional gel electrophoresis (2DE). Carcinogenesis 1992;13:1177-1183.
17. Paradis K, Langford G, Long Z, Heneine W, Sandstrom P, Switzer WM, et al. Search for cross-species transmission of porcine endogenous retrovirus in patients treated with living pig tissue. Science 1999;285:1236-1241.
18. Nyberg SL, Remmel RP, Mann HJ, Peshwa MV, Hu WS, Cerra FB. Primary hepatocytes outperform Hep G2 cells as the source of biotransformation functions in a bioartificial liver. Ann Surg 1994;220:59-67.
19. Wang L, Sun J, Li L, Mears D, Horvat M, Sheil AG. Comparison of porcine hepatocytes with human hepatoma (C3A) cells for use in a bioartificial liver support system. Cell Transplant 1998;7: 459-468.
20. Kobayashi N, Miyazaki M, Fukaya K, Inoue Y, Sakaguchi M, Uemura T, et al. Transplantation of highly differentiated immortalized human hepatocytes to treat acute liver failure. Transplantation 2000;69:202-207.
21. Roberts EA, Letarte M, Squire J, Yang S. Characterization of human hepatocyte lines derived from normal liver tissue. Hepatology 1994;19:1390-1399.
22. Kobayashi N, Fujiwara T, Westerman KA, Inoue Y, Sakaguchi M, Noguchi H, et al. Prevention of acute liver failure in rats with reversibly immortalized human hepatocytes. Science 2000;287: 1258-1262.
23. Kelly JH, Koussayer T, He D, Chong MG, Shang TA, Whisennand HH, et al. Assessment of an extracorporeal liver assist device in anhepatic dogs. Artif Organs 1992;16:418-422.
24. Ellis AJ, Hughes RD, Wendon JA, Dunne J, Langley PG, Kelly JH, et al. Pilot-controlled trial of the extracorporeal liver assist device in acute liver failure. Hepatology 1996;24:1446-1451.
25. Sussman NL, Chong MG, Koussayer T, He DE, Shang TA, Whisennand HH, et al. Reversal of fulminant hepatic failure using an extracorporeal liver assist device. Hepatology 1992;16: 60-65.
26. Ellis AJ, Sussman NL, Kelly JH, Williams R. Clinical experience with an extracorporeal liver assist device. In: Lee WM, Williams R (eds). Acute liver failure. Cambridge: Cambridge University Press, 1997:255-265.
27. el Mouelhi M, Didolkar MS, Elias EG, Guengerich FP, Kauffman FC. Hepatic drug-metabolizing enzymes in primary and secondary tumors of human liver. Cancer Res 1987;47:460-466.
28. Werner A, Duvar S, Muthing J, Buntemeyer H, Kahmann U, Lunsdorf H, et al. Cultivation and characterization of a new immortalized human hepatocyte cell line, HepZ, for use in an artificial liver support system. Ann N Y Acad Sci 1999;875:364-368.
29. Miyazaki M, Mihara K, Bai L, Kano Y, Tsuboi S, Endo A, et al. Immortalization of epithelial-like cells from human liver tissue with SV40 T-antigen gene. Exp Cell Res 1993;206:27-35.
30. Rozga J, Williams F, Ro MS, Neuzil DF, Giorgio TD, Backfisch G, et al. Development of a bioartificial liver: Properties and function of a hollow-fiber module inoculated with liver cells. Hepatology 1993;17:258-265.

31. Jauregui HO, Naik S, Santangini HA. The use of microcarrier-roller bottle culture for large-scale production of porcine hepatocytes. Tissue Eng 1997;3:17-25.
32. Clement B, Desille M, Fremond B, Campion JP, Guguen-Guillouzo C, Bourel M, et al. Hepatocytes in cell therapy [in French]. Transfus Clin Biol 1998;5:80-87.
33. Naik S, Trenkler D, Santangini H, Pan J, Jauregui HO. Isolation and culture of porcine hepatocytes for artificial liver support. Cell Transplant 1996;5:107-115.
34. Takahashi M, Ishikura H, Takahashi C, Nakajima Y, Matsushita M, Matsue H, et al. Immunologic considerations in the use of cultured porcine hepatocytes as a hybrid artificial liver. Anti-porcine hepatocyte human serum. ASAIO J 1993;39:M242-M246.
35. Baquerizo A, Mhoyan A, Shirwan H, Swensson J, Busuttil RW, Demetriou AA, et al. Xenoantibody response of patients with severe acute liver failure exposed to porcine antigens following treatment with a bioartificial liver. Transplant Proc 1997;29: 964-965.
36. Baquerizo A, Mhoyan A, Kearns-Jonker M, Arnaout WS, Shackleton C, Busuttil RW, et al. Characterization of human xenoreactive antibodies in liver failure patients exposed to pig hepatocytes after bioartificial liver treatment: An ex vivo model of pig to human xenotransplantation. Transplantation 1999;67:5-18.
37. Dowling DJ, Mutimer DJ. Artificial liver support in acute liver failure. Eur J Gastroenterol Hepatol 1999;11:991-996.
38. Weiss RA. Xenografts and retroviruses. Science 1999;285:1221-1222.
39. Patience C, Takeuchi Y, Weiss RA. Infection of human cells by an endogenous retrovirus of pigs. Nat Med 1997;3:282-286.
40. Van der Laan LJW, Lockey C, Griffeth BC, Frasier FS, Wilson CA, Onions DE, et al. Infection by porcine endogenous retrovirus after islet xenotransplantation in SCID mice. Nature 2000; 407:501-504.
41. Nyberg SL, Hibbs JR, Hardin JA, Germer JJ, Platt JL, Paya CV, et al. Influence of human fulminant hepatic failure sera on endogenous retroviral expression in pig hepatocytes. Liver Transpl 2000;6:76-84.
42. Gunzburg WH. Xenotransplantation: A summary of the International Business Communications' Fourth International Congress. Liver Transpl 2000;6:388-394.
43. Sandrin MS, McKenzie IF. Recent advances in xenotransplantation. Curr Opin Immunol 1999;11:527-531.
44. Eguchi S, Kamohara Y, Sugiyama N, Kawazoe Y, Kawashita Y, Tamura H, et al. Efficacy and current problems with a porcine hepatocyte-based bioartificial liver: Light and shade. Transplant Proc 1999;31:2014-2015.
45. Riordan SM, Williams R. Extracorporeal support and hepatocyte transplantation in acute liver failure and cirrhosis. J Gastroenterol Hepatol 1999;14:757-770.
46. Eguchi S, Lilja H, Hewitt WR, Middleton Y, Demetriou AA, Rozga J. Loss and recovery of liver regeneration in rats with fulminant hepatic failure. J Surg Res 1997;72:112-122.
47. Sundback CA, Vacanti JP. Alternatives to liver transplantation: From hepatocyte transplantation to tissue-engineered organs. Gastroenterology 2000;118:438-442.
48. Watanabe FD, Mullon CJ, Hewitt WR, Arkadopoulos N, Kahaku E, Eguchi S, et al. Clinical experience with a bioartificial liver in the treatment of severe liver failure. A phase I clinical trial. Ann Surg 1997;225:484-491.
49. Sussman NL, Gislason GT, Conlin CA, Kelly JH. The Hepatix extracorporeal liver assist device: Initial clinical experience. Artif Organs 1994;18:390-396.
50. Gerlach JC, Encke J, Hole O, Muller C, Courtney JM, Neuhaus P. Hepatocyte culture between three dimensionally arranged biomatrix-coated independent artificial capillary systems and sinusoidal endothelial cell co-culture compartments. Int J Artif Organs 1994;17:301-306.
51. De Bartolo L, Jarosch-Von Schweder G, Haverich A, Bader A. A novel full-scale flat membrane bioreactor utilizing porcine hepatocytes: Cell viability and tissue-specific functions. Biotechnol Prog 2000;16:102-108.
52. Maurer HR. Towards serum-free, chemically defined media for mammalian cell culture. In: Freshney RI (ed). Animal cell culture. A practical approach. MacLean, VA: IRL, 2000:15-46.
53. Berry MN, Edwards AM, Barritt GJ. Monolayer culture of hepatocytes. In: Isolated hepatocytes. Preparation, properties and application. Amsterdam: Elsevier, 1991:265-354.
54. Michalopoulos GK. Liver regeneration: Molecular mechanisms of growth control. FASEB J 1990;4:176-187.
55. Dixit V, Arthur M, Reinhardt R, Gitnick G. Improved function of microencapsulated hepatocytes in a hybrid bioartificial liver support system. Artif Organs 1992;16:336-341.
56. Sielaff TD, Nyberg SL, Rollins MD, Hu MY, Amiot B, Lee A, et al. Characterization of the three-compartment gel-entrapment porcine hepatocyte bioartificial liver. Cell Biol Toxicol 1997;13: 357-364.
57. Suzuki M, Takeshita K, Yamamoto T, Ishibashi H, Kodama M. Hepatocytes entrapped in collagen gel following 14 days of storage at 4 degrees C: Preservation of hybrid artificial liver. Artif Organs 1997;21:99-106.
58. Akaike T, Tobe S, Kobayashi A, Goto M, Kobayashi K. Design of hepatocyte-specific extracellular matrices for hybrid artificial liver. Gastroenterol Jpn 1993;28(suppl 4):S45-S52.
59. Naka S, Takeshita K, Yamamoto T, Tani T, Kodama M. Bioartificial liver support system using porcine hepatocytes entrapped in a three-dimensional hollow fiber module with collagen gel: An evaluation in the swine acute liver failure model. Artif Organs 1999;23:822-828.
60. Michalopoulos GK, Bowen WC, Zajac VF, Beer-Stolz D, Watkins S, Kostrubsky V, et al. Morphogenetic events in mixed cultures of rat hepatocytes and nonparenchymal cells maintained in biological matrices in the presence of hepatocyte growth factor and epidermal growth factor. Hepatology 1999;29:90-100.
61. te Velde AA, Ladiges NC, Flendrig LM, Chamuleau RA. Functional activity of isolated pig hepatocytes attached to different extracellular matrix substrates. Implication for application of pig hepatocytes in a bioartificial liver. J Hepatol 1995;23:184-192.
62. Gregory PG, Connolly CK, Toner M, Sullivan SJ. In vitro characterization of porcine hepatocyte function. Cell Transplant 2000;9:1-10.
63. Plant NJ, Horley NJ, Savory RL, Elcombe CR, Gray TJ, Bell DR. The peroxisome proliferators are hepatocyte mitogens in chemically-defined media: Glucocorticoid-induced PPAR alpha is linked to peroxisome proliferator mitogenesis. Carcinogenesis 1998;19:925-931.
64. Kera Y, Penttila KE, Lindros KO. Glutathione replenishment capacity is lower in isolated perivenous than in periportal hepatocytes. Biochem J 1988;254:411-417.
65. Poso AR, Penttila KE, Suolinna EM, Lindros KO. Urea synthesis in freshly isolated and in cultured periportal and perivenous hepatocytes. Biochem J 1986;239:263-267.

66. Lindros KO, Penttila KE. Digitonin-collagenase perfusion for efficient separation of periportal or perivenous hepatocytes. Biochem J 1985;228:757-760.
67. Bader A, Knop E, Boker K, Fruhauf N, Schuttler W, Oldhafer K, et al. A novel bioreactor design for in vitro reconstruction of in vivo liver characteristics. Artif Organs 1995;19:368-374.
68. Bhatia SN, Balis UJ, Yarmush ML, Toner M. Effect of cell-cell interactions in preservation of cellular phenotype: Cocultivation of hepatocytes and nonparenchymal cells. FASEB J 1999;13: 1883-1900.
69. Khaoustov VI, Darlington GJ, Soriano HE, Krishnan B, Risin D, Pellis NR, et al. Induction of three-dimensional assembly of human liver cells by simulated microgravity. In Vitro Cell Dev Biol Anim 1999;35:501-509.
70. Unsworth BR, Lelkes PI. Growing tissues in microgravity. Nat Med 1998;4:901-907.
71. Lazar A, Peshwa MV, Wu FJ, Chi CM, Cerra FB, Hu WS. Formation of porcine hepatocyte spheroids for use in a bioartificial liver. Cell Transplant 1995;4:259-268.
72. Lazar A, Mann HJ, Remmel RP, Shatford RA, Cerra FB, Hu WS. Extended liver-specific functions of porcine hepatocyte spheroids entrapped in collagen gel. In Vitro Cell Dev Biol Anim 1995;31:340-346.
73. Kim SS, Utsunomiya H, Koski JA, Wu BM, Cima MJ, Sohn J, et al. Survival and function of hepatocytes on a novel three-dimensional synthetic biodegradable polymer scaffold with an intrinsic network of channels. Ann Surg 1998;228:8-13.
74. Demetriou AA. Support of the acutely failing liver: State of the art. Ann Surg 1998;228:14-15.
75. Kono Y, Yang S, Letarte M, Roberts EA. Establishment of a human hepatocyte line derived from primary culture in a collagen gel sandwich culture system. Exp Cell Res 1995;221:478-485.
76. Selden C, Shariat A, McCloskey P, Ryder T, Roberts E, Hodgson H. Three-dimensional in vitro cell culture leads to a marked upregulation of cell function in human hepatocyte cell lines—An important tool for the development of a bioartificial liver machine. Ann N Y Acad Sci 1999;875:353-363.
77. Gerlach JC, Schnoy N, Encke J, Smith MD, Muller C, Neuhaus P. Improved hepatocyte in vitro maintenance in a culture model with woven multicompartment capillary systems: Electron microscopy studies. Hepatology 1995;22:546-552.
78. Traiser M, Diener B, Fandrich F. Isolation and cryopreservation of human hepatocytes. Transpl Med 1994;6:84-90.
79. Fautrel A, Joly B, Guyomard C, Guillouzo A. Long-term maintenance of drug-metabolizing enzyme activities in rat hepatocytes after cryopreservation. Toxicol Appl Pharmacol 1997;147: 110-114.
80. Loretz LJ, Li AP, Flye MW, Wilson AG. Optimization of cryopreservation procedures for rat and human hepatocytes. Xenobiotica 1989;19:489-498.
81. Anchordoguy TJ, Cecchini CA, Crowe JH, Crowe LM. Insights into the cryoprotective mechanism of dimethyl sulfoxide for phospholipid bilayers. Cryobiology 1991;28:467-473.
82. Guillouzo A, Rialland L, Fautrel A, Guyomard C. Survival and function of isolated hepatocytes after cryopreservation. Chem Biol Interact 1999;121:7-16.
83. Sun EL, Aspar DG, Ulrich RG, Melchior GW. Cryopreservation of cynomolgus monkey (*Macaca fascicularis*) hepatocytes for subsequent culture and protein synthesis studies. In Vitro Cell Dev Biol 1990;26:147-150.
84. Utesch D, Diener B, Molitor E, Oesch F, Platt KL. Characterization of cryopreserved rat liver parenchymal cells by metabolism of diagnostic substrates and activities of related enzymes. Biochem Pharmacol 1992;44:309-315.
85. Zaleski J, Richburg J, Kauffman FC. Preservation of the rate and profile of xenobiotic metabolism in rat hepatocytes stored in liquid nitrogen. Biochem Pharmacol 1993;46:111-116.
86. Nelson LJ, Newsome PN, Howie AF, Hadoke PW, Dabos KJ, Walker SW, et al. An improved ex vivo method of primary porcine hepatocyte isolation for use in bioartificial liver systems. Eur J Gastroenterol Hepatol 2000;12:923-930.
87. Flendrig LM, la Soe JW, Jorning GG, Steenbeek A, Karlsen OT, Bovee WM, et al. In vitro evaluation of a novel bioreactor based on an integral oxygenator and a spirally wound nonwoven polyester matrix for hepatocyte culture as small aggregates. J Hepatol 1997;26:1379-1392.
88. Flendrig LM, Chamuleau RA, Maas MA, Daalhuisen J, Hasset B, Kilty CG, et al. Evaluation of a novel bioartificial liver in rats with complete liver ischemia: Treatment efficacy and species-specific alpha-GST detection to monitor hepatocyte viability. J Hepatol 1999;30:311-320.
89. Rozga J, Holzman MD, Ro MS, Griffin DW, Neuzil DF, Giorgio T, et al. Development of a hybrid bioartificial liver. Ann Surg 1993;217:502-509.
90. Gerlach J, Trost T, Ryan CJ, Meissler M, Hole O, Muller C, et al. Hybrid liver support system in a short term application on hepatectomized pigs. Int J Artif Organs 1994;17:549-553.